DESIGN AND ANALYSIS OF THE INTERNALLY COOLED SMART CUTTING TOOLS WITH THE APPLICATIONS TO ADAPTIVE MACHINING

Thesis

By

Saiful Anwar Bin Che Ghani

A thesis submitted in partial fulfilment of the

requirements of Brunel University

for the degree of Doctor of Philosophy

January 2013

Abstract

Adaptive machining with internally cooled smart cutting tools is a smart solution for industrial applications, which have stringent manufacturing requirements such as contamination free machining (CFM), high material removal rate, low tool wear and better surface integrity. The absence of cutting fluid in CFM causes the cutting tool and the workpiece subject to great thermal loads owing to higher friction and adhesion, and as a result may increase the levels of tool wear drastically. The increase in cutting temperature may influence the chip morphology which in return producing metal chips in unfavourable ribbon or snarl forms. CFM is difficult to be realized as contaminants can be in various forms in the machining operation and to avoid them totally requires a very tight controlled condition. However, the ecological, economical and technological demands compel the manufacturing practitioners to implement environmentally clean machining process (ECMP). Machining with innovative cooling techniques such as heat pipe, single-phase microduct, cryogenic or minimum quantity lubrication (MQL) has been intensely researched in recent years in order to reduce the cutting temperature in ECMP, thus enabling the part quality, the tool life and the material removal rate achieved in ECMP at least equate or surpass those obtained in conventional machining. On the other hand, the reduction of cutting temperature by using these techniques is often superfluous and is adverse to the produced surface roughness as the work material tends to inherent brittle and hard property at low temperature. Open cooling system means the machining requires a constant cooling supply and it does not provide a solution for process condition feedback as well.

This Ph.D. project aims to investigate the design and analysis of internally cooled cutting tools and their implementation and application perspectives for smart adaptive machining in particular. Circulating the water based cooling fluid in a closed loop circuit contributes to sustainable manufacturing. The advantage of reducing cutting temperature from localized heat at the tool tip of an internally cooled cutting tool is enhanced with the smart features of the tool, which is trained by real experimental data, to cognitively vary the coolant flow rate, cutting feed rate or/and cutting speed to control the critical machining temperature as well as optimum machining conditions. Environmental friendly internal micro-cooling can avoid contamination of generated swarf which can also reduce the cutting temperature and thus reduce tool wear, increase machining accuracy and optimize machining economics. Design of the smart cutting tool with internal micro-cooling not only takes into account of the environmental aspects but also justifies with its ability to reduce the machining cost. Reduction of production cost can be achieved with the lower consumption of cooling fluid and improved machining resources/ energy efficiency.

The models of structural, heat transfer, computational fluid dynamics (CFD) and tool life provide useful insight of the performance of the internally cooled smart cutting tool. Experimental validation using the smart cutting tool to machine titanium, steel and aluminium, indicates that the application of internally cooled smart cutting tools in adaptive machining can improve machining performance such as cutting temperature, cutting forces and surface quality generated. The useful tool life span is also extended significantly with internally cooled smart cutting tools in comparison to the tool life in conventional machining. The internally cooled smart cutting tool has important implications in the application to ECMP particularly by overcoming the stigma of high uncontrollable cutting temperature with the absence of cooling fluid.

Acknowledgement

I would like to express my gratitude especially to my supervisor, Professor Kai Cheng, and my co-supervisor, Dr. Richard Bateman for their valuable advice, guidance, support, motivation and encouragement throughout this journey.

Recognitions are highlighted to Brunel University for their financial support, which made this research achievable. A token of appreciation also go to Universiti Malaysia Pahang, Malaysia for putting their faith in me to pursue my studies to doctoral level.

Special thanks are to my colleagues Dr. Tim Minton, Dr. Chao Wang, Dr. Sarah Sun, Mr. Abdul Hadi Mohamad, Ms. Amirah Mohamad Sahar and Mr Fathullah Ghazali for supporting me with my research work, also to Dr. Frank Wardle, Mr. Paul Yates, and all the technicians for their assistance. I am also grateful to all of the individuals who have directly or indirectly helped me in completing my research.

I would like also to acknowledge my parents of both sides, Che Ghani bin Ambak and Maznah Muftahuddin, and Md Noar and Noraini Md Shah for their love, encouragement and support throughout my research studies.

I deeply indebted to my beloved wife, Nor Aida Zuraimi Md Noar, for her warm comfort and great assistance and for her patience and understanding which has inspired my research work from the beginning to the end.

Table of Contents

Abbreviations

AC   Adaptive control

ACC   Adaptive control constraint

ACO   Adaptive control optimisation

AI   Artificial intelligent

ALE   Arbitrary Lagrangian-Eulerian

BC   Boundary conditions

BUE   Built-up edge

CBN   Carbon boron nitride

CFD   Computational fluid dynamics

CFM   Contamination free manufacturing

DNS   Direct numerical solutions

CFM   Contamination free machining

CNC   Computer numerical control

CP   Commercial pure

DAQ   Data acquisition system

DM   Dry machining

EAA   Extrinsic allergic alveolitis

ECMP   Environmentally clean machining process

EDM   Electrical discharge machining

EDX   Energy dispersive X-ray spectroscopy

EU   European Unions

FEA	Finite element analysis
FEM	Finite element modeling
FOCAS	FANUC open CNC API Specifications
FOD	Foreign object debris/ foreign object damage
GAC	Geometrical adaptive control
GUI	Graphical user interface
HSM	High speed machining
HSS	High speed steel
IGES	Initial graphic exchange specification
IC	Internally cooled/ internal cooling
IDP	Iterative development procedure
IR	Infra-red
IT	Information technology
MEMS	Micro-Electro-Mechanical-Systems
MQL	Minimum quantity lubrication
MRAC	Model reference adaptive control
MRR	Material removal rate
MWF	Metal working fluid
NDM	Near dry machining
NIST	National Institutes of Standards and Technology
PLC	Programmable logic control
PMMA	Poly(methyl methacrylate)

SEM	Scanning electron microscope
SLS	Selective laser sintering
SMS	Smart Machining Systems
STEP	Standard for the exchange of product model data
TC	Thermocouple
TCP/IP	Transmission control protocol and internet protocol
UK	United Kingdom
US	United States of America
USB	Universal serial bus
VI	Virtual instruments
WC	Tungsten carbide
Z-N	Ziegler Nichols method

Nomenclature

A	Area	m²
A_s	Shear plane area	mm²
a_p	Depth of cut	mm
c_p	Specific heat capacity	J/(kg·K)
d	Diameter	mm
F_c	Cutting force	N
F_R	Radial force	N
F_t	Feed force	N
f	Feedrate	mm/rev
h	Convection heat transfer coefficient	W/(m²·K)
KF	Crater front distance	mm
KT	Crater wear	mm
k	Thermal conductivity	W/(m·K)
L	Length	mm
l	Length of the chip	mm
l_e	entrance length	mm
$\dot{m}$	Mass flow rate	kg/min or l/min
P	Pressure	Pa or bar
p	Wetted perimeter of a duct	m
Pr	Prandtl number	
Re	Reynolds number	
r	Radius of a pipe	mm
r_c	Chip thickness ratio	
s	Diagonal distance on the cutting tool	mm
T_t	Tool temperature	K or °C
T_f	Mean fluid temperature	K or °C

t_1	Undeformed chip thickness	mm
t_2	Mean cut chip thickness	mm
t_{sl}	Sublayer thickness	mm
T	Temperature	K or °C
VB	Flank wear width	mm
v	Velocity	m/s
W	Weight of the chip	kg
w	Chip width	mm
$\dot{Q}$	Rate of heat generation per unit volume	W/m³
q_n	Total heat transfer in n direction	W
q''	Heat flux	W/m²
$\dot{\forall}$	Volumetric rate	m³/min

Greek letters

α	Rake angle	°
$\emptyset$	Shear plane angle	°
λ	Frictional angle	°
θ_∞	Work ambient temperature	K or °C
θ_C	Chip temperature	K or °C
θ_{opt}	Optimum cutting temperature	K or °C
θ_R	Relief surface temperature	K or °C
θ_S	Shear plane temperature	K or °C
θ_T	Tool face temperature	K or °C
ρ	Density	kg/m³
$\sigma_{(comp)}$	Compressive stress	MPa or N/mm²
σ_1	Maximum principle stress	MPa or N/mm²
τ	Shear strength of material	MPa or N/mm²

List of Figures

List of Tables

Chapter 1:   **Introduction**

1.1.   **Background of the research**

Technological advancement of cutting tool in *green manufacturing* or environmentally clean machining process (ECMP) as being used by Byrne and Scholta (Byrne and Scholta, 1993) is the quintessential requirement in the complex machining field for enabling high cutting performance of ecological desirable manufacturing and reducing its environmental impacts while maintaining the lowest possible production cost. The term green manufacturing can be viewed from two aspects:

(1) the manufacturing of "green" products, particularly used in renewable energy system or contamination free environment, or

(2) "greening" the manufacturing, i.e. reducing pollution and waste by minimisation of natural source usage, recycling and re-using by-pass products and reducing emissions.

The endeavour by the manufacturers in fulfilling both aspects of green manufacturing is by minimising the dependency of the machining process on metal working fluid (MWF). The two common approaches taken in realising green manufacturing are (1) dry machining (DM) and (2) near dry machining (NDM). In machining, despite the long established benefits of dousing MWFs as shown in Fig. 1-1, the fact that the adverse impacts it poses in the shop floor atmosphere, to the global environment, to the finished parts and to the manufacturing cost has heightened the research interest to eliminate the usage of it in the recent years (the roles and drawbacks of MWFs are compiled together in Table 1-1.

Fig. 1-1: Exposure to MWF can cause; irritation of skin/ dermatitis, bronchitis, occupational asthma (Rosenman et al., 1997), irritation of the upper respiratory tract, breathing difficulties or a more serious lung disease called extrinsic allergic alveolitis (EAA) (Health Safety Executive, 2012)

Table 1-1: The roles and the drawbacks of MWF

Role		Drawback	
(i)	Cooling down the cutting temperature	(i)	Possible contamination to the finished part
(ii)	Reduction of friction between the generated chip and the cutting tool	(ii)	Hazardous to the operator; cause dermatological and respiratory illnesses
(iii)	Reduction of the built-up edge (BUE) and built-up layer (BUL) formations	(iii)	Involving high cost related to the operation, maintenance, disposal and treatment of MWF
(iv)	Inhibiting corrosion		
(v)	Washing away the metal chip		

Green manufacturing is compulsory in the machining of contamination free machining products (CFM), and some specific applications include the manufacturing of medical devices, food and beverage container and highly inflammable magnesium based alloys. Certain aerospace components also need to be machined in green manufacturing because their nature of working that is sensitive to foreign object debris/ foreign object damage (FOD). Selective components that require green manufacturing are shown in Fig. 1-2.
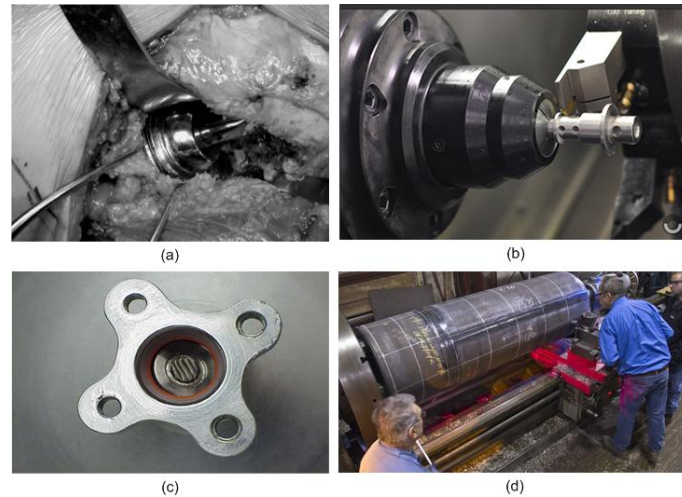
Fig. 1-2: Example of green manufacturing components; (a) a ball-joint for hip replacement (Heisel et al., 2004) (b) machining of magnesium (Reed Prototype and Machining, 2012) (c) FOD sensitive pump component for aerospace (International Aerospace Quality Group, 2007) (d) machining of beverages container (Beverage Machine and Fabricators, 2012)

Currently, the green manufacturing performance with the absence of MWF has been enhanced by the improvement of tool geometry, coating materials and chip breaking technique, however, the effectiveness of green manufacturing requires more than just eliminating coolant; it requires a scientific and methodological approach in managing the heat produced during overall machining operation. Practically the advancement in green manufacturing technologies nowadays, such as tool coatings (Kustas et al, 1997; Rech, 2006), minimum quantity lubrication (MQL) (Kamata et al., 2007), cryogenic cooling (Bermingham et al., 2012) or indirect cutting insert cooling (Ghosh et al., 2005; Frost, 2008) and vibrating as well as rotary tool (Hosokawa et al., 2010), enable the reduction of localised cutting temperature at the tool tip which is detrimental in conventional dry machining but in some cases the heat is required for cutting process because:

(i)   at high temperature the brittle material of the cutting tool will be more ductile so can prevent edge chipping,

(ii)   the heat is beneficial especially in hard-to-cut material to reduce the shear strength of the work-piece material and

(iii) unoptimal cutting temperature is one of the major cause for formation of BUE; commonly discovered in low-speed machining.

Smart cutting tools integrated with 'sensor-fusion' technology can provide process measurement variables such as temperature, force, acoustic emission or any combination of the variables to be used to denote the machining condition in real time. Additional features of the smart cutting tools such as "*plug and produce*" and the temperature management can reduce setting up time and improve green manufacturing performance respectively. Fig. 1-3 shows some smart cutting tools that have been published recently with two of them Fig. 1-3(b) and Fig. 1-3(c) are co-produced by the author at Brunel University.
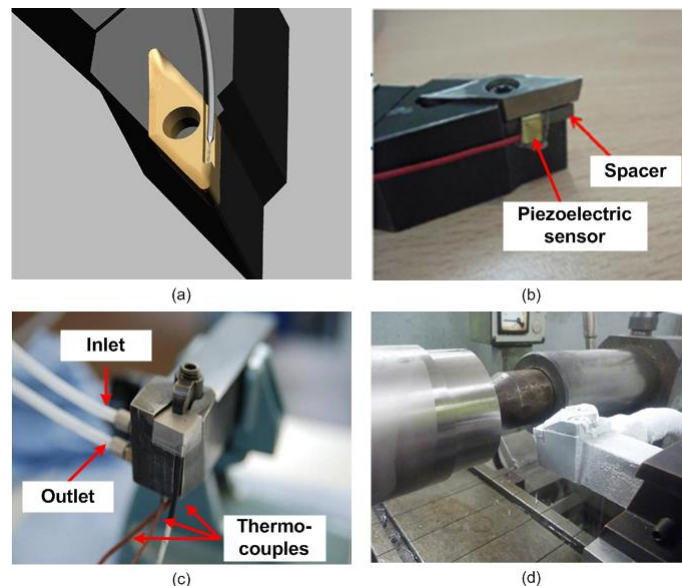
Fig. 1-3: Smart cutting tools; (a) Smart tool with embedded thermocouple from ACTARUS (b) Smart tool with force sensor (Wang et al., 2012), (c) Internally cooled cutting tool with embedded thermocouple (Sun et al., 2011), (d) Cutting tool with internal cryogenic cooling (Bermingham et.al, 2012)

As concluded by Byrne et al. (2003), the development of cutting technologies particularly in green manufacturing or environmental conscious machining as being used in the publication, should be strongly integrated with smart management by using the information technologies. Decades of research have reduced the dependency of machining, which is a process of material removal from work-piece, on the skill requirements of machine tool operators by the advent of computer numerical controlled (CNC) machining. However, a common drawback of CNC machine is that its operating parameter such as spindle speed or feedrate is prescribed conservatively either based on programmer's knowledge and experience or by a relatively static machinability database in the handbooks in order to achieve product quality specifications or to preserve the tool. Therefore, many CNC systems run under inefficient operating conditions which have become an interest to study a smart and adaptive way which provides on-line adjustment of the operating parameters in real time to control optimum cutting condition.

This dissertation and research is part of the ConTemp project that endeavours to develop, test and commercialise a new concept of cutting tool for green manufacturing with an integrated high performance micro cooling device, serving as sensor; actuator system for measurement of tool's temperature and simultaneous cooling of the tool, thus leading to longer tool life and increased part accuracy.

1.1.1. Smart cutting tools integrated with existing machine tool

Cutting tools are one of the key inputs in the cutting process, which the smartness of them can improve process productivity, achieve high machining

accuracy and reduce the manufacturing cost. Smart cutting tool is required in today's manufacturing Although smart machining have been addressed regularly in various academic publications since 1980s, unfortunately, when speaking about smart cutting tools, the community of manufacturing practitioners do not always share a common language. As a matter of fact, smart machining and smart cutting tools have always been used interchangeably although the two aspects represent two different entities in manufacturing. Therefore, it is intended that this research may contribute to an enlightening approach based on a review of the recent developments, challenges and current trends related to smart cutting tools. The design of internally cooled smart cutting tool and its application in adaptive smart machining will elucidate the unique role of the two aspects in realising green manufacturing.

The baseline aims of the development of the smart cutting tools are (i) to improve tool performance by means of extending the tool life and (ii) accommodating a cutting tool with smart features which can substantially contribute to cutting performance. The tool life extension may be an attribute of friction reduction mechanism such as advanced coating materials or techniques or cutting temperature reduction method such as minimum quantity lubrication (MQL) or indirect cooling. The smart features are in-trend with today manufacturing philosophies for lean, agile and green manufacturing. This can be realised by having a modular "plug and produce" cutting tool or integrating the cutting tool with intelligent aspects of information technology such as fusion of thermal and force sensors or probably by diminishing the waste involve in machining. Waste is taken in its most general sense including time, resources and process residuals.

The major challenge that hampers the development of smart cutting tools to date are the difficulties to produce economical smart cutting tools that can work in a hostile environment of machining. Economics here includes the cost associated with development, operation and maintenance cost in exploiting smart cutting tools and their peripheral subsystems particularly in selecting suitable sensors and actuators.

The roadmap for cutting technology illustrated in Fig. 1-4 provides the technological aspects that need to be considered in designing of the internally cooled smart cutting tools. The framework of this research includes the innovation to the process inputs of the machine tool especially the *cutting tools*, *cutting fluid*, *tool material* and *adapted process parameter*. The performance of these innovative aspects is assessed by the machining performance evaluation such as quality assurance (accuracy, repeatability and reproducibility), process monitoring, controls, and artificial intelligence in accordance with the requirements of the change drivers.
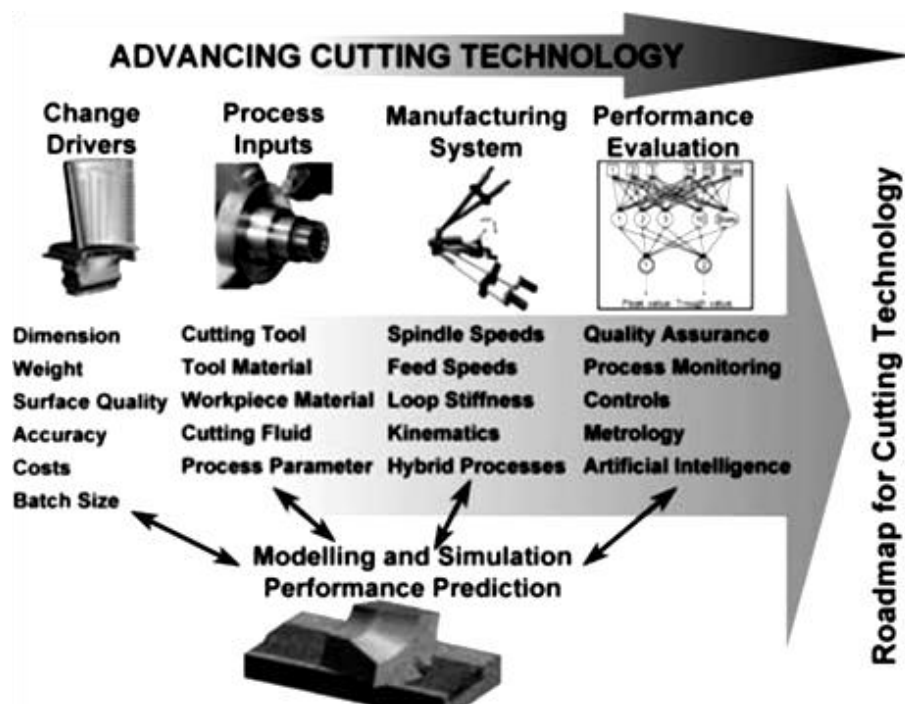
Fig. 1-4: The roadmap for cutting technology (Byrne et al., 2003)

1.1.2. Adaptive machining with optimum machining condition

Adaptive control used in the manufacturing literature does not share the same definition as the one used in control engineering. The application of adaptive control in manufacturing today is realised by means of on-line manipulation of process parameters to obtain optimum machining outputs rather than adaptive changing of real-time error correction algorithms due to condition uncertainty as in control engineering. So due to that adaptive machining might be a more suitable term to be used for this technique.

The benefits of adaptive machining are mainly to increase the economics of machining especially in green manufacturing. Cutting parameters such as feedrate and cutting speed are normally on-line adapted to optimally control the process parameters (e.g. cutting forces or cutting temperatures) in order to obtain higher degree of machining economics such as high accuracy of surface finish, low machine downtime or extended tool life.

Although the benefits of application of adaptive machining is clear, the implementation of even the simplest adaptive machining such as feedrate adaptation based on cutting force measurement from a commercial available dynamometer is quite complex (Masory et al., 1980). The adaptive control system for machining process can easily get unstable while adapting cutting parameters due to the nature of the working system that based on sampled data with non linear variable gain.

1.1.3. Tool-wear/ tool life performance model of an internally cooled cutting tool

Application of MWF in current manufacturing practice is ubiquitious, and a still valid report from 1998 has given an estimated figure of 52% of 640 million gallons of MWFs is consumed in machining annually (Brockhoff and Walter, 1998). Besides the serious drawbacks possess by application of MWFs on health and safety, the cost regarding with the purchase, treat and disposal of MWF in automotive engineering for example can be up to four times higher than the tooling cost, two times higher than general machining cost and can account up to 17% of the cost per part (Brockhoff and Walter, 1998; Sreejith et al., 2000). Thus, operation concerned with sustainability has been looking into green manufacturing as alternatives; in green manufacturing very minimum coolant application is aimed. Even though this approach suggests that higher temperature and more rapid tool wear will occur, with optimum cutting conditions and advance tooling technology (smart tools including the advancement of coating technology and cleaner cooling) an extended tool life and reasonable machining performance are obtainable. Thus there is a need for a scientific approach in modeling of tool life/ tool wear in the function of temperature, fluid dynamics, machining parameters and heat transfer so better understanding of the factors affecting smart tool performance. It is the goal of this work to develop, validate and apply a performance based model of machining process that provides good fundamental in designing internally cooled smart cutting tools for application in green manufacturing. The use of the model will also serve as a mechanism to reduce the machining cost and hence, lessens the environmental impact during the research. The types of modeling and simulation approaches with their capabilities and limitations are visualised in Fig. 1-5(a). Two example results of finite element analysis (FEA) of

coating tool performance and tool performance in high speed machining (HSM) of dry machining are shown in Fig. 1-5(b) and Fig. 1-5(c) respectively.
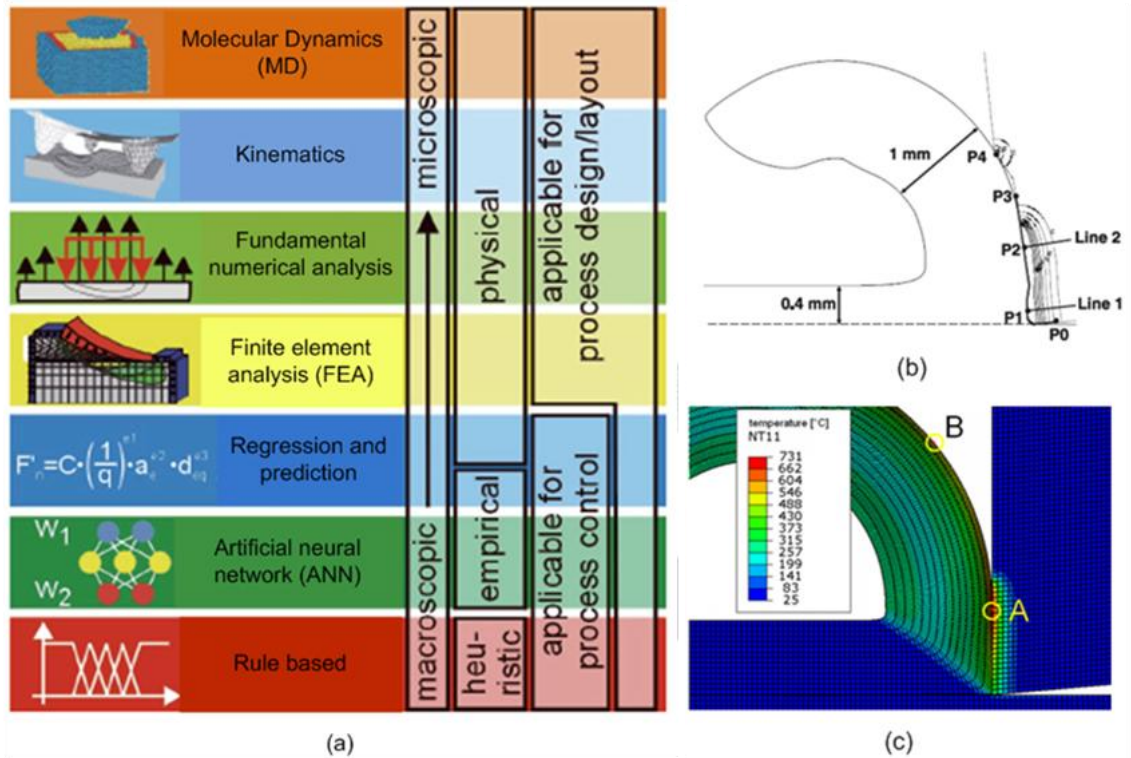
Fig. 1-5: (a) Model types and simulation approaches and their capabilities and limitations (Brinksmeier et al., 2006), (b) FEA simulation of thermo-mechanical behavior of coating tools in dry machining (Kone et al., 2010), (c) FE simulation on tool performance in HSM dry machining (Molinari et al., 2005)

1.2.   **Research motivation, aims and objectives**

Dousing cooling lubricant on a cutting tool is a conventional way to reduce the cutting temperature, to increase the productivity and to extend the tool life. However, the used cooling fluid contains chemical compounds that are harmful to the operator, detrimental to the environment and inefficient to the machining economics. Obviously there is a need for an innovative approach to develop

smart cutting tools for green manufacturing that can perform equally if not better than conventional machining with external flood cooling. The integration of the sensors fusion, information of the state of the tool condition and state of the art of the tool geometry and materials technologies is the key characteristic of a smart cutting tool. The internal cooling, which is one advanced feature introduced to the tool geometry, is aimed to remove the excessive heat generated in machining, and consequently could enable the industry to find a lower cost solution with reduced lead time, to achieve accurate and better surface quality and at the same time to practice environmental friendly manufacturing in order to maintain their competitiveness. Techniques in managing the temperature of the cutting tools have great potential in green manufacturing because it is projected in the coming years that the advancement of cutting tool materials is forecasted to be slow due to it becoming more difficult to do much better than diamond, carbon boron nitride (CBN) and various modern coatings.

While the currently adopted internal cooling concepts have obvious limitations on machining performance (due to remoteness from cutting edge), the ultimate motivation of this research is to control the cutting temperature optimally, thus extending the tool life by reducing the wear impacts while maintaining high machining productivity in an adaptive manner. With the availability of advanced communication on CNC machine tool controller such as wireless serial, Ethernet, high speed serial bus (HSSB) and solid state media, adaptive control has been intensively deployed in improving machining performance especially in green manufacturing of difficult-to-cut materials such as titanium alloy and Inconel. The adaptive machining has the ability to predict the job quality, tool condition and the remaining useful tool life based on sensory feedback and it is also capable in taking appropriate corrective actions when required. However, present technology is still far away from this goal due to

the lack of reliable prediction strategy and robust sensors that can be used in the complex and hostile machining environment. The cost effective aspect of thermocouple and, high accuracy and high response of pyrometer and infrared (IR) camera in contactless measurement of cutting temperature offer the possible application of internally cooled tool to adaptive machining. The motivations for implementation of green manufacturing with adaptive machining are illustrated in Fig. 1-6. The effort to preserve the environment, new laws and regulations imposed on the manufacturers, the needs for recycling of the bypass products and the requirement for manufacturing of contamination free manufacturing (CFM) products are the change drivers towards green manufacturing with smart strategies. The performance of this approach can be assessed based on the job satisfaction, the extended tool life obtained, the reduction in manufacturing cost and the cleanliness of the manufacturing environment.

Fig. 1-6: The motivation for implementation adaptive control in green manufacturing

Modeling of machining operation with internally cooled cutting tool poses an important role to describe the state of the tool condition or the surface finish quality. Moreover, the developed model can also assist the optimisation process without necessitating huge experimental data. The inclusion of internal cooling mechanism alters heat partition in machining, the temperature distribution as well as the stress distribution inside the tool. This requires new model to be developed and tested.

Based on these challenges, the objectives of this research can be formulated as follows:

1) Design of internally cooled smart cutting tools with a closed loop coolant system to reduce the cutting temperature in machining various type of work materials, particularly in machining difficult-to-cut material.

2) Optimise the micro- geometric features involved in the internally cooled tool to enhance heat removal effectiveness without weakening the structural strength of the tool.

3) Develop a model of an internally cooled cutting tool to perform the CFD, heat transfer and mechanical analysis in order to represent the tool performance in producing the required job specification and to predict the tool ife.

4) Develop an adaptive machining network which can synergise the functions of internally cooled smart cutting tool and the adaptive control system (consists of multiple sensors, DAQ modules and appropriate actuators like pump and machine tool motion mechanisms).

5) Extend the benefits of internally cooled cutting tools in adaptive machining through a study of employment temperature difference of the coolant between the inlet and outlet in real-time as process parameter.

Objectives (1), (2) and (3) are based on a combined study of stresses and heat generated effects in orthogonal cutting and the heat transfer and fluid flow in micro-channel followed by physical testing.

Objective (4) explores the concept of adaptive machining to control the cutting temperature in order to extending of the tool life. Objective (5) studies the benefits of extending the concept of internally cooled smart cutting tools through a study of employment the difference in temperature at the inlet and outlet as real-time process condition parameter.

Objectives (4) and (5) will be validated by cutting trials that integrates the whole components in a closed loop system.

1.3.   **Structure of the thesis**

Fig. 1-7 depicts the structure of the thesis. This structure is formulated to answer the questions arose in this research, which are:

(1) Cutting temperature is spatial and temporal dependent that makes the detection of cutting temperature inconsistent. How to identify a highly reproducible cutting temperature spot on a cutting tool?

(2) The cooling technique adopted in the cutting tool. What is the most efficient internal cooling structure?

(3) The structural impact on the tool strength due to inclusion of internal cooling structural. Would the embedding of micro channel close to the cutting edge lead to possible tool fracture in machining targeted materials?

(4) Influence of internal micro channel on cutting temperature and temperature distribution inside the cutting tool. How are the temperature distributions affected by flow in the micro-channel?

(5) Internal cooling structures optimisation. What are the optimum coolant conditions and cooling geometry in maximising heat removal rate?

(6) Tool wear model in the function of cutting temperature. How is cutting temperature related to tool wear?

(7) Internally cooled smart cutting tool in machining different work materials. How does the internally cooled smart cutting tool perform in machining different types of workpiece materials?

(8) Adaptive machining to control cutting temperature, thus improving tool life. Would possibly by adapting cutting parameters based on cutting temperature reduce tool wear?

(9) If by adaptive controlling cutting temperature can extend tool life, what is the most effective on-line (and real time) adaptive control technique that can be utilised?

(10) Smart cutting tool to manipulate temperature difference of the coolant between the inlet and outlet to predict cutting temperature. Would the difference in coolant temperature at the inlet and outlet infer the actual cutting temperature at the tool- chip interface?
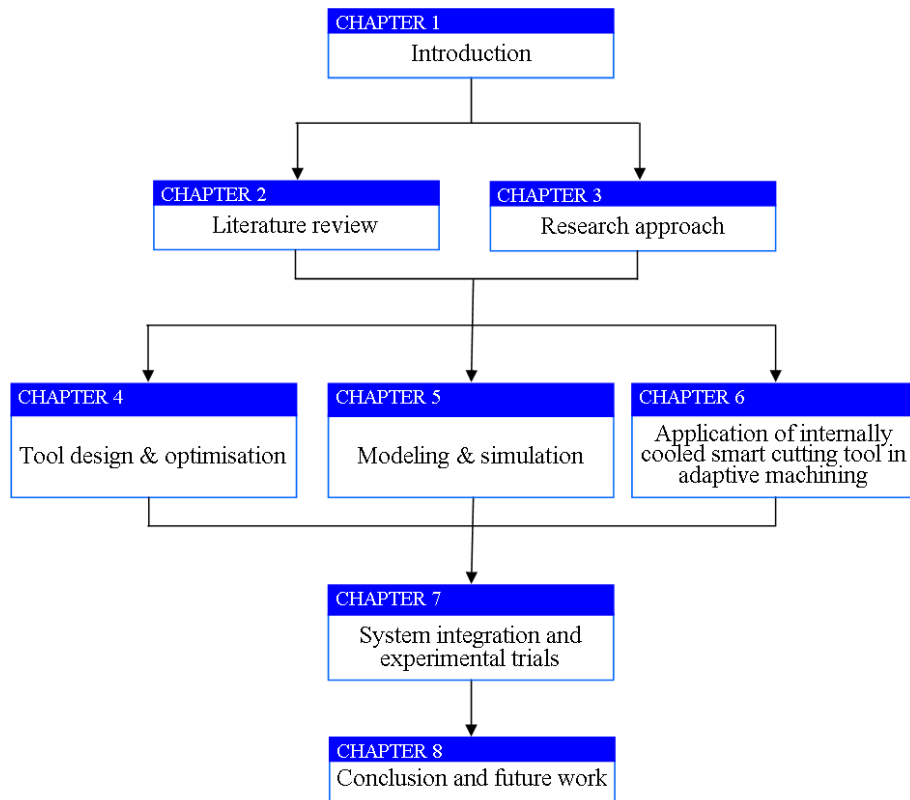
Fig. 1-7: The structure of the thesis

Chapter 1 defines the overall importance of the internally cooled smart cutting tool in improving machining performance and extending cutting tool life in green manufacturing. The background in the advancement of cutting tool technology, adaptive machining, process modeling are also presented.

Chapter 2 describes the review and critiques carried out on the specific subjects to answer the above documented questions. The review can be classified into state of the arts and the challenges in green manufacturing, the advancement in smart cutting tool especially in internally cooled cutting tool and the numerical analysis and simulation approaches for tool performance in green manufacturing environment. The critiques are performed to find the research gap and the technological demands to implement internally cooled smart cutting tools in adaptive machining of green manufacturing.

Chapter 3 describes the research formulation and explanation on experimental facilities.

Chapter 4 and 5 will answer questions number (1) to (6). In chapter 4, the concept of internal cooling techniques will be discussed, the inclusion in the cutting tool, structural and thermal analysis and optimisation. Chapter 5 is dedicated to develop and test the structural, computational fluid dynamics (CFD), heat transfer and tool life models of internally cooled cutting tool in turning operation. The modeling will be supported by empirical results as the models are machining condition specific related.

Chapter 6 describes the development of adaptive control program and CNC-PC interface. The published adaptive control algorithms will be scrutinised and the application suitability with the internally cooled smart cutting tools will be accessed. The questions number (8) and (9) will be answered in this chapter.

Chapter 7 discusses the procedures taken in system integration and the presentation of the results of the cutting trials. The machining trials have been designed to test the performance of internally cooled smart cutting tools in machining different types of work materials, ranging from ductile material, aluminium alloys up to hard to cut materials like steel. Common material for aeronautical components like titanium will also be machined. At the end of the chapter the analysis on the temperature difference between the inlet and outlet temperature will be discussed.

Chapter 8 concludes the work and all the questions predefined in this research are assessed. The contributions of the research will also be highlighted. The thesis is ended with the proposal for future works.

Chapter 2:   **Literature Review**

2.1.   **Introduction**

A thorough and systematic assessment is undertaken so as to recognize the works that have been carried out on the subjects of application of internally cooled smart cutting tool and adaptive machining in green manufacturing. This is to critically review the theoretical background and the state of the art of the research field. It comprises of the review on the state of the art of dry machining (DM) and near dry machining (NDM) as the core working principles of green machining and the common challenges faced in the working environment.

Publications on smart cutting tools as to improving the machining process and adaptive machining as smart cognitive approach to control the machining process variables are then scrutinised in details as benchmark for the design process.

The strategies for designing and implementing internally cooled smart cutting tools to adaptive machining are illustrated in the framework as shown in Fig. 2-1. The framework for the design of internally cooled cutting tools requires a brief revision on the available design techniques such as "total design" and "concurrent engineering".
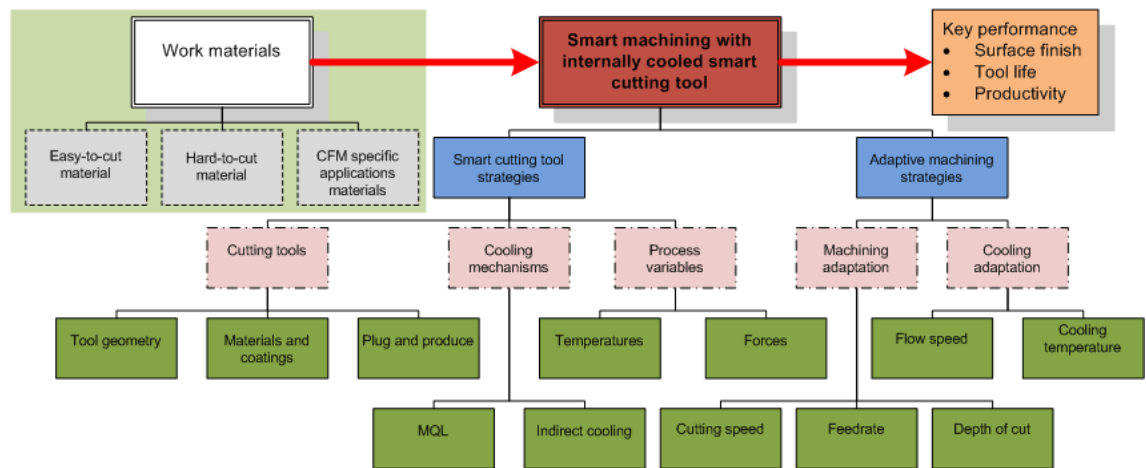
Fig. 2-1: Strategies for implementation of internally cooled smart cutting tools in adaptive machining

2.2.   **Environmental conscious machining**

Green manufacturing has been shifting from a cleaner machining alternative to the highly desired ecological machining practice over the past decade (Weinert et al., 2004; Helu et al., 2012; Shokrani et al., 2012). The increasing sensitivity to environmental and health issues is reflected in the increasingly stringent legislation and national and international standards. Soares (Soares, 1999) mentioned that ISO14000 series of standards have been established with the aim to help industries to manage better the impact of their activities on the environment.

The importance of green manufacturing does not only concern European Union (EU) countries and United States of America (US) but also influences other parts of the world. Quazi et al. (2001) in their discussion on the motivation factors for an organisation in Singapore to adopt environmental management system ISO14000 standards have identified eight main possible factors of the shifting towards ecological favourable ECMP; (i) cost savings, (ii) gaining competitive advantages, (iii) meeting environmental regulation, (iv) meeting customer

expectations, (v) top management concern, (vi) concern over trade barriers, (vii) following head office environmental practice, and (viii) employee welfare.

However, there are also manufacturers particularly in aerospace, automotive, medical and food and beverage industries that are compelled to practice a more stringent control of green manufacturing, i.e. CFM due to the tight regulations imposed on the manufacturing process and consumption of their products or due to the nature of the work materials that prohibits the materials to be machined with metal working fluid (MWF) (International Agency Quality Group, 2007; Salahshoor et al., 2011).

2.2.1. Current research in environmentally conscious machining

Conventional machining processes are not clean, may contaminate the machined parts and can cause pollution (Byrne and Scholta, 1993; Weinert et al., 2004). The use of coolant in machining operation especially in metal cutting comes with a stigma that suggests the resulting aerosolised coolant is harmful to the user and the environment. Much investment has been made to spare machine operators from inhalation of potentially dangerous chemicals found in some MWFs. The most common ailments are reported as dermatitis and hypersensitive pneumonitis (Zachaisen et al., 2011). Adequate protection and extraction systems are now common place to enforce the specified maximum allowance of airborne particles generated by direct, external flood cooling of metal cutting. A figure which stands at 0.4 mg/m^3 has been outlined by NIOSH (National Institute for Occupational Safety and Health, 1998). There is also the cost to the environment to consider. The industrial use of MWF is suggested to produce 400,000 m^3 of waste fluids in the UK annually (Dept. of Trade and Industry, 2000). The amount of waste water produced as a direct result of metal working fluids in the US is reported to be 3.8 to 7.6 million m^3 annually.

The treatment of used-MWF is cost intensive; and with modern coolants and lubrications containing biological components; extra processing procedures are required to fully treat the fluids. Falkinham III has warned in his publication (Falkinham III, 2002) that harmful bacteria (mycobacteria) can be present in MWF even in the presence of disinfectants and bactericides.

The restrictions in dousing of MWFs resulting manufacturing researchers and engineers to take new technical challenges to develop new and alternative technologies which then lead to green manufacturing (Klocke et al., 1997). Byrne and Scholta (Byrne and Scholta, 1993) in their publication about the strategic approach in environmentally clean machining process have outlined several strategies for green manufacturing and one major factor that has been discussed is through the efficient management of cutting and cleaning fluids. Currently researches in green manufacturing are focused in developing two machining strategies:

    (1) dry machining (DM)

    (2) near dry machining (NDM).

The two strategies are driven by the researches conducted worldwide to enable high machining performance of green manufacturing. The current key researches in green manufacturing are summarised in Fig. 2-2. The survey papers have been collected and analysed based on the tooling, the contributions towards understanding of the physics and mechanisms of the dry machining, workpiece materials, numerical modeling and simulations and the application of the smart and sustainable machining.

Research area	Research description	Researcher
Tooling	Tool geometry Tool materials Coatings Cooling	Mills, 1996 Kustas et. al., 1997 Weinert et. al., 2004 Sreejith, Ngoi, 2000
Understanding of the physics and mechanisms	Cutting forces Cutting temperatures Surface finish Tool life/ wear rates	Lahres, Jörgensen 1997 Gekonde, Subramanian, 2002 Nouari et. al. 2003 Kremer, El Mansouri, 2011
Materials	Explosive Hard-to-cut Bio-medical applications Composites	Weinert, König, 1993 Klocke, Eisenblätter, 1997 Salahshoor, Guo 2011 Shokrani et. al., 2012
Numerical modelling and simulations	Process modelling Tool-life/ wear rates modelling FEM simulation MD modelling	Grzesik, 2008 Marksberry, Jawahir, 2008 Bahi et. al., 2012
Smart and sustainable manufacturing	Smart manufacturing Smart machining system Smart tooling Sustainable manufacturing	Davis et al., 2012 Deshayes et al., 2006 Pandey et al., 2013 Byrne, Scholta, 1993

Fig. 2-2: Green manufacturing/ environmentally conscious machining key research areas

The parameters used in selecting the key papers are:

(1) the impact factor of the academic journals where the papers are published such as Wear, CIRP Annals- Manufacturing Technology or International Journal of Machine Tools and Manufacture.

(2) The papers' relevance to the research in sustainable or smart manufacturing

(3) The contribution and achievement of the researchers based on the published results in the selected papers or subsequent papers from the same research groups.

It is worth to mention here that there are several other papers that have been reviewed but not presented here due to similar or collaborated works with other institution such as the publication from Bermingham et al. (2011). The group from Bath University has done an outstanding job in the research of sustainable engineering particularly using cryogenic cooling.

2.2.2. Fundamentals of machining operations

Understanding the fundamentals of machining is an essential prerequisite in developing a suitable machining setup for applying internally cooled smart cutting tool in green manufacturing environment. Generally, the performance of a machining process is quantifiable by investigating the fundamentals mechanics and dynamics of the machining process such as chip morphology, wear mechanisms, the quality of machined component and the tool life.

Literature review has determined that the machining performance is influenced by several factors include tool geometry (nose radius, tool angles and chip breaker), cutting speed, feedrate, depth of cut, work material characteristics and hardness, unstable BUE, and the stability of the machine tool. The stability of the machine tool can be analysed by using modal analysis (Zaghbani et al., 2009). The tribological phenomenon at the contact interface between the cutting tool and generated metal chips plays great influence in controlling the chip formation, surface finish, tool wear mechanisms and wear rate (Gekonde and Subramaniam, 2001). The analysis of the tribological effects on tool performance and cutting process requires knowledge of cutting forces and cutting temperatures. Accurate measurement of these process variables is helpful in optimising tool design and improving machining performance. The forces measurement is used in:

(i)   prediction of machining power requirements,

(ii)   quantitative analysis of the stresses experienced by the cutting tool and

(iii)   indicating the level of rigidness and vibration of machine tool elements, tool holders and other fixtures (Wright et al., 1978; Trent et al., 2000; Gekonde and Subramaniam, 2001).

Dynamometers, devices used to measure the force, have been developed in the last hundreds years and ever since continuously improved in term of measurement accuracy and practicality in machining environment. Temperature, besides stress, is critical in influencing the life of the cutting tools (Trent et al., 2000). As reported by Davies et al. (2007), temperature in machining (both maximum and average) provides important information in machining performance improvement and cutting tools design. By measuring the temperature in machining, (i) surface finish quality can be improved, (ii) tool life span can be predicted and (iii) reliable modeling algorithms of

machining can be developed. Several attempts have been made to determine reliable cutting temperature but none has as yet been selected as standard (Tay, 1993; Bacci da Silva et al., 1999; Abukhshim et al., 2006).
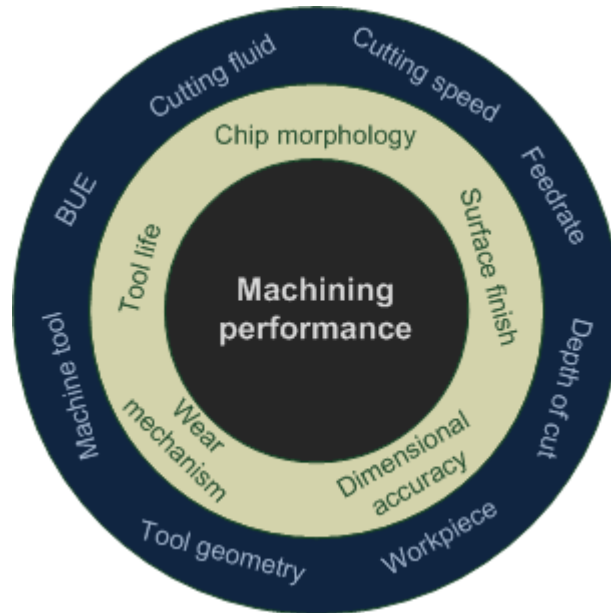
Fig. 2-3: Characterising machining performance and its influential factors

Hitherto, myriad of studies have been carried out to elucidate the effects of machining parameters on the quality of the finished surface, the tool life, wear mechanisms and chip formation (Davies et al., 1996; Young, 2000; Risbood et al., 2003). Yousefi and Icheda (2000) in their ultra HSM of aluminium alloy with standard P20 carbide insert concluded that in general, the surface roughness tends to reduce with the increase in cutting speed. However, between the cutting speed of 100 to 200 m/s the growth of welded of aluminium on the cutting tip causes an increase in surface roughness.

The cutting forces decrease with the increase in cutting speed due to thermal softening of the workpiece material (Gente et al., 2001). It is reported in several cases where the cutting force reaches its minimum when the cutting speed is

increased but increases again when the cutting speed is further increased (Fang et al., 2009).

2.2.3. Work materials

Research in ECMP has cut a wide variety of workpiece materials ranging from easy-to-cut aluminium alloys (List et al., 2005) to difficult-to-cut hardened steel (Lalwani et al., 2008) and advanced aerospace materials (Abdel-Aal et al., 2009). Work materials affect the tooling performance in a direct way and selection of proper work materials is largely dependent on applications, i.e. components and products. Different industrial sectors require specific materials, such as stainless steel and titanium alloys for medical devices, aluminium alloys for aerospace, magnesium alloys and composited for automotive, hardened steel for moulds and silicon for electronics. However, the cutting performance or machinability characteristics of these materials vary widely due to respective mechanical, physical and chemical attributes. There are many materials especially free machining materials that are easily machined in ECMP. Free machining materials are materials like steel which have additives to increase the materials' machinability at the expense of its ductility.

Titanium and superalloys are common material in aerospace and aeronautical industry. They are extremely difficult to machine materials except at low cutting speeds because machining of them accelerating the tool wear. The slow rate in machining these materials exacerbates the machining cost because it is common practice to remove over 90% of the blank material in the process of fabricating a single component.

The availability of common materials to be cut in different machining operations in ECMP are consolidated in Table 2-1.

Table 2-1: The application of ECMP in different machining process with different work materials (Klocke et al., 1997)

Process	Material				
	Aluminium		Steel		Cast iron
	Cast alloys	Wrought alloy	High alloyed bearing steel	Free cutting, quenched and tempered steel	GG20–GG70
Drilling	MQL	MQL	MQL	MQL/DRY	MQL/DRY
Reaming	MQL	MQL	MQL	MQL	MQL
Tapping	MQL	MQL	MQL	MQL	MQL
Thread forming	MQL	MQL	MQL	MQL	MQL
Deep hole drilling	MQL	MQL		MQL	MQL
Milling	MQL/DRY	MQL	DRY	DRY	DRY
Turning	MQL/DRY	MQL/DRY	DRY	DRY	DRY
Gear milling			DRY	DRY	DRY
Sawing	MQL	MQL	MQL	MQL	MQL
Broaching			MQL	DRY	DRY

2.2.4. Smart machining

There has been a consistent endeavour for continuous improvement in the machine tools and the machining process to respond to the requirements for better quality and higher precision products at lower costs. Deshayes et al. (2005) from National Institute of Standards and Technology (NIST) has presented the application of Smart Machining Systems (SMS) in machining operation to produce the first and every product correct, to improve the response of the production system to changes in demand, to realise rapid manufacturing and to provide data on an as-needed-basis with two-fold aims; to improve the performance of production systems and reduce production costs. Smart machining should provide the following capabilities (Deshayes et al., 2005; Jerard et al., 2009 and Davis et al., 2012):

(1) Self recognition and communication of their capabilities to other parts of

the manufacturing operation

(2) Self monitoring and optimising the operations

(3) Self assessing the quality of their work

(4) Self learning and performance improvement over functional period

For a successful implementation of environmentally conscious machining, selections of optimum cutting parameters and cooling technique for a given cutting tool, workpiece material and machine tool are vitally important. In order to decrease environmental and health hazards, change from wet flooding cutting to dry/ near-dry cutting is highly recommended (Weinert et al., 2004). Despite the proposal of various innovative techniques to replace the wet flood cooling such as minimum quantity lubrication (MQL), internal cooling and self-lubrication coatings the machining principle is still dependent on basic mechanics and dynamics of chip formation. It is, therefore, quintessential for the development of an effective internally cooled cutting tool to understand the factors which influence the generation of heat, the flow of heat, and the distribution of temperature in the cutting tool, work-piece and chip especially around the cutting edge.

Adaptive machining provides an automatic control to improve tool life, productivity or the quality of the surface finish. Depending on the machining requirements, certain technique will be applied to achieve the objective. In aerospace industry for example, the accuracy of surface integrity and residual stresses are the major requirements since any discrepancies to the ever stringent specifications of the aeronautic parts might cause the components damage sooner than the life cycle or fail their functionality (Frankel et al., 2012). For automotive industry, improvement in effective tool life while dry machining aluminium, steel and magnesium can contribute significantly to the production cost (Dasch et al., 2009; Marksberry et al., 2008; Weinert et al., 2004). In small and medium industries (SMEs), prediction of the tool life and on-line monitoring of the process variables are too detrimental to the operational cost

and the quality control of the production is rather loose due to the lack of investment in the business which led to limited resources (human power, time, money, scale) available (Bititci et al., 2012). For SMEs the challenge to achieve the production target has always become the priority and thus it is convenient if the productivity can be controlled at the maximum rate.

The application of adaptive control in manufacturing is commonly for improving the machining performance of computer numerical controlled (CNC) machine tools (Koren, 1988; D'Errico, 1997; Risbood et al., 2003; Cus, 2008). Inarguably the advent of CNC machine tools has enabled the machining operation to be less dependent on the manual skills of machine operators. Despite the advancement, the machining parameters, such as cutting speed, feedrate and depth of cut, must still be prescribed based on part programmer's experience and knowledge. It often occurs that the cutting parameters are programmed with conservative values, which are not as high as they possibly could be, in order to reduce the risk of tool failure. The reason of selection of non high productive values may also possibly due to the lack of complete knowledge of the part programmer about the complex thermo-physical process of machining.

Literature reviews outlined three main techniques in the application of adaptive control in machining. Adaptive control constraints (ACC) and geometric adaptive control (GAC) are the most common two techniques of adaptive control applied for roughing and finishing operation respectively. ACC manipulates the machine parameters, such as feedrate or speed, in real time to control the operating point, which is normally fed to the adaptive system by a sensor, to be on the constraints throughout the whole process. In GAC, the quality of the surface finished is controlled in real time by compensating for the errors caused by tool deflection and wear. ACO (adaptive control optimisation)

represents techniques with adaptation strategy to extremise the key performance index of the machining economic function by means of automatic control of the machining parameters within the bound of system and process constraints.

The application objectives of these techniques depend on the requirement, facilitated systems, availability sensors and operational type of the manufacturing. Typically ACC helps manufacturing to achieve the objective to improve the productivity by increasing the material removal rate (MRR) in rough machining operation. Depending on the workpiece material and geometrical complexity of the product, the improvement in production rate can be as high as 80% by implementing ACC in comparison to conventional CNC cutting (Koren, 1988). GAC is applied to achieve objectives of:

(1) achieving required dimensional accuracy and

(2) maintaining consistent surface finish of a machined product.

The dimensional accuracy and surface finish are influenced directly from the generation of wears on the cutting tool particularly the flank wear and crater wear. These variables attenuate during machining but they cannot be measured in real time which makes it difficult to know the accurate actual workpiece dimension and the quality of surface finish. GAC approach uses the condition of tool as the criteria to determine the state of dimensional accuracy and surface quality. Obikawa and Shinozuka (Obikawa and Shinozuka, 2004) have reviewed two common tool conditions recognition techniques, i.e. threshold method and artificial neural networks. Threshold method is a robust classifier into two categories, i.e. safe or hazardous condition. Artificial intelligent techniques like artificial neural network (ANN) also have high ability of learning that they have been applied to the classifications of more complicated conditions. The application of ACO, as briefly mentioned before, is associated

with the objective of improving dominating performance indices in machining economics. In general, ACO deals with multiple machining variables to achieve a specific economic goal, for instance, automatic controlling of cutting force by means of manipulating spindle speed and feed rate to achieve high MRR without radically curtailing the tool life (Wang et al., 2012).

2.3.   **Smart cutting tools**

Development of a smart cutting tool is essential in realising smart machining in environmentally conscious machining as illustrated in Fig. 2-1. "Smartness" of a cutting tool has not been clearly defined and standardised as yet. Based on the review (Byrne and Scholta, 1993), this can be attained with the introduction of smartness into a cutting tool to satisfy the three main aspects of an ideal cutting tool, i.e. ecology, technology and economy, as shown in Fig. 2-4.
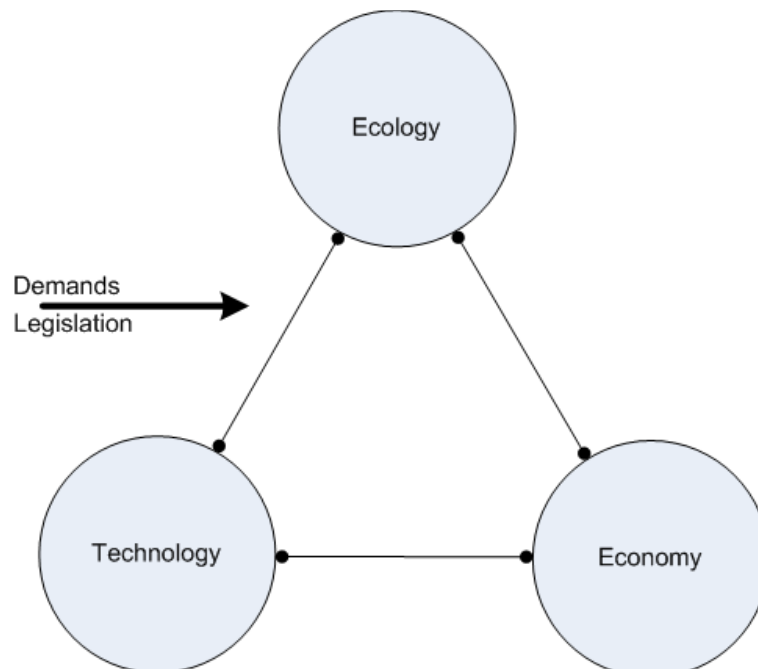
Fig. 2-4: The balance between economy, technology and ecology in realising ECMP (Byrne and Scholta, 1993)

Based on the key aspects proposed by Byrne and Scholta (Byrne and Scholta, 1993) as illustrated in Fig. 2-4 and the issues highlighted by Deshayes et al. (2005), there is a need for a smart cutting tools with the following features:

(1) Addressing the communication of all information needed to fabricate a product that satisfies customer needs.

(2) Accommodating sensor fusion that can increase the confidence in tool and process monitoring.

(3) Possessing the characteristics of plug and produce for easy re-configurability.

(4) Environmental friendly in terms of the application of the tools in machining.

2.3.1. Cutting tools technology

From the point of ECMP the challenges in machining with the absence of MWF demand for a new challenge on cutting tool technologies. It is essential that the roles of cutting fluids are addressed in the development of the tool for ECMP. Tool materials, coatings together with tool geometries are the most important factors determining effective tooling performance. The tool geometry, materials and coatings shall be suitable for high temperatures and thus high cutting speeds allow the machining operation with lower cutting forces (Byrne and Scholta, 1993). Byrne and Scholta (1993) added more that the application of intelligent sensors aids the automatic manufacturing by means of monitoring the physical parameters, assisting in data acquisition, communication and diagnostics. It is also a general consensus that machining downtime and machine setting up are cost that associates closely with green and agile

manufacturing. Thus, the new cutting tool for ECMP must possess a "plug and produce" capability (Wang et al., 2012).

Cutting tool materials for improving ECMP cutting tool

The materials chosen for cutting tool regardless for conventional machining or ECMP must possess a number of important properties to avoid excessive wear, fracture failure and high temperatures in cutting. Hardness (or also called hot hardness) at elevated temperature is the most important factor in choosing cutting materials, so that the hardness and strength of the cutting edge can be preserved at high temperature. Toughness, wear resistance, surface finish, chemical inertness and thermal conductivity are other major characteristics of the tool materials. The criteria of typical cutting tool materials were compared and documented by Childs (2000) and their applicable work materials are displayed in Table 2-2 and Table 2-3, respectively.

Table 2-2: Comparisons of different cutting tool materials (Childs, 2000)

	Hot hardness	Tough-ness	Wear resistance	Thermal shock resistance	Cutting speed	Surface finish	Material cost
High speed steel (HSS)	Low	High	Low	High	Low	Low	Low
Carbide	↓	↑	↓	↑	↓	↓	↓
Ceramic	↓	↑	↓	↑	↓	↓	↓
Carbon boron nitride (CBN)	↓	↑	↓	↑	↓	↓	↓
Diamond	High	Low	High	Low	High	High	High

Table 2-3: Common tool materials and their applicable work materials (Childs, 2000)

	Soft non-ferrous	Cast iron	Carbon and low alloy steels	Hardened steels	Nikcel-based alloys	Titanium alloys
HSS	√	X	O	X	X	X
Carbide	√	√	√	O	√	O
Ceramics	X	√	√	O	√	X
CBN	X	O	X	√	O	O
Diamond	√	X	X	X	X	√

(√: Good, O: Suitable, ×: to be avoided)

2.3.2. Cooling technique for the smart cutting tool

The cooling application in machining plays an important role in reducing the localised cutting temperature and many cutting operations cannot be carried out without the application of coolant (Bermingham et al., 2012). It is well recognised that the management of heat generation and the heat extraction in machining operation is vitally crucial in order to achieve extended tool life and component quality. Astakhov (2006) has reported that according to the first law of metal cutting by Makarow, the highest machinability is achievable when the cutting process is carried out at a critical machining temperature which is also known as optimal cutting temperature, θ_{opt}. At the θ_{opt} the highest ratio of the cutting material hardness to the workpiece material hardness is achieved. It is better to have better understanding in cutting temperature first before studying the effectiveness of cooling in machining.

Shaw (1984) has defined four important temperatures that involve in machining. The summary of the four main temperatures and their effects are displayed in Table 2-4. It is worth to mention that   the work ambient

temperature, θ_∞ is the ambient temperature in the machine tool and it should be duly noted that the ambient temperature does not necessarily be the same as the room temperature.

Table 2-4: Temperatures in machining

Temperature	Symbol	Effects
Shear plane temperature	θ_S	• Influence on flow stress to sustain materials' plastic deformation. • Major influence on tool face temperature (θ_T) and relief surface temperature (θ_R).
Tool face temperature	θ_T	• Influences crater wear development • Influences the size and stability of BUE
Relief surface temperature	θ_R	• Influences wear land development
Chip temperature	θ_C	• Most accessible temperature • Not greatly influenced by the cutting speed
Work ambient temperature	θ_∞	• Direct influence on θ_S, θ_T and θ_R.

The early works in defining cutting temperatures (i.e. before 1930) were mainly by measuring the mean temperature of tool-chip interface using tool-work dynamic thermocouple technique as reported by Shaw (1984) and recently by Davies et al. (2007). While this value may be adequate for some applications, it is generally not as useful as compared to temperature distributions. Numerous researchers have also started to associate the cutting temperature with temperature fields as it was observed that the onset of crater wears of the tool commonly developed along the tool rake face some distance away from the cutting edge which this point has been identified as the position of maximum

cutting temperature (Chao and Trigger, 1958; Usui et al., 1984). Due to practical limitations to obtain the maximum cutting tool temperature, some publications (Young, 1996; Korkut et al., 2007) proposed the use of chip-back temperature to represent the process temperature.

The cooling effect of cutting fluids allows the cutting tool to have extended tool life by maintaining the cutting temperature lower than thermal softening temperature of the cutting tool material and reducing the thermal induced wear such as diffusion, adhesion and oxidation.

Application of cryogenic cooling in machining process has received great recent interest due to the intrinsic environmental benefits it carries (Yildiz and Nalbant, 2008; Khan and Ahmed, 2008; Bermingham et al., 2011). Liquid nitrogen which is normally used as cryogenic coolant is safe, non toxic and evaporating to environment without leaving mess and residual on the machine tool and machined component has been used successfully by many researchers (Khan and Ahmed, 2008; Bermingham et al., 2012). However, several drawbacks have been identified in practical usage of the cooling technique, viz. (i) it requires constant coolant supply, (ii) ice build up around the cutting tool and tool holder, (iii) the fluid is not re-usable and (iv) it cannot be used for management of swarf size and swarf evacuation.

Minimum quantity lubrication (MQL) offers the manufacturers with greener and cost effective cooling alternative in comparison with wet flood cooling (Marksberry and Jawahir, 2008; Fratila, 2010; Shokrani et al., 2012). MQL also provides an alternative for machining process in which DM cannot be applied especially where the machining accuracy and high surface quality are of importance. It has been reported in some cases, the application of MQL can be more expensive because they require additional equipment which is normally

not equipped with the standard machine tool. In addition, the used lubricant either in mist or gaseous form is not reusable as they vaporise after application. This, on the other hand, the application of MQL can contribute to the reduction of total machining cost by eliminating the disposal cost and the cost associated with the maintenance and cleaning of the machine tool, work part and generated chips.

2.4.   Tool life and tool wear

Tool lifespan is parameterised by the amount of tool wear. It is disclosed in several publications (Young, 1996; Ay et al., 1998; D'Errico, 1998; Dimla Snr., 2000) that the progression of tool wear is closely associated with the consistently increase of machining temperature which at one critical point accelerates the wear formation.

Tool life can be generally defined as the usable period of time that has elapsed beginning from a point when a fresh tool starts cutting until before the onset of tool failure which causes the cutting tool failed to produce acceptable or desired workpieces (Axinte et al., 2001; ISO 3685:1993; Kwon et al., 2003). Literature survey shows that there is no standard method for measuring tool life. However, based on the literature review the determination methods of tool lifespan can be broadly categorised as follows:

(1) Progressive tool wear (Axinte et al., 2001; ISO 3685:1993; De Chiffre et al., 2000)

(2) Surface roughness (Kwon et al., 2003)

(3) Abrupt tool failure (Axinte et al., 2001)

(4) Predictions by theoretical or empirical modeling (Usui et al., 1984; Chungchoo et al., 2002)

Methods (1) to (3) require the variables to be directly measured during machining. On the other hand, method (4) is accomplished by predicting the tool life based on theoretical considerations (Meng et al., 2000), or by empirical modeling (Choudhury et al., 1999).

The first and second method employs the direct measurement of gradual growth of tool wear or increment in workpiece surface roughness as the criteria to determine the useful life of a cutting tool. International Organisation for Standardisation (ISO) has published standard in 1977 and a revised version in 1993 (ISO3685:1993) with the aim to unifying tool life testing procedures in turning operation by means of measuring wear on the tool faces. Although this method is independent of workpiece material and geometry, this method however, is practically less useful because it does not say much about the quantity of machinable product or the quality of the surface finish.

Abrupt tool failure such as chipping, fracture or deformation is the most obvious machining phenomena to terminate the useful tool life. This phenomenon however, as explained by Hastings and Oxley (1976), is only observed if incorrect or unsuitable cutting conditions are selected.

The major complications to utilise the above mentioned methods as standard procedure for determining tool life are mainly due to the fact that tool wear, surface roughness, tool fracture, cutting forces and cutting temperature are stochastic variables and their experimental spread can largely vary from one operation to another. It is also often observed that the same experiment when it is performed on two different machine tool yields different results (Axinte et al., 2001, De Chiffre et al., 2000).

Direct measurement of tool wear has been accepted as a norm in determining the tool life (ISO3685:1993). If a machining operation is performed with suitable and optimum cutting parameters, the wear produced will dominantly occur at flank and rake faces with other types of tool failure such as chipping, fracture, deformation etc. are almost negligible.

Fig. 2-5 shows two images of the wear regions; the left hand side depicts the locations of crater wear and flank wear while the divided zones of the flank wear, which are identified in ISO3685:1993 (1993), are displayed. Zone C is part of the cutting edge at the tool nose, zone N is the farthest quarter of the worn cutting edge length, b_w, and zone B is the quasi straight region in between zone C and zone N (Astakhov, 2004).
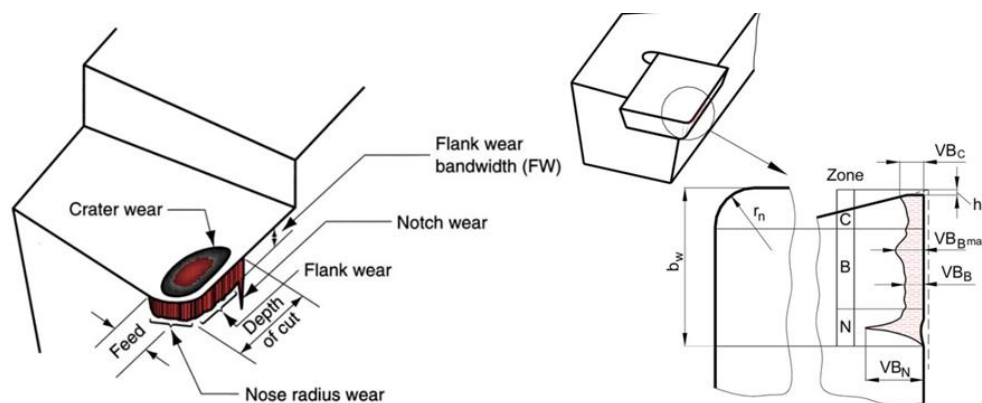
Fig. 2-5: Tool wear regions (Astakhov, 2004)

The criteria adopted for measuring tool wear of carbide tools are recommended as follows:

(a) The average width of the flank wear land, VB_B= 0.3 mm, if the flank wear land is considered to be regularly worn in zone B

(b) The maximum width of the flank wear land $VB_{B,max}$= 0.6 mm, if the flank wear land is not considered to be regularly worn in zone B.

Notch wear, VB$_N$= 1mm can also be used as a tool life criteria but the assessment of this variable is normally subjective and insufficient.
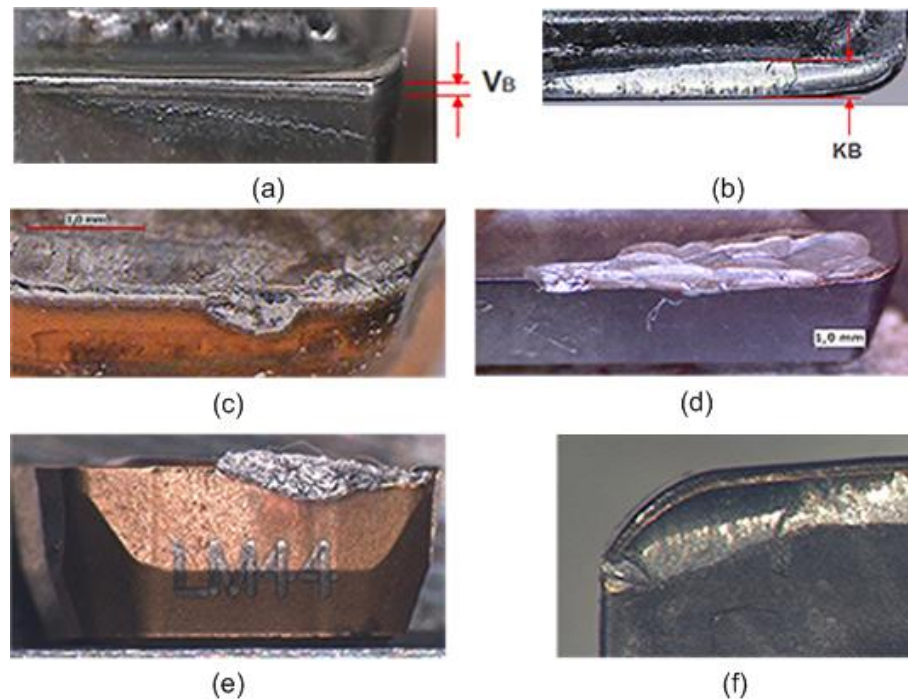
Fig. 2-6: Types of tool wear and tool failure; (a) flank wear, (b) crater wear, (c) chipping, (d) tool breakage, (e) BUE and (f) plastic deformation (Sandvik, 2012)

Wear mechanisms in normal cutting can be categorised into four main groups, which are oxidation, abrasion, adhesion and diffusion (Hastings and Oxley, 1976; Trent et al., 2000). As explained earlier, in normal cutting no abrupt tool failure should happen, and most of the wear processes will concentrate on the major flank side and rake face (Fig. 2-5). Fig. 2-7 shows the total wear curve which shows that all the wear mechanisms in normal cutting are temperature sensitive. At low cutting temperature (which is due to soft cutting or high cooling rate) only adhesive and abrasive processes are dominant. Meanwhile as the cutting temperature gets higher than a certain critical temperature thermal

induced wears, i.e. oxidation or diffusion are activated and dominate the total wear.
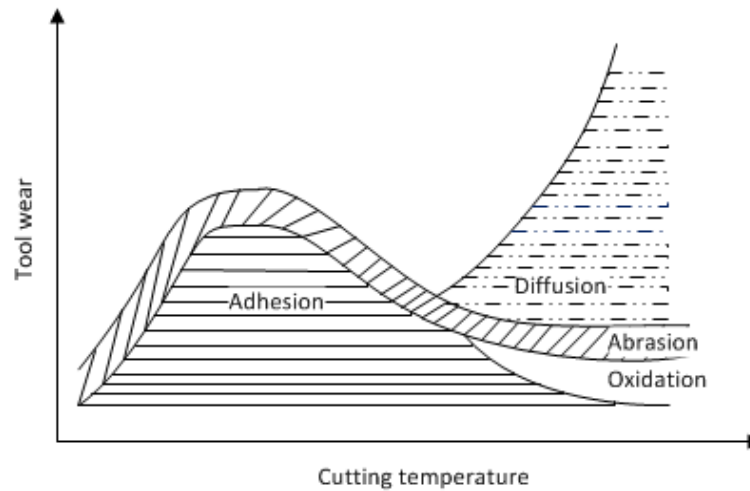
Fig. 2-7: Total wear mechanisms as function of cutting temperature (Hastings and Oxley, 1976)

Oxidation is thought to contribute to the wear of tungsten carbide cutting tools, particularly at the outer edges of the contact zones, where the temperatures are high and there is free atmospheric contact. The deep grooves observed on either side of the chip flow path on the rake face of some cutting tools, particularly straight tungsten carbide cobalt grades are believed to be the result of oxidation effects. A similar groove on the flank face at the end of the wear land remote from the tool nose is usually considered to be due to oxidation effects. Such a groove is also known to appear when machining materials with abrasive surface scale, or a material which severely work hardened. It has also been suggested in (Jacobson et al., 2001) and (Bin et al., 2007), that oxidation is responsible for a general weakening of the tool matrix and thus expediting the failure of the tool. However, a slight oxidation is helpful to minimise total tool wear. The generation of oxidation wear isolates the tool from the workpiece which in return reducing adhesion and diffusion.

Of the other three wear processes, i.e. abrasion, adhesion and diffusion, only the latter two are generally reported as being the causes of tool life termination. Although some researchers (Shaw, 1984) attribute tool wear to abrasion it is difficult to see how the abrasive process can responsibly contribute to the characteristic wear curve as mentioned previously.

Abrasion is essentially a process of micro-cutting which produces chips and leaves grooves. It is of interest that Trent (Trent et al., 2000) was unable to detect any significant signs of abrasive wear in an extensive metallurgical study of the wear process of carbide cutting tools when machining iron and steel. The classification of abrasive of metals is based on metal hardness-to-abrasive hardness ratio (H/H_A) (Pintaude et al., 2009). Earliest investigation of H/H_A has been carried out by Tabor (1954) and he pointed out that for one material to abrade another, the abrading material must be at least 20% harder than the abraded surface and there would be relatively few particles in the workpiece material exhibiting such characteristics.

Adhesion and diffusion mechanisms, both of which show a high degree of sensitivity to cutting temperatures are sufficient together to explain the characteristics shape of the tool wear of Fig. 2-7. In the low temperature range adhesion, a welded junction that is formed by the mechanism of friction and wear between metals at the contact surface is the principal factor controlling tool wear. Experimental studies (Hastings and Oxley, 1976; Kitagawa et al., 1997) show that the adhesive wear rate increases with the temperature increment until the amount of wear is maximum when the temperature is beyond a certain point for instance 600°C as reported by Hastings and Oxley (1976) and thereafter falling off rapidly with further increase in the temperature. As the adhesion wear mechanism tends to become less dominant in causing tool wear with the rising cutting temperature, the diffusion wear mechanism

becomes significant and increases rapidly with increases in temperature. Diffusion wear is a type of wear that is a result of atomic transfer at contact asperities (Nouari et al., 2003; Sutter et al., 2007). It is reported by Kitagawa et al. (1997) on works using carbide tools that at temperatures above $800°C$ diffusion becomes the dominant factor in tool life. Considering the dominant role of diffusion in determining the wear rate of cutting tools in the higher temperature range, and the exponential relationship between the diffusion rates and temperature it is not surprising that experiments have shown that tool life is highly dependent on the cutting temperature.

2.5.   **Numerical modeling and simulation**

The development of a new concept of cutting tool requires considerable investment of time and resources (Trent et al., 2000). The influence of process features such as tool geometry, cooling fluid and cutting parameters on the chip morphology, cutting temperatures, cutting forces, finished product dimensionality and cutting tool life need to be investigated systematically (Shaw, 1984; Trent et al., 2000). The direct experimental approach to study these influences is expensive and time consuming. Theoretical modeling and computer simulation of the cutting process can potentially reduce the number of design iterations and result in a substantial cost savings. CIRP working group (van Luttervelt et al., 1998) has identified the primary objective of modeling of machining operations as to develop a predictive capability for machining performance in order to facilitate effective planning of machining operations to achieve optimum productivity, quality and cost.

Heat and mass transfer in liquid flow in micro-channels has been an area of interest recently due to wide application of Micro-Electro-Mechanical Systems (MEMS). The ability to predict pressure drop and heat transfer characteristics for a given micro-channel geometry and operating conditions is of paramount importance to the design and performance assessment of a micro-channel heat sink.

Generally, the associated heat flux at the heat sources in a cutting tool is much higher than that in MEMS devices. However, the dimensions of the micro-duct in the concept of internally cooled cutting tools are of similar order to that found in typical MEMS devices. Thus, the studies available in literature related to the application in MEMS will assist in understanding the fluid flow behaviour and determining the associated pump power.

2.5.1. Thermal and fluid model

Based on the moving heat source method by Carslaw and Jaeger (1959), several analytical models of steady state temperatures in metal cutting have been presented (Trigger and Chao, 1951; Hahn, 1951; Loewen and Shaw, 1954). All these models assume that the bulk of deformation energy is converted into heat with most of the heat transferred to the deformed metal. In the case of rapid deformation process, heat generation can lead to high localised temperature since the heat has no time to be conducted away from the deformed metal, and the conditions become essentially adiabatic.
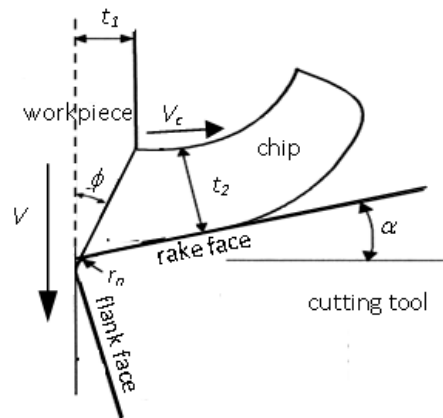
Fig. 2-8: Simplification of the orthogonal cutting mechanism

Simplest model of orthogonal cutting was developed by Trigger and Chao (1951) and from the model a relationship of cutting temperature, θ –speed, v can be derived:

$$\theta = Kv^m \qquad (2.1)$$

Where K is experimentally obtained and m depends on the materials combination of the tool and work-piece.

Contact area on the rake face, A_r, is usually ill defined due to the fact that there is no universal method to measure, calculate and predict the area of contact between the tool and the chip. The contact area is in most cases controlled by the length of contact, L (see Fig. 2-9). The length of contact, L is bigger than uncut chip thickness, t_1 or feed, f and it may be as high as ten times longer as t_1. In orthogonal cutting process, the width of the region of contact is usually about the same size of the depth of cut.

The generation of heat in secondary shear zone is a consequent of the deformation of the chip along the rake face to which sliding friction is added. A significant percentage of the friction energy generated at the tool-chip interface is transmitted to the tool until a thermal equilibrium of the tool is reached. In

this area two friction phenomena take place by dry machining. Up to a certain distance from the cutting edge the shear stress controls the adhesion of the chip to the cutting tool (denoted by L_1 in Fig. 2-9) and from that point the shear stress will decrease due to the reduction of slide friction (after Coulomb's law) until the point where the chip loses contact with the rake face of the tool (denoted by L_2 in Fig. 2-9). In some publications with regard to the three dimensional friction processes, some other form of frictions might occur in the transition zone between the two friction phenomena, L_1 and L_2. The friction coefficient of the tool-chip is dependent to machining entrance angle as well as the rake angle of the tool.

Between the tool flank face and finished work surface, a tertiary zone is defined by the elastic deformation and rubbing effect between the two surfaces. The frictional heat generated at the tertiary zone is more intense as the tool gets less sharp. The generated heat and consequent elevated temperature from this zone controls tool life, quality, tolerance and the integrity of the finished surface.
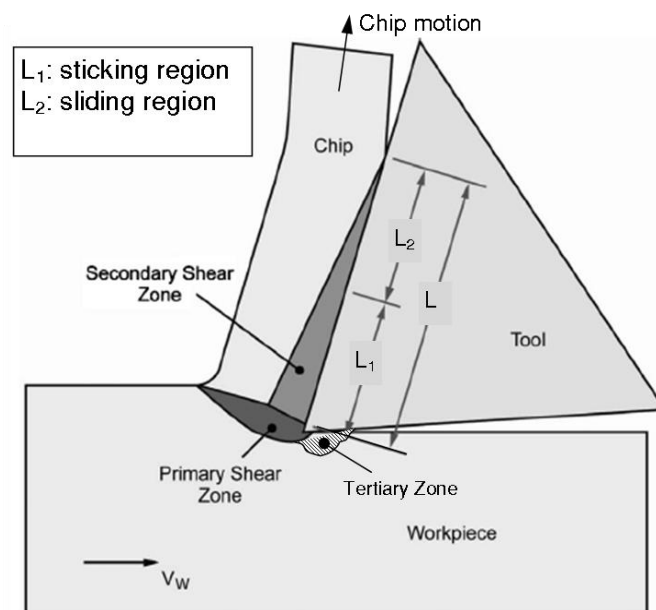
Fig. 2-9: Schematic illustration of heat generation during orthogonal machining

Due to vastness of this research area, this section presents specific literature overview of the application of internally cooled cutting tools in single phase force convection flow in micro- channel. It is worth mentioning, that the topics related to hydro-dynamic and thermal-dynamic developing flows have been excluded from this review and most of the literatures covered pertain to fully developed conditions.

Single phase flow

In single phase flows with channel diameters in the order of 10 - 100μm, Sharp and Adrian (2004) have indicated an early transition from laminar to turbulent flow and possible deviations of friction factors from conventional correlations. Reynolds number, Re and Darcy's friction factor, f_0 are two important non-dimensional parameters to represent fluid flow regime.

Re, which characterizes the effect of the inertial and viscous forces and is a significant indicator to the laminar to turbulent transition in fluid flow, is given as

$$Re = \frac{\rho V_{flow} D_h}{\mu} \tag{2.2}$$

where, ρ is the fluid density, V_{flow} is the fluid flow speed, D_h is the hydraulic diameter and μ is the fluid dynamic viscosity.

Darcy's friction factor, f_0 which relates the pressure loss due to frictional effect along the a specific length of a duct to the average velocity of the fluid flow , is given by,

$$f_0 = \frac{2D_h \Delta p}{\rho L_d V_{flow}^2} \tag{2.3}$$

In the above equation L_d represents the length of the duct meanwhile Δp represents the pressure drop in the system. Papautsky et al. (2001) compiled a comprehensive study of the results of microscale (for a pipe with internal diameter in the order of 10^{-6}) single phase internal flows and concluded a 60% reduction in f_0 compared to the macroscopic theory at the same Re.

The study also declared that no reliable data existed for the Re for laminar to turbulent transition as Re varies with the type of fluid used, shape and size of the pipe and the surface roughness. Moody (1944) has developed the well known Moody diagram to correlate f_0, surface roughness and Re for fully developed flow in a circular macro-scale pipe. Kandlikar and Grande (2003) proposed a modified Moody diagram to consider the effect of reduction in the cross-sectional area in micro-channels or pipes with significant relative values of surface roughness.

Nusselt number, Nu, a dimensionless parameter that indicates the ratio of convection to conduction of heat transfer across normal to a boundary, should be constant in a fully developed laminar flow in a micro-channel.

On the basis of the experiments, the following equations 2.4, 2.5, 2.6 and 2.7 were proposed for determining Nu.

$$Nu = Nu_{Gn}(1 + F) \tag{2.4}$$

where Nu_{GN} is calculated from the calculation proposed by Gnielinski in the function of Re, f and Prandtl Number, Pr:

$$Nu_{GN} = \frac{(f/8)(Re - 1000)Pr}{1 + 12.7(f/8)^{1/2}(Pr^{2/3} - 1)} \tag{2.5}$$

Here, f is Fanning friction factor and is given as:

$$f = (1.82 \log Re - 1.64)^{-2} \tag{2.6}$$

and F is the adopted factor to adjust Gnielinski correlation and it depends on Re, channel diameter, D_c and hydraulic diameter, D_h.

$$F = C \cdot Re(1 - (D_c/D_h)^2 \tag{2.7}$$

For the equation 2.7 the empirical constant, C is given as $7.6 \cdot 10^{-5}$.

2.5.2. Tool wear/ tool life model

Shaw (1984) has mentioned that predominance of wear mechanism is dependent on the machining conditions. This notion is justified by the number of attempts that have been made to develop methods for accurately predicting the effects of machining parameters on the tool life over the past decades (Marksberry et al., 2008; Axinte et al., 2001; Kwon et al., 2003).

A common approach for establishing the tool life models is based on the understanding that useful tool life is limited by the amount of wear occurring on the tool faces. A review on empirical and numerical tool life models are summarised in Table 2-5. Since the previous notion proposed by Shaw (1984) about the direct relationship of the tool life and cutting parameters, it can be seen that the trend in modeling the tool life has been to extend Taylor's basic tool life equation.

Table 2-5: Summary of empirical and theoretical tool life models for dry machining

No.	Tool-life/tool-wear equation	Constants determination	Reference
1	Taylor's basic equation: $T = \dfrac{C}{V^n}$	C and n are empirical values and currently available from many reference sources	Arsecularatne et al., 2006 Koren, 1977
2	Taylor's reference-speed based equation: $V/V_R = (T_R/T)^n$	n is determined from experiment and is available from many reference sources	Marksberry and Jawahir, 2008
3	Taylor's extended equation: $T = \dfrac{C_2}{V^p f^q a_p^r}$	All constants (C_2, p, q and r) are experimentally determined	Niebel et al., 1989
4	Temperature-based tool-life equation: $\theta T^n = C_3$	n is found between 0.01 and 0.1 and C_3 is experimentally determined	Oxley, 1989
5	Taylor's extended equation including cutting conditions and tool geometry: $C \propto [(\cot\beta - \tan\alpha)^n F(\alpha,\beta)^{1/\varepsilon}]^{-1}$	The influence of α and β can be theoretically determined as partial contribution to Taylor's constant C	Lau et al. 1980

6	Taylor's extended equation including cutting conditions and workpiece hardness: $T=C_4V^{n}f^{fm}d^{pr}q^{s}t^{iu}j^{x}$	Requires excessive tool-life testing to determine all constants (C_4, n, m, p, q, t, u and x)	Wang and Wysk, 1986
7	Taylor's extended equation including cutting conditions and workpiece hardness: $V=C_5/(T^{m}f^{y}d^{x}(\text{BHN}/200)^{n})$	All constants (C_5, m, y, x and n) are experimentally determined	Wang and Wysk, 1986 Zdeblick et al. 1981
8	Taylor's extended equation including chip groove effect factor and a tool coating effect factor: $T = T_R\,W_g\,(V_R/V)^{W_c(1/n)}$ where $W_c = n/n_c$ and $W_g = km/f^{n1}d^{n2}$	Constants (k, n_1, n_2 and n_c) are experimentally determined; m is the machining operation effect factor (with $m = 1$ considered for turning)	Jawahir et al., 1995

Some researchers have taken further step to predict the rate of certain wear mechanism in machining for a better control and thus, to allow a higher degree of improvement to the machining performance. The tool wear rate models that have been developed were claimed to be able to provide rich information about the wear growth rate for the wear mechanisms by knowing several process variables that have to be obtained from experiment or theories (Kwon et al., 2003; Bin et al., 2007). Takeyama and Murata's wear model (Takeyama and Murata, 1963), where dW/dt is the rate of tool wear, in consideration of abrasive wear and diffusive wear is formulated in following equation.

$$\frac{dW}{dt} = G(V,f) + D\exp\left(-E/RT_c\right)$$

(2.8)

where $(G, D = \text{constants})$

This model has been analysed by Mathew (1989) by using carbide tool in machining carbon steels and results validated that the diffusion equation can be used effectively to predict the rate of tool wear based on the average tool-chip interface temperature. Mathew (1989) expanded the explanation by mentioning that for cutting temperature higher than 800°C, the first abrasive term $G(V,f)$ can be neglected because above this temperature the wear rate is highly dominated by temperature-sensitive diffusion process.

It is generally accepted that for carbide tools under practical cutting conditions, the wear rate is dominated by a temperature-sensitive diffusion process, in particular at higher cutting speed (Mathew, 1989). Mathew (Mathew, 1989) analysed the tool wear of carbide tools when machining carbon steels and result has shown that although Takeyama and Murata's diffusion equation (equation 2.8) can be used effectively to compute the rate of tool wear based on average tool-chip interface temperature, the first abrasive term $G(V,f)$ can be neglected when the cutting temperature gets higher than 800°C.

2.5.3. Structural simulation

The cutting and feed forces in conventional machining operations have been an area of interest for researchers over the last century due to the importance of predicting the edge fracture, chipping and other mechanical tool-failure mechanisms due to the generated mechanical stresses. Mackerle (2003) has reported over 100 publications related to structural analysis of cutting tool have been published between 1976 and 1996 alone. Structural analysis of cutting tool can be performed with the aims

(i) to understand the effects of geometric, materials and process parameters to tool performance,

(ii) to compute residual stress in the tool during machining,

(iii) to study the effect of tool wear and failure, and

(iv) to optimise design parameters.

Among the numerical procedures, the finite-element methods (FEM) are the most frequently used. In applying finite element methods to metal cutting, two formulations, Lagrangian and Eulerian, are generally used. While the Lagrangian approach is usually applied to solid mechanics problems, the Eulerian formulation is used in problems where a control volume is involved like fluid mechanics (Shaw, 1984).

In the Lagrangian formulation, the nodes associated with the workpiece are fixed in space and the nodes associated with the tool are fed into it while a layer (chip) is removed from the workpiece. While this approach is well suited for transient analysis, it is not really suitable for steady state machining as small time steps are needed to ensure accuracy and the calculations have to be carried out over large intervals (Strenkowski, 2004).

In Eulerian formulations, the nodes associate with the cutting tool are evaluated as fixed in space while the work material and the presumed chip shape/ zone is treated as a fluid passing through a control volume. Since, the volume of the flowing chip is known (presumed), fewer elements are required for convergence and accuracy and to obtain steady solutions. While the computational load is greatly reduced if the Eulerian formulation is adopted, it requires an external predictive model to predict the dimensions of the flowing chip on the rake face (Stephenson, 2006).

Recently, an Arbitrary Lagrangian-Eulerian (ALE) method, applicable to problems of high strain rates and possessing characteristics of both solid and and fluid flow, has been applied to metal cutting (Olovsson et al.,1999; Movahhedy et al., 2000; Ceretti et al., 2007). The ALE formulation uses an algorithm which decides upon the motion of all degrees of freedom of the mesh for every time step of the analysis, such that the resulting mesh retains an optimal shape and condition with minimal increase in the computational load.

2.6.   **Design methodology**

High performance of green manufacturing requires optimum design considerations of machining parameters and cutting tool as the decisions made during design stage will significantly affect the machining performance (Yang, 2001). There should be a structured and holistic approach to balance between technology, economy and ecology aspects in fulfilling the demands and at the

same time meeting the legislation restrictions as proposed by Byrne and Scholta (1993).

The design methodology should encompass the assessment on the market/ user needs, the cost incurred, the technological availability up to the after sale support. Two design techniques have been looked into details; Pugh's total design and concurrent engineering. Both techniques offer systematic iterative approaches to simultaneously integrated design of a product or process and their related development procedures including manufacture, support and deployment strategies, which as a result encouraging for a more evolutionary approach to the design process.
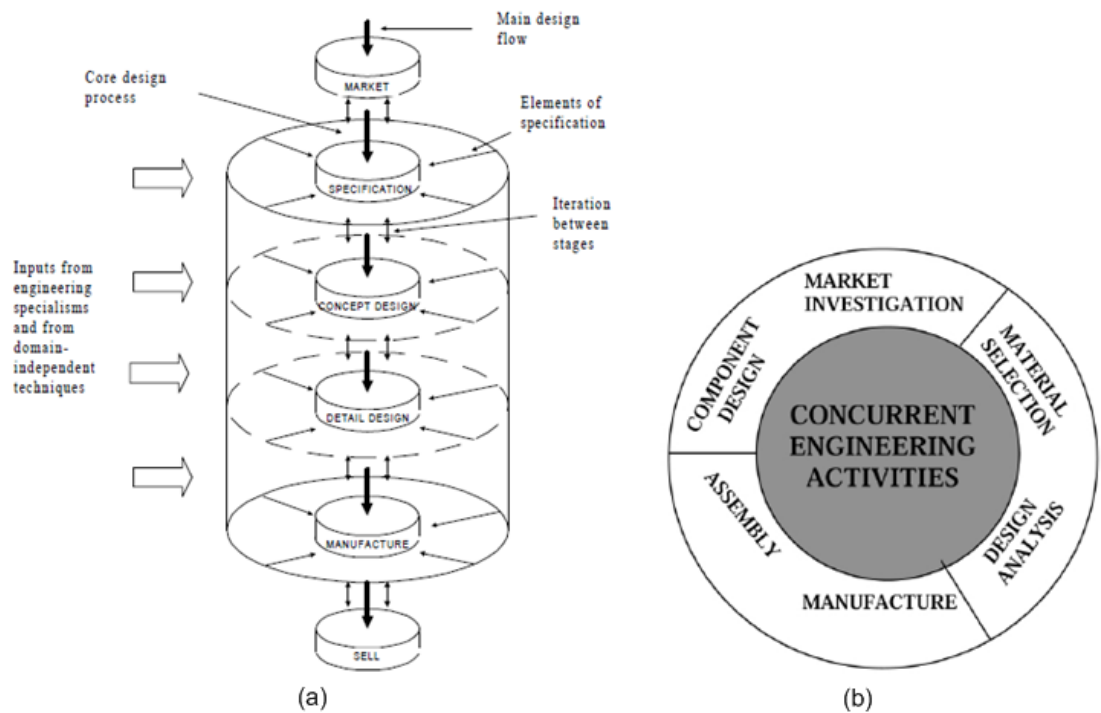
Fig. 2-10: Product development design, (a) Total design (Pugh and Clausing 1996) and (b) concurrent engineering (Prasad, 1996)

2.7.   **Conclusions**

Based on the critical literature review carried out, the following research gaps are identified:

- The design of an internally cooled cutting tool requires a methodological optimisation to enhance the machining performance by incorporating high performance internal cooling device, advanced coating materials and well accepted tool geometry in order for it to be used in the green manufacturing.

- A comprehensive model that synergises CFD-FEA plays a key role to allow the application of internally cooled smart cutting tool in the adaptive machining environment.

- The integration of internally cooled smart cutting tool in adaptive machining requires a holistic approach in selecting robust multiple sensors, high rate of DAQ system and stable communication interface.

Based on the identified research gaps, research approach in Chapter 3 is designed to fill the technological deficiencies and the contributions will be discussed in details in Chapter 4, 5, 6 and 7.

Chapter 3:   **Formulation   of   the   Research Approach**

In this chapter, the framework to achieve the objectives outlined in the research is formulated. This step holds an immense importance in this research since it contributes directly to the design, simulation, experiment, optimisation and implementation of internally cooled cutting tools in the adaptive controlled machining. As explained in the part "thesis structure", there are ten main questions that need to be answered in this research. In order to answer the ten questions, six work packages are formulated as shown in Fig. 3-1. The six work packages are:

    (1) reviewing of the related work,

    (2) holistic formulation of the research approach,

    (3) design and optimisation of the internally cooled smart cutting tool,

    (4) modeling and simulation of the structural, thermal, CFD and tool life of the cutting tool,

    (5) application of the internally cooled smart cutting tool in adaptive machining and,

    (6) system integration and experimental trials with different types of work materials.

The strategies and work carried out in each work package are designed with the aim of answering the questions and of achieving potential contributions in the research. The flow diagrams in Fig. 3-1 shows the work required to fulfil the strategies.
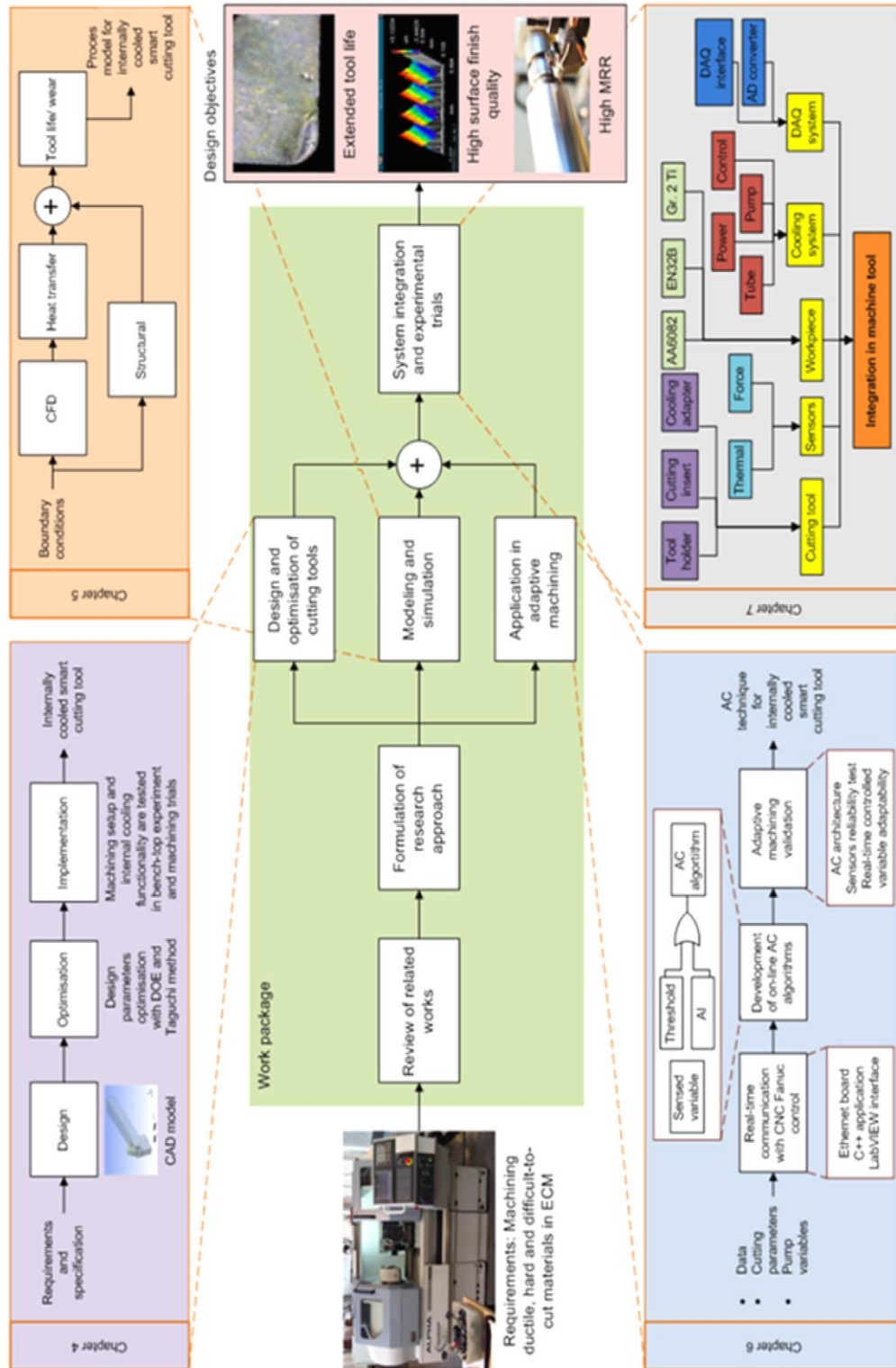
Fig. 3.1: Roadmap for the development of the internally cooled smart cutting tools with application to adaptive machining

It is widely accepted by manufacturing engineers that tool geometry, combination of workpiece-tool materials, machine tool, coolant application and process parameters are major factors in influencing machining performance. With consideration to include all these factors in designing internally cooled smart cutting tools in a scientific manner requires huge resources and almost impossible to be completed within the time frame of a Ph.D. research. Thus the major considerations have been set as the research platforms and can be summarised as follows:

(1) The cooling structure is designed on a basic commercially available tool.

(2) In order to model the tool in orthogonal cutting, single turning tool is selected.

(3) Tungsten carbide is chosen as the main cutting tool material due to the fact that it is cost effective, adequate hardness to accommodate internal structure and widely used in industry. However, in the preliminary studies high speed steel (HSS) tools are also used especially when the studies do not require for a specific material.

(4) The cutting trials of the internally cooled tools are performed on the CNC lathe machine.

(5) The effects of tool geometry, internal cooling liquid parameters, and machining parameters on internally cooled smart cutting tool behaviors need to be scientifically studied so a comprehensive model can be used for further development and optimisation.

3.1.   Numerical models development

In this section, the numerical models of machining are developed. The main purpose of developing numerical models is to enable the process of designing internally cooled cutting tools with minimal input from cutting trials. Among

the models covered are forces model, temperature model, tool life model, surface roughness model, CFD and heat transfer models and tool mechanical structure model.

Over the last several years, commercial packages (ABAQUS, DEFORM, and ADVANTEDGE) have enabled detailed calculations of machining mechanics and, to a limited extent, heat transfer. However, computational models can be complex to build and the software as well as the computation hardware can be expensive to purchase. For these reasons a simplified approach was used that was based on finite element (FE) modeling (Tay, 1993). The models were developed based on the steady state orthogonal machining and were simplified with certain degrees of assumptions which can potentially give not as accurate results as the transient computational simulation provided by the commercial packages. However, it has been proven that this approach suffices for engineering calculations, where the objective is to develop order-of-magnitude estimates of the cutting forces and the amount of heat transfer to the tool.

3.1.1. Structural analysis

Theories in the mechanical structure of materials, which address the assumptions regarding structural loads, geometry and material properties, are usually not valid near concentrated forces or moments, especially those located near a stress concentration zone (cracks, hole, corners etc.) (Hibbeler, 2008). The internally cooled cutting tool falls in this category due to the proximity of the micro-channel and bottle cap shape of the insert to the cutting and feed forces. Thus, analytical expressions available to calculate the maximum stresses due to a hole in a plate under tensile, torsion or bending cannot be applied (Young et al., 2002). However, an FE model (approximation solution at convergence) can

be used to obtain the stress distribution in an internally cooled cutting tool, but only physical testing can ultimately validate the results. The reader should not consider the stresses presented in this thesis as accurate to those obtained in the actual cutting process, as the FE models are based on simplified assumptions about force distributions in the metal-cutting process. It is also not practical to validate the mechanical FE result experimentally because the effects of temperature and chemical reaction could not be simply included in the model. Having said that, it can be concluded that the purpose of the FEA analyses is to compare design parameters trends, provide a reasonable starting point for feasibility testing, and give insight into what trends may exist in the actual process as parameters changed.

The main objective in the development of mechanical modeling is to use static three dimensional FEM models that can compute the mechanical loads on the conventional tool insert and internally cooled cutting tool insert. The assessment includes the mechanical effect on the cutting inserts particularly after the embedding of internal cooling features and as the basic platform for geometrical design optimisation.

In summary the procedure for mechanical analysis can be broken down as follows:

    (1) Design geometrical models of conventional cutting tool insert and internally cooled cutting tool insert.

    (2) Define and analyse the effects of mechanical load in actual machining

    (3) Define the boundary conditions for the FEM

    (4) Perform FEM on ANSYS Workbench.

3.1.2. Thermal analysis

Localised high temperature at the contact interface between the cutting tool and the sliding chip is difficult to be directly measured as the location is constantly obscured throughout the cutting. The thermal model of a machine tool should account for the heat exchange situations such as heat conduction, heat transfer across contact zones (tool-chip-workpiece-cooling mechanism), radiation, and convections (natural and forced). The models should preferably be applied in 3D, and the procedure is:

(1) Use finite elements method rather than finite volume method, since the modeling involves steady state mechanical, thermal and fluidic interaction. ANSYS Fluent will be used to solve the numerical simulation.

(2) The model calculates the temperature distribution as a function of heat generation

(3) Heat sources are introduced in the primary deformation zone, secondary deformation zone and along sliding frictional zone

(4) Location and shapes of these zones are determined from literature and model results

(5) Thermal, mechanical and fluidic properties of the materials and the boundary conditions are included in the model

3.1.3. CFD analysis

The main assumption in CFD analysis is that the flow is always in single phase since the temperature increase will never exceed the fluid saturation temperature. The flow regime of the internal cooling liquid influences the heat

transfer coefficient, pressure drop and flow pattern. However, flow pattern is not an issue for a single phase flow.

Pressure drop calculation will determine the size and energy of the pump. Characterising heat transfer coefficient either by manipulating the flow velocity and temperature at inlet or by increasing the contact area of water ensures that the cutting temperature can be optimally controlled.

3.1.4. Wear analysis

Machining without lubrication fluid is a stigma as there is a connotation that higher friction and a rapid temperature raise will encourage tool wear. Tool wear is an important factor to limit the tool life. Severe tool wear will influence the surface finish too. However, high cutting temperature is not necessarily bad for the tool.

As described by Hastings and Oxley (1976), the cutting temperature is exponentially proportional to the cutting speed. In the cutting trials performed by Loladze as reported in the same publication (Hastings and Oxley, 1976), the certain minimum regions of cutting wear detected in the middle range of cutting speeds tested. The results indicate that by determining the optimum cutting speed, optimum working temperature can be controlled and consequently the occurrence of tool wear can be reduced.
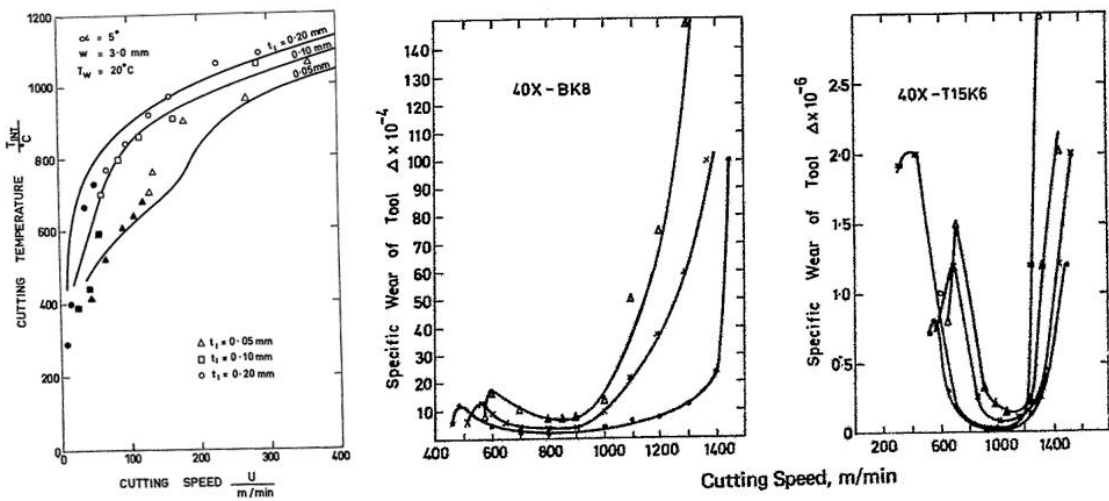
Fig. 3-2: Cutting temperature-cutting speed relationship and specific wear-cutting speed relationship (Hastings and Oxley, 1976)

Several correlations in predicting the tool life have been published. Most of them were derived and expanded from Taylor's equation and they require data from the experiment to fit the equation's constants. Despite extensive uses from the research community in expanding Taylor's equation, the equation addresses the relationship between the tool life and cutting parameters only. For the application of adaptive machining a more dynamic equation than this is required as the cutting parameters are expected to change throughout the cutting process. Wear rate equations from Usui et al. (1984) for example are interesting to be investigated as they can describe the wear mechanism and the rate of it happen at certain cutting parameter or cutting temperature.

At present, most of the tool-life/ wear models that have been published require experimental and empirical data such the one required in Taylor's tool life equation. An attempt to apply analytical model developed by Takeyama and Murata (1963) has been carried out by Attanasio et al. (2010), but the model needs to be solved with advanced Deform 3D FEM software. His result showed

good agreement between simulated and experimental outcome in machining AISI 1045 steel bars with ISO P40 carbide insert.

Other researchers such as Zhou et al. (1995) and Fu et. al. (2011) have investigated the possibilities of using artificial intelligent (AI) techniques to predict wear development. Application of artificial neural network (ANN) to characterise the tool wear, and clustering and analysing of the tool wear stage using fuzzy logic have been respectively studied by Zhou et al. (1995) and Fu et al. (2011).

3.2.   Cutting process simulation

The ultimate aim of the simulation of the cutting process is to optimise the geometrical design of internally cooled smart cutting tool with the minimum number of cutting trials.

With the boundary conditions obtained from the publications of earlier researcher and self-conducted experiments, the process parameters that intended to be studied are listed as structural analysis of the tool, temperature distribution on the rake face and inside the tool as well as the heat generated during machining.

The simulations are performed in ANSYS workbench environment. For this research, transient simulations are not required because the purpose of the simulations is not to model the whole machining process, and then validate the results of the simulation by experiments. Rather, the simulation has been used as a standard engineering tool to give guidance in specifying the internally cooled cutting tool geometry and machine settings in the experiments.

3.3.   **Design of an internally cooled cutting tool**

The actual work to design internally cooled cutting tools starts in this section. Three cooling approaches selected are manifold design, jet impingement cooling and open plan structure.

The designs have been modeled mainly on computer-aided design (CAD) software Pro/Engineer. However, during the design process other CAD environments like Solidworks and ANSYS Design Modeler have also been used due to several reasons like license restriction, simulation convenience, complex features optimisation etc. The exchange of CAD data from one environment to another gets easier nowadays owes to the advent of neutral data format such as Initial Graphics Exchange Specification (IGES) and Standard for the Exchange of Product model data (STEP).

The design approach needs to consider the following aspects:
  (1) Low thermal conductivity of tungsten carbide.
  (2) Trade-off between tools' mechanical and thermal properties.
  (3) Internal structure as close as possible to the cutting edge.
  (4) Big temperature difference between cutting zone and cooling fluid is required.
  (5) The minimum modification to the conventional machining tool.

The aspects written above have led the design to be analysed structurally and thermally. The development of the internally cooled cutting tool is simulation driven although the final development still requires the input from real cutting trials since the dynamic factors of machining can be simulated accurately. The

simulations are conducted on ANSYS workbench environment. The advanced feature in DesignXplorer of ANSYS workbench allows the designs to be optimised systematically by describing the relationship between the design variables (i.e. coolant type, cooling structure geometry, cooling temperatures, speed etc.) and tool performance (i.e. stresses, temperature distribution, heat removal rate etc). The design exploration uses Design of Experiment (DOE) together with Taguchi method to assist the optimisation judgment.

The simulation driven internally cooled cutting tool development is accomplished by the prototype built up and physical cutting trials as illustrated schematically in Fig. 3-3.
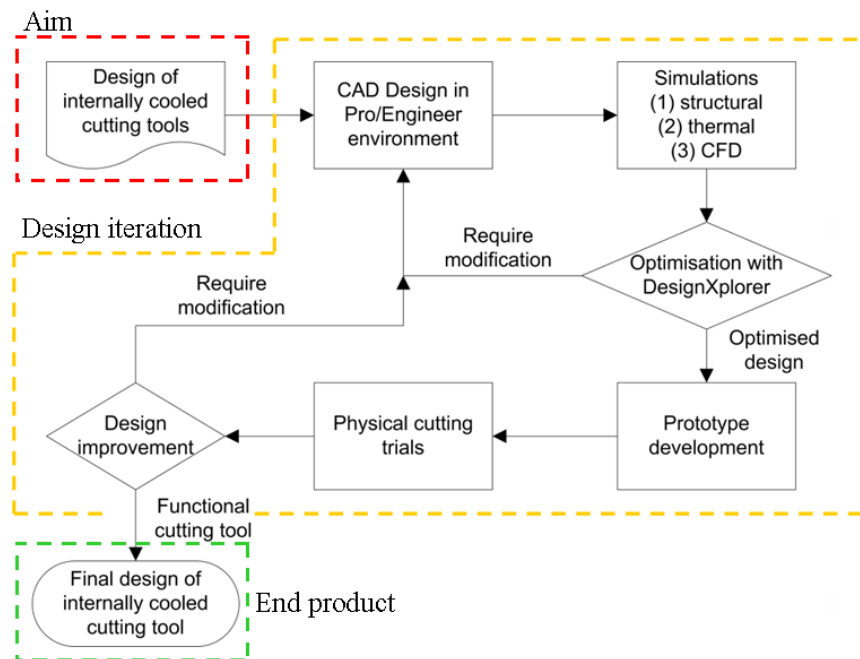
Fig. 3-3: Design process of internally cooled cutting tools

3.4.   **Preliminary cutting trials**

Two major observations are expected from the preliminary cutting trials. Firstly, the cutting trials will be used to validate the models of machining when internal cooling is introduced. Secondly, the cutting trials will also be used to further study the effect of internal cooling on machining performance, chips formation, process parameters (i.e. forces and temperature) and tool wear mechanisms.

Since the throughputs of both observations are the same, then they can share the same experimental setup. The experimental setup can be divided into internal lathe machine setup (confined with dashed line) and external lathe machine setup as illustrated in Fig. 3-4 .
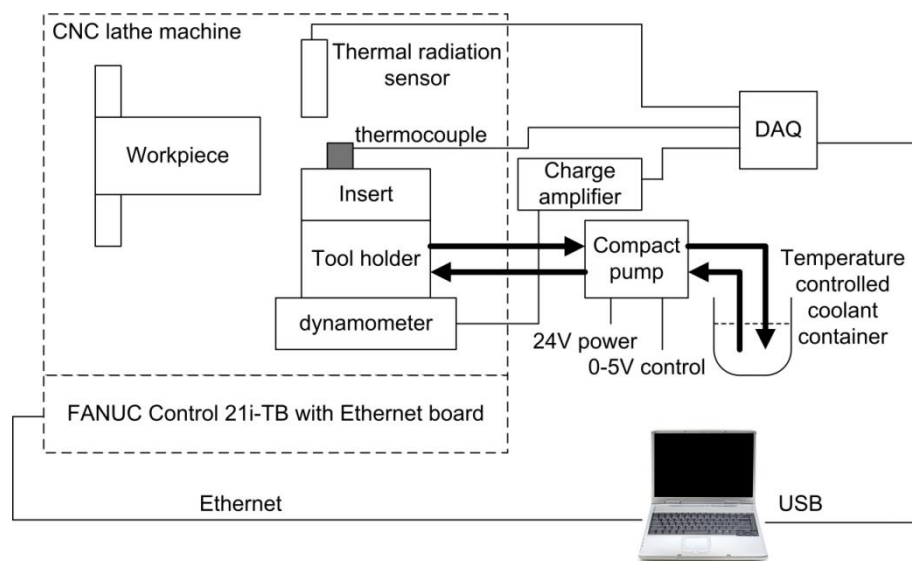
Fig. 3-4: Experimental setup

Internal lathe machine setup consists of cutting tool module (i.e. cutting inserts, tool holders, thermocouples and inlet and outlet tubes for internally cooled tools), workpiece with the support of tailstock and communication setup with CNC control. The model of the CNC lathe machine tool is Alpha Colchester

Harrison 600 Group with Fanuc Control model FANUC 21iTB. FANUC 21iTB allows the communication over the Ethernet version which is realized by the socket communication (TCP/IP communication) with FANUC Ethernet Board

Although tungsten carbide is chosen as the preferred tool material, but high speed steel (HSS) tool has also been tested in this research. However, the usage of the HSS tool was mainly at the preliminary stage to build the working prototype of internally cooled tool and to assess the effectivenss of the internal cooling concept. Based on the modeling built, the geometry of the tool insert to be used in this research is best when it is in its simplest shape as more features on the tool insert may mislead the benefits of the internal cooling. Therefore, the insert type selected is SNUN120408 (refer Appendix E). The cutting insert is in basic square prism shape (Fig. 3-5 (a)). It is attached to the tool holder by means of clamping and normally the insert and the tool holder require supporting plate in between of the two parts. This configuration, especially for the tool holder CSBNR 2525M12-4 is ideal for embedding internal cooling structure from the point of views of designing, prototyping and implementation at machine tool. As further shown in Fig. 3-5(b), for the internally cooled tools the cutting insert has been modified in bottle cap shape, supporting plate has been replaced with internal cooling adapter and two holes have been drilled in the tool holder for inlet- outlet coolant circulation.
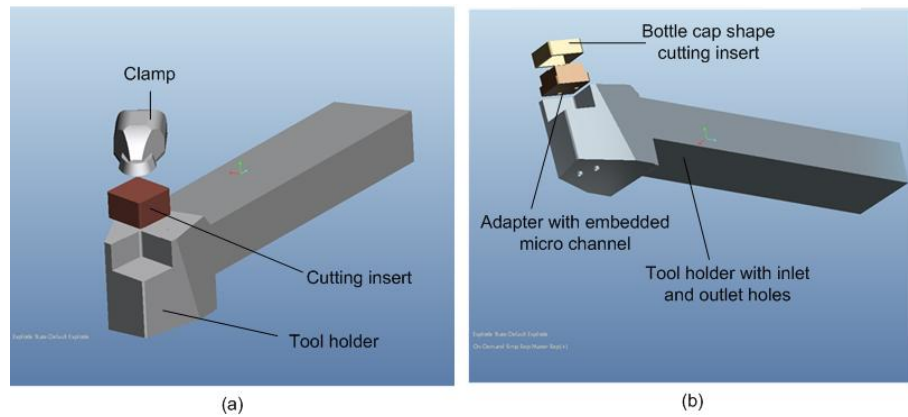
Fig. 3-5: Explosive views of (a) conventional cutting tool (b) internally cooled cutting tool

Most of the the fabrication and modification works of the components of the internally cooled tool module have been conducted with the available facilities in the workshop of School of Engineering and Design, Brunel University. The only part outsourced was for the machining of the cutting insert into bottle cap shape since the high residual stress created from the conventional machining may weaken the subsurface structure of the tool (as shown by a failed tool in Fig. 3-6(a)). The earlier attempt to electro discharge machine (EDM) the insert has failed due to the fact that the composition of the insert materials contains non-conductive material which does not effectively react with the electrode (Fig. 3-6 (b)). Therefore, more advanced technologies which can create complicated three dimensional features that made of a wide range of material groups without creating adverse effects are necessitated. A partner in the ConTemp Project consortium, C.F.K CNC-Fertigungstechnik Kriftel GmbH (CFK), who has a speciality in selective laser sintering (SLS) process can offer solution for the insert modification (Fig. 3-6 (c)).
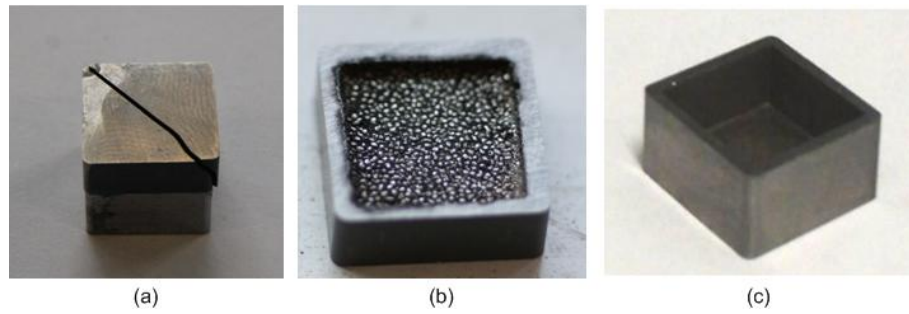
Fig. 3-6: Cutting inserts; (a) high residual stress causes tool breaks, (b) wrong electrode to EDM the WC insert and (c) optimal SLS fabricated bottle cap shape insert

The thermal sensors utilised in this study were a laser pyrometer and a thermal imaging infrared (IR) camera. The models of the two instruments can be referred in Appendix B.

The cooling adapters were fabricated on the 5-axis CNC machining centre Kern in the Advanced Machining and Enterprise Engineering, Brunel University lab (Fig. 3-7). The technical drawing and the CNC programming codes can be found in Appendix C and Appendix D respectively. The cooling adapters have been pre-fabricated using Polymethyl methacrylate (PMMA) to visibly ensure the accuracy of the machining. The working version of the cooling adapter is made of stainless steel due to the fact that stainless steel is poor thermal conductor metal with 16.26 W/m.K conductivity, k (see Table 3-1 for k of different metals) and the high stiffness of stainless steel can provide adequate support against chatter and high localized force.

Fig. 3-7: Machining the cooling adapter on 5-axis Kern machine

Table 3-1: Thermal conductivity, k of different metals (Matweb.com)

Metal	Thermal conductivity, k at 25°C / W/m·K
Aluminium	220
Carbon steel- 0.5%C	54
Copper	386
Stainless Steel	16.26
Titanium	15.6
Tungsten	180

An off-the-shelf tool holder (CSBNR 2525M 12-4, produced by Sandvik) was modified so that the inlet and outlet tubes for the internal-coolant could be attached on the bottom and side surfaces, respectively (Fig. 3-8). The 2mm diameter channels for the inlet and outlet have been machined accurately by the process of drilling and at the end of each channel and at each channel a thermocouple is attached to measure the entrance and exit coolant temperatures, T_{in} and T_{out}.
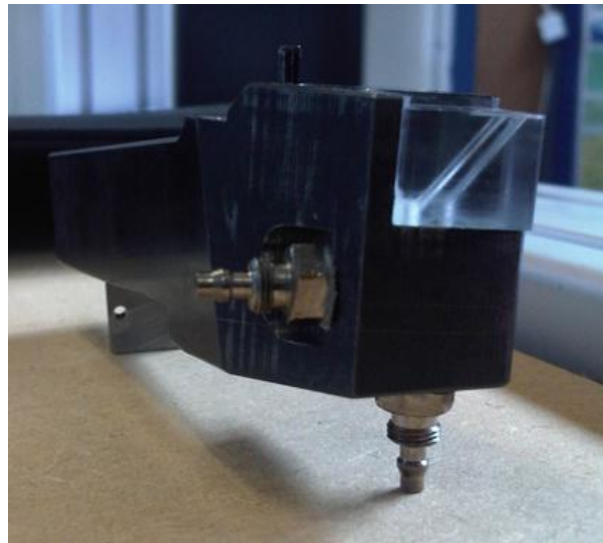
Fig. 3-8: A modified tool holder with a replica of plastic adapter

Beneath the tool holder, a 3D force measurement equipment, dynamometer from Kistler is used. To increase the sampling accuracy of data acquisition resources, only forces in the directions of cutting, F_c, and feed, F_t are acquired. The charge amplifier of the dynamometer needs to be set according to the calibration certificate (Appendix F) and the dynamometer once mounted in the machine tool needs to be calibrated using force gauge to determine the transfer function (Fig. 3-9).

Fig. 3-9: Calibrating the dynamometer using force gauge

The charge amplifier (Fig. 3-10) is securely located outside the machine tool and connected with the dynamometer via a metal -shielded cable. The voltage signal converted by the charge amplifier is sent to the monitoring signal on the PC via DAQ interface from National Instrument.

Fig. 3-10: Charge amplifier

The C-series DAQ interface model cDAQ 9172 (Fig. 3-11) can accommodate different modules. For this research two modules have been used; Voltage analogue I/O module NI9264 and CJC calibrated temperature module NI9123. NI9264 as marked with 1 in Fig. 3-11 has four BNC ports which increases the signal to noise ratio and the NI9123 as marked with label 2 can accommodate 16 wired thermocouples.
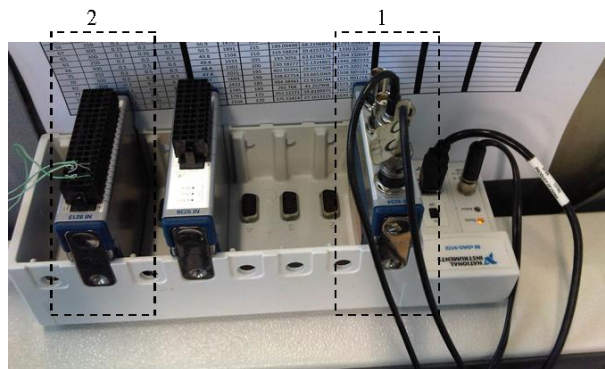
Fig. 3-11: DAQ interface

The DAQ interface is connected to developer environment software, LabView 10.0 on the PC via USB.

On the other hand, the peripheral system to circulate the cooling fluid in a closed-loop cooling circuit consists of a micro-pump, temperature controlled container and voltage supply units. The working principle of the micro diaphragm pump is based on reciprocating displacement technology (see Fig. 3-12). The twin heads pump motors are operated at 24V DC and can be controlled with 0-5V DC.

1   Exhaust valve
2   Inlet valve
3   Working chamber
4   Diaphragm
5   Eccentric
6   Connecting rod
7   Pump drive
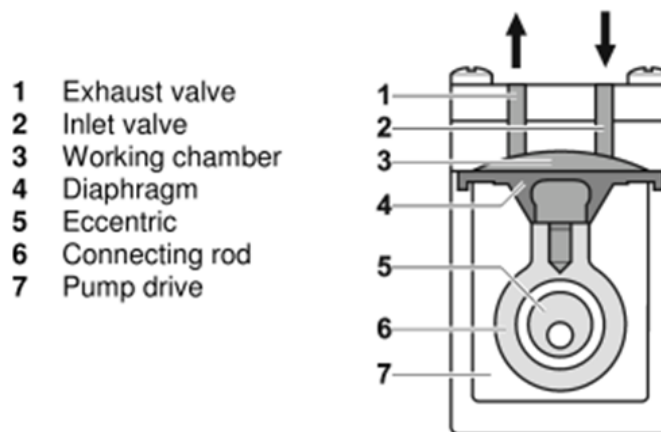
Fig. 3-12: Working principle of the micro-diaphragm pump

The cooling fluid is pumped through the tool from an insulated container and the temperature of the coolant is controlled by a chiller made by Thermo Cube (Fig. 3-13).

Fig. 3-13: Temperature setting on Thermo Cube

The first cutting trial was carried out with two folds objectives; (1) to test the functionality of the internally cooled cutting tool in the real machining environment and (2) to collect machining data for process modeling. For this experiment a TiN coated insert was used because it can improve sliding behaviour at the flank and rake face due to its low friction coefficient. Six temperature points are observed on the surface of the cutting inserts to map the temperature distributions on the surface of the insert. Five black spots were marked on the rake face of the insert so the pyrometer could be targeted to measure the point temperature. The position of the black spots from the cutting edge can be referred in Table 3-2. Temperatures at the inlet and outlet were also acquired during the machining. The cutting insert used and the identification of the 5 spots are displayed in Fig. 3-14.
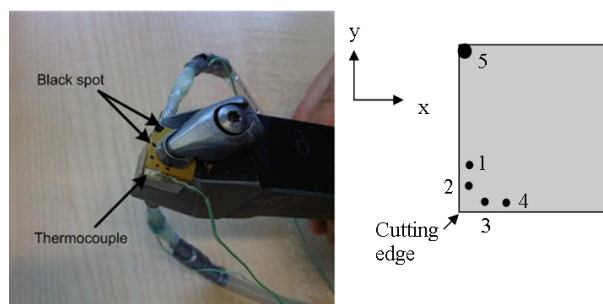
Fig. 3-14: Cutting tool for the first experiment

Table 3-2: The position of the black spots from the cutting edge

Spot	x (mm)	y (mm)
1	1	4
2	1	2
3	2	1
4	2	4
5	0	12

For the second experiment, tool module with internal cooling system is utilised to study the effects of internal cooling in machining. Three types of workpiece materials have been cut (i.e. AA6082, EN32B mild steel and commercial pure (CP) titanium grade 2). The three materials represent three groups of common workpiece materials in machining (i.e. ductile materials, hard materials and difficult-to-cut materials).

The effects that are anticipated to be observed in the machining are machining performance (i.e. tool life and surface finish quality), chips formation, process parameters (i.e. cutting forces and cutting temperatures) and tool wear mechanisms.

The norm in determining the tool life is systematically written in the ISO 3685:1993. For sintered carbide tool the common criteria used to reject the tool are:

(1) The maximum width of flank wear land VB_B max = 0.6 mm or the average width of the flank wear land, $VB_B = 0.3$ mm.

(2) The depth of crater wear, KT / mm obtained by the formula

$$KT = 0.06 + 0.3f \qquad (3.1)$$

where f is the feed rate.

(3) The crater front distance reduces below $KF = 0.02$ mm.

(4) The crater breaks through at the minor cutting edge producing poor surface finish.

The measurement equipment used to measure the tool wear are TESA Vision System and Dino-Lite digital microscope. The surface roughness of the finished surface is measured under Zygo surface profiler.

3.5.   Development of communication and control for adaptive machining

The communication interface is the core of the adaptive machining system because it interfaces all the integrated hardware like the machine tool, the cooling system and the sensors. The system integration for the adaptive machining is illustrated in Fig. 3-15.
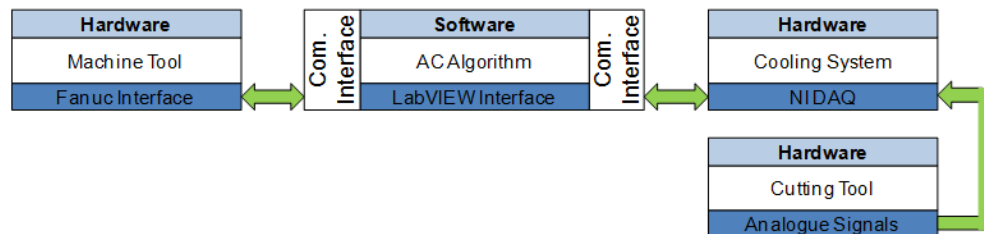
Fig. 3-15: System integration for adaptive machining

The communication interface application is developed in LabVIEW environment. In the LabVIEW program the logic for AC algorithm is also developed. Three techniques for AC algorithm have been shortlisted to be tried in this experiment as follows:

(1) Tool life-temperature equation

$$\theta T^n = C \tag{3.2}$$

Where n is found between 0.1 to 1 and C is experimentally deteremnied constant.

(2) Takeyama and Murata's wear rate model

$$\frac{dW}{dt} = G(v.f) + D \cdot e^{-E/R \cdot \theta} \tag{3.3}$$

Where G and D are experimentally determined constant and θ is the cutting temperature.

(3) Threshold control

Threshold control is by determining the optimum cutting region, within which the minimum wear mechanisms and rate of wear occurs.

3.6.   Improvement of the smart cutting tool

The ability of internally cooled cutting tool to machine materials, particularly common aeronautical material- titanium at high material removal rate in green manufacturing is an advantage to machining cost. The main challenges in machining titanium are:

(1) high chemical reactivity,

(2) low thermal conductivity,

(3) relative high hardness and strength and

(4) gross inhomogeneous plastic deformation in cutting of the titanium hamper the development of HSM cutting tool for green manufacturing of titanium (Komanduri, 1982; Bermingham et al., 2011).

Current slow removal rate exacerbates the machining cost with the contamination of chips. The machining cost of cutting titanium can be significantly reduced by improving material removal rate, thermal

management, the possibility of direct recycle of the chips, lubrication strategies and particularly tool design (Bermingham, et al., 2011). Therefore the improvement needs to be performed in a holistic manner in order to balance between the technological, economical and the environmental aspects. Due to the complexity of machining process especially with absence of cooling lubricant, the improvement of the cutting tool requires some problems to be addressed pragmatically rather than scientifically. Besides that artificial intelligent tool and analysis of variance (ANOVA) technique with the aid of sensors fusion are also utilised to facilitate the decision making process.
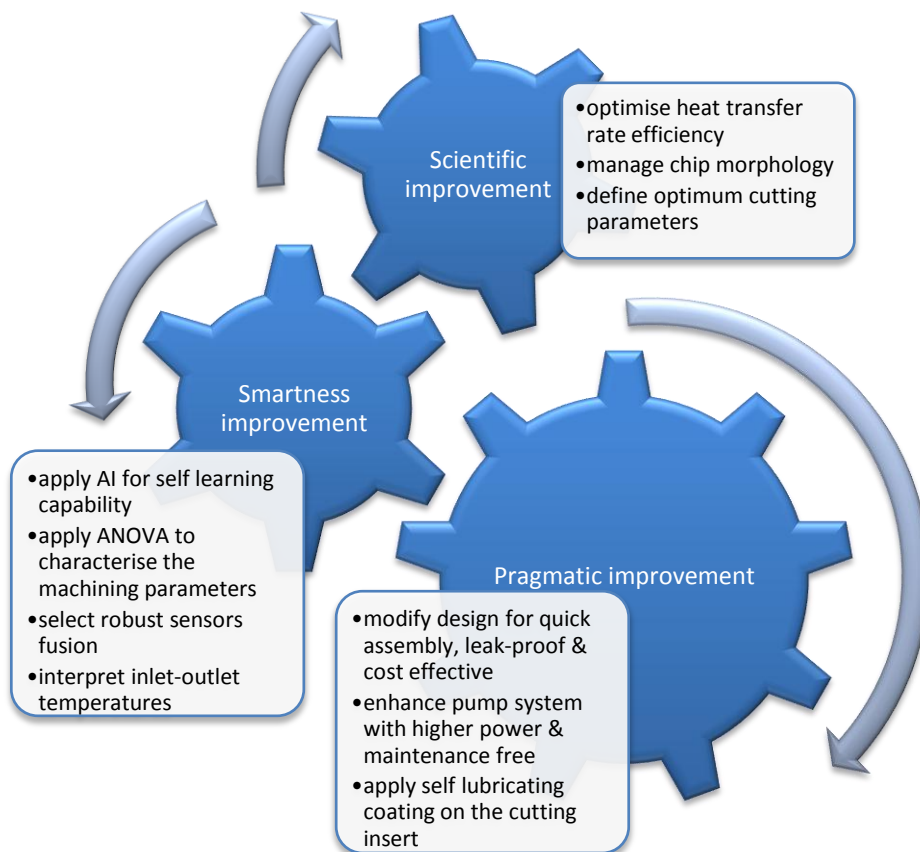
Fig. 3-16: Improvement of smart cutting tools with consideration of scientific, pragmatic and smart aspects

Chapter 4:   **Design of the Internally Cooled Smart Cutting Tool**

Design of internally cooled cutting tools has partially adopted the principle of total design method by Stuart Pugh (Pugh and Clausing, 1996). Fig. 4-1 illustrates the systematic core design which consists of imperative activities in the process of design and development of internally cooled cutting tools. It starts with the identification of the demand and requirements from the end-users, particularly the needs for high machining economics efficiency in green manufacturing.
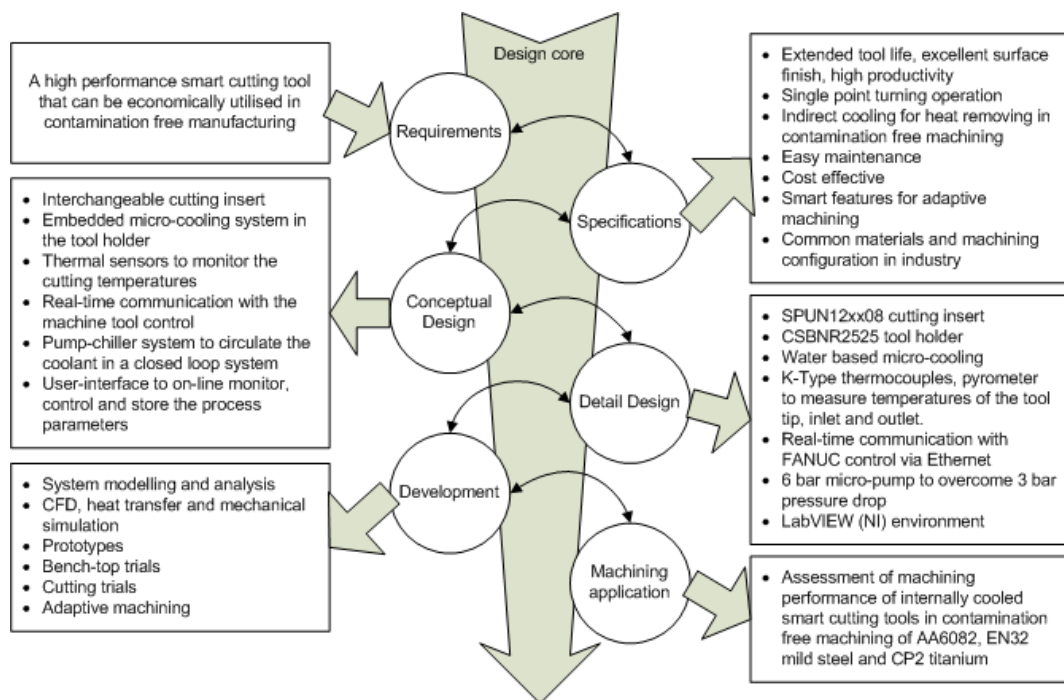
Fig. 4-1: Design core in designing pre-production internally cooled smart cutting tools

In the next stages, i.e. specifications, conceptual design, detail design and development, the scientific as well as pragmatic input from various engineering disciplines are taken into considerations. Each stage is designed to fulfil the requirements set for internally cooled cutting tools, i.e. performance in green manufacturing, ease of installation in the current machine tool configuration, low maintenance, manufacturing and operational cost effective and smart features for practical manufacturing such as plug and produce and user-friendly data exchange interface. The flow of the design stages is actually an iterative process where the outcome of every stage is continuously checked to ensure it satisfies the design core.

Technical aspects have been formulated and evaluated in a holistic manner in the development stage. The synthesis between manufacturing and intelligent system required the development of internally cooled smart cutting tool to be carried out based on the principles of iterative development procedure (IDP) where the key elements, i.e. planning ; analysis and simulation; prototype manufacture; deployment; testing and evaluation, are in cyclic flow allowing for a more evolutionary approach to the development. In the analysis, the boundary conditions for the application of internally cooled smart cutting tool have been defined. Analytical models for the fluid behaviour, heat transfer and mechanical structure have been developed to provide better understanding of the influence of the main process parameters. Simulating the models especially in three dimensions can significantly improve the time required for development stage since the number of experimental trials can be reduced. The optimised model yielded from the results of analysis and simulation shall be manufactured and assembled as first prototype.

Internally cooled cutting tools evolve under three major iterations that rectifying unforeseen problems which could not be identified and simulated in the previous stage, such as sealing problems, assembly time, residual stress inherited from the manufacturing process of the supplier, impurity in the materials, aliasing of sampling rate and combination effect of intense stresses and temperature at the contact region. Internally cooled cutting tools emerged from the optimising iterations are robust to cut different materials without the aid of MWF and are effective to extend the tool life, machine good surface finish and/or increase productivity.

From the design three main components that will be used for adaptive machining of contamination free materials are internally cooled cutting tools, coolant supply system and adaptive control with user interface.

Generally, it can be formulated that the design of internally cooled cutting tools involves following procedures:

(1) Design of an internally cooled cutting tool based on the geometrical model of a conventional cutting tool with software Pro/Engineer

(2) Definition and analysis of the effects of mechanical as well as thermal loads on the proposed design

(3) Determination of the boundary conditions for the FE models

(4) Execution of the finite element analysis (FEM) in the simulation environment of ANSYS workbench.

4.1.   Design baselines

A set of baselines have been used to design the internally cooled (IC) smart cutting tools as listed below:

(1) Least modification to existing machining configurations.

(2) Highest heat transfer rate

(3) Trade-off between mechanical and thermal properties

(4) Cost effective

(5) Plug and produce smart cutting tool

Machine tool configurations such as tool holders, tool geometries and tool materials are guided by industrial standards. By following these standards it is assured to design an IC smart cutting that can fit into machine tool.

As reported in the patents and standards related to cooling technique in machining:

(1) The heat transfer in direct flood cooling is by forced convection, and

(2) the heat transfer in indirect cooling is by conduction.

It is important to consider the fact that cutting tool especially the carbide type is made of poor thermal conductivity material. Thus, the challenge lies in the effort to remove the heat efficiently through conduction across poor conductive materials.

One solution is by minimising the thickness of the tool, thus the coolant can effectively remove the heat from the localised heat zone. This solution, however, might weaken the mechanical structure of the tool. A systematic study will be performed to study the effects of the tool thickness on the tool temperature, structural strength and impact resistance. Tool temperature

reflects the ability of the heat sink to reduce the maximum cutting temperature of the tool without the expense of the mechanical strength of the cutting insert.

The solutions proposed will consider the economic factor as well. The elements to quantify the cost efficiency of the design of IC smart cutting tool proposed include the energy required to operate the IC smart cutting tool, the cost associated with the sensor utilized and the coolant selection.

The last aspect in the design baselines is the plug-and-produce features of the internally IC smart cutting tools. The machining process parameters measurements and the data processing capabilities often make the cutting tool to be application and machine tool specific. It is therefore a requirement for special considerations to be taken while designing the internally cooled smart cutting tool to make sure the cutting tool has following characterics (Davis, 2012):

    (1) greater manufacturing complexity
    (2) dynamics-based economics
    (3) responsive radically to different performance objectives

4.2.   Design approach

The design of an IC smart cutting tool is effectively an optimisation of a commercially available cutting tool in the aspect of thermal behaviour to extend the tool life and machining performance.

$$q_x = -kA\frac{dT}{dx} \qquad\qquad (4.1)$$

Based on the fourier's law of the heat conduction (equation 4.1), the cooling structure which will be introduced in the cutting tool module should obey following criteria to effectively remove huge amount of heat:

    (a) smallest distance to heat zone

    (b) largest contact area of cooling fluid

    (c) biggest temperature difference between heat source and heat sink.

The cutting insert geometry should be in simplest form to understand precisely the effect of internal cooling on machining performance. Lathe cutting insert of ISO SNUN or SPUN (see Appendix E for the ISO standards geometry for indexable inserts) are used as insert geometry as they don't have chip breaker and the attachment of the insert to the tool holder by means of clamping can allow sufficient space to accommodate cooling structure. It is also decided to select tungsten carbide as the material for the cutting insert as this material is the most popular material used in the industries.

Thermocouples and compact infrared (IR) camera or pyrometer will be utilised as fusion sensor to provide feedback signal for adaptive machining control.

4.3. **Design proposal**

The design proposal for the IC smart cutting tool can be characterised based on the design baselines and the design approach written above.

Three main components of an IC smart cutting tool that need to be designed are the tool holder, tool insert and internal cooling structure. The geometries of the components are crucial in determining the fitness of the module into the machine tool.

The development stage of the IC smart cutting tool will use lathe machine tool Alpha Colchester as trials test-bed. Therefore, all the modifications will be based on the requirements to fit with this machine tool without neglecting the universal aspect of the internally cooled tool to be used in other machine tools.

The biggest challenge in fitting the designed IC smart cutting tool in Alpha Colchester machine tool is with the size of standards tool holder normally used on this machine, i.e. square section of the tool handle is 20mm × 20mm. This geometry is too small to accommodate the inlet and outlet tubes. Therefore, a bigger size of tool holder (i.e. 25mm × 25mm square section of the tool holder) is opted where slight modification to the handle's thickness needs to be made to fit the tool holder into the machine where proper centre line can be set.

The selection for the tool holder, insert geometries, insert materials and internal cooling techniques are listed in Table 4-1. The cutting tool modules (Fig. 4-2) commonly comprise a cutting insert that is held in a tool holder by a clamp that can be tightened against the holder by a screw. In some cases supporting adapter is used sandwiching between the cutting insert and tool holder to provide additional support during machining.

Table 4-1: Proposal of design elements

Design elements	Selection
Tool holder	CSBNR 2525 M
Insert geometries	(1) SNUN 120408
	(2) SPUN 120408
Insert materials	(1) High speed steel (HSS)
	(2) Tungsten carbide (WC)

Internal cooling techniques	(1) single phase micro-channel (below 1 mm cross sectional area) (2) jet impingement cooling (3) open-plan cooling

The selected insert, in square shape (SNUN type), fits into the pocket at the end of the tool holder where the cutting edge of the insert is directed towards the workpiece to engage with the material to cut. The advantage of this shape of tool insert is, when the edge worn out, the insert maybe rotated ninety degrees or flipped upside down to expose a fresh edge to the workpiece. By this way the tool can effectively have eight cutting edges. If the cutting insert is designated with clearance angle (e.g. SPUN insert), the number of effective cutting edges is reduced to four.
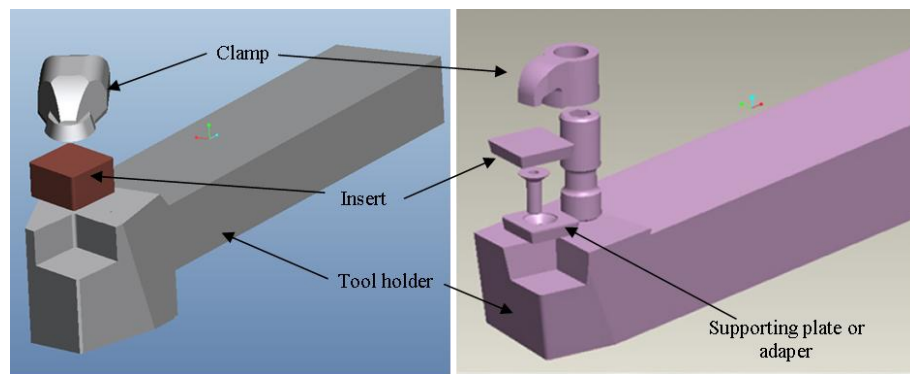
Fig. 4-2: Standard cutting tool module

Fig. 4-3 shows the unexploded CAD view of conventional tool (top) and a cutting tool that has been modified to apply internal cooling to the cutting insert (bottom).
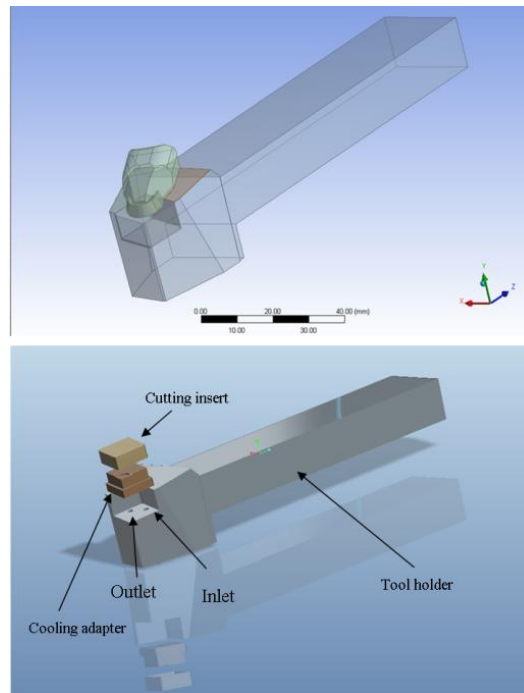
Fig. 4-3: CAD design of the commercial available cutting tool module (top) and customised internally cooled tool components (bottom)

The cutting insert is characterised by a bottle-cap shape with the cavity forms heat sink when assembled together with the cooling adapter. Different internal cooling techniques can be applied to the cutting tool depending to the shape of cooling adapter and means of circulating the coolant around the tool. Micro-channels are formed in the tool holder to supply and remove the coolant from the cooling adapter. Cooling channel with cross sectional area of less than 1 mm² (hence micro-channel) needs to have high cooling capability with the tiny geometry since bigger channel will affect the tool mechanical strength.

The coolant supplied is water based since water has a high specific heat capacity, c_p (approximately 4,180 J/kg·K). Some anti-corrosion additive might be added to the water to avoid oxidation of the metallic parts when exposed to the water.

As shown in Table 4-1, three internal cooling techniques selected for this research are single phase micro-channel, jet impingement cooling and open plan design. The proposed designs are shown in Fig. 4-4.

Manifold cooling channel   Jet impingement cooling   Open plan cooling
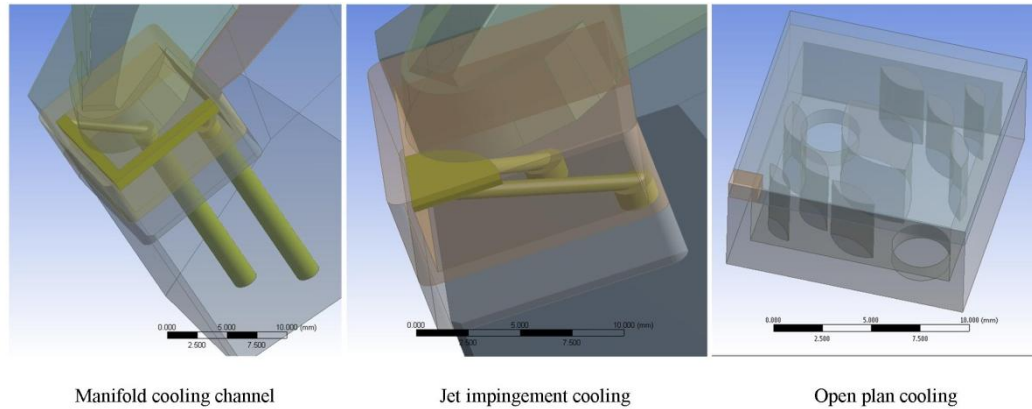
Fig. 4-4: Internal cooling designs

The designed cooling channels have cross sectional area of less than 1 mm. All the cooling techniques are supplied with single phase fluid with the temperature of the fluid varied between 5°C to 30°C. For most simulations particularly the heat transfer and fluid dynamics analysis, the FEMs are not modeled with the tool holder to spare computing power as shown for open plan cooling. Therefore, boundary conditions need to be determined and verified experimentally.

4.4.   Results and discussion

The presentation of the results is mainly in two parts. Firstly the results of the computer simulation is presented and then followed by preliminary results of the cutting trials.

4.4.1. Numerical analysis

Based on the orthogonal cutting diagram of lathe turning operation in Fig. 4-5, the component of force acting on the rake face of the tool in the direction tangential to the workpiece radius at point of contact with the cutting edge is called cutting force, F_c. It acts in the direction of cutting velocity, v, and in most cases this is the largest of the three force components. The force component acting on the tool in the direction of feed is called feed force and is often referred as F_t instead of F_f due to the fact that this force is tangential to the main cutting force, F_c. The third component that is acting in the workpiece radial direction is the smallest of the force components and is noted as F_r. This force in modeling orthogonal cutting is usually ignored.
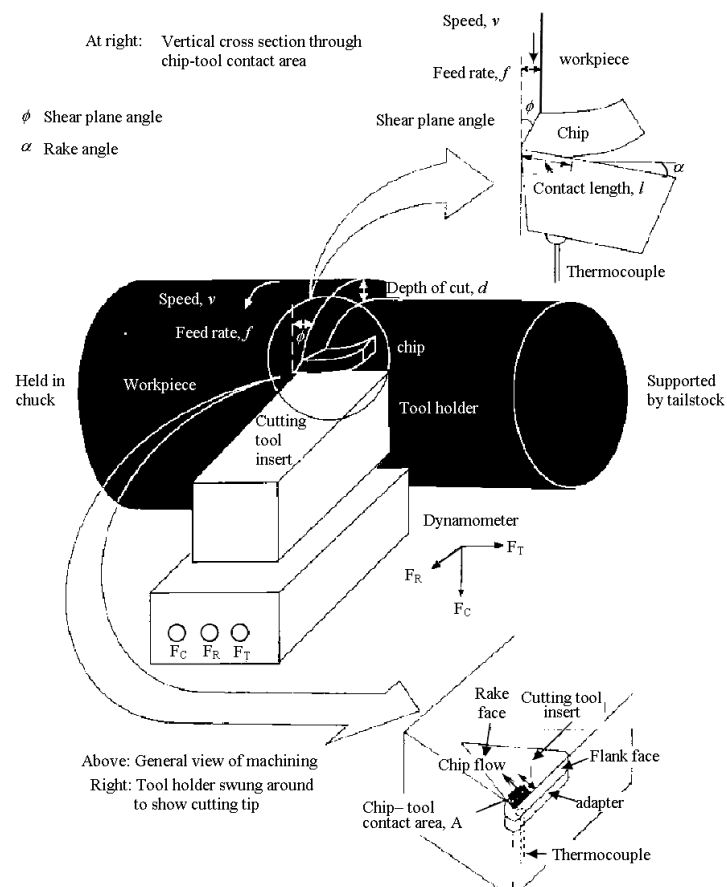
Fig. 4-5: Overview diagram of orthogonal cutting operation

Numerical calculation of the two major force components in orthogonal cutting, i.e. cutting and feed forces requires geometrical parameters of undeformed chip thickness, t_1 (the feed), chip width, w (depth of cut) and shear plane angle, ϕ to be known.

Shear plane angle is,

$$\tan \emptyset = \frac{r_c \cos \alpha}{1 - r \sin \alpha} \tag{4.2}$$

where r_c is the chip thickness ratio.

$$r_c = {t_1}/{t_2} \tag{4.3}$$

t_2 is the mean chip thickness and is calculated as follows:

$$t_2 = \frac{W}{\rho w l} \tag{4.4}$$

W and l is the weight and length of a piece of chip that need to be measured. The density of the workpiece, ρ is assumed to be unchanged during chip formation.

With τ is shear strength of a material, cutting force and feed force can be computed based on Merchant's shear plane analysis.

The main cutting force acts on the tool/workpiece direction is:

$$F_c = 2 w t_1 \tau \cot \emptyset \tag{4.5}$$

and the feed force acts normal to the main cutting force can be obtained by:

$$F_t = w t_1 \tau (\cot^2 \emptyset - 1) \tag{4.6}$$

By obtaining these forces, further analysis physical phenomena on the tool rake face such shear stresses, temperatures, etc. can be performed. Also as per definition that the coefficient of friction equals the ratio of the force in the direction of sliding chip to the force normal to the sliding interface, therefore the coefficient of friction on the rake face of the tool can be written as:

$$\mu = \frac{F}{N} = \frac{F_c \sin \alpha + F_c \cos \alpha}{F_t \cos \alpha + F_t \sin \alpha} \qquad (4.7)$$

$$= \frac{F_c + F_t \tan \alpha}{F_c - F_t \tan \alpha} = \tan \lambda \qquad (4.8)$$

where F and N respectively represent frictional force and normal force on the rake face and λ represents frictional angle (see Fig. 4-6).
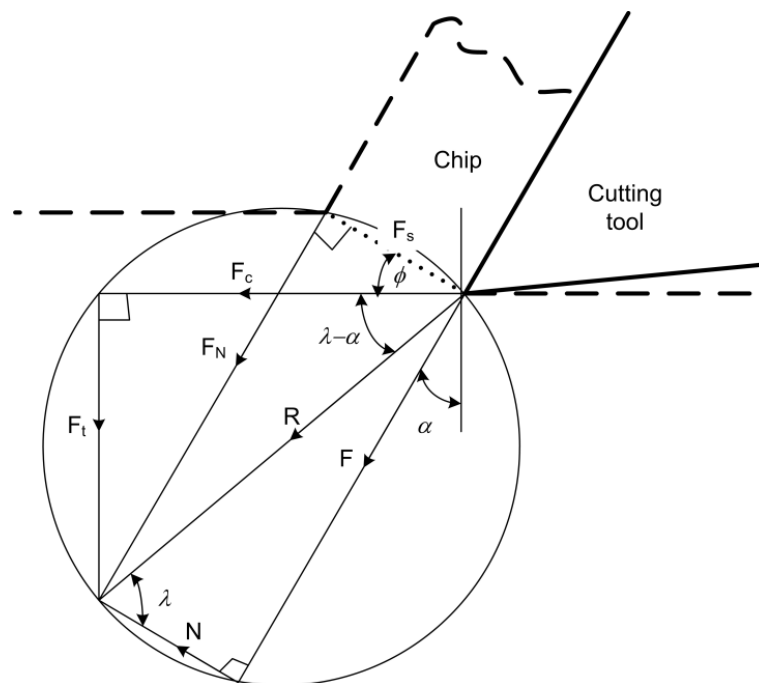
Fig. 4-6: Merchant's force circle

Moreover by obtaining the cutting force and feed force the more significant parameters in the shear zone such as shear force, normal force, shear stress and normal stress can be calculated.

From the Merchant's force diagram in Fig. 4-6 the forces act on the shear plane are derived to be

Shear force,

$$F_s = F_c \cos\emptyset - F_t \sin\emptyset \qquad (4.9)$$

Normal force,

$$F_N = F_c \sin\emptyset + F_t \cos\emptyset \qquad (4.10)$$

Using these shear and normal forces, the shear stress and normal stress may be found from the following equation:

Shear stress,

$$k_s = \frac{F_s}{A_s} = \frac{[F_c \cos\emptyset - F_t \sin\emptyset] \sin\emptyset}{wt_1} \qquad (4.11)$$

Normal stress,

$$\sigma = \frac{[F_c \sin\emptyset - F_t \cos\emptyset] \sin\emptyset}{wt_1} \qquad (4.12)$$

where $A_s = shear - plane\ area,$

$$A_s = \frac{t_1 w}{\sin\emptyset} \qquad (4.13)$$

By definition power consumed in machining (mostly to run the spindle) equals force times speed.

$$P = F_c v \qquad (4.14)$$

From literature the machining efficiency of the power required to perform machining can obtain specific energy, U to predict temperature rise as proposed by Nathan Cook (model developed by cutting various workpiece materials).

$$\Delta T = \frac{0.4U}{\rho_c} \left(\frac{V t_1}{K} \right)^{0.333} \tag{4.15}$$

Stresses on the tool are primarily calculated.

Normal stress,

$$S = \frac{F}{A} \tag{4.16}$$

Common cutting force, F_c, in machining hard to cut material is 500N. Unconventional cutting insert is assumed to have square face of 12mm×12mm. Using equation above the normal stress acts on the tool is 3.47MPa.

4.4.2. Simulation

The ultimate aim of the computer simulation is to design internally cooled tools which can efficiently preserve the tool against thermal load without alleviating the mechanical strength. The boundary conditions defined in the simulation can aid the optimisation process by reducing the process dependency on cutting trials.

Fig. 4-7 shows the temperature distribution in cutting tool with conventional tungsten carbide insert when heat of 40W (same as Loewen and Shaw, 1954) is

applied. The high temperature gradient (about 50K/mm) is observed in the vicinity of the tool tip. Maximum temperature of 563K (290°C) is recorded at the cutting edge but the temperature has dropped until 441K (169°C) at the opposite orthogonal edge.
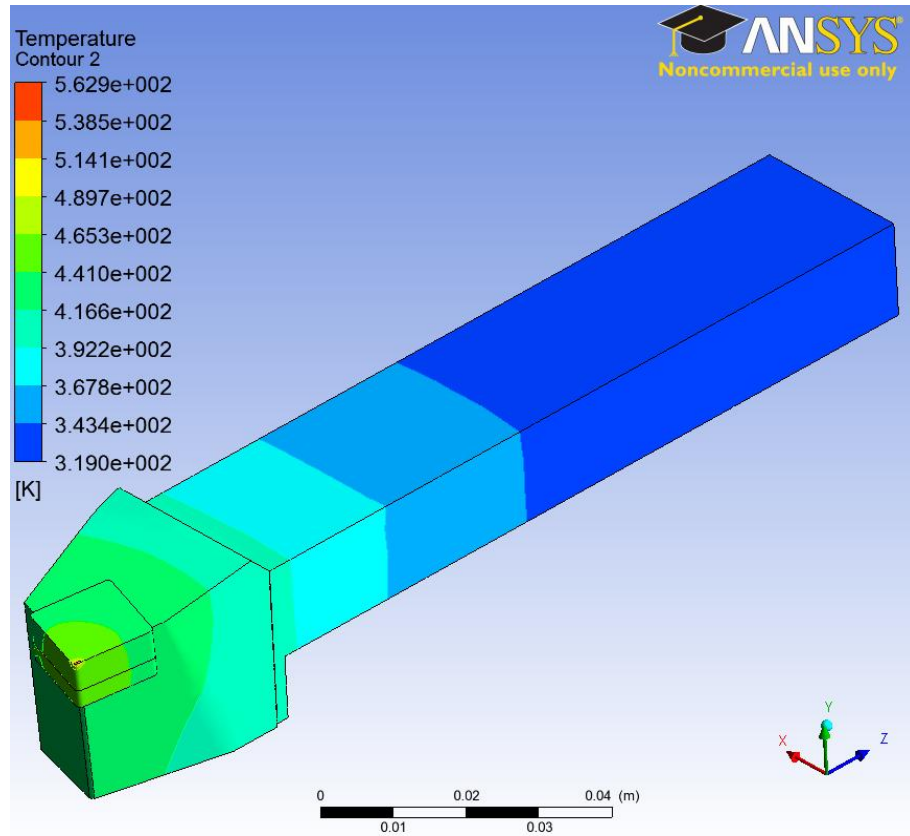
Fig. 4-7: Temperature distribution with 40W heat applied

The thermal model of the cutting tool and applied boundary conditions are developed based on the 2D model proposed by Tay et al. (1974) and Dogu et al. (2006) as illustrated in Fig. 4-8.

The locations at where the boundary conditions were applied are translated in the 3D generation of the FEA models. The simulation does not require the model to include the chip and the work-piece, since the objective of the

simulation is to observe the temperature distribution in the work-piece when a constant heat flux is applied.
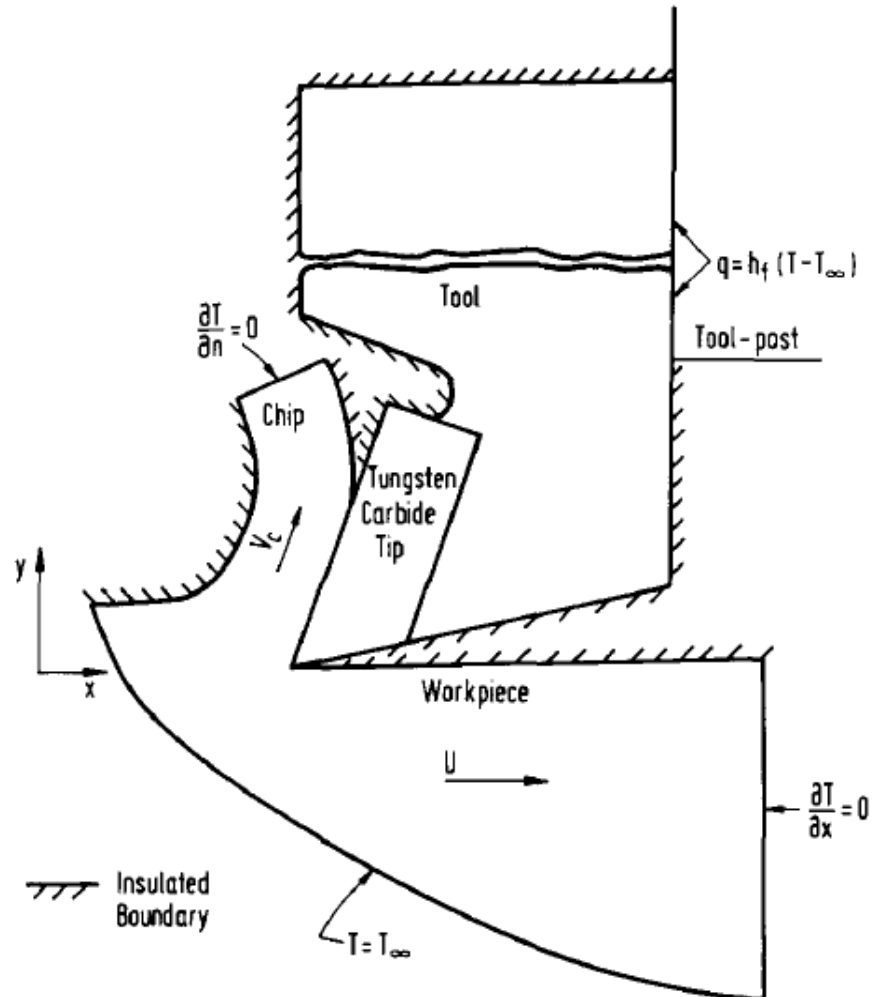
Fig. 4-8: Boundary conditions used by Tay et al., (1974) and Dogu et al., (2006)

Table 4-2 shows the variation of maximum temperatures on the cutting tool when different amounts of heat are applied. The full simulation results can be referred in Appendix H.

Table 4-2: Maximum tool tip temperatures produced when different heat transferred to the tool

Heat (W)	Max. tool temperature (K)
5	317.95
10	348.24
20	391.13
30	494.37
40	562
50	700.34
60	851.41
70	1004.9
80	1108.79
90	1210.54
100	1315.01
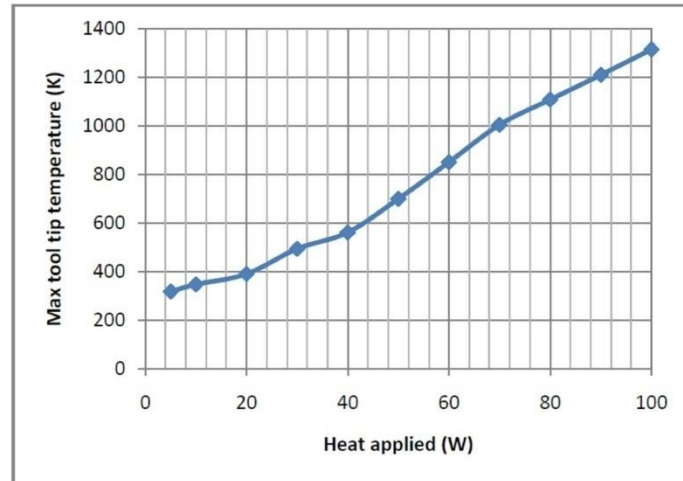
Removal of heat from the tool by fluid obeys the principle of forced convection

$$Q = \dot{m}c_p\Delta T \tag{4.17}$$

where specific heat capacity, c_p of water is approximately 4,180 J/kg·K.

Re-arranging the equation 4.17 to estimate mass flow rate that needs to be supplied in order to remove 40W of heat with the increase of coolant temperature of 3 K is:

$$\dot{m} = \frac{Q}{c_p\Delta T} \tag{4.18}$$

Thus it results a coolant supply of 0.003 kg/s, which is relatively small and easily obtainable with micro-channel cooling. By knowing the density of the water used, the mass flow rate can be converted to volume flow rate if required.

Designing internal cooling structure requires design variables to be tested. The design processes for micro-channel cooling and jet cooling are documented in publications Sun et al. (2011) and Che Ghani et al. (2011a, 2011b) respectively.

Sun et al. (2011) have studied the effects of insert top thickness, vertical and horizontal sides' length of the triangular section and inlet channel diameter on the cooling capability of micro-channel internal cooling. It is suggested that the diameter of the micro-channel has a significant effect on the cooling capability while no interactions between the design parameters are observed in influencing the temperature distribution.

Che Ghani et al., (2011b) have studied the effects of distance between the channel and the bottom of the heat source, the channel diameter and the coolant temperature on the temperature of the cutting tool by jet cooling. A significant effect by coolant temperature is obtained while the effects of other factors are not really pronounced to be considered. This is in agreement with the suggestion in the patents and standards related to indirect cooling technique in machining that biggest difference between coolant and temperature and heat source temperature is desired to increase heat removal rate. Based on the study, the diameter of the cooling channel of 800μm has been chosen due to manufacturing factor and mechanical strength it provides.

Generally, cutting tool with internal open plan cooling design (Fig. 4-4) produces slightly lower maximum tool tip temperature compared to the tools with micro-channel and jet cooling when similar flow speed is supplied. Heat of 60W is supplied to the tool to observe the cooling capability of the IC smart tool when utilised in machining hard to cut materials like titanium and Inconel. It is observed that all the three designs of internally cooled tool can effectively reduce the cutting temperature with the least reduction of temperature demonstrated by single phase micro-channel (Fig. 4-9). Nevertheless, the reduction of about 200K from 851K to 650K is significant in protecting the tool

since this reduction can enable the tool of carbide material to avoid critical diffusion wear activation region, 711°C or 984.15K (Yang, 2001). Both micro-channel design and jet cooling design show no further improvement as the flow speed increases. Marginal temperature difference can be seen when open plan cooling is used. This indication discounts the necessities for high coolant volume and big pump size required by open plan cooling.
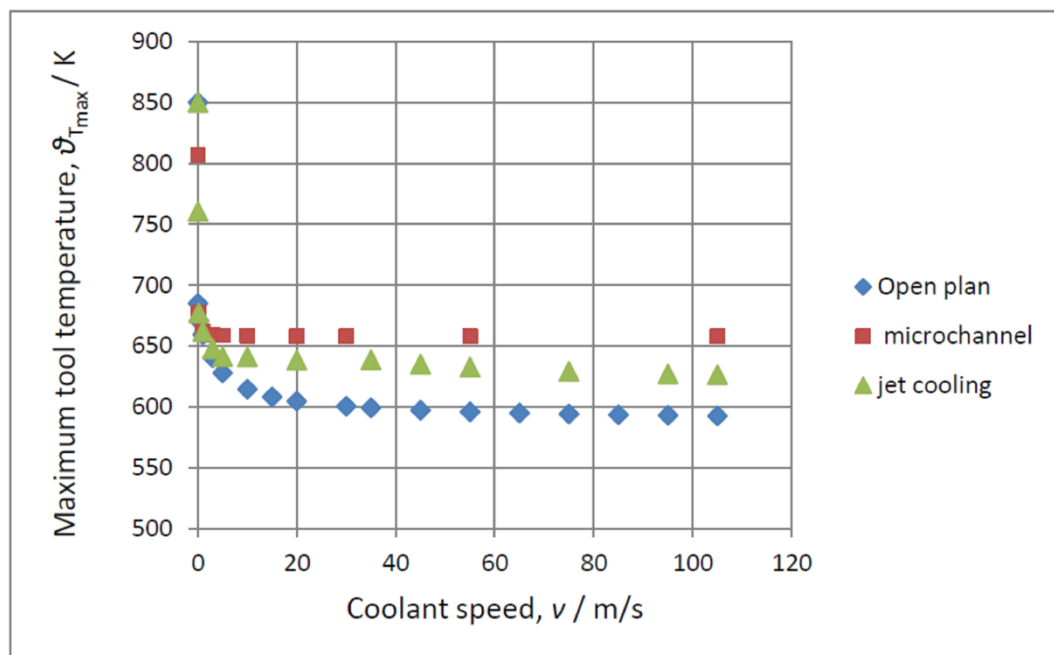
Fig. 4-9: Cooling capability assessment of different cooling technique with 60W heat supplied

Design with single phase micro-channel of 800μm diameter is simulated when heat transferred to the tool varied from 5W to 100W and the maximum tool temperatures obtained are compared with the simulated results of conventional dry machining tool as shown in Fig. 4-10.
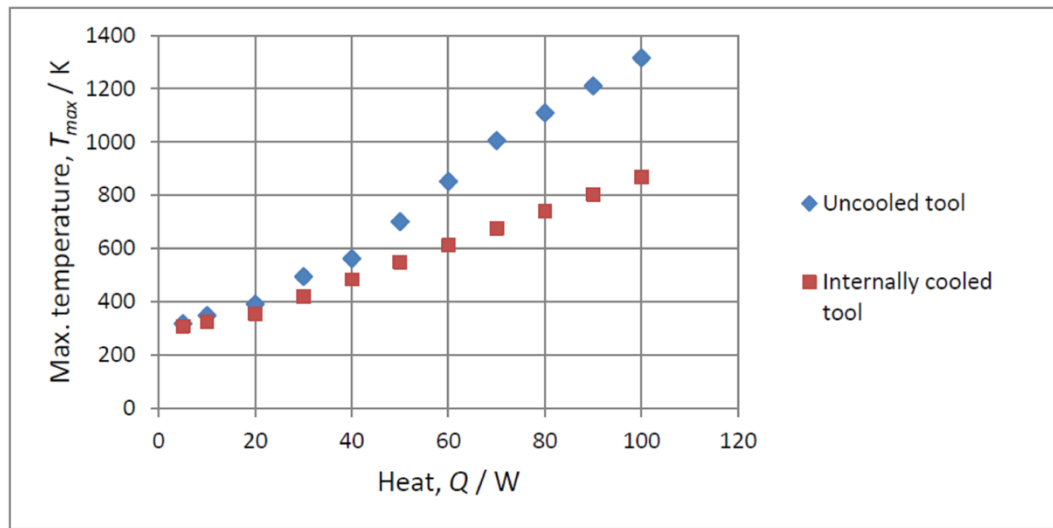
Fig. 4-10: Simulation of internally cooled (800µm diameter microchannel) and uncooled tools

4.4.3. Experiment

The objectives of the experimental study are (1) to effectively assemble a working module of an internally cooled cutting tool, (2) to test the cooling capability of the cutting tool and compare it with the numerical simulations and (3) to assess internally cooled tool performance in actual cutting trials.

The objectives (1) and (2) can be achieved by building a bench-top test facility which comprises all relevant components such as tool holder, pump and tubes, thermal sensors and data acquisition system. Objective (3) requires the tool to be assembled in a machine tool. Thus CNC lathe ROMI Bridgeport was chosen as an experimental platform to test the tool.

Fig. 4-11 schematically illustrates the bench-top test facility setup that constitutes components of internally cooled cutting tool.

Fig. 4-11: Test rig setup for the internally cooled cutting tool

Tool holder is held firmly on a bench. At the end pocket of the tool holder a cutting insert and supporting adapter are fitted (Fig. 4-2). For internally cooled cutting tool customised made cutting insert and cooling adapter (Fig. 4-12) are sealed together to ensure proper coolant circulation can be supplied. For the preliminary trials only single phase internal cooling tool will be tested due to simplicity of fabrication of this design. Two front edges of the cooling adapter are chamfered and at the end of both chamfers two micro holes (800μm diameter) are drilled to form inlet and outlet channels as depicted in the right hand side of Fig. 4-12.

Fig. 4-12: Bottle cap shape cutting insert (left hand side), and micro-channel design cooling adapter (right hand side)

When the cutting insert and cooling adapter are assembled together as shown in Fig. 4-13, a cooling channel with triangular section will be formed. Non-hardening, non-setting and high temperature resistant mounting grease is applied between the contact surfaces of the cutting insert, cooling adapter and tool holder to seal the components together. The technical data sheet of the mounting grease is attached in Appendix G.
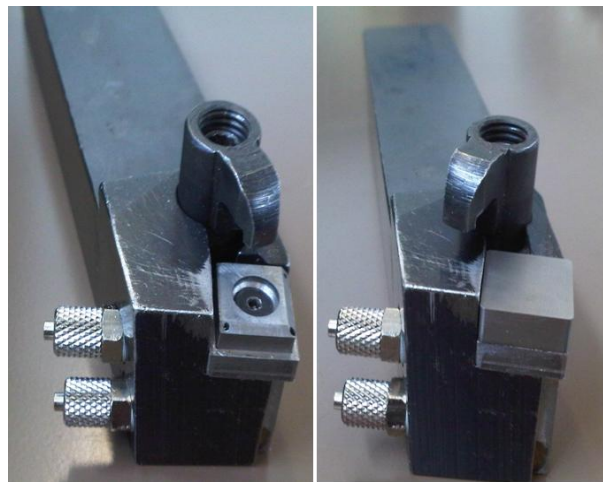
Fig. 4-13: Assembly of the internally cooled cutting tool

Fig. 4-14 shows a soldering iron with specially shaped end acts as a heat source; it can provide a uniform contact area with adjustable constant temperatures in the range of 30 to 350°C to be applied on the tool. Prior to the heating, the temperature of the heat source is ensured to reach the desired temperature by using a type T (copper-constantan) thermocouple. Type T thermocouples have high sensitivity, i.e. ±0.5 for temperature range: -40°C < T < 150°C, and $0.004 \times T$ for temperature range: 125°C< T< 350°C.
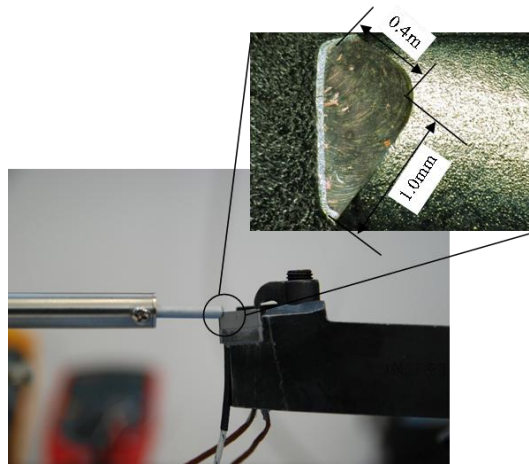
Fig. 4-14: Application of heat source on the tool (inset: the geometry of the soldering iron)

The bench-top experiment is performed to achieve the first objective by means of assessing the functionality of the whole components when assembled together. The cooling fluid is pumped through the internally cooled tool and a container at the highest mass flow rate (0.4 l/min) in a closed loop circuit by using a peristaltic pump (Fig. 4-15). Pure water is used as the cooling media. Three K type (chromel- alumel) thermocouples are used in this experiment; one embedded below the heat source and two to measure the inlet and outlet temperatures (see Fig. 4-14). K type thermocouple is selected for the real machining based on the large working range of the thermocouple of this type (-50< Temperature range< 1300°C) and its resolution (0.1°C).

The temperatures data obtained from this experiment are acquired by a universal serial bus (USB) 16-channel thermocouple module NI9213 and the data is stored for post processing and further analysis.
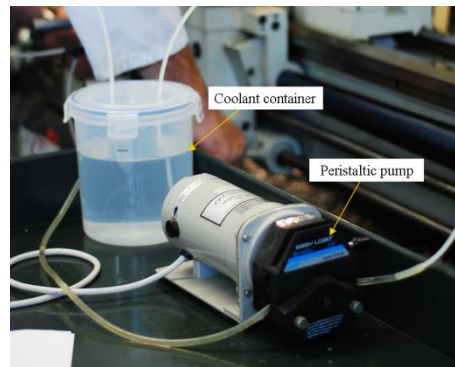
Fig. 4-15: Pump and container to circulate the coolant in closed loop circuit

The functionality of the internally cooled tool system will determine the accomplishment of objective (1). The coolant is pumped through the system and a heat source with constant temperature of 100°C is applied. Fig. 4-16 shows the acquired tool temperature when the coolant is switched on and off. Two observations can be seen from the trial; (1) a temperature reduction of about 30°C can be obtained by turning on the internal cooling and (2) the thermocouple is reasonably quick in measuring the temperature.
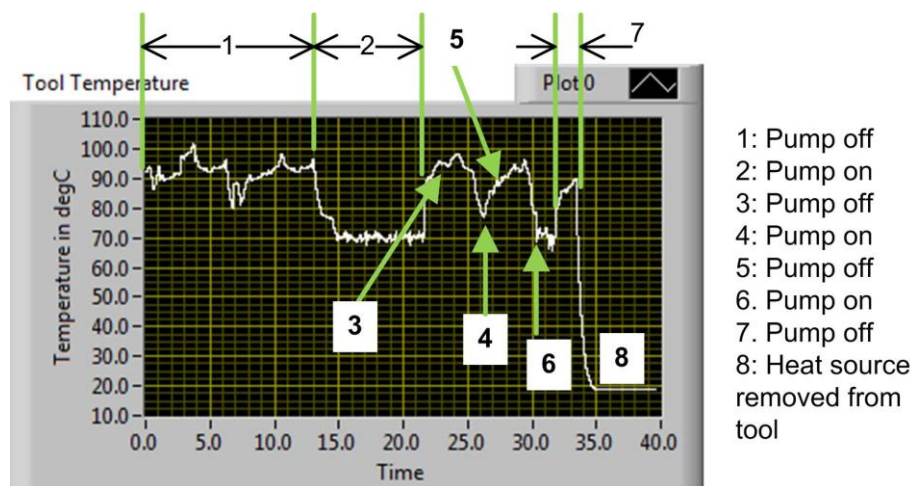
Fig. 4-16: Screen shot of benchtop trial results

The temperature distributions on the flank face and rake face of the tool is observed by using IR thermal camera. Fig. 4-17 and Fig. 4-18 show the IR

images of thermal distribution on the flank (top) and rake (side) faces when a constant temperature of 100°C is applied. In Fig. 4-17, it can be seen that the colour in the vicinity of the cutting edge changes from orange to pink which indicates the reduction of temperature.
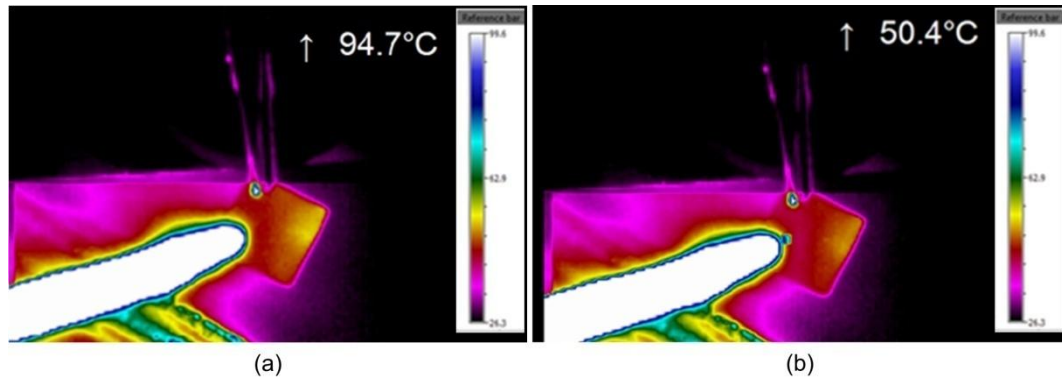
Fig. 4-17 : Temperature distribution on the rake face; (a) cooling off, and (b) cooling on
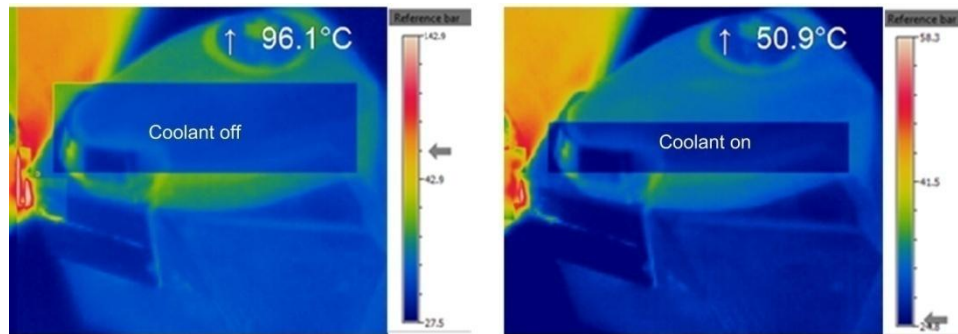
Fig. 4-18 : Temperature distribution on the rake face (coolant on and off)

The objective (2) and objective (3) can be achieved by applying the internally cooled cutting tool in real cutting trials (Fig. 4-19). The tool is used to cut aluminium alloy AA6082 with cutting parameters listed in Table 4-3.
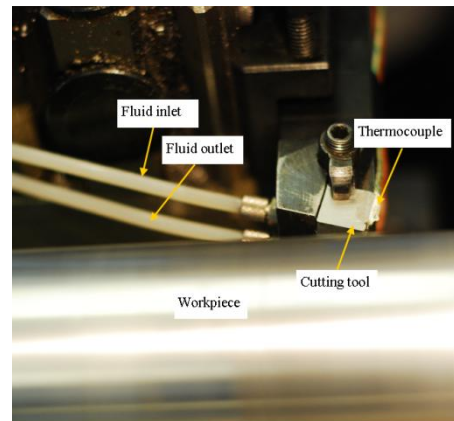
Fig. 4-19 : Setting up the internally cooled tool on lathe machine.

For the preliminary experiment the insert used is of high speed steel (HSS) material. The reason of the usage of this material is because HSS is a more conductive material than WC which is more favourable in the modification process using EDM.

Table 4-3: Machining parameters for preliminary experiment

Machining parameter	Value
Cutting speed [rpm]	1100
Depth of cut [mm]	0.5
Feed rate [mm/rev]	0.1888
Cutting travelled length [mm]	200
Coolant inlet velocity [m/min]	0.4
Coolant supplied temperature [˚C]	22
Insert material	HSS

Four cutting trials (from four available cutting edges of an insert) comprising of two cutting trials in conventional dry machining (DM) and two cutting trials of dry machining with internally cooled cutting tool (IC) were performed to assess the cooling capability of internally cooled cutting tool. For IC cutting trials the water based coolant is supplied at 0.2 l/min (0.4 m/min) through an internal

cooling channel of 0.045 mm² cross sectional area. It is observed that dry machining cutting trials are influenced by the ambient temperature meanwhile a more steady cutting trials obtained by applying internal cooling Fig. 4-20. Generally, the average of the measured steady state cutting tool temperature is reduced from 106°C to 51°C (improvement of over 50%) with the application of internal micro-channel cooling.
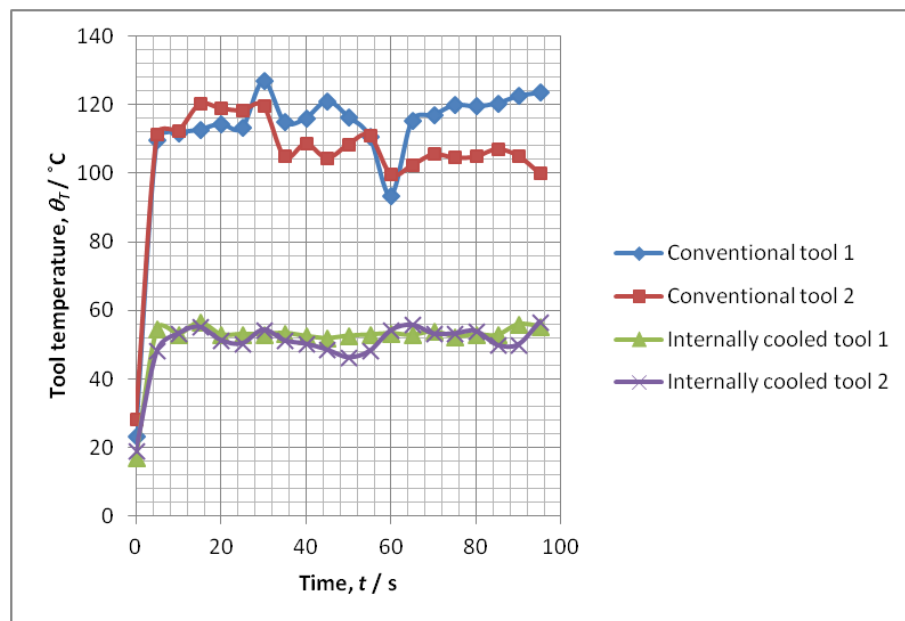
Fig. 4-20: Preliminary results of cutting trials

4.5.   **Conclusion**

In this chapter, three approaches of internally cooled smart cutting tools, i.e. single phase micro-channel, jet cooling and open plan have been designed and assessed. The internally cooled smart cutting tools were characterised based on commercial tool holder configurations that constitute of cutting insert, supporting adapter and a tool holder. This approach allows the cutting tool to be fitted directly on a machine tool.

The embedding of the cooling structure in the adapter rather than in the cutting insert enables all the four cutting edges of the cutting insert to be utilised in machining. The low cost to fabricate cutting insert can also be economically changeable once all the cutting edges worn out or if different type or grade of cutting insert is needed.

The simulations show that high temperature reduction can be achieved with internally cooled cutting tool with minimum allowable mechanical safety factor of 2 when the bottle-cap shape of insert has wall thickness of 1mm. Application of internally cooled tool in dry machining can reduce the tool temperature up to 35% which in most aggressive machining cases enables the tool to work below critical diffusion wear activated temperature for carbide tool.

The assessment on the three designs of internal cooling showed that all the three approaches were effective in reducing the cutting tool temperature when the nominal heat fluxes in machining were applied. The simulation also indicated that the high temperature was only localised at the cutting tip which has discounted the application high coolant volume by open plan cooling. So for the application in adaptive machining the cooling techniques are just limited to micro-channel and jet cooling. Experiment has proven that the internally cooled cutting tool can be used in real machining environment. Due to marginal advantage of higher power consuming open plan design, the design will not be further investigated in this research. Experimental cutting trials show that over 50% temperature reduction can be achieved in dry machining with the application of internally cooled smart cutting tools. Bigger temperature reduction of the cutting tool obtained in experiment compared to simulation is because of the location where the temperature has been measured in machining.

Chapter 5:   **Modeling and Simulation for the Tool Design and Analysis**

The computational modeling of a physical process analysis constitutes three main steps:

(i)   problem definition

(ii)   mathematical model

(iii)   computer simulation

Development of ideal mathematical equations to precisely pose a machining process is difficult due to the geometrical, physical, thermal and chemical complexities of the process. Therefore, introduction of simplifying assumptions is required in order to reduce the complexity of the mathematical model and make the numerical or exact solution to represent the machining process possible. The accuracy of the numerical model can be improved by determining the suitable boundary and initial conditions which are obtained experimentally.

Introduction of internal cooling (IC) alters the thermal and mechanical behaviours in machining process which consequently affects the machining performance such as tool wear development and surface roughness of the finished product. In this research, modeling enables quantification of the performance of a machining process with internally cooled smart cutting tool in terms of temperature reduction and tool life.

The analysis, modeling and simulation of CFD, thermodynamics and tool life of an internally cooled cutting tool can be summarised in the following five steps:

(1) The modeling of CFD, thermodynamics and tool life modeling of a turning process with internally cooled cutting tool require pre-determination of the heat sources.

(2) The regime of the cooling fluid has pronounced influence in determining the heat removal capability in a closed loop cooling system. Obviously the effects of fluid conditions (e.g. type, temperature and viscosity of the fluid) and the fluid speed need to be analysed and modeled to quantify the amount of heat removed.

(3) Based on the obtained CFD results, the thermodynamics (i.e. temperature distribution and maximum tool temperature) analysis and modeling of a turning process with internally cooled cutting tool can be performed. With the CFD results as well the temperatures of the fluid at the inlet and outlet can also be predicted.

(4) Utilising the cutting tool temperature obtained by heat transfer model, the wear rate models of an internally cooled cutting tool can be developed.

(5) Relative tool life of cutting tool with internal cooling and conventional can be computed based on the wear rate model.

5.1.   Analysis and simulation of mechanical loads

The mechanical simulation of FEM-computational model requires a development of CAD-model of conventional and internally cooled cutting tool inserts. The CAD models were mostly developed in Pro/Engineer software, and then later they were exported to ANSYS Workbench for the static structural simulation. The meshed models of conventional cutting insert and internally cooled cutting tool insert are displayed in Fig. 5-2.

The models are complemented with the boundary conditions, fixed support positions and material properties. The attachment of the insert on the tool holder is by means of clamping. The positions at where the insert is fixed to avoid displacement and tilting are shown with the green colour in Fig. 5-1.
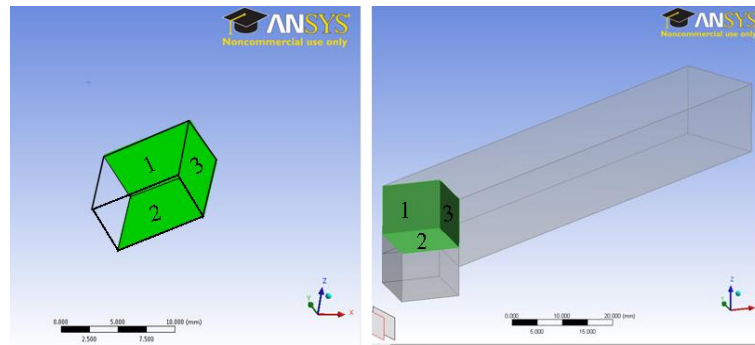
Fig. 5-1: Position of the fixed supports on the insert by the tool holder

In the FEM-modeling following mechanical loads are considered:

    (1) Components of the cutting forces

    (2) Pressure from internal cooling liquid in the micro-channel.

The cutting forces have been measured in the experiment by mounting the tool holder on a Kistler dynamometer (model 9257B). Theoretically only two component forces, viz. in cutting direction and feed direction, are effective in orthogonal turning operation, thus only two charge amplifiers (model 5070A) were required. The cutting trial was performed using conventional cutting tool to machine a grade-2 CP titanium with cutting speed of 80m/min, feedrate of 0.1 mm/rev and depth of cut of 0.5 mm. The machining trials produced the average cutting force and the average feed force in the magnitude of 243.7 N and 128.4 N, respectively. Selection of average cutting forces is sufficient for static simulation. The recorded cutting force and feed force were displayed in

the top left part of Fig. 5-2. The increased in cutting force towards the end of the machining was due to the impact by the continuous chip that gathered around the cutting tool.
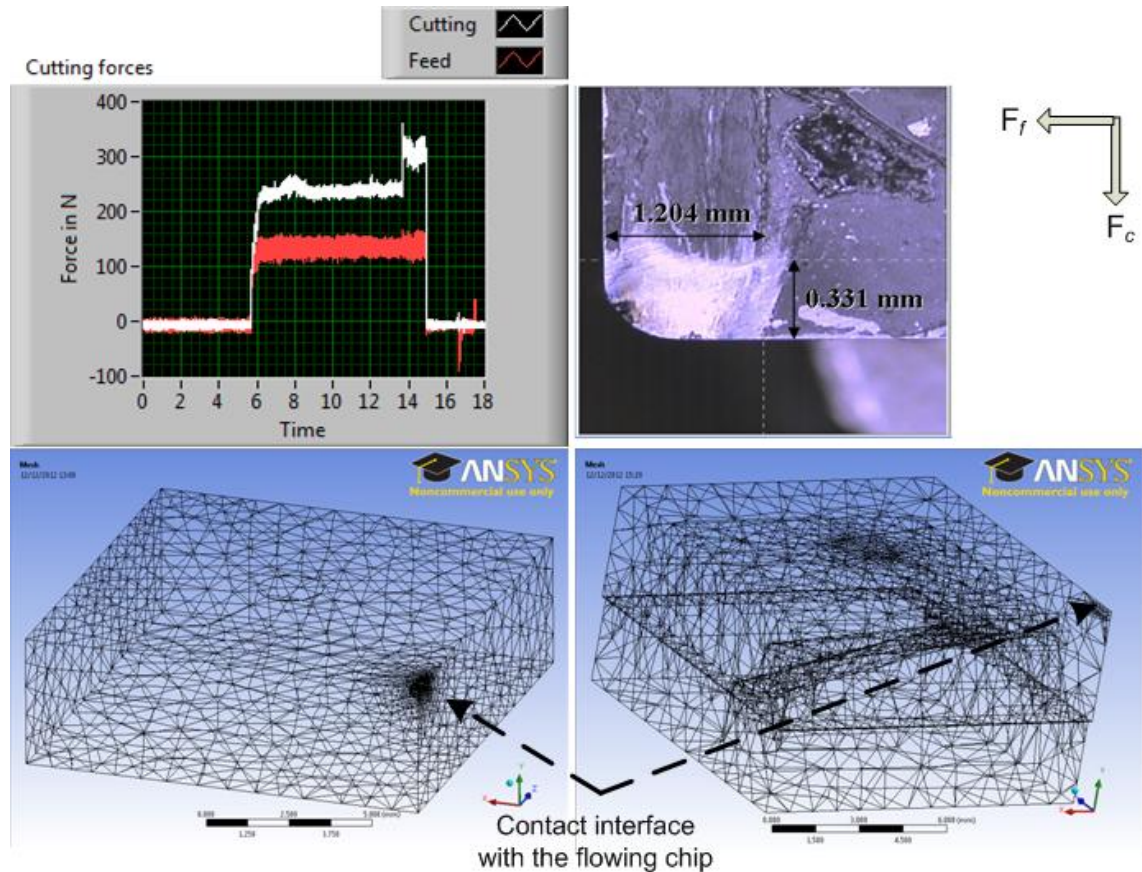
Fig. 5-2 : Cutting forces used and the model of conventional insert and internally cooled insert

The cutting forces were applied at the contact zone between the flowing chip and the cutting tool. The dimension for the contact area was also obtained from the experiment. The contact size of 1.2mm × 0.3mm that has been used for static structural simulation will also be used in CFD simulation.

Cutting insert is considered to be constituted of brittle materials. In this case, the maximum principle stress (σ_1) will be the limit for tool failure. Cemented

carbide will retain most of its strength at elevated temperatures. Thus the rise in temperature should not significantly influence the validity of this strength calculation. Positive principle stress corresponds to tensile stress and negative principle stress corresponds to compressive stress. For brittle materials, ultimate compressive stress should be used as material parameter to determine the allowable stress. Tensile strength is not suitable to gauge the strength of tungsten carbide because it is too brittle and accurate readings cannot be obtained. Tungsten carbide has compressive strength of 2.683 GPa or kN/mm^2 (matweb.com). In addition, inhomogeneities of the material and operating conditions with a safety factor of 1.5 should be considered to determine the allowable stress.

(a)   (b)
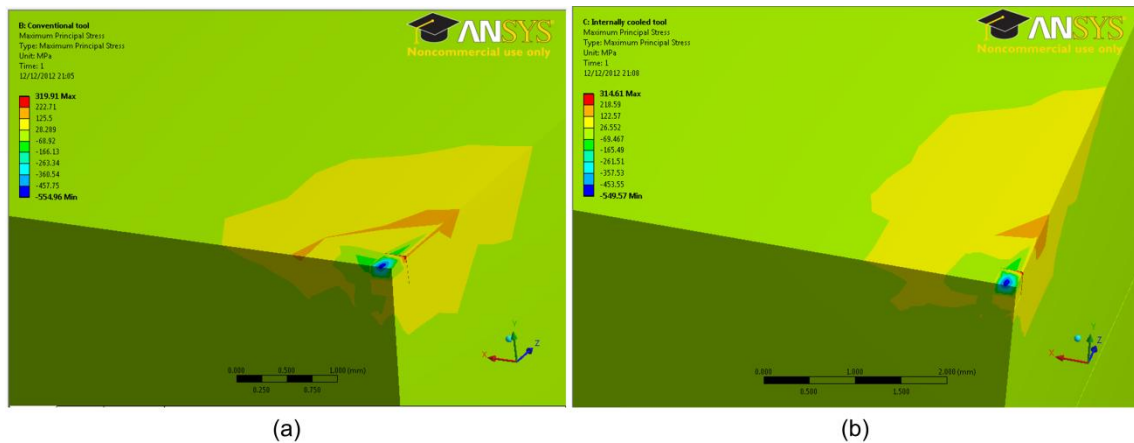
Fig. 5-3 : Maximum principle stresses in the cross sectional view of maximum distribution. (a) conventional cutting tool, and (b) internally cooled cutting tool

The pressure of the coolant on the insert wall and on the micro-channel has also been simulated. However, the pressure is too small in comparison with the materials so it can be neglected.

In a nutshell, the compressive stress, which is used as a parameter to determine the strength of a material shows that embedding a micro channel in a cutting

insert does not affect its strength. In fact the simulated compressive strength of an internally cooled cutting tool insert is still far below the allowable 1.5 safety factor which enables the cutting insert to do a more aggressive cutting or the cooling micro-duct can possibly be brought closer to the contact zone to enhance heat transfer capability (see Table 5-1).

Table 5-1: Simulated stress (see Fig. 5-3) and allowable stress for tungsten carbide insert

	Allowable	Conventional insert	Internally cooled insert
$\sigma_{(comp)}$/ GPa	1.79	0.55496	0.54957

5.2. Boundary conditions of a turning process with internally cooled cutting tools

When metals are deformed plastically, especially in conditions of high localised deformation, a significant amount of heat can be generated. As a result the temperature of the components involved in machining may be increased. The energy conversion in a machining process is not a direct process but actually a compilation of several energy formation stages. The compilation follows the theory of energy conservation where there is no energy dissipation in the system. Some energy is consumed in chip formation, whilst some others generated in the internal and on the surface of the workpiece by the processes such as:

- Plastic deformation based on the temperature distribution
- BUE
- Crack formation
- Tension on the finished surface, and
- Chemical reaction through oxidation

In DM, the heat distributes itself mainly into the workpiece, the cutting tool and the chip with the assumption that no losses of heat to the environment due to natural convection and radiation. If flood cooling is applied, a portion of heat will also be convected by the cooling fluid. In the case of application of internally cooled cutting tool in dry machining process, indirect cooling is effective as heat sink by removing the heat from the cutting tool by means of flowing fluid.

5.2.1. Heat sources

Heat sources definition is useful for the analytical analysis and the simulation of CFD, thermodynamics and wear model of the machining with internally cooled cutting tool. Generally there are three heat sources that occur in a machining process (explained in Chapter 2) and these three heat sources are also applied in a machining with internally cooled tools. As depicted in Fig. 5-4 the three heat source zones are primary shear plane, secondary shear zone and tertiary friction zone.
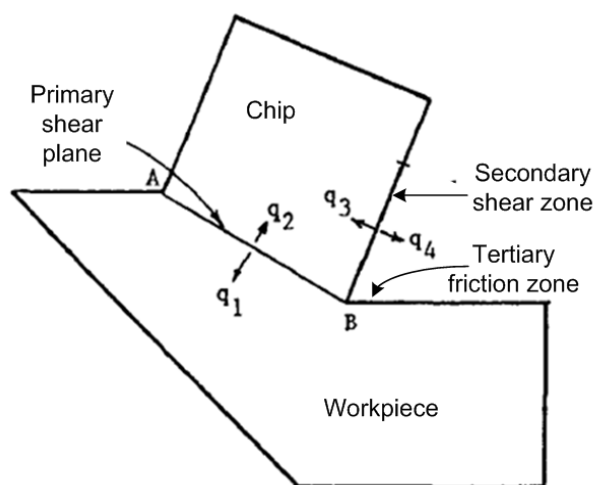
Fig. 5-4 : Heat sources and heat transfer mechanisms in DM

(Dutt and Brewer, 1964)

The primary shear zone is a free dissipation energy zone (q_1 and q_2) and the heat generated in tertiary friction zone is in the analysis and simulation negligible based on the assumption that the cutting tool is sharp. From the basic definition for the modeling and simulation of CFD and thermodynamics process of the machining with internally cooled cutting tool, the contact interface in the secondary shear zone will be considered in the simulation as input for the heat local distribution (q_4).

In a nutshell, the heat generation in machining consists of multiple complicated energy conversion process. The effort to model the temperature distribution in the machining especially inside the tool requires the representation of the thermal model to be simplified. The model representation must include the system limitations with clear definition of initial and boundary conditions.

5.2.2. Heat transfer

The heat transfer inside the cutting tool in DM can temporally be divided into three stages. The first stage is happening right in the beginning of a turning process in the heat source zones explained before, where these zones are heated up relatively quickly in a high localised manner. In the second phase of the heat transfer the enthalpy increases, i.e. the energy is stored locally and the heat is then conducted to the direct adjacent area of the cutting tool. The final stage is where the temperature is assumed to be asymptotically stable.

The heat supplied through the tool-chip contact interface and dissipated through the conduction to the chip, cutting tool and workpiece as well as lost to the environment by means of natural and forced convection must follow the law of energy conservation. Should no energy be stored or dissipated from the

controlled domain, the process will be considered as steady. The modeling and simulation of the machining process with internally cooled cutting tool only considers the case of steady state condition.

5.3.   **Computational fluid dynamics (CFD) modeling**

CFD analysis in the domain when the internal cooling is embedded in the cutting tool due to its contribution in providing fundamental influence on heat transfer needs to be performed before further analyses on thermal, mechanical and wear development can be conducted. The objectives are to obtain:

(i)   the types of flow regime, and

(ii)   the flow speed topography of the cooling fluid.

The analytical models of flow, laminar and turbulent of the cooling fluid with inhomogeneous temperature distribution as well as the heat source and the heat sink in a machining process with internally cooled cutting tool requires three partial differential equations of:

- Mass conservation energy or continuity equation
- Motion or momentum equation
- Energy equation

Governing continuity fluid equation for a fixed volume element $dV = dx \cdot dy \cdot dz$ in transient flow at time, t is given in the following equation:

$$\frac{\partial \rho}{\partial t} + \frac{\partial(\rho v_x)}{\partial x} + \frac{\partial(\rho v_y)}{\partial y} + \frac{\partial(\rho v_z)}{\partial z} = 0 \tag{5.1}$$

Since the cooling fluid will not change phase while exchanging heat, it will be considered as incompressible fluid. Thus, the following simplification valid for the:

$$\nabla v = \frac{\partial v_x}{\partial x} + \frac{\partial v_y}{\partial y} + \frac{\partial v_z}{\partial z} = 0 \tag{5.2}$$

The determination of motion equation (which is also known as a momentum equation) firstly assumes that the water as Newtonian incompressible fluid. Under consideration of Newtonian fluid the shear stress, τ can be written as:

$$\tau = \mu \frac{dv_x}{dy} \tag{5.3}$$

Newtonian fluid suggests that the shear stress, τ correlates linearly with the transverse velocity gradient dv_x/dy. The fluid which does not exhibit this property should be treated as rheology. Since the cooling fluid used in this research fits the assumption of Newtonian incompressible fluid, the Navier-Stokes equation of motion for the three dimensional fluid can be formulated in the following form:

$$\frac{dv_x}{dt} = f_x + \frac{1}{\rho}\left(\frac{\partial \sigma_x}{\partial x} + \frac{\partial \tau_{xy}}{\partial y} + \frac{\partial \tau_{xz}}{\partial z}\right) \tag{5.4}$$

$$\frac{dv_y}{dt} = f_y + \frac{1}{\rho}\left(\frac{\partial \tau_{yx}}{\partial x} + \frac{\partial \sigma_y}{\partial y} + \frac{\partial \tau_{yz}}{\partial z}\right) \tag{5.5}$$

$$\frac{dv_z}{dt} = f_z + \frac{1}{\rho}\left(\frac{\partial \tau_{zx}}{\partial x} + \frac{\partial \tau_{zy}}{\partial y} + \frac{\partial \sigma_z}{\partial z}\right) \tag{5.6}$$

Thus the above presented equations will be used to find solution for the fluid flow regime in the internally cooled cutting tool. In consequence, the heat transfer problem should be dealt with the energy equation that solved by using Fourier differential equation:

$$\frac{d\theta}{dt} = a\left(\frac{\partial^2 \theta}{\partial x^2} + \frac{\partial^2 \theta}{\partial y^2} + \frac{\partial^2 \theta}{\partial z^2}\right) \tag{5.7}$$

The exact determination of the heat transfer in laminar and turbulent flow requires a system of three partial differential equations. An integration to solve multiple number of heat transfer conditions simultaneously is not possible because of the dependent effects by the geometry, the boundary conditions (BC) and the initial conditions (Frost, 2008). Therefore, further analysis of the flow state and the calculation of the resulting flow velocity distribution is conducted on the principle of the similarity theory. A numerical calculation of the heat transfer with regards to the flow in the internally cooled tool based on the differential equation system using the CFD simulation is presented in section 5.5.

The numerical calculation of the internally cooled cutting tool requires the innovative system to be divided into three main components as in Table 5-2.

Table 5-2: The components of the IC cutting tool for CFD analysis

System components	Modeling interest
Inlet	Modeling fluid velocity distribution profile to obtain inlet BC for micro-channel.
Internal cooling micro-channel	Modeling of flow regime characteristics and heat transfer behaviour in the micro-channel.
Outlet	CFD modeling to determine outlet BC of the micro-channel.

Each component is assumed to have a circular cross section, ϕ and geometrical length, and they will be dealt separately with their unique BCs (see Fig. 5-5).

No.	Part	Length (mm)	ϕ (mm)	Surface
1	Tube	5000	2.0	Smooth
2	Hole	5.0	2.0	Smooth
3	µ-channel	10.0	0.8	Smooth
4	Heat sink	$\pi \times (3.0mm)^2 \times 0.3mm$		Smooth
5	µ-channel	12.0	0.8	Smooth
6	Hole	5.0	2.0	Smooth
7	Tube	5000	2.0	Smooth
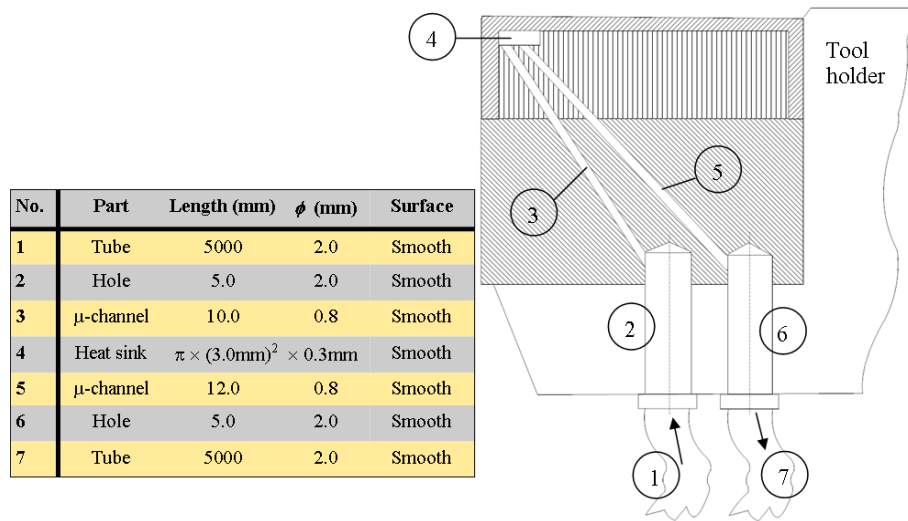
Fig. 5-5 : The components of IC smart cutting tool for CFD analysis

The modeling of the fluid behaviour at the inlet will provide important BC for the heat transfer calculation in the cooling micro-channel. The fluid speed distribution at the inlet is influenced by the pressure and mass flow rate of cooling fluid. By assuming no heat loss from the micro-channel to the adjacent tool holder and plastic tubes, the amount of heat removed by the fluid can be calculated from the equation 5.8:

$$\dot{Q}_{fluid} = (\vartheta_{fluid,inlet} - \vartheta_{fluid,outlet}) \cdot c_p \cdot \dot{V} \cdot \rho \qquad (5.8)$$

where $\dot{Q}_{fluid}$: heat removed by the fluid

ϑ: temperature

c_p: specific heat capacity

$\dot{V}$: volume flow rate

ρ: density of the fluid

The equation 5.8 can also explain the reason why water is chosen to be the cooling fluid in the internally cooled cutting tool. Besides the aspects of

availability and environmental friendliness, the physical properties of water are also an advantage in removing heat in machining with internally cooled cutting tools. Water has respectively high heat capacity and very high heat conductivity; two vital properties in determining heat removal capability of the cooling system.

Since the water will be used in the single phase cooling micro-channel, the properties of the water below the boiling point of $100°C$ are observed as in Table 5-3.

Table 5-3: Physical and thermal properties of water (Incropera and DeWitt, 2007)

Temp. ϕ °C	Density ρ kg/m³	Spec. heat capacity c_p J kg/K	Dynamic viscosity μ 10^{-6} Pa s	Kinematic viscosity ν 10^{-6} m²/s	Thermal conductivity k W/(mK)	Prandtl Number Pr
0	1000	4217	1750.0	1.789	0.569	12.99
22	998.0	4181	959	1.006	0.606	6.62
42	991.1	4179	631	0.658	0.634	4.16
62	982.3	4186	453	0.478	0.656	2.88
82	970.9	4199	343	0.364	0.671	2.14
100	957.8	4217	279	0.294	0.680	1.76

5.3.1. Internal cooling fluid velocity

The modeling of cooling fluid velocity is based on the approximation analysis of an incompressible fluid. The observation of the friction loss and resistance loss of the fluid in the cooling micro-channel is formulated in the following mathematical term of pressure drop, Δp (Incropera and DeWitt, 2007):

$$\Delta p = \left(\lambda \cdot \frac{1}{d}\right)\frac{\rho \cdot v^2}{2} + \sum \zeta \cdot \frac{v^2}{2} \qquad (5.9)$$

where λ: channel friction coefficient

d: diameter of the internal channel

ρ: density of the used fluid

v: flow velocity

ζ: friction coefficient of the channel

The first term on the right hand side of the equation 5.9 is for the friction loss and the second term on the right hand side of the equation is for the resistance loss in the integrated cooling tool.

Basic aspect in the CFD modeling of the cooling fluid in the internally cooled cutting tool is the flow types of the fluid regime; i.e. laminar flow and turbulent flow. Internal flow is used as the domain for the modeling. In an internal laminar flow, the fluid particles flow in streamlines parallel to the domain axis. The streamlines are assumed to never intercept with each other. In stationary laminar flow the fluid velocities at an arbitrary location in the domain is always constant at all time. In stationary turbulent flow, the flow speed distribution is changing by time but the mean speed is maintained constant. The fluid particles become chaotic and high speed of the particles is observed across the mean fluid speed vector which consequently affects the momentum exchange and heat transfer behaviour in radial direction. Thus, a better heat distribution per overall cross sectional area of the fluid is obtained with the turbulent flow, whilst in laminar flow the heat transfer across the flow direction is merely by means of convection (Launder and Sharma, 1974). The observation gives in-depth understanding in designing aspects of the internally cooled tool with the objectives to achieving high heat transfer rate.

The fluid behaviour will affect the cooling capability of the internally cooled cutting tools. As described in Chapter 2, two non-dimensional parameters used to represent fluid flow are the Reynolds number, Re, and the Darcy's friction factor, f_0. Re, which generally defined as the ratio of forces interaction, is useful in characterising the type of fluid regime in micro-channels.n In smooth pipe Re values for internal flow between 2300 and 4000 are assumed to be transition laminar to turbulent regime (Joseph and Yang, 2010). As shown in the equation 5.10 the Re can be written as a function of the density, ρ, speed, v, and dynamic viscosity, μ of a fluid and the length of the channel.

$$Re = \frac{\rho \cdot v \cdot L}{\mu} \qquad (5.10)$$

By considering the mass flow rate, $\dot{m}$ of the fluid and assumption of mean fluid speed in a closed conduit, Re can be re-written as

$$Re = \frac{2\dot{m}}{\pi r \mu} \qquad (5.11)$$

where r is the radius of the micro-channel.

The equation 5.11 can be also re-written in the function of fluid average velocity, v, length, L and kinematic viscosity, ν as below:

$$Re = \frac{v \cdot L}{\nu} \qquad (5.12)$$

For non-circular tubes, Re is determined by hydraulic diameter, D_h. Thus, Re can be defined in the function of wetted perimeter of a duct, p as:

$$Re = \frac{4\dot{m}}{\mu \cdot p} \qquad (5.13)$$

where

$$D_h \equiv \frac{4A_c}{p} \qquad (5.14)$$

At the point of transition the value of Reynolds number is known as critical Reynolds Number, Re_{crit}. As mentioned before, the transition from laminar to turbulent in an internal pipe can happen in the region of $2300 > Re_{crit} > 4000$. As a guideline for modeling it can generally assumed that beyond $Re = 2320$ the fluid behaves in turbulent manner (Incropera and DeWitt, 2007).

For modeling purposes, the flow velocity is assumed with its mean velocity at water temperature of 20°C. The Reynolds number of the flow at each component as defined in Fig. 5-5 is then calculated. The results of the calculation are recorded in Table 5-4. The results show that Reynolds number are distributed in the range of 528 and 6604. In the table, the grey highlighted Reynolds numbers are the numbers that are higher than 2320 which indicates turbulent flow.

Table 5-4: Reynolds number of the cooling fluid (20°C) flow inside the parts of internally cooled cutting tools.

Volumetric rate l/min	Reynolds Number						
	Part 1	Part 2	Part 3	Part 4	Part 5	Part 6	Part 7
0.1	528	528	1321	2553	1321	528	528
0.2	1057	1057	2641	5107	2641	1057	1057
0.3	1585	1585	3962	7660	3962	1585	1585
0.4	2113	2113	5283	10214	5283	2113	2113
0.5	2641	2641	6604	12767	6604	2641	2641

By taking the assumption that the flow with Re>2300 is turbulent, it can be seen in Table 5-4 that the majority of the flow types in part 3 and 5 (the micro-channels) is turbulent. Only for the flow rate of 0.1 l/min laminar flow can be obtained throughout the internally cooled cutting tool. Based on the advantage of turbulent flow in exchanging heat as explained before, it is specially intended to have high turbulent flow in the Part 4 (heat sink). Thus, minimum volumetric rate of 0.3 l/min is safe to be supplied by the pump in order to ensure the turbulent flow in the micro channel, which consequently can allow the cooling device to achieve the optimal heat transfer.

With this mass flow rate it is predicted a fluid with Reynolds number of 3962 will flow in the internally cooled cutting tool. The Reynolds number is significantly high to explain the turbulent flow regime in the micro-channel. It is also worth mentioning that the volumetric rate of 0.2 l/min is also considered to be used in this experiment if the pressure drop resulted with 0.3 l/min volumetric rate is too high for the pump.

Based on the assumption that the fluid is Newtonian; an important characteristic of this fluid is that the tangential force (shear stress) is proportional to the fluid velocity. Hence, this means that the fluid has only small resistance to any deformation. Due to viscosity the fluid velocity gets smaller in the flow profile. In the middle of the flow the velocity of the fluid is the highest whilst the velocity in the direction of flow gets smaller as the observation goes towards the boundary layer of the flow (almost zero velocity). So the boundary conditions when the internal pipe radius is R can be written as follows:

$$r = R : v = 0$$
$$r = 0 : v = v_{max}$$

For the laminar flow in a circular cross sectional pipe based on the Stoke's law (Incropera and DeWitt, 2007) is:

$$v(r) = \frac{\Delta p}{4 \cdot \eta \cdot l} \cdot (R^2 - r^2)$$

(5.15)

Based on the formula it can be predicted the temperature distribution profile will be parabolic.

Different flow behaviour occurs in turbulent flow especially in the fluid region near to the pipe wall. The velocity profile of a turbulent flow in the region near to the entrance of the pipe is visualized based on the theory in Welty (2008) and Incropera and DeWitt (2007) in Fig. 5-6. It can be seen in the turbulent region there is a quasi-laminar sublayer near to the pipe wall with the thickness of the quasi-laminar sublayer is represented by t_{sl}.
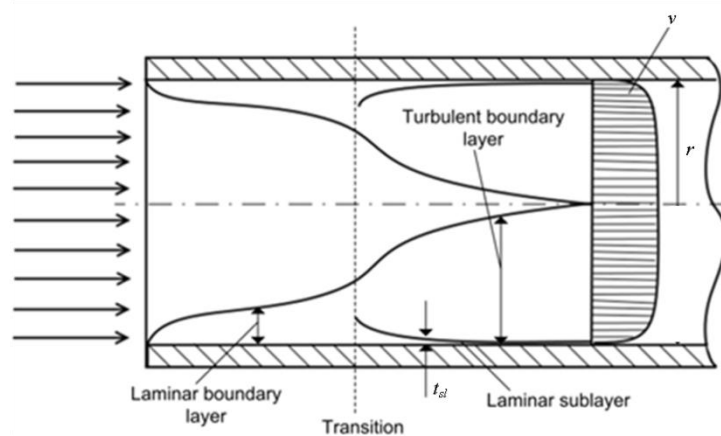
Fig. 5-6 : Velocity profile in turbulent flow in the region near pipe entrance

In the fully developed region of the fluid the velocity profile of the fluid flow is parabolic; same as in laminar flow. The boundary conditions are dependent on the fluid viscosity, average fluid velocity and the surface roughness of the domain. The bigger the Reynolds number the flatter (less parabolic) the velocity profile of the fluid flow in the fully developed region will be.

To map a velocity profile, it is required to determine the length for the velocity profile to be fully developed after entering the component of the pipe. The length is commonly represented as entrance length, l_e. The formula to measure the l_e in laminar regime is written below (Welty, 2008):

$$l_{e,laminar} = d \cdot 0.0575 \cdot Re \tag{5.16}$$

Where d is the diameter of the micro-channel (equals to $2r$ as in Fig. 5-7)

There is no report available on the prediction of entrance length for a fully developed turbulent velocity profile. Therefore, for modeling purposes of the flow inside the parts of the micro-channel with turbulent regime is assumed to be fully developed.

The main difference in flow velocity profile function between the turbulent and laminar flows are that in a fully developed flowthe Reynolds number does not play any influence in determining the velocity profile of turbulent flow. This is supported and explained by Prandtl deviation in interpolation formula for fluid velocity profile (Frost, 2008):

$$\frac{v}{v_{max}} = \left(1 - \frac{r}{R}\right)^{\frac{1}{n}} \tag{5.17}$$

In this equation R is the external pipe radius and r is the internal distance in radial direction from the pipe axis. The exponential function $1/n$ is a slowly function of Reynolds Number and the surface roughness of the wall. The exponent n is found to vary from a value of 6 at $Re=4000$ to 10 at $Re=3,200,000$ and n is taken as 7 at Reynolds number of 10^5 (Welty, 2008).

To determine the velocity profile and the velocity, v of the flow, the maximum velocity, v_{max} should be identified first. Generally the average fluid velocity can be calculated with the equation 5.18 (Welty, 2008):

$$\bar{v} = \frac{\dot{V}}{A} = \frac{2}{R^2} \int_0^R v(r)dr \tag{5.18}$$

Substituting the radius value in the Prandtl derivation in the equation 5.18 produces an equation that describes the ratio of the average fluid speed to the maximum inlet speed as follows:

$$\frac{\bar{v}}{v_{max}} = \frac{2 \cdot n^2}{(n+1) \cdot (2n+1)} \tag{5.19}$$

Considering Part 3 (refer Fig. 5-5) with the Reynolds number of 3962 and n value of 4 when a mass flow rate of 0.3 l/min is supplied, the maximum velocity in the stationary turbulent region is 5.61 m/s and when the equation above is applied will yield an average middle velocity of 3.99 m/s.

So the complete velocity profile of fluid in the micro-channel can be formulated in an equation to be used as boundary conditions for the later CFD simulation as follows:

$$v(r) = 5.61 \cdot \left(1 - \frac{r}{0.0004}\right)^{\frac{1}{4}} \frac{m}{s} \tag{5.20}$$

As stated in the theory, the fluid velocity at the wall of the conduit is zero. The isotach of the velocity is in circular form about the conduit axis. The velocity profile properties of the other main parts of the internally cooled cutting tool are compiled in Table 5-5.

Table 5-5: Fluid profile properties in turbulent regions

Part	D mm	$\bar{v}$ m/s	Re	n	v_{max} m/s
1	2.0	0.0008	1584.9	N/A	0.0016
2	2.0	0.159	1584.9	N/A	0.319
3	0.8	0.3986	3962.2	4	5.61
4	0.3	7.706	7660.1	6.3	9.74
5	0.8	0.3322	3962.2	4	4.66
6	2.0	0.16	1584.9	N/A	0.322
7	2.0	0.0004	1584.9	N/A	0.0008

Based on the mathematical model presented above, the pressure drops and friction coefficient can be calculated. The pressure drop, $\Delta p = p_1 - p_2$ associated with fully developed flow from the positions along the axis of the tube identified as x_1 and x_2 may be expressed as

$$\Delta p = -\int_{x_2}^{x_1} dp = f\frac{\rho u_m^2}{2D}\int_{x_2}^{x_1} dx = f\frac{\rho u_m^2}{2D}(x_2 - x_1) \tag{5.21}$$

where f is a friction factor. For fully developed laminar flow f is given as

$$f = \frac{64}{Re} \tag{5.22}$$

The analysis of friction factor for fully developed turbulent flow is complicated and commonly obtained empirically. The Re for turbulent flows predicted in the internally cooled cutting tool when is supplied with 0.3l/min mass flow rate of coolant satisfies the correlation proposed by Petukhov (Petukhov, 1963):

$$f = (0.790 \cdot \ln Re - 1.64)^{-2} \tag{5.23}$$

$$3000 \lesssim Re \lesssim 5 \times 10^6$$

The pump required to overcome the resistance to flow associated with this pressure drop may be expressed as:

$$P = (\Delta p)\dot{\forall} \tag{5.24}$$

Where $\dot{\forall}$ is volumetric rate which in an incompressible fluid may be expressed as

$$\dot{\forall} = \dot{m}/\rho \tag{5.25}$$

Table 5-6 shows the analytical results of the pressure drop, Δp and pressure required, P by the pump to flow the cooling fluid with the mass flow rate of 0.3 l/min to pass through each section of the internally cooled cutting tool.

Table 5-6: Pressure drop and pressure required to flow the coolant in the internally cooled cutting tool

Part	D_h m	Length m	Re	f	u_m m/s	Δp Bar	P Bar
1	0.002	5	1585	0.04038	0.00080	0.00003	0.00016
2	0.002	0.005	1585	0.04038	0.31888	0.00512	0.02557
3	0.0008	0.01	3962	0.04157	0.39860	0.04120	0.20565
4	0.0005	0.0005	7660	0.03397	7.70600	0.21814	1.88758
5	0.0008	0.012	3962	0.04157	0.33217	0.03434	0.17137
6	0.002	0.005	1585	0.04038	0.32218	0.00523	0.02610
7	0.002	5	1585	0.04038	0.00081	0.00003	0.00016

5.4.   Thermodynamics analysis and modeling

5.4.1. Heat transfer in internally cooled cutting tool

The result from the CFD analysis are utilised in thermodynamics analysis in order to simulate the performance of the internally cooled cutting tool in

machining. The heat transfer in turning process only considered the cutting tool as domain. The energy transferred to the cutting insert in the form of heat will be modelled and simulated.

Considering Fourier's law, one dimensional heat transfer can be expressed in the form of heat flux in the function of temperature gradient as:

$$\dot{q} = -k\frac{\partial \theta}{\partial x} \qquad\qquad (5.25)$$

The negative sign indicates the direction of heat transfer from high temperature to low temperature. The above equation can be re-written in the form of heat flow as:

$$\dot{Q} = \dot{q} \cdot A = \frac{k}{x}(T_1 - T_2) \cdot A \qquad\qquad (5.26)$$

The notations used are as illustrated in Fig. 5-7.
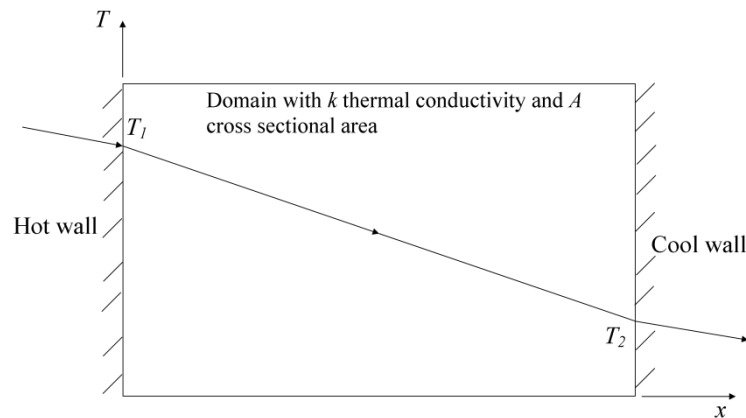
Fig. 5-7: Heat conduction between two walls of different temperatures

5.4.2. Factors influencing heat transfer

The study of heat removal rate of the internally cooled cutting tools requires the fundamental understanding on the important factors that can increase heat transfer. Based on the equation 5.26, it can be formulated that the rate of heat transfer increases when the thermal conductivity of the material is high, or

when the temperature difference or the temperature gradient is enlarged or when the heat flux is applied at a bigger area. The transfer rate of heat can also be improved by reducing the distance between the hot and cold walls.

Based on this argument, the improvement of heat transfer rate of the internally cooled cutting tools with specific pre-determined tool geometry and tool material can only be realized by either minimising the distance between the heat source and the heat sink or by reducing the internal cooling fluid.

The reduction of the distance between the effective internal cooling micro-channel and the cutting edge must be critically designed so that the critical minimum distance which can weaken the mechanical structure of the cutting insert can be avoided. As discussed in Chapter 4, the FEM models of the internally cooled cutting tools are simulated against mechanical stresses in machining and a comparative study against the conventional solid cutting insert is performed.

5.4.3. Heat transfer in 3D

Based on the principle of energy conservation in the first law of thermodynamics the equation for 3D heat transfer can be derived as in equation 5.27 (Incropera and DeWitt, 2007).

$$\rho \cdot c_p \left(\frac{\partial T}{\partial t} \right) = k \left(\frac{\partial^2 T}{\partial x^2} + \frac{\partial^2 T}{\partial y^2} + \frac{\partial^2 T}{\partial z^2} \right) + \dot{q}_i \tag{5.27}$$

The left term, which is a function of material density, ρ, heat capacity at constant pressure, c_p, temperature difference, ∂T, and elapsed time, ∂t, indicates the amount of heat stored in the volume element and the right hand

terms comprise the amount of heat flow in each direction vector (x, y and z). $\dot{q}_i$ in particular represents the amount of heat generated as well as absorbed by the controlled volume. With this governing equation the thermal behaviour in a smart cutting tool with internal cooling can be modeled and analysed by means of coupling with the result from CFD analysis.

(1) By experiment, boundary condition of temperature in the function of displacement and time can be determined.

(2) The result can be used to correlate the heat flux normal to the contact area with the displacement and time through following relationship:

$$-k\frac{\partial T}{\partial n}\bigg|_t = q''$$

(5.28)

(3) This result can then be utilised as boundary conditions in the heat transfer simulation of internally cooled cutting tool using ANSYS Fluent.

The amount of heat removed by the internal cooling fluid can be calculated by:

$$\dot{Q} = h \cdot A \cdot \left(T_t - T_f\right)$$

(5.29)

with A is the tool-chip contact area, T_t is the internal surface temperature, T_f is the mean fluid temperature and h, the convection heat transfer coefficient which can be expressed in the form of

$$h = \frac{\dot{Q}}{\left(T_t - T_f\right)}$$

(5.30)

The heat transfer coefficient can be calculated using Nusselt number (Incropera and DeWitt, 2007).

$$h = Nu \cdot \frac{\lambda}{d_{hyd}} \tag{5.31}$$

Since heat is transferred by means of forced convection in internally cooled cutting tool, the Nusselt-number is a function of Reynold's number and Prandtl number (these numbers have been determined in the CFD analysis section.)

$$\overline{Nu} = \frac{\overline{h}L}{k_f} = f(Re_L, Pr) \tag{5.32}$$

$\overline{h}$: convection heat transfer coefficient
L: characteristic length $\left(\frac{surface\ area}{perimeter}\right)$
k_f: thermal conductivity of fluid

There are several empirical correlations published by previous researchers such as Hausen, Gnielinski and Kraussold (reported by Frost (2008)), but it has been studied that the results of each correlation do not have much different. Hence, the correlation obtained from the theory of the boundary layer for the forced convection in turbulent flow is used.

$$Nu = 0.03965 \cdot \frac{Re^{0.75} \cdot Pr}{(1 + 0.35 \cdot (Pr - 1))} \tag{5.33}$$

Using equation 5.33, Nusselt number at the heat sink segment (part 4) for cooling fluid with corresponding Reynolds number and Prandtl number for different fluid temperatures (as listed in Table 5-3) have been calculated and shown in Table 5-7. Consequently, heat transfer coefficient can be calculated using the obtained Nusselt number.

Table 5-7: Nusselt numbers and heat transfer coefficients of internally cooled cutting tool for the temperature range of 0°C to 100°C

θ_f, °C	Pr	Re	Nu	h, W/m²K
0	13.749	4302	53.01729	6.66E+04
20	7.024	7660	73.36149	9.22E+04
40	4.350	11784	89.79043	1.13E+05
60	3.025	16370	101.5847	1.28E+05
80	2.221	21754	110.5146	1.39E+05
100	1.744	27307	116.5423	1.46E+05

With the heat transfer coefficients obtained as in Table 5-7, the amount of heat removed can be calculated based on the simulation result by ANSYS CFX that will be performed in the next section (Section 5.5).

5.5.   CFD simulation on the internally cooled cutting tool with thermal loads

CFD simulation and thermal analysis of internally cooled cutting tool are performed with the strategy summarised as follows:

(1) Apply and simplify CAD model of internally cooled cutting tool from Chapter 4

(2) Define boundary conditions with the selected mesh

(3) Perform CFD simulation and thermal analysis

(4) Analyse the results of the simulation

(5) Design optimisation

There are several numerical methods to be used in solving CFD and thermodynamics problem such as Finite Different Method (FDM), Finite Volume Method (FVM) and Finite Element Method (FEM). The CFD simulation and thermal analysis of internally cooled cutting tools are performed with the simulation software ANSYS Workbench with Fluent.

The CAD model was developed with the software Pro/Engineer and later the model was transferred for the simulation, which was performed on the platform ANSYS Workbench R13.0.

5.5.1. Modeling and defining boundary conditions

The key step in 3D simulation of CFD and thermodynamics for the cooling liquid in the micro–channel are the correct mesh size for CAD model and the establishment of boundary conditions.

Critical attention needs to be paid in meshing the CAD model for CFD and thermodynamics analysis as the model consists of structural and fluid parts. Unsuitable mesh particularly for internally cooled cutting tool may result in divergence solution or conflict for the software in performing fluid-solid interaction computation.

The meshing methods and the example of meshed internally cooled cutting tool are shown in Fig. 5-8.

Meshing methods:
Tool holder: Patch independent method
Cutting insert: Patch conforming method
Contact zone: sweeping method
Fluid in micro channel: Programmed
controlled 5 layers inflation

Number of nodes: 1256131
Number of element: 725983
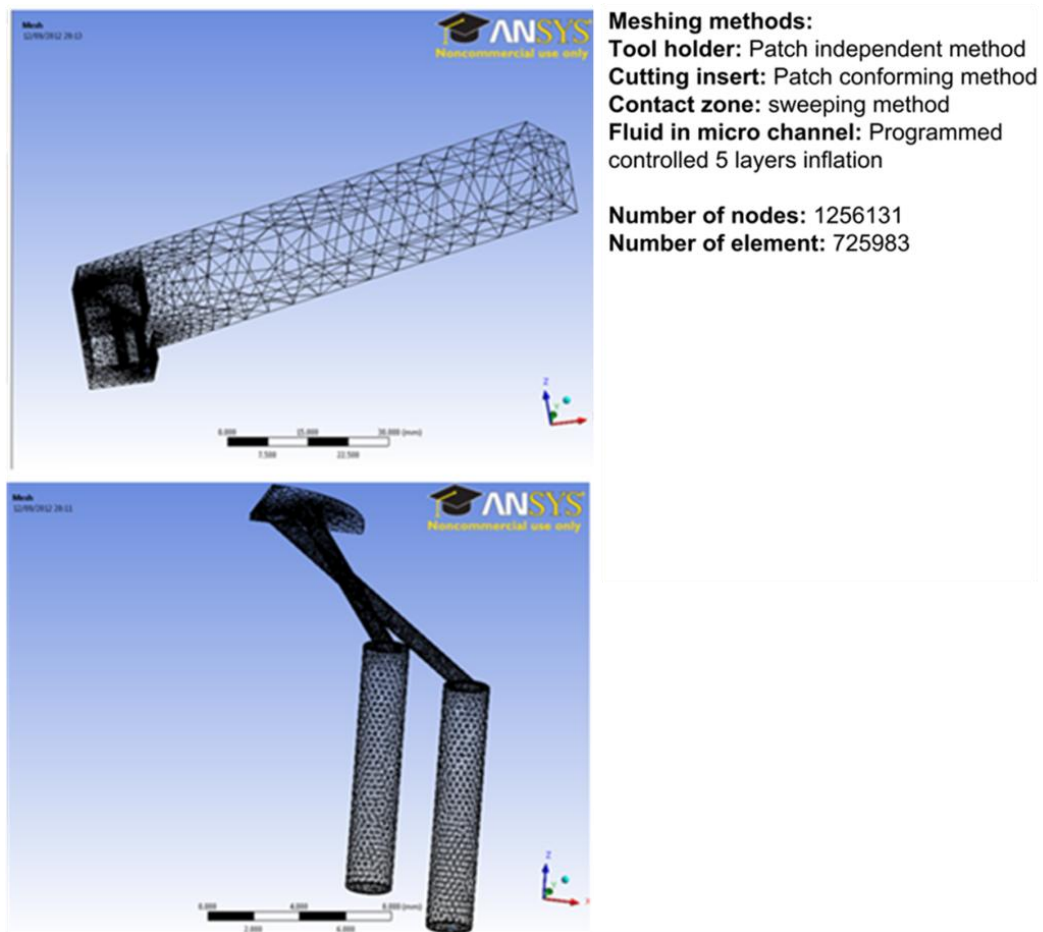
Fig. 5-8 : Meshing of the internally cooled cutting tool

The complete development of CAD model and suitable meshing lead to the next development steps, i.e. setting of boundary conditions, selection of turbulent model and determining the solving algorithm. The CAD models and mesh selection for conventional tool (Fig. 5-10 (a) and Fig. 5-10(c) respectively) and for internally cooled smart cutting tool (Fig. 5-10 (b) and Fig. 5-10(d) respectively) has been simplified from the actual aesthetic geometry to enlighten computational process.

The boundary conditions consider the heat source from the machining, the heat transfer with the ambient and the heat transfer and fluid dynamics of the cooling fluid in the micro-channel. The study of the boundary conditions from

the heat source at the contact zone has been conducted in the section 5.4.1. The required cooling fluid parameter as discussed in section Computational fluid dynamics is set to the cooling boundary conditions. Other surfaces except the end of the tool holder were set to be adiabatic and the end the tool holder is set at ambient temperature. Ambient temperatures considered are in the range of 20°C to 30°C. Adiabatic boundary condition for the rest of exposed surface is based on the boundary conditions set by Tay et al. (1974).
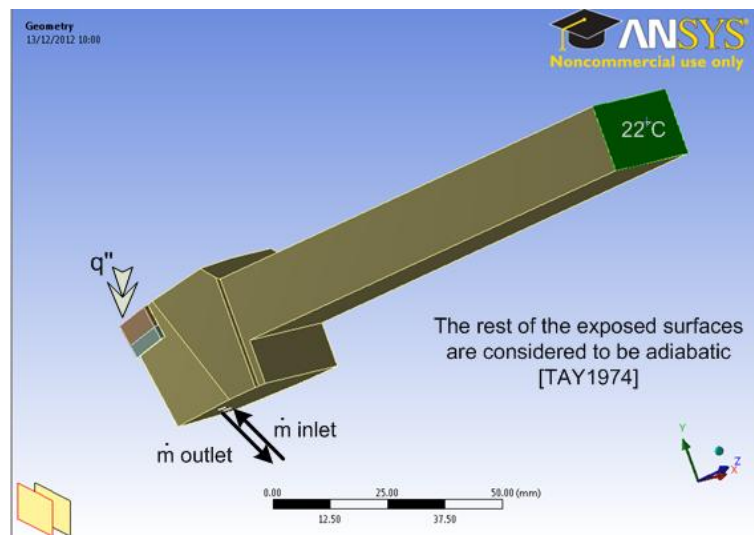
Fig. 5-9 : Boundary conditions for CFD and thermodynamics analysis

The $\kappa - \varepsilon$ model has been chosen for the computation of CFD model in ANSYS Fluent software. Among the available commercial CFD software, these are the most widely used to model the turbulence. The main advantage of utilising this model is due to its modeling cost-benefit ratio. The cost that is meant here is the cost of time to run this model and the associated computational hardware. The particular benefit of this model is the high quality of the computed results. The basic equations for this model are not going to be included here. Launder and Sharma has written a good explanation about this model in their publication (Launder and Sharma, 1974). The fundamental of the model is based on the

solution of two transport equations that represent the turbulent properties of a flow. The first transported variable is κ, the turbulent kinetic energy that determines the energy in the flow, whereas the second transported variable is ε, the turbulent dissipation that determines the scale of the turbulence. The precondition for the application of the model is a fully developed turbulent flow. Basically turbulence models are used in addition to the direct numerical solution (DNS) of the conservation equations for mass, momentum and energy. However, computation of the conservation equations by DNS is limited by the available computing power, thus turbulence models like $\kappa - \varepsilon$ is used. The turbulence modeling allows an approximation flow behaviour description and thus enables the computation of the turbulent flow with the computer hardware resources available at Brunel Univeristy. The basic idea of turbulence modeling is that the turbulent flow should not be accurately modelled in terms of spatial and temporal. Instead, the flow variables are modeled by dividing them into a time-average value and an associated amount of fluctuation. This division is based on the Reynolds equation. Based on the division, the system equation that is yielded from the energy conservation equations can be averaged. The additional unknowns appear as the correlation factors in Reynolds stress. This fluctuation value contains the information that has been removed by the time averaging the instantaneous values (Launder and Sharma, 1974). Different approaches can be used to model these tensors and one of them is $\kappa - \varepsilon$ model.

In addition to the turbulence model a selection of the numerical solution algorithm is required. This is due to the fact that there is no separate equation for the pressure in the Navier-Stokes equations. Pressure derivation is part of the equation system, which is composed of the conservation laws of mass, momentum and energy, but the continuity equation does explicitly contain

pressure. This makes the solution of this equation system gets more difficult. The presented cooling system is based on internal circulation of water, thus the coolant used is an incompressible fluid. The incompressible fluid, in contrast to compressible fluid, does not dependent on pressure and density. Therefore, the continuity equation provides no information on the present pressure field.

In ANSYS Fluent a list of pressure correction schemes called "Pressure-Velocity Coupling" is available to carry out the numerical calculation of the pressure to solve the problem. The basic approach here is firstly, to calculate the velocity components of the momentum equations. The obtained velocity components are then corrected together with the pressure by a pressure correction procedure in accordance with the continuity equation. Overall, this is an iterative process until the continuity equation and the momentum equations are satisfied. ANSYS Fluent provides four pressure-velocity coupling algorithms to perform the iteration.

    (1) SIMPLE (Semi-Implicit Method for Pressure Linked Equations),

    (2) SIMPLEC (SIMPLE-Consistent)

    (3) PISO (Pressure Implicit solution by Splitting of Operators) and

    (4) Coupled

SIMPLE algorithm that was developed based on Patankar (Patankar, 1980) is a widely-used pressure-velocity coupling scheme and was also used in this simulation. The corrective procedure in the scheme uses a relationship between velocity and pressure corrections to enforce mass conservation and to obtain the pressure field. One problem with the SIMPLE scheme is that it can be rather slow. Alternative to SIMPLE, ANSYS Fluent user can also chooses SIMPLEC algorithm, which has similar procedure to the SIMPLE but SIMPLEC uses

different expression for the face flux correction to accelerate the convergence. PISO algorithm, which is also an improvement to SIMPLE algorithm offers improvements to the calculation efficiency by performing additional corrections, i.e. momentum correction/ neighbour correction and skewness correction. These two corrections basically help the new velocities and the corresponding fluxes to satisfy the momentum balance after the pressure-correction equation is solved. Coupled algorithm is the coupling of these Skewness- Neighbour corrections. This algorithm offers a more accurate adjustment of the face mass flux correction especially for models with high degree of skewness by using the normal pressure correction gradient.

Correct setting of computational options and boundary conditions means that the smooth running of CFD simulation. 500 iterations have been selected to allow the computation to reach convergence. The simulation results can be analysed straight from the ANSYS Workbench interface.

5.5.2. CFD analysis and simulation on thermodynamics of internally cooled cutting tools

The results of CFD and thermodynamics simulation will be analysed from the following three points of view.

(1) Cutting temperature reduction in application of internally cooled cutting tools.

(2) CFD model to predict maximum cutting temperature.

(3) Heat transfer between the solid and cooling fluid.

Fig. 5-10 (e) and Fig. 5-10 (f) show simulated temperature distribution on cutting tool when machining mild steel EN32B at cutting speed 250 m/min,

feedrate 0.2 mm/rev and depth of cut 0.5 mm for conventional cutting tool and internally cooled cutting tool respectively.
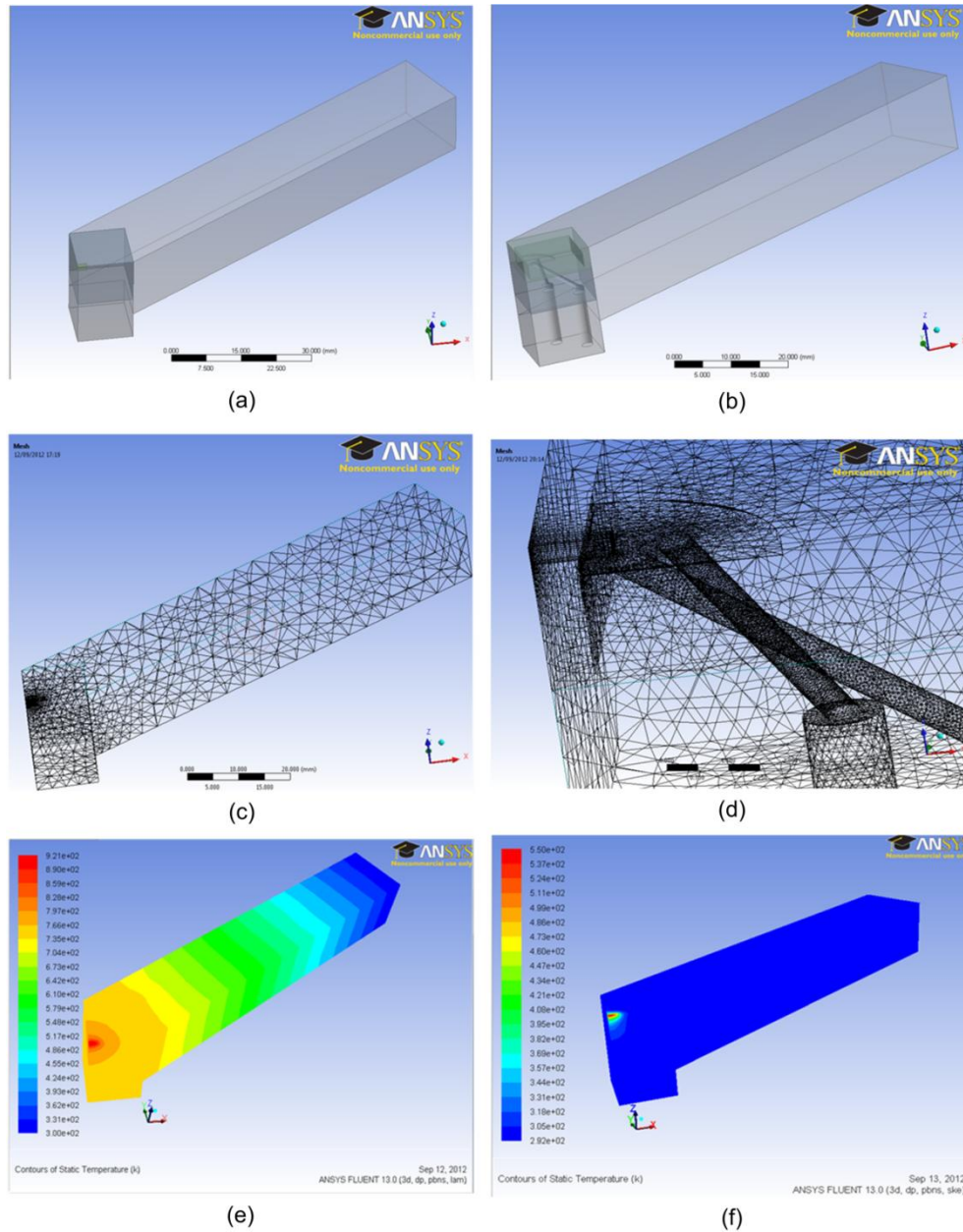
Fig. 5-10 : CFD simulation of heat transfer when machining of steel EN32B with carbide inserts at cutting speed 250 m/min, feedrate 0.2 mm/rev and depth of cut 0.5 mm

Cooling fluid with volume flow rate of 0.3 l/min has been supplied internally to the cutting tool through a micro-channel of 0.8 mm diameter. The simulation result shows that the maximum temperature of 921K recorded on conventional tool could be reduced to 550K by applying internally cooled cutting tool. The temperature distributions between the two tools show a significant different trend as well. Temperature rise on the tool holder is almost insignificant when internally cooled cutting tool is applied. The result gives good indicator that the cooling system is adequate to absorb the transferred heat to the tool.

The results of the simulation of cooling fluid are shown in Fig. 5-11. In the Fig. 5-11(a) the maximum temperature of the fluid is 326.3K (53.3°C) which is well below the boiling point of water. The temperature difference simulated between the inlet and outlet is approximately 10°C. Fig. 5-11(b) displays the velocity distribution of water in the internal cooling manifold. The agreement of the simulated model with continuity theory should be validated by the amount of fluid supplied and removed from the domain.
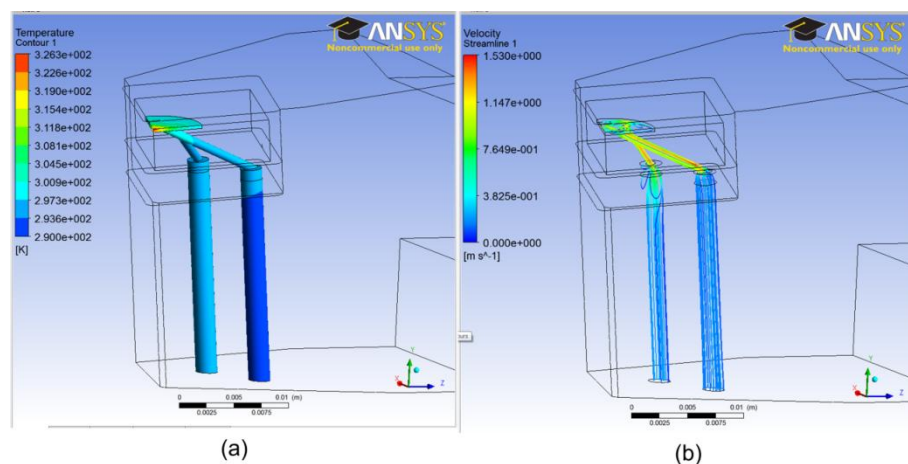
Fig. 5-11 : Cooling fluid's CFD and heat transfer simulation results: (a) fluid temperature distribution, (b) fluid velocity distribution

A monitor line has been drawn along the diagonal surface of each cutting insert starting from the cutting edge to investigate the temperature propagation in the tool. It can be seen in Fig. 5-12 that both cases (conventional uncooled tool and internally cooled tool) exhibit sharp drop of cutting temperatures after the cutting edge and the temperature attenuates linearly within the distance of 2 mm from the cutting edge and the curves exhibit exponential decay afterwards. The temperature of the cutting tool at the position further than 2 mm is approximately similar as ambient temperature (305K) with the application of the internally cooled cutting tool whilst the temperature inside the conventional uncooled cutting tool is still high (600K).

Uncooled conventional tool   Internally cooled tool

Tool material: Tungsten carbide
Cooling fluid: Water
Coolant speed: 0.3 l/min
Microchannel diameter: 800μm
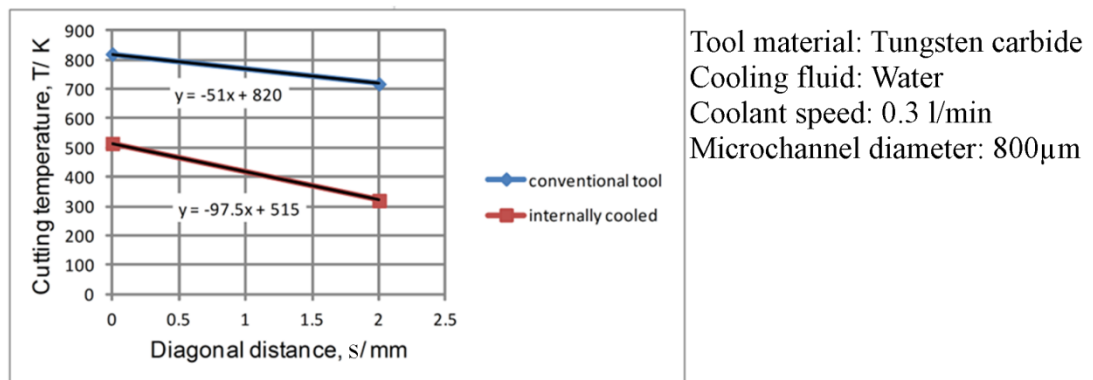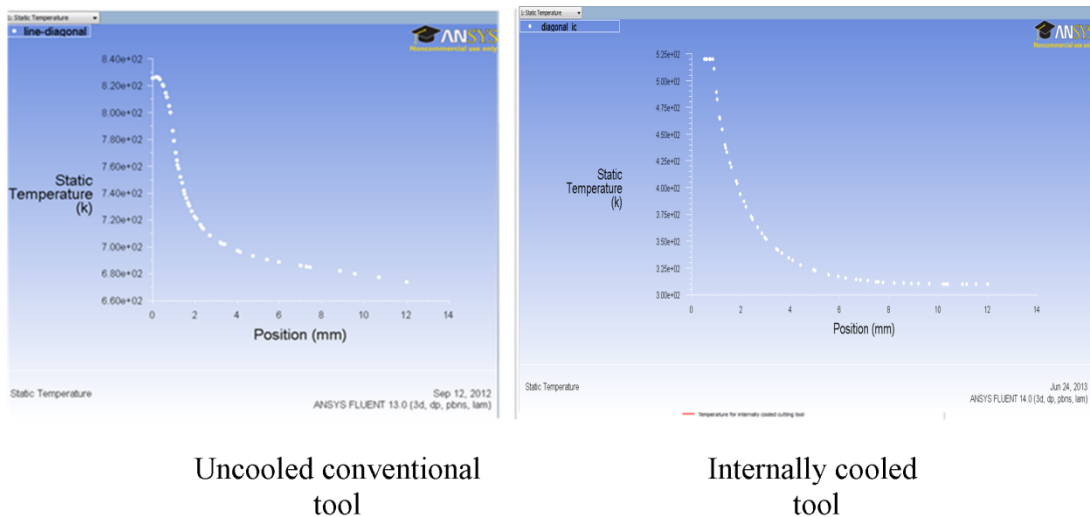
Fig. 5-12 : Temperature from the cutting edge along the diagonal of the insert

The relationship of the cutting temperature and the distance, s in mm is useful for prediction of maximum cutting temperature, T_{max} in actual machining. T_{max} can provide information about process phenomena such as BUE, tool failure or surface finish quality. Linear relationships between T_{max} , s and measured temperature, T_{meas} within 2 mm distance along the rake face for both tools are as follows:

Conventional tool: $T_{max} = 51s + T_{meas}$

Internally cooled tool: $T_{max} = 97.5s + T_{meas}$

The relationships correlate well with the conductivity theory:

$$T_{max} = \frac{\dot{q} \cdot s}{k} + T_{meas} \tag{5.34}$$

5.5.3. Validation of the simulation of CFD and heat transfer

The CFD model has been validated with experimental trials. For this purpose aluminium alloy AA6082 has been machined with a carbide tool at a set of uniform cutting parameter but with variations of supplied mass flow rate. The coolant has been pumped at 9 levels of flow rate as shown in Fig. 5-13. AA6082 was used in this experiment because of its low wear rate on carbide tool. This can enable a single edge of a carbide insert to be used for the whole experiment. The experimental setup is the same as in Chapter 4. Besides validating the result at the measured points, the ability of internally cooled cutting tool to reduce the cutting temperature can also be observed.

From the experiment (Fig. 5-13), it can be concluded that (i) internally cooled cutting tool can reduce the cutting temperature, (ii) both simulation and experiment agreed that the changes in cutting temperature is very marginal when the flow rate is changed and (iii) discrepancies of about 10% -15% should be expected when predicting a cutting temperature with the developed model.
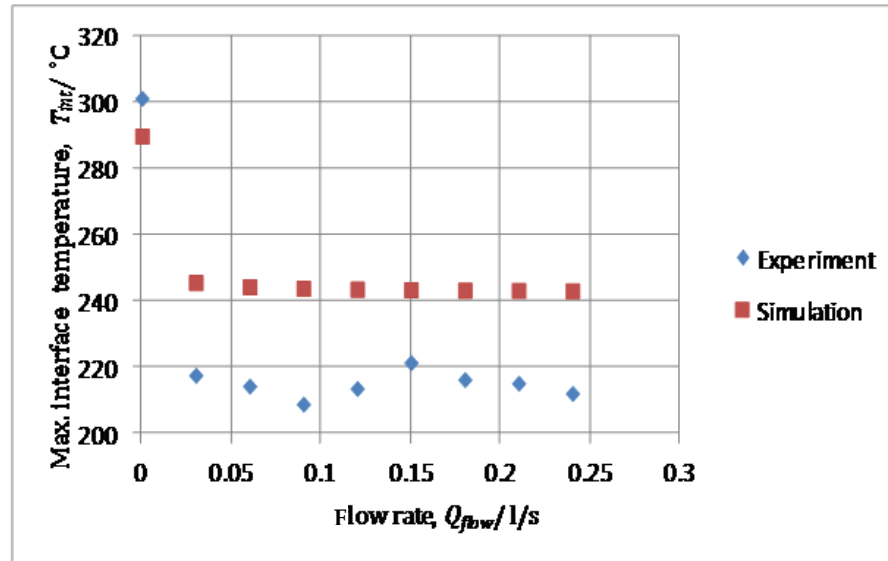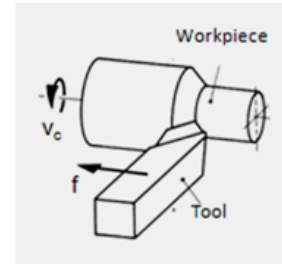
Fig. 5-13: Validation of CFD model with cutting trials

5.5.4. Optimisation of internally cooled cutting tool for application in adaptive machining

Optimisation of cooling geometry for this research has been performed and published by Sun et al. (2011) and Che Ghani et al. (2011). The optimisation results showed that micro-channel diameter, the distance between the nozzle (channel's end that closest to the heat source) and the downside of the insert, the thickness of the insert and the thickness of side wall of an insert do not interact with each other in influencing cooling capability.

The most pronounced factor that affects the effectiveness of the cooling is the size of the micro-channel. This is aligned with the theory that the bigger the contact size the bigger heat transfer coefficient will be.

5.6.   Tool wear

During the cutting process, the tool removes a certain part of a workpiece by a process of intense plastic deformation at high strain rate within the shear plane and the tool-chip contact interface. As a result, the cutting face experiences a high temperature and a great mechanical pressure. Improper temperature management will seriously affect the amount of tool damage because of the elevated temperature.

5.6.1. Tool wear and tool life modeling

The tool life modeling has been conducted with the machining of titanium owes to the inherent difficult-to-cut material properties of titanium that expedites the process of tool wear. Selection of two levels for each variable has been made and the randomised order of cutting matrix and the tool life results are compiled in Table 5-8. The carbide cutting insert with CVD diamond coating has been used for this experiment. The CVD diamond coating is helpful in machining hard-to-cut material due to its inherent self-lubricating property.

Table 5-8: Cutting matrix and the tool life results

Cutting ID	Speed/ m/min	Feed/ mm/rev	Depth/ mm	Flow/ l/min	Tool life/ min
1	120	0.1	1	0.5	14.6
2	80	0.2	1	0	19.9
3	80	0.2	0.5	0.5	37.4
4	80	0.2	0.5	0	20.5
5	120	0.2	0.5	0	4.2
6	80	0.1	1	0	54.1
7	120	0.1	0.5	0	14.3
8	80	0.1	0.5	0.5	102.4
9	120	0.1	1	0	11.1
10	120	0.2	1	0.5	5.2
11	120	0.2	0.5	0.5	7.6
12	120	0.2	1	0	2.6
13	80	0.1	0.5	0	70.1
14	120	0.1	0.5	0.5	22.6
15	80	0.2	1	0.5	26.8
16	80	0.1	1	0.5	77.2

Based on the extended tool life equation:

$$T = \frac{C_1}{v^p \cdot f^q \cdot a_p^r} \qquad (5.35)$$

The coefficients can be determined by linearising the equation.

$$\log T = \log C_1 - p \cdot \log v - q \cdot \log f - r \cdot \log a_p \qquad (5.36)$$

Coefficients p, q and r are determined from the graph in Fig. 5-14 while alternately keeping the variables constant. The obtained coefficients are displayed in Table 5-9.

Table 5-9: Experimentally obtained coefficients for conventional and internally cooled tool

	C_1	p	q	r
Conventional	93263347.6	4.1916	1.766	0.3628
Internally cooled	77056273.08	3.95295	1.5098	0.518025

So respectively the tool life model for conventional tool and internally cooled tool while machining grade 2 CP titanium are:

$$T = \frac{93 \cdot 10^6}{v^{4.19} \cdot f^{1.77} \cdot a_p^{0.36}} \qquad (5.37)$$

and

$$T = \frac{77 \cdot 10^6}{v^{3.95} \cdot f^{1.5} \cdot a_p^{0.52}} \qquad (5.38)$$
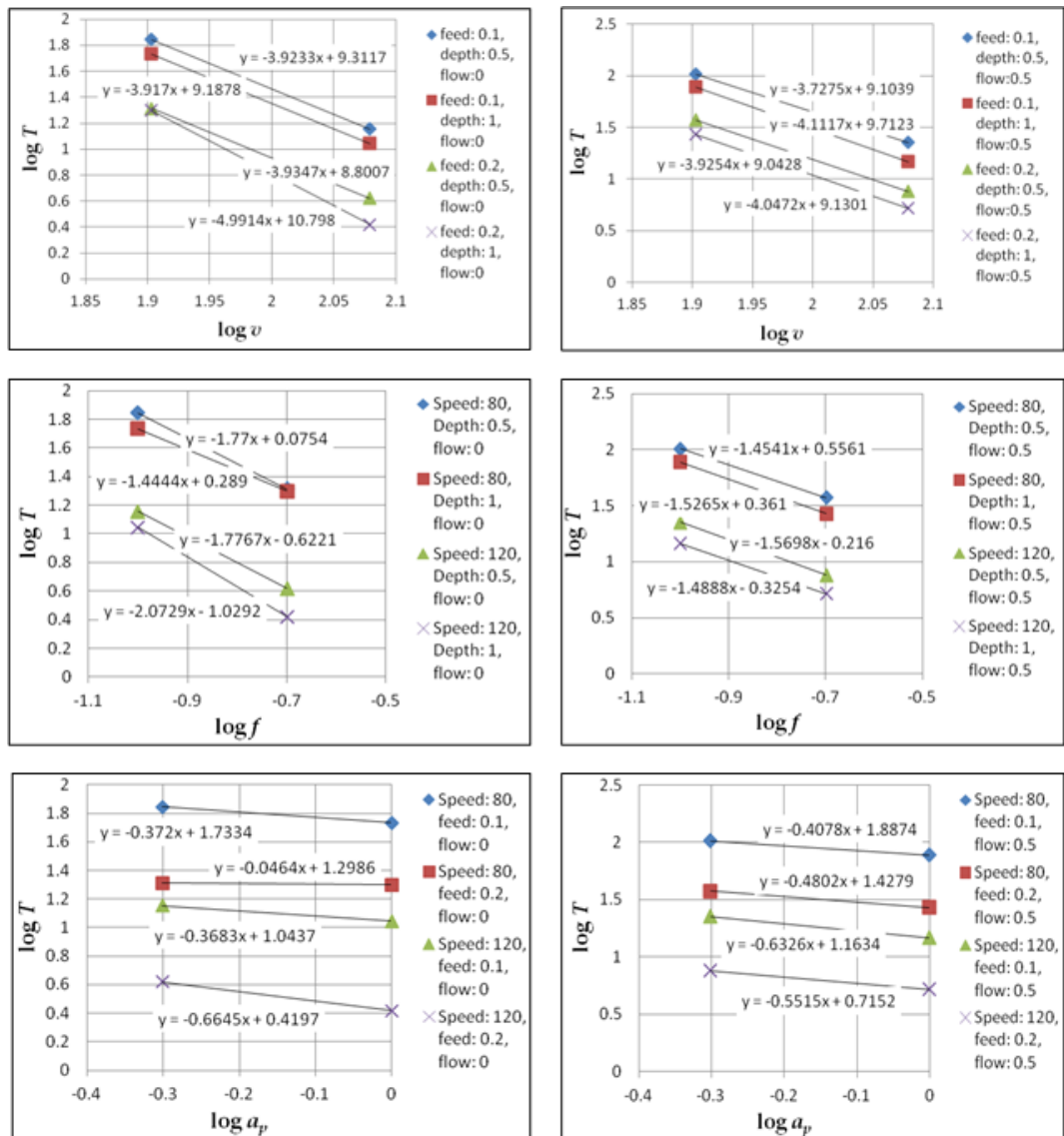
Fig. 5-14 : Determination of coefficients

5.6.2. Validation

Simple validation has been performed on the recently developed models by re-fitting in the experimental matrix. The experimental tool life is compared with the computed tool life from the model and the error between the numbers is determined.

Based on the variations calculated in the Table 5-10, the tool life for a given set of cutting parameters for conventional and internally cooled carbide cutting tool in machining aluminium, AA6082 can be predicted with the model developed with the discrepancy of less than 20%.

Table 5-10: Tool life model validation

Cutting ID	Speed/ m/min	Feed/ mm/rev	Depth/ mm	Flow/ l/min	Experiment	Model	Variation
1	120	0.1	1	0.5	14.6	15.06	3.24
2	80	0.2	1	0	19.9	16.87	17.90
3	80	0.2	0.5	0.5	37.4	37.60	0.63
4	80	0.2	0.5	0	20.5	21.69	5.32
5	120	0.2	0.5	0	4.2	3.96	5.08
6	80	0.1	1	0	54.1	57.37	5.66
7	120	0.1	0.5	0	14.3	13.48	5.86
8	80	0.1	0.5	0.5	102.4	107.09	4.40
9	120	0.1	1	0	11.1	10.49	5.46
10	120	0.2	1	0.5	5.2	5.29	1.82
11	120	0.2	0.5	0.5	7.6	7.57	0.48
12	120	0.2	1	0	2.6	3.08	14.75
13	80	0.1	0.5	0	70.1	73.78	5.05
14	120	0.1	0.5	0.5	22.6	21.56	4.76
15	80	0.2	1	0.5	26.8	26.26	2.01
16	80	0.1	1	0.5	77.2	74.78	3.19

Chapter 6:   Adaptive Control with the Internally Cooled Smart Cutting Tool

The main requirements in machining are:

    (1) Highest machining accuracy

    (2) Maximum productivity

    (3) Longest effective tool life

    (4) Minimum production cost

    (5) Shortest machine down-time

It is always a tall order to fulfil all the requirements mentioned above especially in ECMP, hence the current practice will only control one or two requirement(s) and compromise the rest.

By reducing dependency of the machining on external lubricant and by circulating the cooling fluid internally through embedded micro-channel in a cutting tool, the *production cost* can be reduced tremendously as the coolant can be continuously recycled in a closed loop system (saving through minimising waste and extra treatment process), smaller pump can be utilised (cheaper pump for low mass flow rate) and less complex chemical components for the cooling fluid is required (only elements to improve thermal conductivity, specific heat capacity and transfer coefficient are required).

Machining down-time can be due to servicing, maintenance, cleaning, inspecting, tool changing and problem rectifying. Reducing machining down time can provide instant beneficial effects on the efficiency of manufacturing

production. Short duration stops due to inspection or minor problem rectification and long duration stops which contribute significantly to production efficiency can be minimised by monitoring the machining process variables (e.g. cutting forces, cutting temperatures or surface roughness) so the unscheduled stops are only carried out when it is necessary.

Since the requirements of minimising production cost and shortening machining down time can be addressed by using internally cooled smart cutting tool, other specified requirements, viz. improving machining accuracy, productivity and effective tool life could be only fulfilled in an economic manner by having an adaptive control system. As explained before, adaptive control in machining does not involve complex error compensation algorithms as in typical adaptive control of control engineering but it just shares the same concept of adapting of certain process parameter to control a constrained condition.

Adaptive control in machining is a smart solution to deal with the sporadic changes in machining conditions, especially in association with the wear rate of a cutting tool. The machining today is rather static since it highly depends on the experience and skills of the machine operators to produce desired output. This practice often leads the machining process to operate at inefficient conditions. Ideally, as the wear mechanisms induced in the machining process, the machine parameters need to be cognitively manipulated in order to control the effective tool life, surface roughness or manufacturing productivity. For this working principle a control law that adapts itself to the changing parameters should be developed. Adaptive control system for machining process, as illustrated in Fig. 6-1, is basically is a feedback system that treats the

computerised numerical controlled (CNC) as an internal unit of the whole adaptive control system.
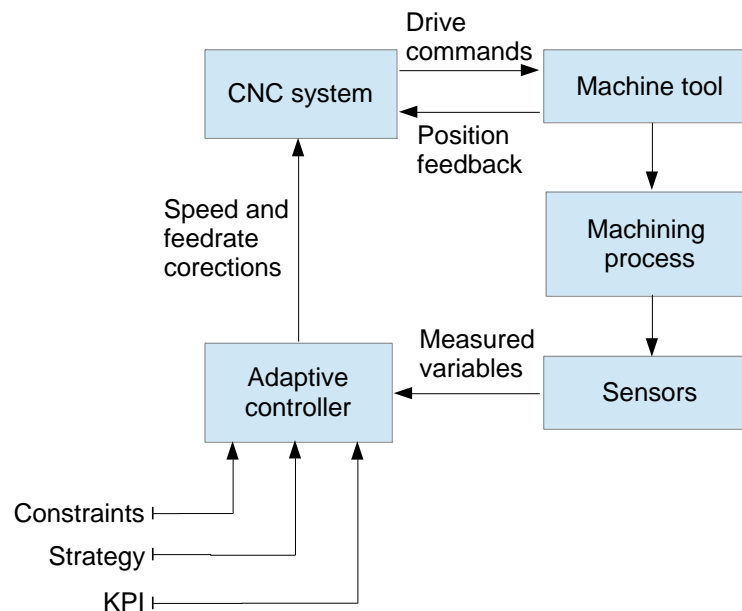
Fig. 6-1: Adaptive control system for machining (Koren, 1988)

6.1.   Adaptive control techniques

Adaptive control in manufacturing is primarily developed to overcome the problem related to static manner of CNC machine tool which causes the typical productivity achievable to be not as high as ideally possible.

The availability of communication with the controller of a CNC machine tool and the needs for higher degree of control on productivity and surface quality has greatly expedited the development of adaptive control (AC) techniques for metal cutting as summarised in Fig. 6-2 (Koren, 1988). These techniques were developed based on on-line control of the machining parameters with reference to the measurements of the machining process state variables, such as cutting

temperature, torque or deflection. These techniques have been explained in details in Chapter 2 and Chapter 3.

Adaptive Control Techniques

- **Adaptive Control Constraint (ACC)**
  - process parameters are manipulated in real-time to maintain a specific process variable (e.g. forces or temperature) at a constraint value.
  - common application: Roughing operation
- **Geometric Adaptive Control (GAC)**
  - driven by the need to maintain product quality despite the structural changes in the process (e.g. tool deflections and tool wear)
  - common application: Finishing operation
- **Adaptive Control Optimisation (ACO)**
  - manipulation of cutting parameters by integrating feedback signal and prediction system to optimise process outputs (MRR, accuracy, cost).
  - common application: cost efficient enhancement

Fig. 6-2: Adaptive control techniques

Based on the review of the techniques above ACC and ACO approaches have been selected for the application of internally cooled cutting tool in machining. Since low cutting temperature, which can be obtained by applying internally cooled cutting tool, does not necessarily assure good surface quality or long tool life, a set of optimum cutting process parameters needs to be maintained in order to minimise the generation of tool wear. Tool wear plays direct role in determining dimensional accuracy and surface finish quality of the workpiece.

For this research the adaptive control system will automatically select the required values for the process control valuables (i.e. cutting speed, feed rate or coolant flow rate) based on the on-line process measurements (i.e. cutting

temperature, inlet-outlet temperature or cutting force) to achieve a particular machining requirement.

The biggest challenges in applying ACO are to find suitable sensors that are reliable to indicate the condition of the cutting tool and to determine and develop comprehensive machining performance indices. Alternatively an approach similar to model reference adaptive control (MRAC) technique can be utilised to correlate the process measured variables with the tool condition and surface roughness. The error obtained by real time comparing the measured value with the referenced value will be used to cognitively adapt the cutting parameters. The schematic diagram of the adaptive control used for internally cooled cutting tool is shown in Fig. 6-3. Denoting y is the output from the machine tool, y_m is the output from the referred model, u_{AC} is the adapted input to the machine tool from adaptive controller and e is the error which represents the difference between the measured output and the model output. The role of controller gain is to provide the system with stability over adaptability.
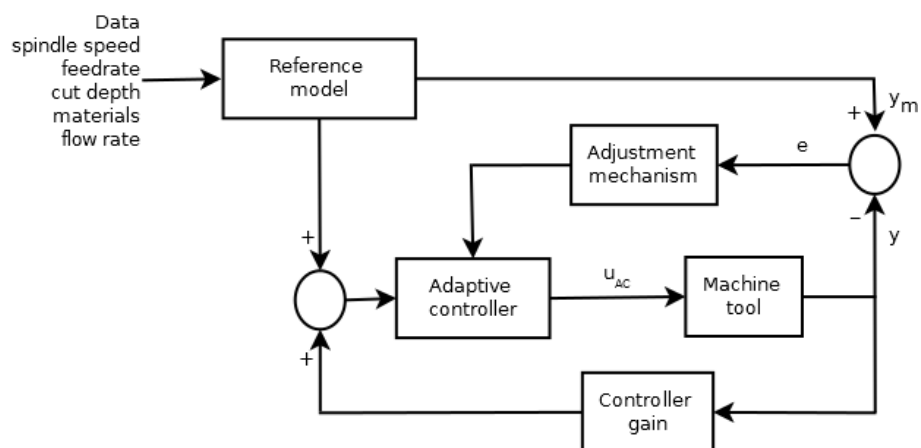
Fig. 6-3 : Block diagram of AC for internally cooled cutting tool based on MRAC approach

6.2.   Communication with machine tool controller over Ethernet

In order to be able to on-line modify the adaptable parameters such as cutting speed, feedrate or coolant flow rate in real time a communication with machine tool CNC controller and pump controller must be established. The acquired information are then correlated with the process model, which is developed by means of training with actual machining data. Lathe machine tool Alpha Colchester in the mechanical lab of Brunel University uses CNC controller FANUC 21i-TB. This model of FANUC control allows Ethernet version to communicate with the CNC side by the "Embedded Ethernet function". The Ethernet mechanism of CNC machine as provided by FANUC is illustrated in Fig. 6-4. It can be explicitly seen that the communication between the user computer and the CNC controller of the machine tool is realized by socket communication (TCP/IP communication). Physical network connection between the personal computer and the CNC is realized by interfacing the two devices through Ethernet ports using local area network cable (Fig. 6-5).
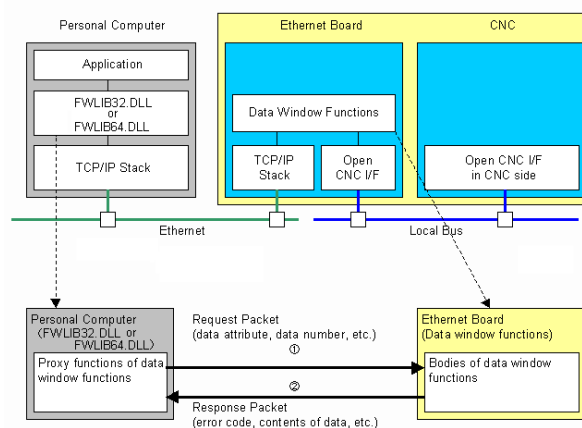
Fig. 6-4 : Communication mechanism with the CNC machine through Ethernet board (www.fanucfa.com)

In summary four main steps need to be carried out before establishing the communication with the CNC controller:

(1) Setting of TCP/IP on the personal computer side.

(2) Setting of the Ethernet board and Embedded Ethernet Function in the CNC side.

(3) Physical connection between personal computer and CNC machine tool.

(4) Programming an application to call FOCAS (FANUC Open CNC API Specifications) library.

Fig. 6-5 : Physical network connection through the Ethernet port on the machine tool

FOCAS enables the reading and writing of CNC data from the controller via Ethernet. The sequence diagram of an application program for the communication with the CNC controller is depicted in Fig. 6-6.
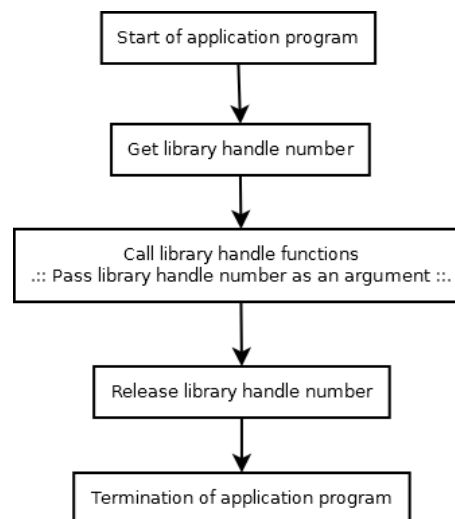
Fig. 6-6 : Flow chart of the sequence in communication application program

An example of the application program that is written in C++ programming environment with the aim to get the reading of the actual tool position, feedrate, spindle speed and constant surface speed is as below and an example of the output is as shown in Fig. 6-7.

```cpp
#include <iostream>
#include "Fwlib32.h"
#include <winsock.h>
#include <time.h>
#include <string>

using namespace std;

int main()
{

    unsigned short h;

    short ret;

    ret=  cnc_allclibhndl3("192.168.1.1",  8193,  10,  andh); //communication
established
    if (!ret)
    {

        // call library handle functions
        struct odbdy buf;

            cnc_rddynamic (h, -1, sizeof(buf), andbuf);
            printf ("actual feed=%ld\n", buf.actf);
            printf ("actual speed=%ld\n", buf.acts);
            printf ("radial=%ld\n", buf.pos.faxis.machine[0]);
            printf ("axial=%ld\n", buf.pos.faxis.machine[1]);
```

```cpp
                struct odbcss srpm;
                    cnc_rdspcss( h, andsrpm ) ;
                    printf ("linear speed=%ld\n", srpm.sspm);

    } else {
        printf ("ERROR!(%d)\n", ret);
        cout<<"connection failed"<<endl;

    }

    //release cnc handle
    cnc_freelibhndl(h);

    return 0;
}
```

The essential information for developing the application program is described in a manual provided by FANUC in FOCAS ½ CANC/PMC Data Windows library. The recommended programming languages for developing the application program are Visual Basic 6.0 or Visual C++ 6.0 and Visual Studio 2010 for Windows 32 bit and Windows 64 bit respectively.
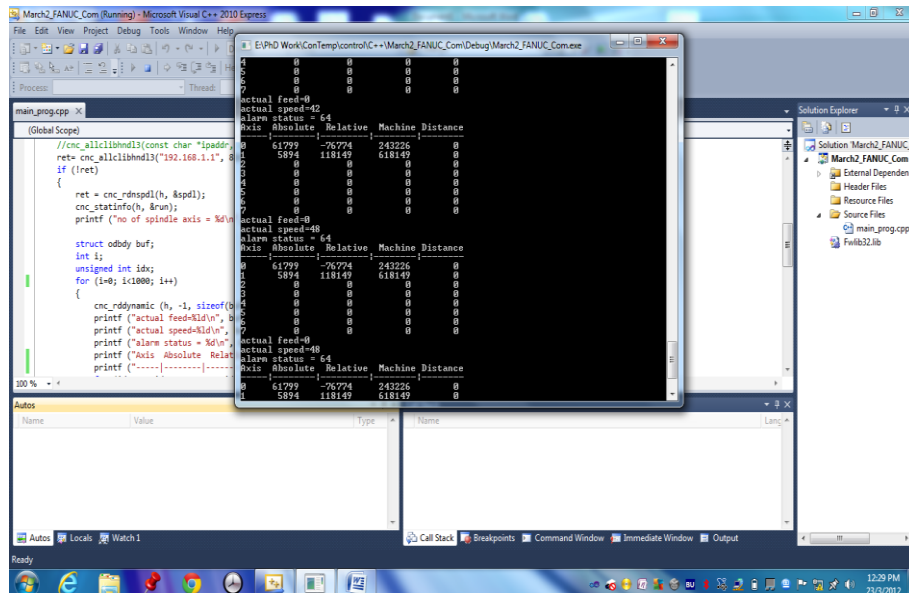
Fig. 6-7 : Screenshot of the communication with FANUC control of the machine tool via Ethernet

As depicted in Fig. 6-7, the position of the two axes which correspond to the position of the tool in axial and radial axes, the feed rate of the tool holder in both directions and the speed of the spindle are transferred to the personal computer at the rate of 250ms.

The adaptive control for the machining with internally cooled cutting tool requires the application program, which can be written in C++ or visual basic, to be launched and executed from LabVIEW environment. LabVIEW is a programming software utilizing graphical programming language – "G". All programs in LabVIEW environment are coded by connecting icons (subprograms, controls and indicators) with wires (refer to the right image in Fig. 6-8). If necessary LabVIEW can call other source codes for example from C++ like in the case of FANUC application program in this project. The LabVIEW interface consists of a front panel (communication with user) and block diagram (code), as shown in Fig. 6-8. LabVIEW has excellent capabilities of managing very complex data structures, signal acquisition and processing because it fully integrates with the available data acquisition system (DAQ system) from National Instruments. The adaptive control algorithm and tuning are written in LabVIEW for input from sensors acquisition, measurement and processing so it is a natural choice to integrate the communication program also in LabVIEW.
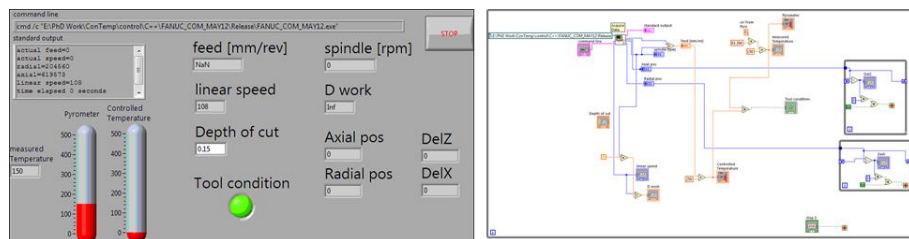
Fig. 6-8 : Front panel and block diagram of LabVIEW programming environment

 The FANUC application program is launched in LabVIEW by using System Exec vi which requires the name and address path of the source code to be input and a unique subprogram (as in Fig. 6-9) is assigned for this routine so the communication can be called conveniently at anytime in LabVIEW program in the later stage of development.
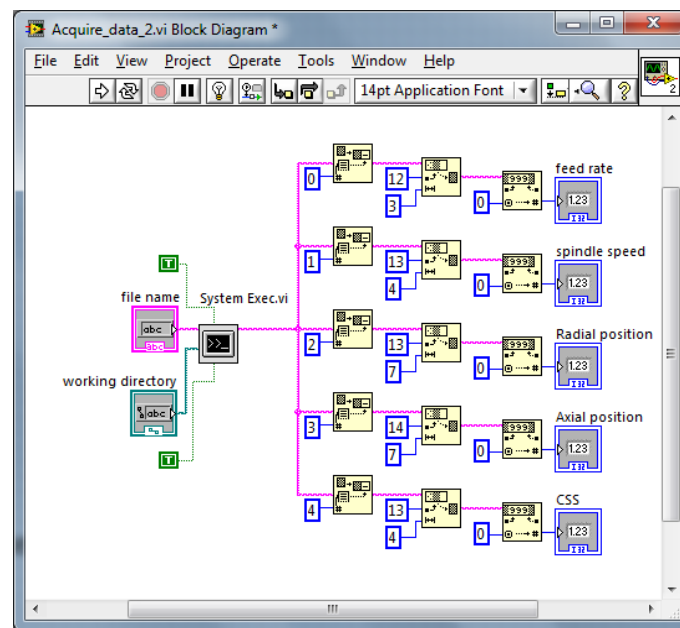
Fig. 6-9 : Sub VI for translating C++ output in LabVIEW

6.3.   **Pump control**

Flow control of the cooling fluid is one of the controlled variables for the adaptive machining with internally cooled cutting tools. The control of the flow by manipulating the pump power is more acceptable by industries rather than machining parameters adaptation because it doesn't change the setup of the machine tool. Besides that, the machining parameters do also influence the surface integrity, changing them might directly change the surface topography. Controlling pump power (either by adapting coolant mass flow rate or

adapting cooling fluid speed) has major advantage over machining parameters adjustment because the standard cutting parameters setting to machine a product can be kept the same while the cutting temperature that affects the effective tool life and thermal expansion of the workpiece can be minimised.

For this research two types of pumps have been tested. The two pumps differ in the size, control and configurations. The differences can offer flexibility in application in the machine tool setup, especially when dealing with different machine tools and their configurtions. One is micro-diaphragm liquid pump from company KNF Neuberger. The pump is equipped with four connecting leads, which are positive (red) and negative (black) power supply cables and a pair (green and white) of 0-5V control cables (see Fig. 6-10).
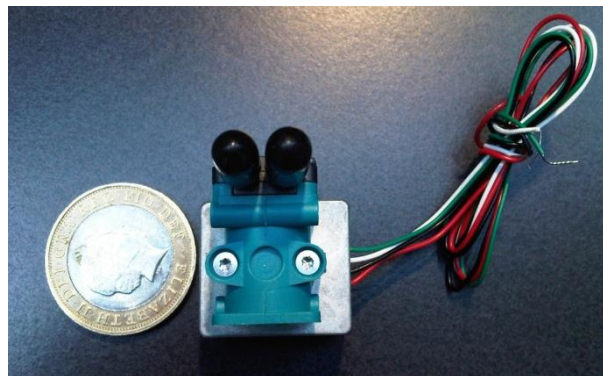
Fig. 6-10 : NF60-DCB Micro-diaphragm pump

The other pump is industrial pump that can supply the cooling liquid up to 30bar. This pump is mounted in a mobile system that constitutes of a tank, electrical cabinet, valve, filter and a chiller. The complete mobile system is powered and controlled by programmable logic control (PLC) TwinCAT by Beckhoff Automation Technology as shown in Fig. 6-12.
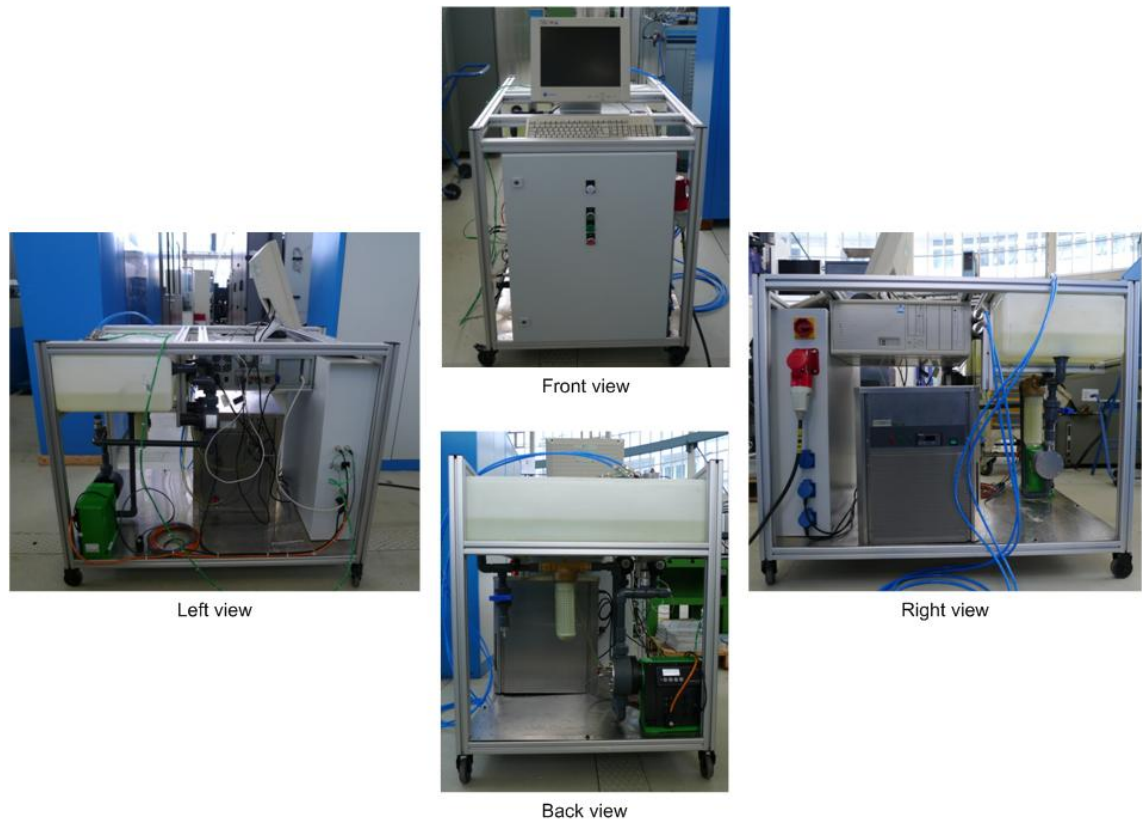
Fig. 6-11 : Heavy duty pump-chiller mobile system

The Beckhoff I/O hardware board is connected to the host PC via TCP/IP network. Upon establishing the connection, the hardware needs to be configured using the TwinCAT System Manager on the host PC. The TwinCAT PLC control requires PLC programmes to be written. The advantage of PLC programming languages of TwinCAT is that the compiled project is XML based which makes it available to be opened with internet browser.
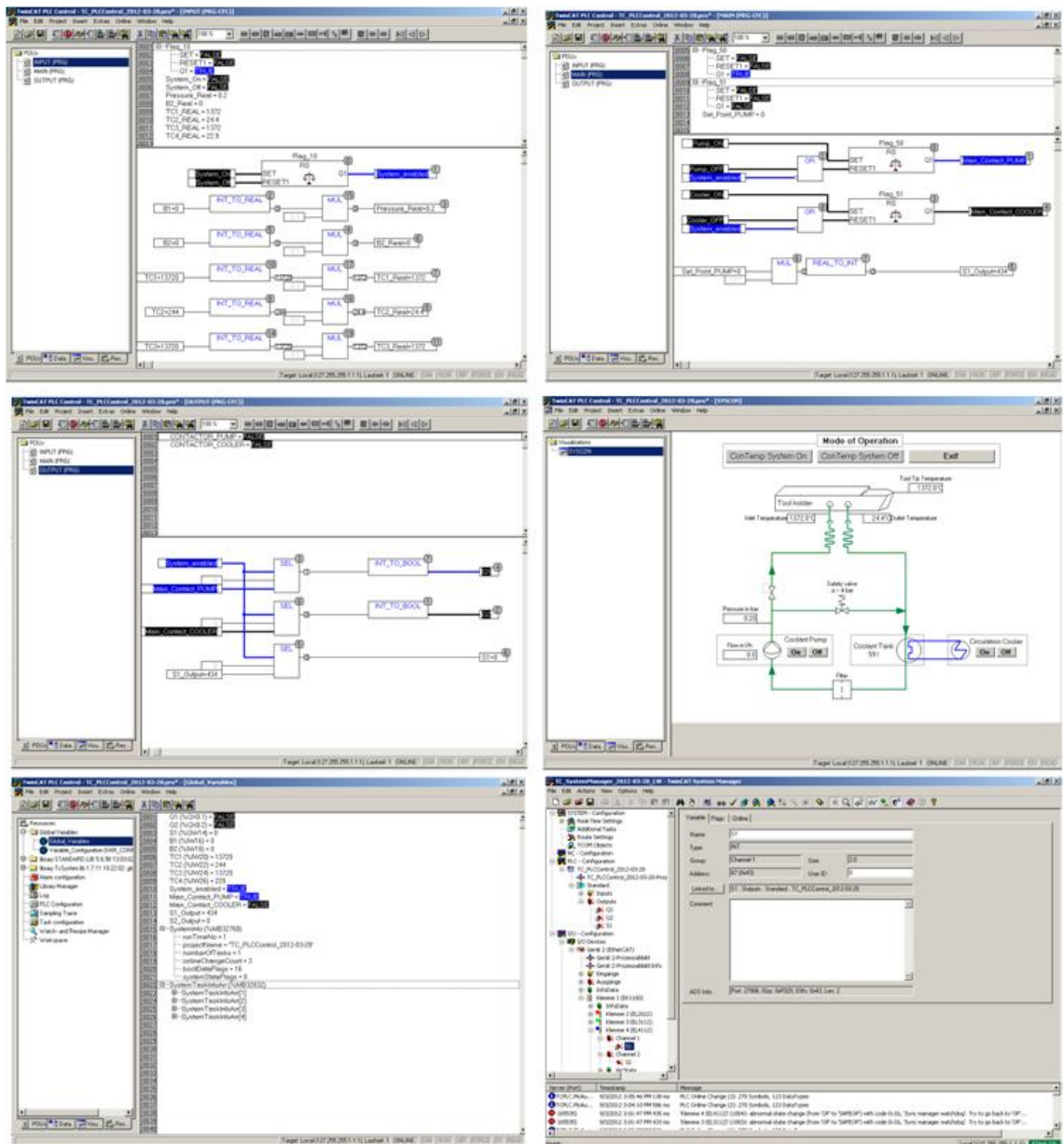
Fig. 6-12 : TwinCAT PLC Control and PLC system manager

6.3.1. Direct voltage control

NF60-DCB twin head brushless DC micro-diaphragm pump can be controlled by analogue voltage output (AO). For this project the pair of 0-5V control cables is connected to spring terminals voltage AO module NI9264 from National Instrument. This module is then attached to the compactDAQ chassis NI cDAQ

9172 which can accommodate eight I/O modules in one chassis and the signals of these modules are accessible in real time by the LabVIEW application program on the personal computer via USB.

Another concern of the twin head diaphragm pump is the hydraulic configuration to optimise the fluid flow rate. The selections of the material and stiffness of the tube, T-joints, type of fluid and the configuration of the hydraulic connection influence the flow of the coolant. The inlets of the both heads are joint together for the priming process and the fluid from the outlets of the two heads are coupled together to be circulated into the micro-channel which is embedded in the cutting tool. The coupling configuration can be seen in Fig. 6-13.

The ideal pressure drop of the system has been calculated in Chapter 5. From the simulation it is obtained that the maximum mass flow rate of 0.005 kg/s with the 6 bar pumping capacity of the micro-diaphragm pump can be achieved while circulating pure water with some anti-corrosion additive through an internally cooled cutting tool.
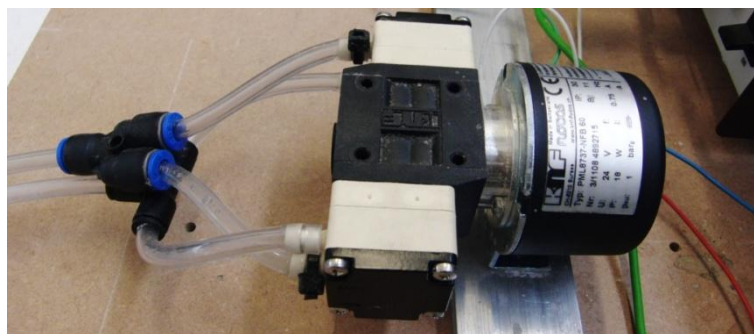
Fig. 6-13 : Hydraulic configuration to optimise the double heads pump

Table 6-1 shows the experiment result to measure the mass flow rate when varying the pump from 1 to 5V in the interval of 1V. It can be seen that only a narrow range of mass flow rate can be controlled. The result is plotted in Fig. 6-14 and the curve describes a linear correlation between the mass flow rate and the controlled voltage. The linear characteristic of the pump is modeled as:

$$\dot{m} = 0.0003V_c + 0.0036 \tag{6.1}$$

Table 6-1: Pump flow rate measurement

Voltage	fluid mass flow rate, $\dot{m}$ / g/min				m_{ave}
V_c / V	m_1	m_2	m_3	m_{ave}	(kg/s)
1	231	231.5	234	232.17	0.0039
2	254.5	252.5	256	254.33	0.0042
3	275.5	284.5	281.5	280.50	0.0047
4	299.5	295.5	296	297.00	0.0050
5	309	311	301	307.00	0.0051
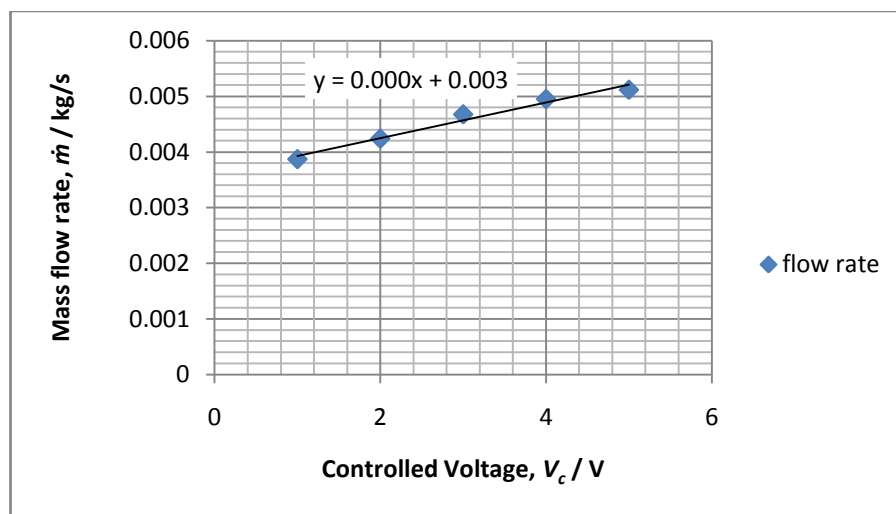
Fig. 6-14 : Mass flow rate versus controlled voltage

6.3.2. PLC control

One partner in ConTemp project, Technical University Berlin has developed a more industrious pump with temperature control and mobile capability. This pump is powered and controlled by PLC using Beckhoff system. Beckhoff system requires Twincat program to manage the control program, I/O devices assignment and signals with other program exchange.   In the variables definition window in Fig. 6-12, I and Q in front of the variable declaration denote the description of a variable either input or output respectively. The "%" sign means that the variable can be used externally, for instance in LabVIEW environment. Then the variables used in the PLC programs need to be assigned to the I/O ports in the TwinCAT System Manager. Selection of the target system into which the PLC project is to be loaded is the next step to do. Finally the user needs to login before creating a boot project.

Fig. 6-15 depicts the graphical user interface (GUI) of the pump-chiller program in the PLC TwinCat program. Among the variables in the GUI are two relays to power the pump and the chiller, a control for fluid flow rate manipulation, three temperature inputs for the thermocouples at the tool tip, inlet and the outlet of the tool and one input from the pressure transducer.
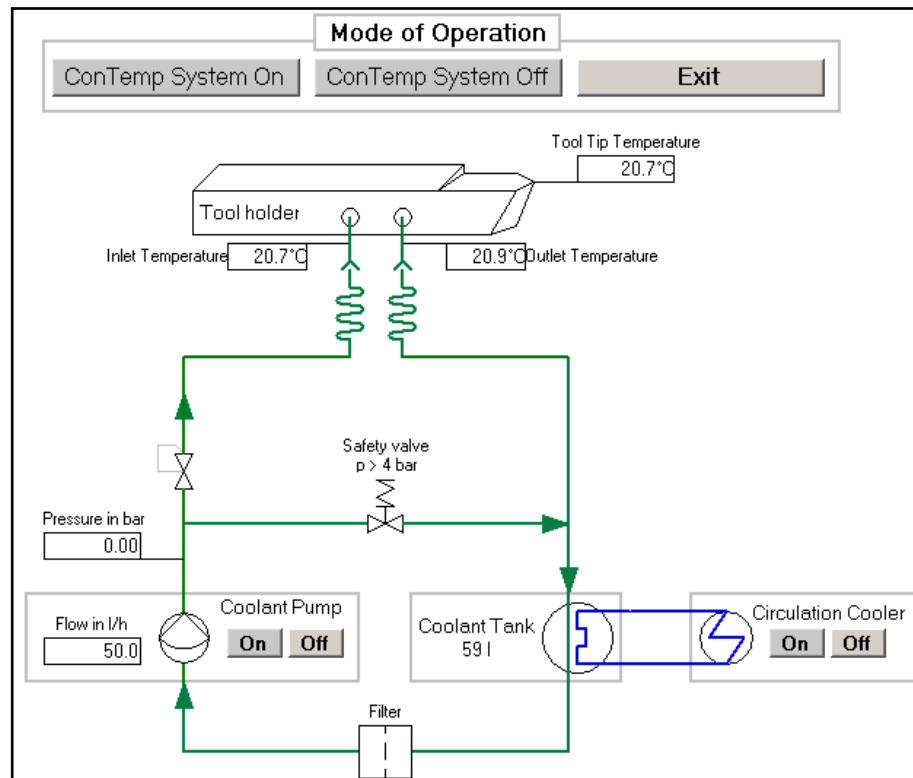
Fig. 6-15 : GUI of pump on Twincat program

These variables can be read and controlled in LabVIEW environment by using ADS.OCX control. This control is available in ActiveX container (Functions palette >> Connectivity >> ActiveX). For this interface AMS Net ID and AMS Server Port need to be inserted. These numbers can be found in the TwinCAT properties under AMS Router tab and PLC Settings respectively. Beckhoff Automation LLC (Beckhoff, 2011) documents the full procedures in using National Instruments LabVIEW with TwinCAT I/O.

Fig. 6-16 : LabVIEW-TwinCAT communication interface block diagram

The interface is then converted into a subVI and can be used in the main adaptive control application program. The signals obtained in real time can be used to correlate with the tool condition model and the index can be displayed on the user interface as in Fig. 6-17. The error (difference) between the measured temperature and the reference temperature from the model is used to adjust the coolant flow rate by manipulating the pump power.

Fig. 6-17 : Front panel of LabVIEW after integration with signals from TwinCAT

The calibration of the pump against the mass flow rate has been carried out on all three different cooling designs and the results are consolidated in one graph as shown in Fig. 6-18. The conclusion of the result can be said that the size of the pressure head of the pump does not significantly contribute to the micro channel as the higher the pressure applied the bigger the back pressure will be. Therefore, a bypass with a pressure relief valve should be made available in the case of excessive built up pressure.
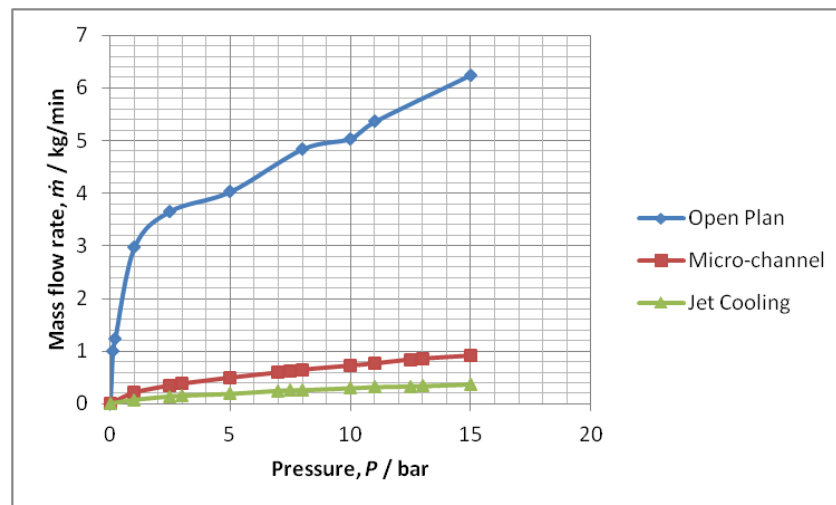
Fig. 6-18 : Mass flow rate versus pump pressure

6.4.   Development of the adaptive control algorithm and its tuning

Two approaches can be utilised in developing the algorithm for adaptive control.

(1) ACC – Controlling tool temperature to avoid critical temperature which activates BUE, BUL or rapid crater or flank wear.

(2) ACO – Controlling KPI based on developed productivity, wear and surface roughness models to optimise machining performance.

Schematic diagram shown in Fig. 6-19 can be used to design the operational flow of ACO but it can also be simplified to design the working principle of adaptive machining with ACC. The machine tool is driven based on the tool holder positions and speed commands from the NC and the actual measured tool holder's positions and speed are fed back in real time to the NC. Communication with the machine tool controller as described in 6.2 allows the variables to be monitored in "Performance monitoring" subsystem. Integration the machining process with thermal sensors, flow rate transducers and dynamometer enable the "Data acquisition and model fitting" subsystem to describe the machining performance in real time and subsequently the information gathered will be used to optimise machining performance from the viewpoints of productivity, surface roughness, tool life or any combination of the key indices by adapting the cutting parameters. The controlled parameters are always inspected to be within the boundaries of predefined constraints.
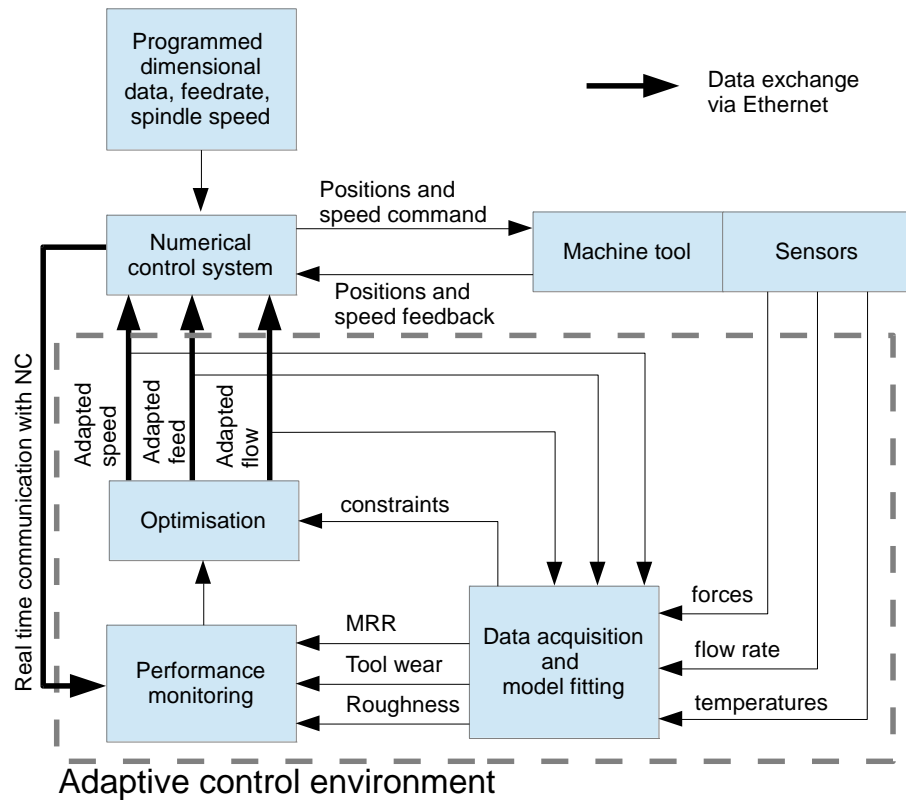
Fig. 6-19 : AC machining with the internally cooled cutting tool

The realisation of adaptive machining with internally cooled cutting tool can be performed online and semi real time. Real time adaptation of pump flow rate can be realised by characterising the tool temperature in the function of coolant flow rate. However, real time adaptation of CNC machine parameters could not be realised during the framework of this research is mainly due to the reasons written below.

(1) Real time machining parameters adaptation requires special study on stability and adaptability of the motion control of the CNC machine. The study involves modeling the transient state of the response variables with different tool-workpiece materials combination for different operational cutting parameters, which to cover all of these is not the main aim of this project.

(2) Adaptation of machining parameters requires the adaptive control to access and modify the drives commands of FANUC NC control which by doing this can breach the warranty agreement from the machine tool manufacturer.

(3) The sensor and actuator for adaptive machining should be fast enough to respond quickly to upsets. As it is scientifically proven, machining temperature which is measured at certain distance from the cutting edge is not an optimum selection to give sufficiently fast feedback for the adaptive control.

The results of cutting trials are analysed to develop tool wear model, surface roughness model and material removal rate model. The challenges in developing a generic model in metal machining are mainly due to continuously changing in dominant effects of thermal, physical and mechanical interactions. Hastings and Oxley (1976) have explained that at optimum selection of cutting parameters, low cutting speed can cause the adhesive effect to dominate the type of wear on the cutting tool while if the cutting speed is increased the wear will be influenced almost solely by thermal induced wear. These phenomena require implementation of a highly dynamic control with real time awareness.

Due to this limitation an adaptive control technique based on ACC has been decided to be used for the machining with internally cooled cutting tool. Two types of ACC control techniques are developed and tested. The first technique is using ACC to single control the cutting force. Firstly, the relationship between the cutting force and the cutting parameters is established. It is discovered from the trials that cutting speeds selected doesn't really influence the cutting force in machining aluminium alloy AA6082. On the other hand, the feedrate applied from 0.05 to 0.25 mm/rev gives a significant region of cutting

force to be controlled. The relationship between the cutting force and the feedrate is shown in Fig. 6-20(b). By assuming the recommended feedrate of 0.15mm/rev as the optimum feedrate, the obtained relationship is integrated in the ACC system. The flow diagram of the ACC is illustrated in Fig. 6-20.
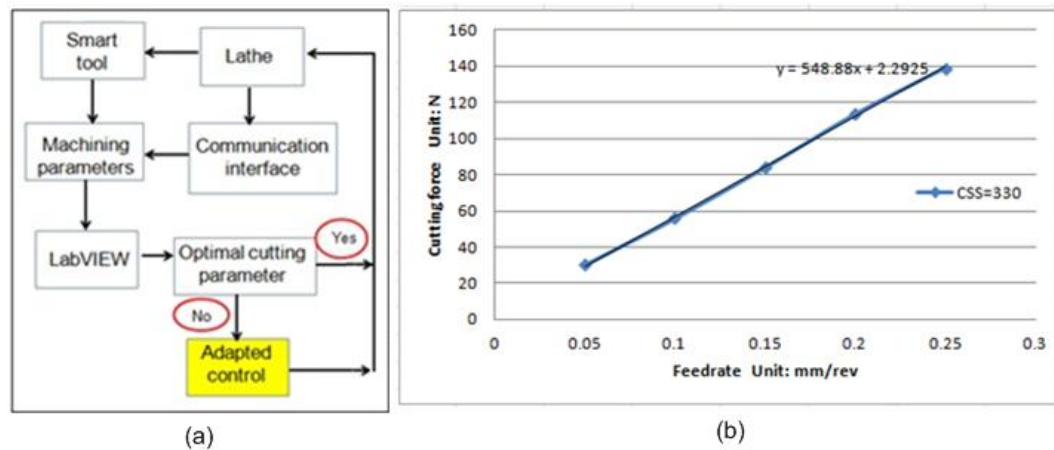
Fig. 6-20 : ACC with cutting force as the constraint; (a) flow chart of ACC with force constraint and (b) the relationship between cutting force and feedrate

The flow control of the second technique is shown in Fig. 6-21. The flow diagram of the control uses the controlled values for specific application in machining of mild steel EN32B. The values can be changed with other values but the users need to have prior knowledge about the optimum cutting parameters of the machining. For this trial, temperature feedback sensed by the embedded thermocouple is used to adapt the internal coolant flow rate and cutting speed. The optimum cutting temperature has been obtained experimentally and the region of the optimum cutting temperature has been determined between 300°C and 350°C.
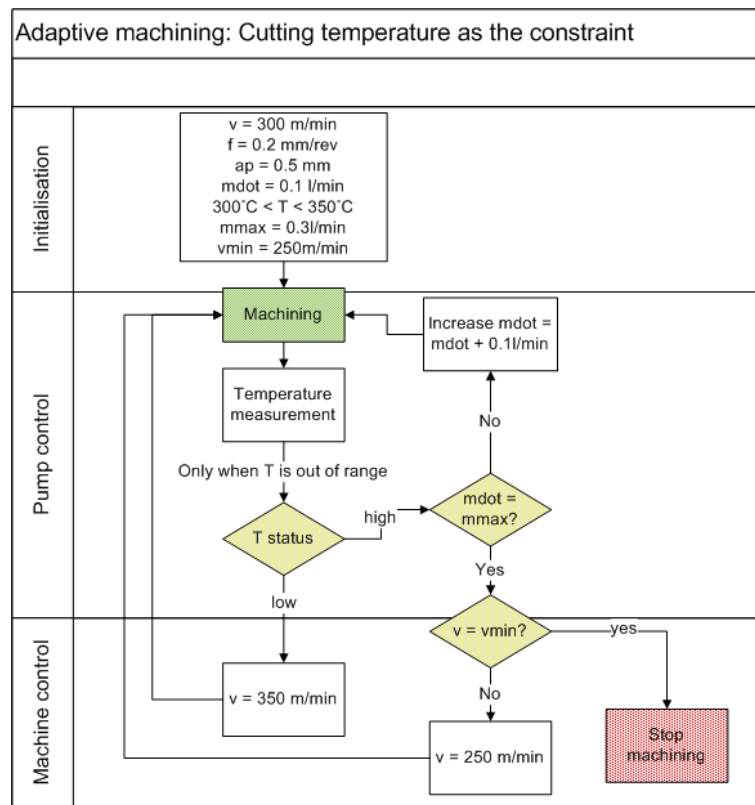
Fig. 6-21 : Adaptive machining of EN32B with the internally cooled cutting tool

Control system needs to be properly tuned in order to make the process variability reduces, efficiency increases, energy cost minimises and production rates maximise. Controller tuning refers to the selection of tuning parameters to ensure the best response of the controller. If a control system is tuned too slow, the response obtained will be too sluggish which disables the controller to handle upsets (which is common things to happen in highly dynamic process of machining operation) and it will take too long to reach setpoint. In contrast, if too aggressive tuning is chosen the loop of the system will go overshoot or become unstable. Based on the process model and the operation needs for a fast response but robust control the PID control is tuned with Ziegler-Nichols method or also known as Z-N rule. Z-N rule is a heuristic method for tuning of PID control that attempts to produce good values for the three PID gain parameters, K_p, t_I, t_D with the aim of achieving good regulation (disturbance

rejection). For this purpose, two measured feedback loop parameters, i.e. T_u, the period of the oscillation frequency at the stability limit and K_u, the gain margin for loop stability need to be derived from real measurements. Based on the cutting trials, the PID gain parameters have been determined for the coolant flow control has been determined as listed in Table 6-2.

Table 6-2: Classic Z-N Rule tuning chart and the derived PID gains from the experiment

Control	Proportional gain, K_P		Integral gain, t_I		Derivative gain, t_D	
P	$K_u/2$	0.20				
PI	$K_u/2.2$	0.18	$1.2K_P/T_u$	2.88		
PID	$0.60*K_u$	0.24	$2*K_P/T_u$	4.8	$K_P*T_u/8$	0.003

6.5.   System validation

In this section the functionality of adaptive machining architecture and the control algorithm is tested. In details, the following four main validations need to be performed.

(1) Functionality test of the ACC architectures.

(2) Measurement reliability of the force sensor and thermal sensors to feed back the control variables.

(3) On-line adaptability of machining parameters to control the cutting force and tool temperature when the signal requires them to do so.

(4) Real time adaptability of pump power with the change of sensed temperature.

For validating the first technique, an aluminium alloy AA6082 blank has been prepared as in the Fig. 6-22. The blank has different height of shoulders as to provide different cutting forces. The idea is, if the cutting force is lower than optimum, in this case 80N, the feedrate will be increased so the productivity increases. On the other hand, if the cutting force is bigger than optimum, as in the case of cutting bigger depth of cut, the feedrate will be reduced so the cutting tool is protected.
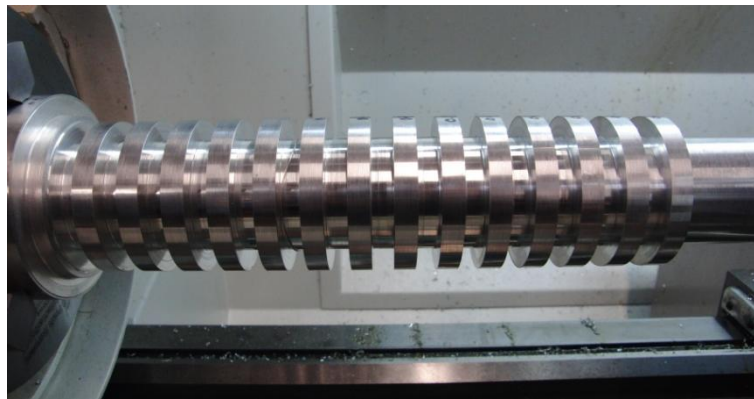
Fig. 6-22 : Workpiece with different shoulders' height

The cutting result is shown in Fig. 6-23. It can be seen that each height is repeated 3 times. The reason for the blank to be designed such a way is that (i) when the first shoulder is cut the force signal will be used by controller to adapt the feedrate for the next cut, (ii) when the second shoulder is cut, the new adapted value will tell the validity of the control algorithm and (iii) the cutting force signal in the three shoulder is used for testing the reliability and accuracy of the piezo force sensor. The force curve in Fig. 6-23 is an average of the static forces.
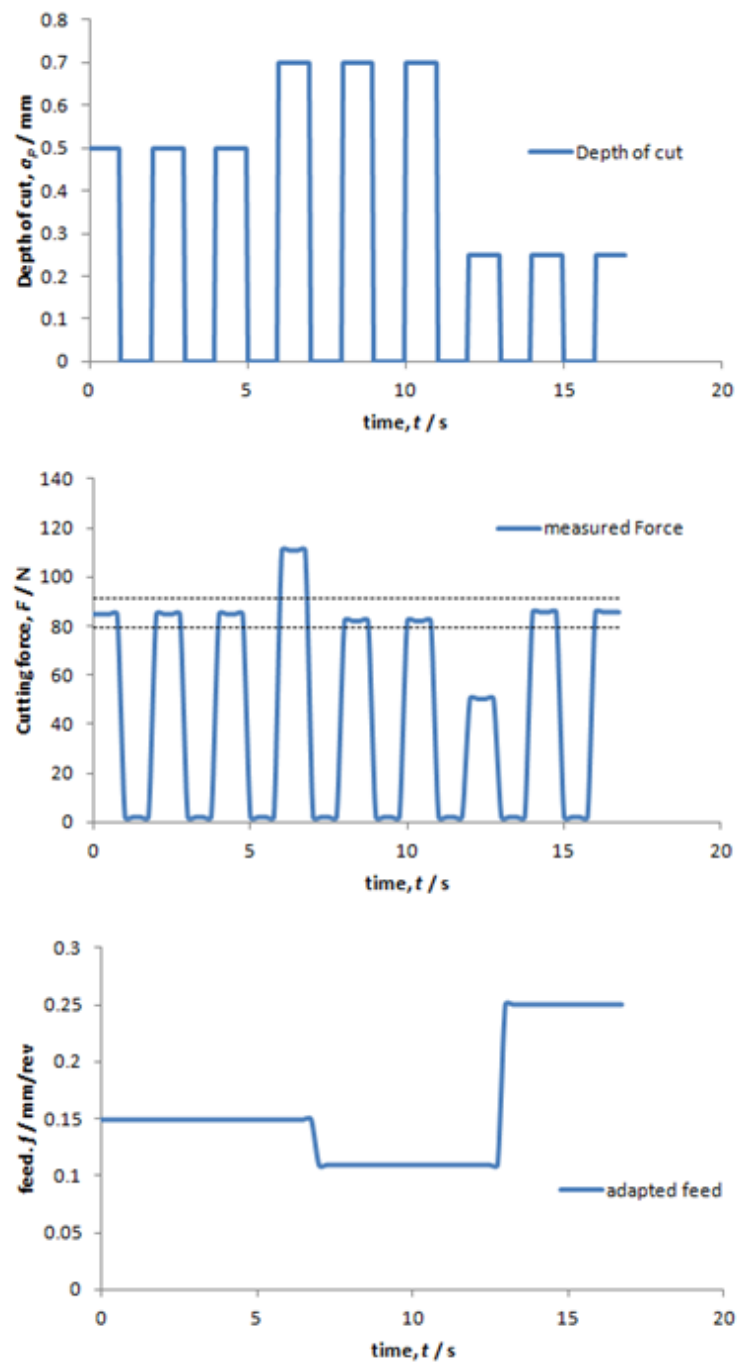
Fig. 6-23 : Validation results for adaptive machining control

With the same idea as in the first technique, the second technique uses a more practical and complex approach. The primary control is on coolant flow rate and if the flow rate reaches the maximum, where no more control of coolant flow rate is allowed, the control of cutting speed will take place.

For this purpose, gate control is programmed on LabVIEW to manage the cases. Three levels of coolant flow rate are used: 0.1, 0.2, 0.3 l/min and three levels of cutting speed are also used for cutting speed; i.e. 250 m/min, 300 m/min and 350 m/min. The variables are only adapted if the cutting temperature is out of the optimum range. Low temperature detected means low cutting speed. Low cutting speed is not only adverse on productivity but it can also activate adhesion wear. So in this case, the cutting speed should be increased.

The tool will start to wear as the cutting operation goes on and the blunt tool requires higher work to deform the work-piece.

The larger amount of work imposed on the tool causes the temperature to raise. If the temperature exceeds the maximum optimal temperature range limit of 350°C, the level of the volume flow rate is checked. If the coolant flow rate does not yet achieve the maximum flow limit (0.3l/min), it will then be increased by 0.1l/min. And the same routine as before is repeated without interrupting the cutting process.

Should the cutting temperature be still higher than the upper limit of optimum cutting temperature range, the increment of volume flow rate of 0.1 l/min is adapted to bring down the cutting temperature. However, this is the maximum volume flow rate allowed with this pump since it has been proven that higher flow rate than this just gives a very marginal change to the cutting temperature.

If the cutting temperature is still beyond its optimum range, the adaptive control will reduce the cutting speed to 250 m/min. Without interrupting the cutting process, the monitoring system will continue observing the cutting temperature and if the temperature goes beyond the maximum limit again the

machining will stop to allow the operator to manually verify the condition of the cutting tool.

For this experiment, a set of cutting trials with cutting length of 2000m was tested on each conventional uncooled tool and internally cooled smart cutting tool. A blank of mild steel EN32B with nominal (original) diameter of 63mm was used for this experiment and the cuts have been performed continuously started with the adaptive machining and followed with conventional dry machining. The tools' condition and surface roughness are investigated.

Fig. 6-24 shows the images of the conventional insert and internally cooled tool insert taken with TESA Vision 200 microscope. Obvious flank wear can be observed on the conventional insert. Although, the wear on the rake face of the conventional insert is not dominant but notch wear has occurred on the tool edge. Meanwhile, slight flank wear can be also detected on the internally cooled cutting insert. This might indicate that the response of the adaptive system is not fast enough to prevent the wear. However, at this stage this judgement is not concrete enough to be concluded as both cutting have only tested once for each tool.

2000m (conventional)   2000m (adaptive)
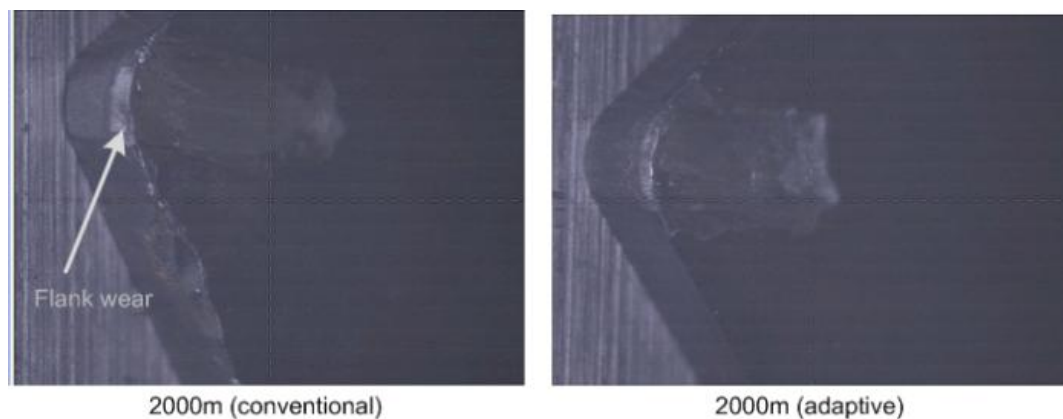
Fig. 6-24: Tools condition after 2,000m dry machining

The surface finish of the workpiece is also observed by measuring each condition twice, once after 1000m cut and the other one after 2000m. The measurements show that better surface roughness can be obtained with adaptive machining process. The surface finish of conventional dry machining is totally unacceptable after 2000m cut. This may be due to the flank wear formed at the tip of the conventional insert. After 2000m cut whilst with the adaptive machining tool, the obtained surface roughness is still low and in fact it is better than the previous 1000m cut. Possible explanation for this might be (i) optimum temperature reached which has lowered the shear strength of the workpiece material thus softens the material or (ii) the elevated temperature causes an increase in the ductility of the tool material.
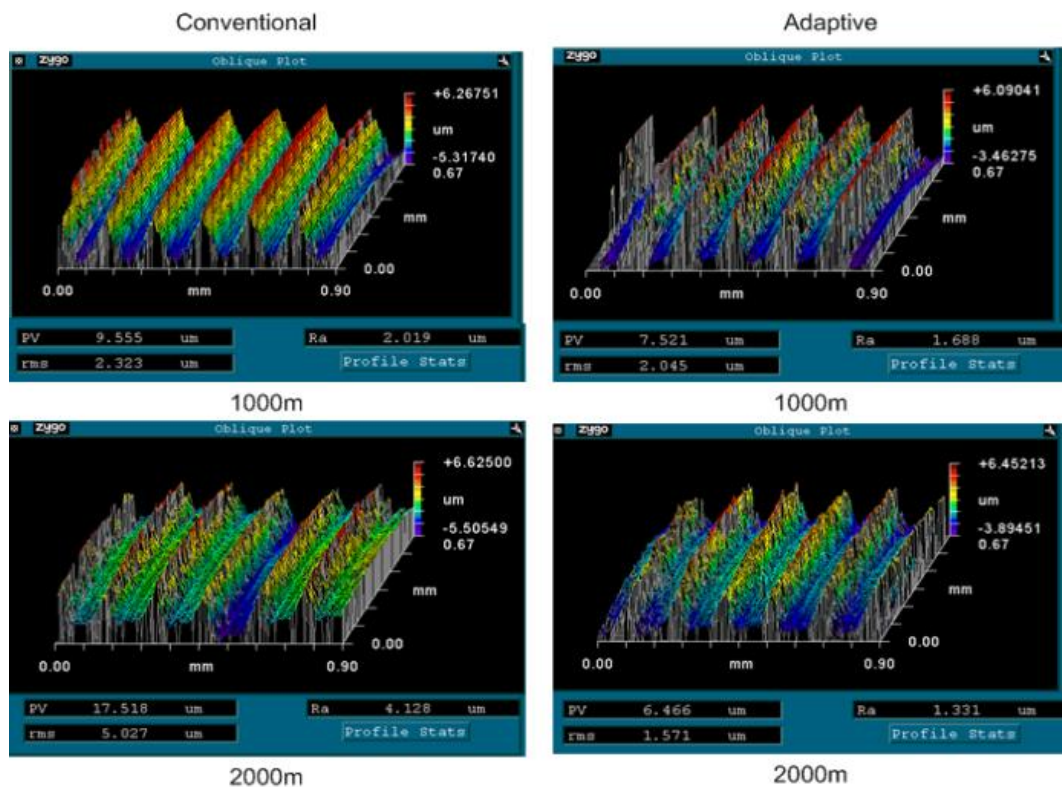
Fig. 6-25: Surface roughness of adaptive machining with the internally cooled smart cutting tool

Chapter 7: System Integration, Cutting Trials, Results and Discussions

This chapter describes the experimental setup, the relationship between cutting parameters and cutting temperature when internally cooled cutting tools are applied, and the comparison of the machining outcomes such as cutting tool life and surface roughness for the machining with internally cooled cutting tools and conventional machining with commercial standard cutting tool insert. Further it presents some results about manipulation of coolant temperature to predict cutting temperature.

The work in this chapter is not going to validate again the FEA and analytical models that have been proposed earlier with the current experimental conditions. The analytical models have been used as reference for adaptive machining, especially in monitoring the tool conditions and in maintaining desired surface roughness. The FEA models, on the other hand, are rather used as a standard engineering tool to give guidance in specifying the internally cooled cutting tool geometry and machining constraints and settings in the experiments.

7.1. Experimental setup for adaptive machining

Cutting insert (type SNUN12xx08 and SPUN12xx08) constitutes of tungsten carbide that bonded with 6% cobalt has been used in this project. This particular geometry of an insert is normally not recommended for dry cutting due to the absence of chip breaker, but was chosen so that the associated wear rate would be relatively steeper, thus could minimise the consumption of work-piece

materials especially in machining the expensive ones like titanium. The cutting insert is modified by embedding micro-channel that is to supply the coolant closest to the heat source in order to remove the heat from the tool optimally. Fig. 7-1 illustrates the tool geometry for a complete cutting tool which consists of a square shape of cutting insert with geometry type SNUN12xx08 and a tool holder of geometrical type CSBNR 2525 M 12-4. The image on the right shows the modified cutting tool with a bottle cap shape cutting insert and a supporting adapter. The bottle cap shape of cutting insert enables the micro-channel to align its cooling position directly beneath the heat sources for optimum conduction heat transfer. The modification of the cutting insert requires a special consideration about the residual stress that might be introduced when forming the bottle cap shape

.
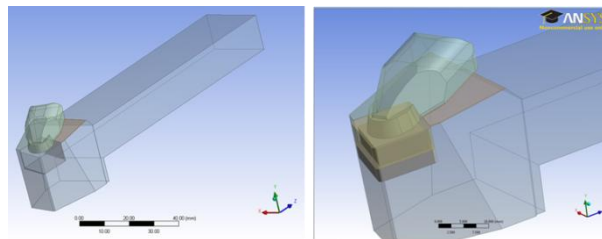
Fig. 7-1 : Cutting tool; (l) commercial tool geometry, (r) modified tool insert for accommodating micro channel

Another modification that needs to be precisely carried out is to fabricate two holes in the tool holder for attachment with the inlet and outlet hoses. Misalignment at this stage may cost unnecessary pressure loss or leakage. The final views of the tool are displayed in Fig. 7-2 with the image on the left shows the tool from the viewpoint of cutting edge and on the right is the image from the major flank view.
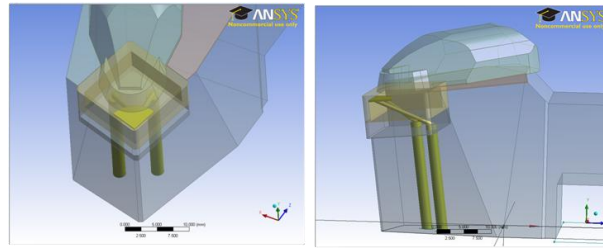
Fig. 7-2 : Internally cooled cutting tool

The machining trials are performed on an Alpha Colchester Harrison 600 Group CNC lathe. In Fig. 7-3 , the machine set-up is displayed. In the figure it can be seen a special jig that holds the tool holder is attached to the dynamometer so the cutting forces in 3 dimensions can be measured. Also the pyrometer that measures a point temperature on the rake face, the work-piece, the inlet hose and the outlet hose is shown in the image.
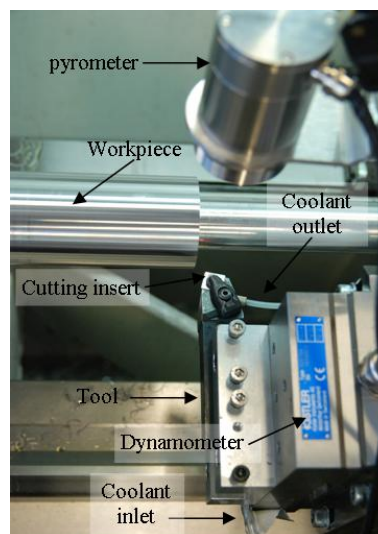
Fig. 7-3 : Machining set-up

Fig. 7-4 shows the subsystems that constitute the whole system for the experiment. The machine tool interface can only be accessed by trained operators and on the interface important control buttons to set the machining parameters like cutting speed, feed rate and depth of cut are available.

Emergency stop button can be found at the interface too. Next to the machine tool sits cooling peripheral. The cooling system consists of a micro-diaphragm liquid pump, a tank and power units. The pump peripheral is arranged to be closest to the machine tool in order to minimise pressure loss. The signals from the machine controller and thermal sensors are acquired by a DAQ system from National Instrument in real time. The data are simultaneously transferred to the monitoring PC and control PC for further actions.
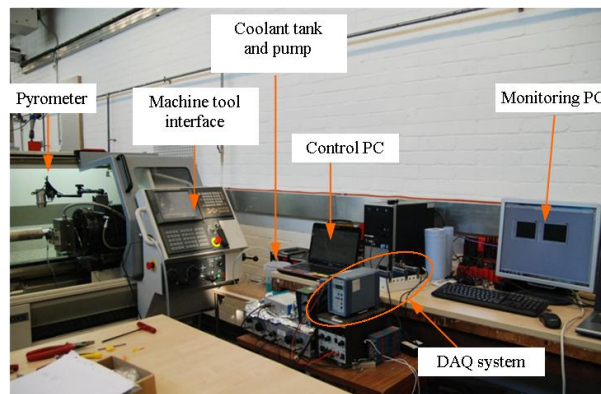
Fig. 7-4: Subsystems for experimental cutting trials

Standard procedures have been practiced during the research to ensure reliable and repeatable results can be obtained. Measurement units such as pyrometer, thermocouples and dynamometer have been calibrated against known values or standard device prior usage to determine the transfer factors. As can be seen in the Fig. 7-5, a pyrometer is calibrated against a black body to determine the emissivity. For a range of 150°C to 350°C, the values in the range of 0.78 and 0.63 have been identified as suitable emissivity to measure uncoated tungsten carbide surface and Ti-N coated tungsten carbide surface respectively. In calibrating the 3D dynamometer, a force calibrator has been used. The calibration is performed in two directions which represent the cutting and feed forces direction. Forces in the range of 20N to 100N and 20N to 250N have been

applied to calibrate dynamometer in feed (as shown in the Fig. 7-6) and force
direction respectively. These ranges have been identified as nominal forces in
machining aluminium, steel and titanium with the selected cutting parameters.
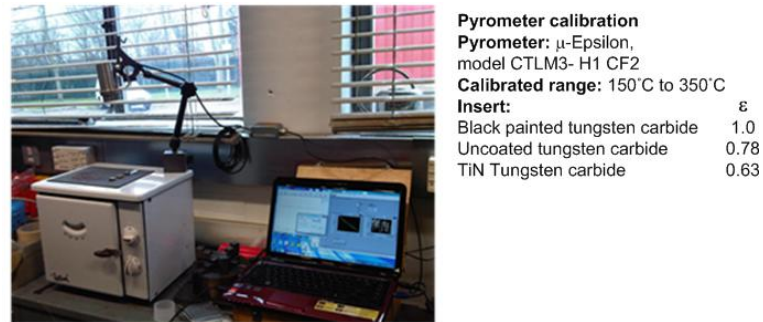
Fig. 7-5 : Pyrometer calibration

Initially, a random initial value will be set in the LabVIEW acquisition program
for the transfer function of the cutting force and feed force. Then force is
applied by the force calibrator on the cutting tool which is attached on the
dynamometer and the reading from the dynamometer is recorded and plotted
in a graph. The gradients of the obtained trend line are the new transfer
function values and will be used in the data acquisition LabVIEW programme.
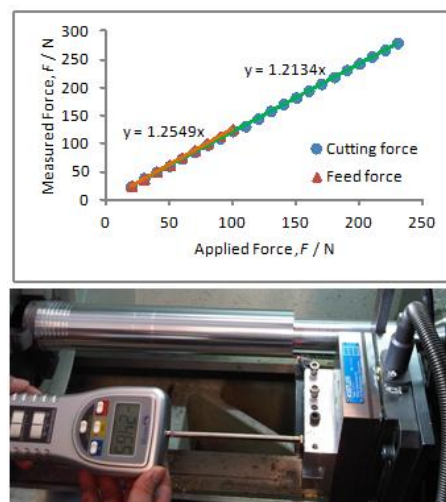
Fig. 7-6: Dynamometer calibration

7.2.   **Machining different types of materials with the internally cooled smart cutting tool**

The selection of materials for cutting trials with internally cooled cutting tool is based on the demand for machining the materials in contamination-free manufacturing environment. Aluminium, steel and titanium, despite their substantial consumption in manufacturing, possess significant challenge for machining with the absence of cooling fluid due to their inherent physical, chemical and thermal properties.

Aluminium is widely used as design features by many global leading manufacturers to express high-end products, ranging from audio-video to automotive applications. Thus, the surface finish of the product needs to achieve high tolerance control. Should machining process can produce the required surface quality, after-treatment operations can be eliminated and this can help in reducing the manufacturing cost. Keeping surface errors at a minimum is a challenge in machining aluminium due to the facts that the material is sensitive to thermal expansion and it is prone to adhere to the cutting edges. At elevated temperature cobalt, which acts as a binder in tungsten carbide tool, reacts with aluminium which causes the aluminium to chemically bond with the exposed cobalt at the cutting edge of the tool. The adhesion of aluminium on the tool expedites the formation of built-up edges (BUE) that make the cutting tool ineffective. The control of cutting temperature and optimum cutting conditions are an extreme importance to enable a high quality surface finish of aluminium to be produced.

Machining of steel has always been an important manufacturing process. Mechanical and physical properties of steel make it a major component in a versatile range of industrial applications including hygienic applications such as drinking and food uses, medical devices and pharmaceutical equipment. The machining conditions particularly the supply of cooling fluid for hygienic applications are critical as it may contribute directly to the consumers either by dietary intake, implants or level of efficacy of the product. The hardness of steel is commonly influenced by the amount of carbon content. On the other hand, the higher the content of carbon steel the lower the melting point of the composite will be. Chip formation of steel creates localized high stress and high temperature on the tool tip. The combination of both effects can drastically curtail the tool life.

Titanium has been widely used in aerospace, biomedical, automotive and petroleum industries because of their good strength-to-weight ratio and superior corrosion resistance. However, the machining of titanium poses a critical challenge due to its tendency to work harden during the machining process, high cutting temperature at the tool chip interface, high cutting pressures, chatter and its reactivity with the cutting tool materials at temperature higher than 500°C. In addition, its low conductivity and low modulus of elasticity impede its machinability. At low cutting temperature, the chemical affinity of the titanium with cutting tool materials may lead to adhesion, which results in a poor work-piece surface finish. Thus, it is an essential for a technique to adaptively control the process parameters to optimally machine titanium to achieving a balance between good surface finish, extended tool life and productivity.

Recent review article by Sharma et al. (2009) describes how developments in coolant technologies including indirect cooling have enabled faster cutting speeds and/or extended tool life when machining difficult to cut materials. Cooling the heated zones internally enables the generated heat to be withdrawn efficiently via conduction. Conduction of heat is directly dependent on the thermal conductivity of the medium, the distance between the heat source and the heat sink and the temperature difference. This advantage may control the amount of heat which is helpful in reducing the cutting forces to be supplied to the cutting tool. As a result, higher optimum cutting parameters can be applied without exerting excessive high thermal load and mechanical pressure on the cutting tool.

The application of internally cooled cutting tool with adaptive control is also beneficial in machining those materials in a ECMP environment because (i) optimum cutting parameters can be controlled and (ii) wear mechanisms which characterise high sensitivity to cutting temperature can be manipulated. These advantages may enable the cutting tool life to be extended, surface finish to be improved and abrupt tool failure to be avoided. However, the experiments to validate these hypotheses necessitate an extremely careful plan because:

(1)   each experiment requires fresh cutting edge to avoid bias,

(2)   tool life investigations require the tool to be used until the onset of tool failure, thus sufficient amount of work materials is needed,

(3)   measurement of tool wear and surface finish have to be performed offline under special measurement equipment.

In summary the cutting parameters and the machining objectives of the final experiments are displayed with their corresponding materials in the Table 7-1.

Table 7-1: Cutting parameters

Material	Grade	Speed, v / m/min	Feed, f / mm/rev	Depth, a_p/ mm	Flow, m/ l/min	Machining objectives
Titanium	CP2	80	0.1	0.5	0	tool life
		120	0.2	1	0.5	
Steel	EN32	100	0.1	0.5	0	surface
		150	0.15		0.17	roughness
		200	0.2		0.5	adaptive
					1	control
					1.75	
Aluminium	AA6082	150	0.1	0.2	0	tool life
		250	0.2	0.3	0.2	surface
		300	0.3	0.5	0.3	roughness
		330				adaptive
						control

7.3.   Cutting trial results and discussions

The experimental results will be displayed and discussed separately for each material. The results will address the challenges in machining of those materials and will discuss the observations recorded in machining with internally cooled cutting tools. At the end of the discussion some conclusions on the performance of the internally cooled smart cutting tool in machining the aforementioned materials and recommendations for improvement will be drawn.

7.3.1. Machining aluminium alloy AA6082

Cutting trials were started with machining aluminium alloy AA6082 at different cutting speeds while the other cutting parameters, i.e. feedrate and depth of cut are kept constant. The cutting speed is increased 25 m/min for every trial and each trial is performed for 20 minutes. The machining was performed initially with conventional tools (145 cuts) and then with internally cooled cutting tools with coolant flow rate of 0.3 l/min in the next round (145 cuts). In order to accomplish these cutting trials 10 bars of AA6082 with the original diameter of 63 mm and allowable tool travel length of 300 mm were used. The tool flank wear, VB which was used as the tool life criterion, was measured under TESA vision system at the end of each trial. A used cutting edge will be marked and turned to a new cutting edge for the next trial until all the four cutting edges of a tool insert were used-up. Fig. 7-7 shows the result of the cutting trials. It can be seen that the flank wear characteristic of conventional tools observes a bell shape curve. It is important to remark that for cutting trials at low cutting speed especially in the range of 175 m/min to 275 m/min, the machine needs to be stopped intermittently for several times during machining due to the formation of BUE. Despite the manual removal of BUE, the sizes of the flank wear land of the cutting tools in this speed range are very high and the surface finish quality is also unacceptable (Fig. 7-9). On the other hand, when machining was carried out with internally cooled cutting tool, the flank wears obtained were more stable for the whole tested speeds range and BUEs were hardly seen on the tool tip. A possible explanation for this is that the elevated temperature which causes the exposed cobalt to react with aluminium was not reached due to efficient heat removal from the internally cooled cutting tool. Another possibility is that the adhesive wear activating cutting speed has been shifted to

the right, but this assumption cannot be tested since the spindle of this machine tool is not capable to rotate any higher.

Tool: SNUN 12XX08
Workpiece: AA6082
Process: Cylindrical turning

f: 0.1 mm/rev
a_p: 0.5 mm
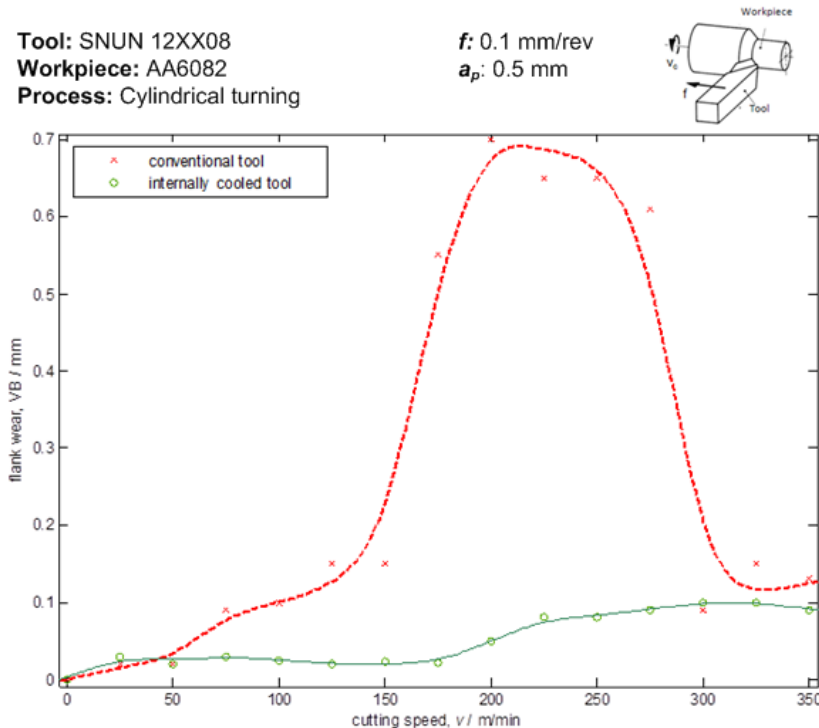
Fig. 7-7 : Flank wear of carbide tools when machining at different cutting speeds

The chips morphology has also been observed (Fig. 7-8). The chips produced are continuous as the ductility of the AA6082 prevents the chip to be broken especially at elevated temperature. The absence of chip breaker does not allow enough shear stress to break the chip. Besides BUE, it was also observed that at the cutting speed of 250m/min serrated chip happen with conventional tool. The chip serration of AA6082 is due to the onset of instability in the cutting process which results from competing thermal softening and strain hardening mechanisms in the primary shear zone (based on the observation by Komanduri (1982)).
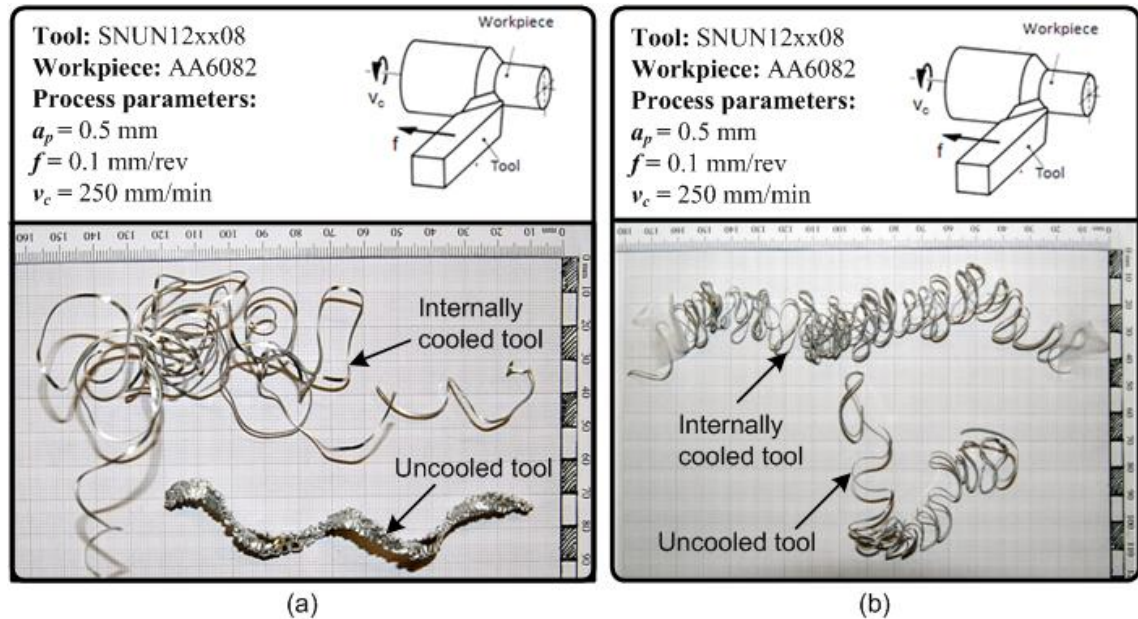
Fig. 7-8 : Chip morphology of machining AA6082; (a) $v = 250$m/min, and (b) $v = 330$m/min

The qualities of surface finish obtained for machining with internally cooled cutting tool are also generally much better than conventional which in the range of 0.5 μm to 1.2 μm. Generally, the surface roughness with the internally cooled cutting tool decrease with the increase in cutting speed. Since the cutting of aluminium can only be performed in the conventional cutting speeds region on this machine tool, it is not really an advantage of using internally cooled cutting tool to control optimum cutting conditions as the conventional cutting tool could also machine the AA6082 with high material removal rates (MRR) and good surface finish qualities. Further study may be required to extend the machining time as 20 minutes may be too short to observe the wear effect in machining AA6082 on carbide tool.
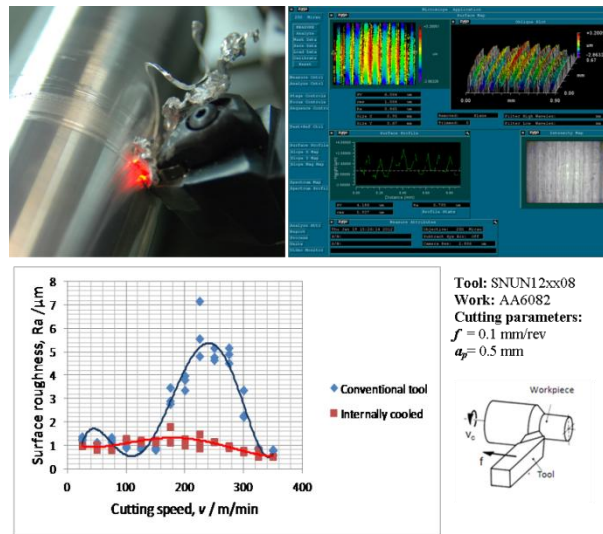
Fig. 7-9 : Cutting speed effects in machining AA6082

An experiment has been conducted to assess the effect of mass flow rate in removing heat from the tool. The result as has been discussed in Chapter 5 shows that the mass flow rate does not play significant role in reducing the cooling temperature. This is probably due to the fact that AA6082 is a soft material so the amount of heat generated and conducted inside the tool is relatively low. As mentioned by Hastings (1976) and Shaw (1984), the machining performance is influenced greatly by the cutting variables in a complex relationship in machining. In order to see the effect of machining parameters on the cutting performance with internally cooled cutting tools a set of cutting trials with four cutting variables; i.e. cutting speed, federate, depth of cut has been designed. The mass flow rate is kept constant at maximum as the author cannot see any point in manipulating this variable for this experiment. Surface roughness is considered as one of the criteria to gauge the performance of a tool. Six bars of AA6082 with the original diameter of 63 mm have been used for this experiment and the machining variables and the experimental results are displayed in Table 7-2.

Table 7-2: Obtained surface roughness, Ra when machining AA6082 with internally cooled tools

No.	speed, v / m/min	Feed, f / mm/rev	Depth, a_p / mm	time, t / s	Surface roughness, Ra / µm			
					Trial 1	Trial 2	Trial 3	Average
1	330	0.1	0.2	107.27	0.68	0.66	0.64	0.66
2	330	0.1	0.3	102.70	0.71	0.78	0.67	0.72
3	330	0.1	0.5	97.56	0.72	0.88	0.73	0.78
4	330	0.2	0.2	46.73	0.74	0.77	0.72	0.74
5	330	0.2	0.3	44.55	0.87	0.85	0.8	0.84
6	330	0.2	0.5	42.13	0.75	0.81	0.84	0.80
7	330	0.3	0.2	26.78	0.8	0.9	0.74	0.81
8	330	0.3	0.3	25.40	0.83	0.86	0.89	0.86
9	330	0.3	0.5	23.88	0.82	0.92	1.01	0.92
10	300	0.1	0.2	74.68	0.61	0.85	0.6	0.69
11	300	0.1	0.3	70.37	0.7	0.88	0.72	0.77
12	300	0.1	0.5	116.87	0.7	0.77	0.83	0.77
13	300	0.2	0.2	56.12	0.68	0.7	0.7	0.69
14	300	0.2	0.3	53.66	0.81	0.72	0.85	0.79
15	300	0.2	0.5	50.89	0.95	0.72	0.87	0.85
16	300	0.3	0.2	32.45	0.8	0.85	0.88	0.84
17	300	0.3	0.3	30.89	0.93	0.89	0.82	0.88
18	300	0.3	0.5	29.15	1.03	0.9	1.07	1.00
19	250	0.1	0.2	99.89	0.71	0.8	0.69	0.73
20	250	0.1	0.3	94.55	0.73	0.69	0.75	0.72
21	250	0.1	0.5	88.67	0.82	0.75	0.79	0.79
22	250	0.2	0.2	41.92	0.74	0.75	0.74	0.74
23	250	0.2	0.3	39.40	0.88	0.76	0.92	0.85
24	250	0.2	0.5	36.64	0.99	0.71	1.09	0.93
25	250	0.3	0.2	47.20	0.87	0.74	0.85	0.82
26	250	0.3	0.3	45.19	1.03	0.83	0.98	0.95
27	250	0.3	0.5	42.93	1.13	0.9	1.14	1.06
28	150	0.1	0.2	205.61	0.63	0.68	0.63	0.65
29	150	0.1	0.3	196.04	0.65	0.66	0.66	0.66
30	150	0.1	0.5	185.35	0.69	0.7	0.7	0.70
31	150	0.2	0.2	88.37	0.72	0.74	0.73	0.73
32	150	0.2	0.3	83.82	0.72	0.73	0.73	0.73
33	150	0.2	0.5	78.79	0.83	0.71	0.79	0.78
34	150	0.3	0.2	49.79	0.74	0.84	0.79	0.79
35	150	0.3	0.3	46.91	0.83	0.84	0.85	0.84
36	150	0.3	0.5	43.77	0.89	0.81	0.87	0.86

Selective data points have been chosen for detail analysis. The surface roughness in the function of cutting speed and feedrate has been analysed at two extreme levels of depth of cut and two sets of graphs have been produced in Fig. 7-10 to assist the analysis. In general, good surface finish can be obtained at low feedrate. Interestingly, cutting speed which is proportional to cutting temperature did not show a direct relationship with the surface roughness. The best surface roughness was when the cutting speed is above 300 m/min and the feedrate is the smallest, i.e. 0.1 mm/rev, while the worst quality of surface roughness was obtained when the AA6082 was cut at the cutting speed of 250 m/min and high feedrate.
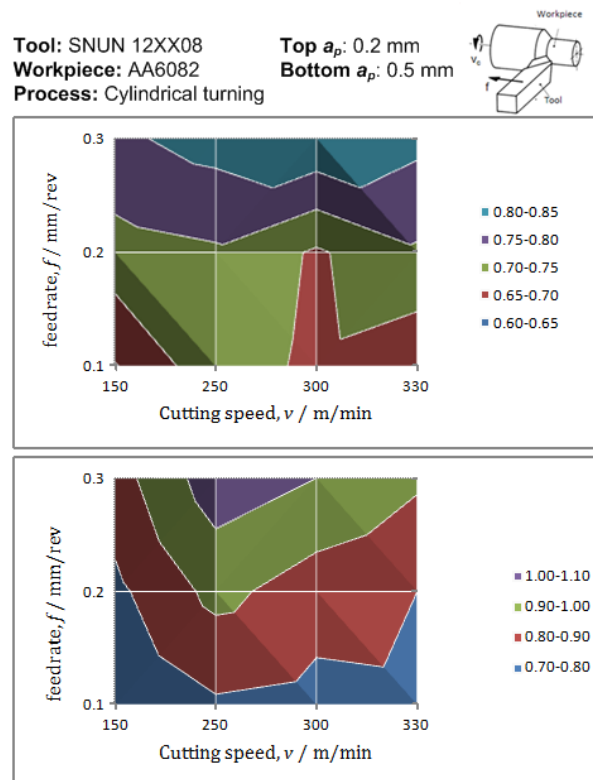
Fig. 7-10 : Surface roughness contour in machining AA6082 with the internally cooled cutting tool

Temperature readings and forces measurements have been referred in order to explore scientific explanation for this interesting relationship. Dry machining of AA6082 in conventional cutting and with internally cooled cutting tools with a constant depth of cut, a_p, of 0.5 mm and 2 levels of feedrate, f = 0.1 mm and 0.2mm, and 3 levels of cutting speed, v = 250 m/min, 300 m/min and 350 m/min yields temperature and forces results which are displayed in Fig. 7-11 and Fig. 7-12 respectively. In Figure 10, both graphs show that reductions of cutting temperature of about 40% can be obtained by utilising internally cooled cutting tool. However, too low temperature recorded when machining with the cutting speed of 250 m/min might cause bigger work is required to cut the AA6082.
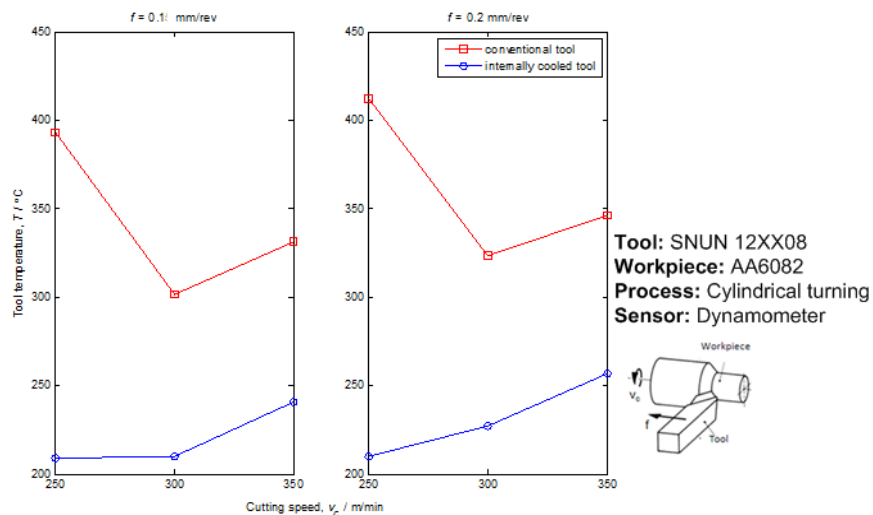
Fig. 7-11 : Tool temperature in machining AA6082

The graph on the left hand side of Fig. 7-12 shows that the biggest feed force of the machining with internally cooled cutting tool was acquired at the lowest cutting speed. Two assumptions can be made here: (i) the feedrate is too big for the cutting speed or (ii) the heat to overcome the yield strength of the work material is not sufficient for the workpiece to be machined. However, the first assumption can be cancelled out with the graph on the right as the feed force

attenuates. Then a conclusion can be drawn here that a certain amount of heat is necessary in machining to ensure a high performance from a cutting tool.
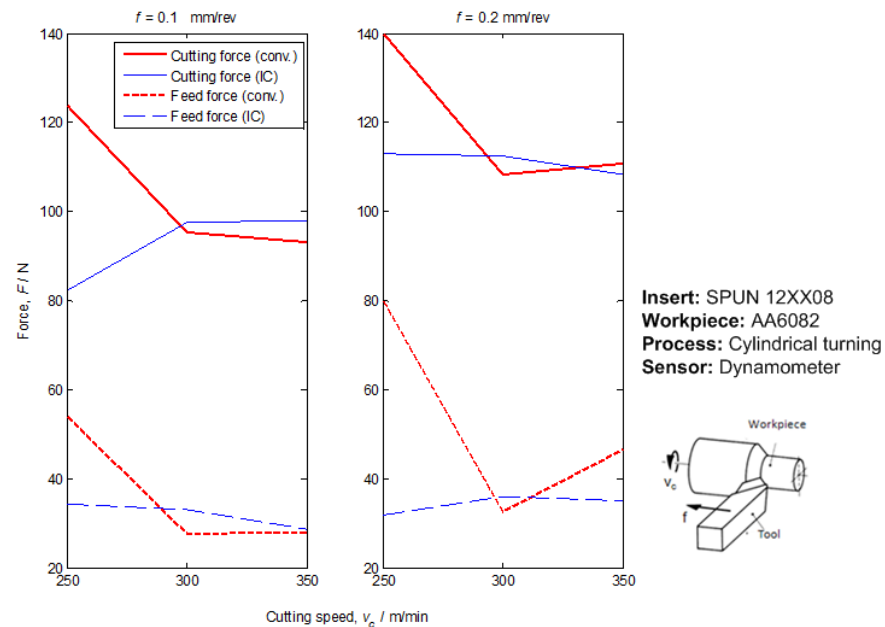
Fig. 7-12 : Cutting forces in machining AA6082

7.3.2. Machining mild steel EN32B

Machining of mild steel EN32B has been performed with the third configuration version of internally cooled cutting tool (please refer to Chapter 4; Design of internally cooled cutting tool). The third version of internally cooled cutting tools is the results of continuous improvement approach adopted in the development of this innovative tool. This new version tool has solved practical issues in using the tools such as leaking and sealing, manufacturing complexity, rubbing and self-lubricating, and non-standard temperature measurement.

Front view: 1mm thick SPUN
cutting insert sits on the fully
enclosed cooling module
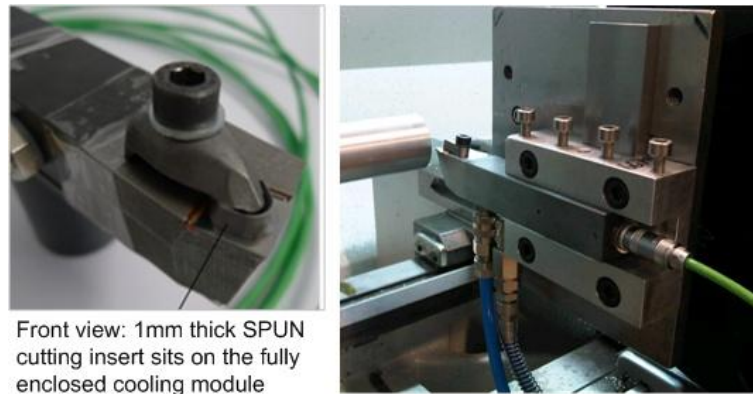
Fig. 7-13 : Mark III internally cooled cutting tool

Cutting parameters as in Table 7-1 have been used in machining mild steel EN32B. Since the importance of suitable cutting parameters has been established in the previous experiment, the effect of cutting parameters especially feed rate on the process variables will be the primary test in machining EN32B. The aims of machining EN32B can be summarised as follows:

(1) Investigate the effect of feed rate on tool temperature and surface roughness.

(2) Investigate the effect of cutting speed on tool temperature.

(3) Investigate the effect of coolant flow rate on cutting temperature.

(4) Investigate the effect of coolant flow rate on cutting forces (cutting and feed).

(5) Investigate the relationship between cutting temperature and surface roughness.

Fig. 7-14 shows the results of varying the feedrate on machining with internally cooled cutting tool. Constant cutting speed, depth of cut and coolant flow rate have been set in this experiment. Generally it can be seen that the tool temperature correlates quite well with the surface roughness. Both variables

increase with the increase in feedrate. The increment trend is also relatively linear with the rate of change in feedrate. Based on this observation, an arbitrary feedrate can be selected for the experiment to investigate other cutting variables as they are all equally significant.
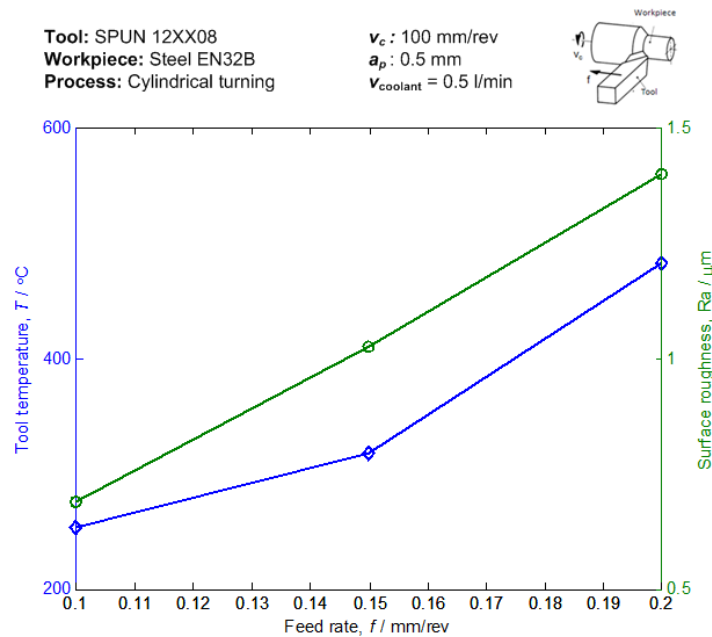
Fig. 7-14 : Effect of feed rate on surface roughness in machining steel EN32B

The next experiment is for investigating the effects of coolant flow rate on the tool temperature under different levels of cutting speed (aim number (2) and (3)). The experiment is performed in conjunction with the aim number (4) and (5). As can be seen in the Fig. 7-15 , internally cooled cutting tool is effective in reducing the cutting temperature for all cutting speed. The tool temperature correlates linearly with the cutting speed at low coolant flow rate, i.e. 0.17 l/min and 0.5 l/min but the relationship gets more complicated as the coolant flow rate increases. If the results are analysed in the view point of cutting speed, it can be seen that the coolant effects are too marginal for the machining with cutting speed of 100 m/min and 200 m/min. Interestingly the cutting

temperatures amplified when the coolant flow rate was set above 1.0 l/min in machining with cutting speed of 150 m/min.
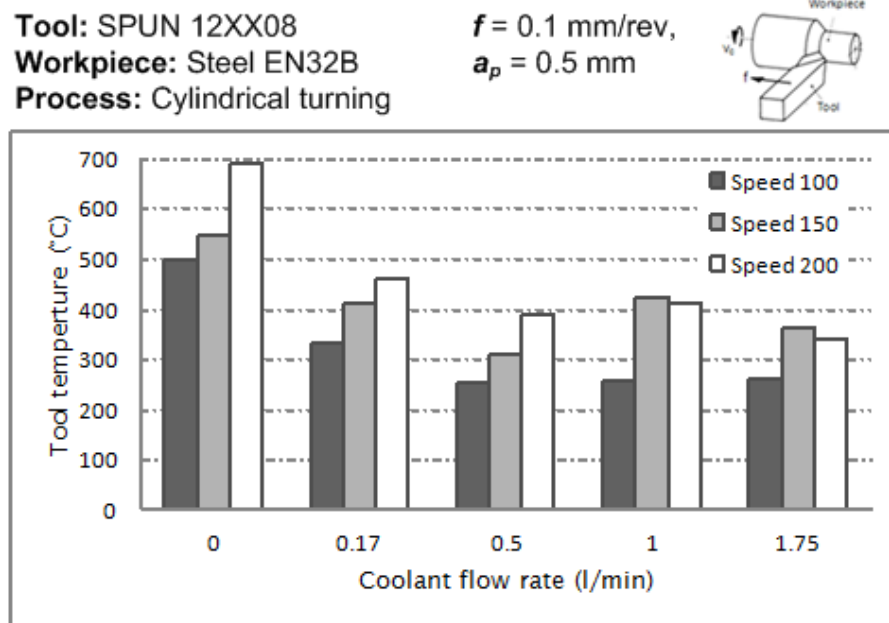
Fig. 7-15 : Tool temperature obtained from machining steel EN32B

Investigation of cutting forces has been performed to see the work carried out during the machining. The cutting force and feed force of the machining with 150 m/min cutting speed has been scrutinised. At coolant flow rate of 1.0 l/min and 1.75 l/min, the cutting forces of 150 m/min machining are peculiarly high in comparison with the readings recorded for the 100 m/min and 200 m/min. Further analysis on thermo-chemical-mechanical analysis should be performed to understand this phenomenon as diffusion and oxidation may take place during the cutting. Such in depth-study is not included in the framework of this research.
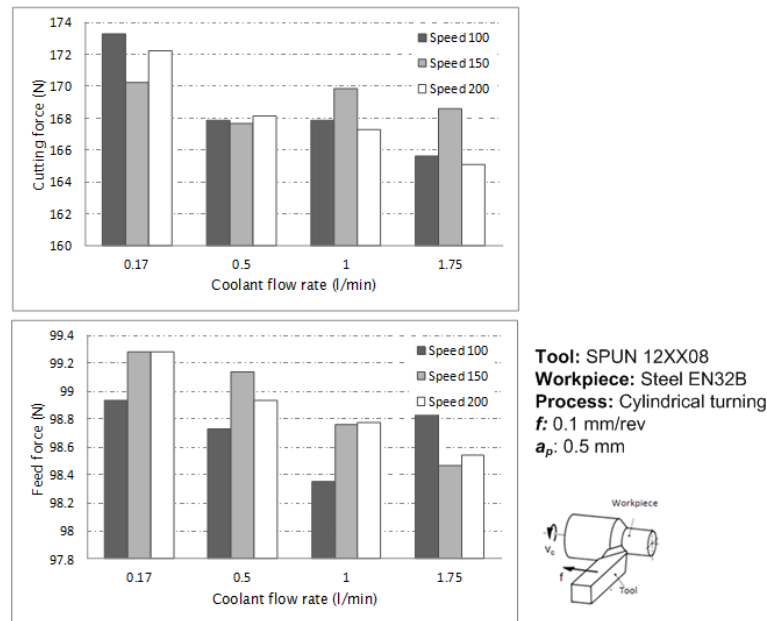
Fig. 7-16 : Cutting forces (top) and feed forces (bottom) acquired in machining

steel EN32B with cutting speed and coolant flow rate are varied

Again, the results of cutting temperature and surface roughness are displayed

side by side in Fig. 7-17 to show the correlation of the two process variable.

Both contour diagrams show maximum values of cutting temperature and

surface roughness at cutting speed of 150 m/min and coolant flow rate of 1.0

l/min. Some adhered metal were seen on the cutting tip and this metal is

analysed under EDX with 30keV accelerating voltage and the result shows that

the metal composed of mainly Mn, Si and C. It is elucidated that the chemical

composition welded at the cutting edge is the same as the workpiece material.

The welding mechanism can be explained with the help of labels A and B in the

Fig. 7-18. The heat generated from the energy conversion in the primary and

secondary deformation zones may reach the melting point of steel EN32B

which then soften some thin layers of the chip. The softened thin layer may

become very soft and flow at the contact interface between the tool face and the

flowing chip or stick to the rake face of the tool. The layer that is closed to the

point A, experiences high pressure due to the thickest thickness of the chip and will stick to the back face of the chips flow with them during machining. Meanwhile, the softened layers at the vicinity of point B, the thinnest area of the chip may remain at the cutting edge due to low pressure and accumulate themselves to form BUE. The formation of the BUE on the cutting edge causes "squeezing effect" which diverts the flow of the chip in the opposite direction (feed direction). The thicker the BUE the larger the side flow and large side flow produces high surface roughness (Yousefi et al., 2000). The best surface roughness was obtained when the cutting speed was the highest and the coolant flow rate was maximised. With this final result a conclusion can be drawn that internally cooled cutting tool can produce a better surface finish provided that the optimum cutting speed is applied. Feedrate is suitable variable to be manipulated in adaptive control as it is linearly correlated with cutting temperature.
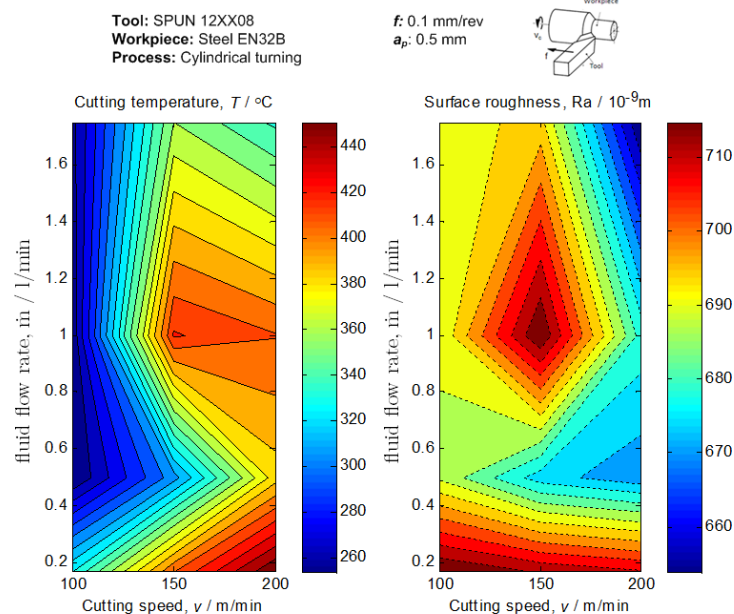
Fig. 7-17 : Cutting temperature and surface roughness contour of machining of EN32B
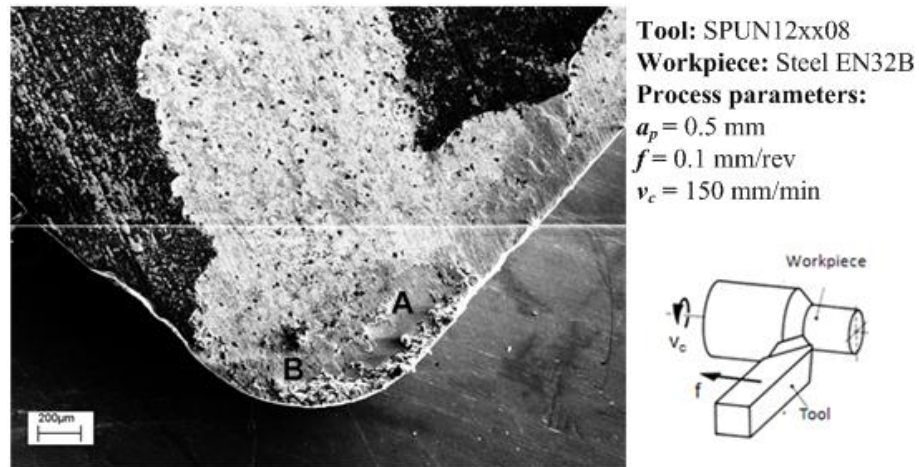
Fig. 7-18 : SEM image of cutting tip after machining mild steel EN32B with the internally cooled cutting tool

7.3.3. Machining Grade 2 CP Titanium

Machining of grade 2 commercial pure (CP) titanium has been performed with the second version of internally cooled cutting tools configuration (please refer to Chapter 4; Design of internally cooled cutting tool). Second version of an internally cooled cutting tool is an internally cooled tool with major modification to the insert geometry. With the same tool holder as in the first version, the second version has replaced the bottle-cap shape cutting insert with a 1mm thick plate of cutting insert. The cutting insert is also equipped with 11° clearance angle. So the new cutting insert geometry falls in the standard category of SPUN. Fig. 7-19 depicts the replica of the modified design of the version 2 internally cooled cutting tools. For this experiment, CVD diamond coated inserts have also been used to observe the effect of the diamond which has been claimed by several papers (Shen, 1996; Lahres et al., 1997; Shimada et al., 2004) that it possesses self lubricating characteristics.
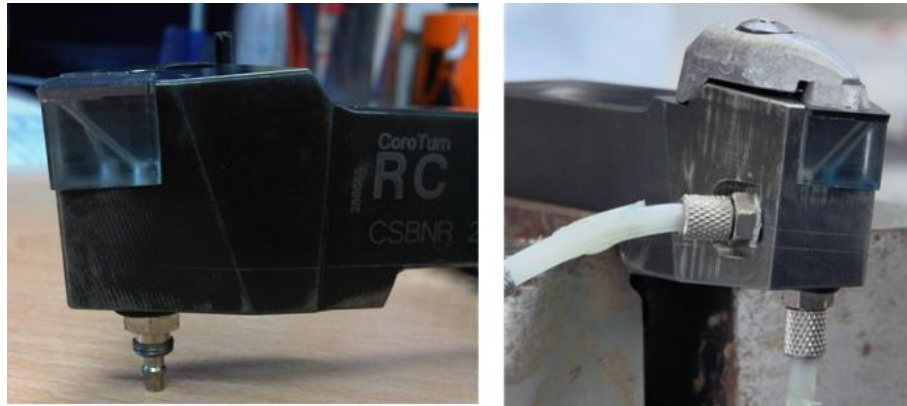
Fig. 7-19 : Mark II replica of the internally cooled cutting tools

The experimental results are displayed in Fig. 7-20. Surprisingly in turning titanium the tool life of the uncoated internally cooled tool was shorter than the lifespan of a conventional (uncooled) cutting tool. A possible explanation for this based on the previous publications (Hastings and Oxley, 1976; Kitagawa et al., 1997) is that the wear characteristics cannot be explained by temperature alone. The low temperature resulted from efficient internal cooling might result in an increase of the dominance of adhesion in controlling wear formation. The used cutting edge has been inspected under the scanning electron microscope (SEM) and energy-dispersive x-ray spectroscopy (EDX) to see the condition of the cutting edge. Accelerating voltage of about 30keV was applied to the specimen to increase the resolution under low vacuum (LV) observation with both backscattered electron image and secondary electron image. Magnification of 50× at 7.2 mm measured distance was also applied. It is found that the content of titanium is hugely dominant in the region close to the cutting edge as shown in the EDX-analyser at the bottom image of Fig. 7-21.
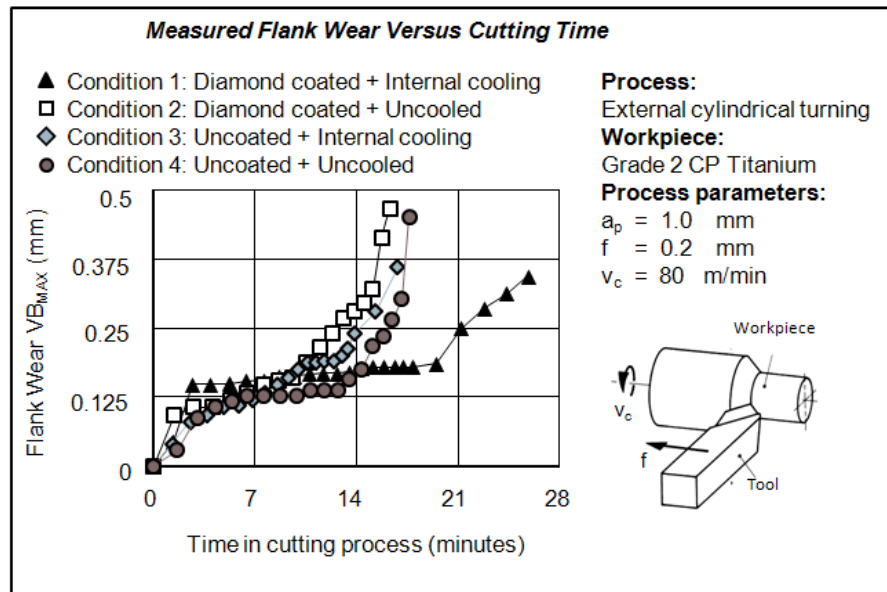
Fig. 7-20 : Experimental results in machining grade 2 CP titanium

The machining with diamond coated inserts showed big improvement when applying internally cooled cutting tool. Although, the coated diamond can provide lubricating effect at the contact interface between titanium chip and cutting tool, but diamond cannot withstand the combination effect of high pressure and high temperature. It is reported that diamond diffuses with ferrous materials at temperature of about 650°C (Shimada et al., 2004). By applying internal cooling beneath the contact region assisted by the high thermal conductivity of diamond, the localised high temperature can be spread and reduced. If tool failure is judged by rapid development of tool wear, the internally cooled cutting tool with CVD diamond coating can enhance the useful tool life to more than 30% than conventional dry machining.
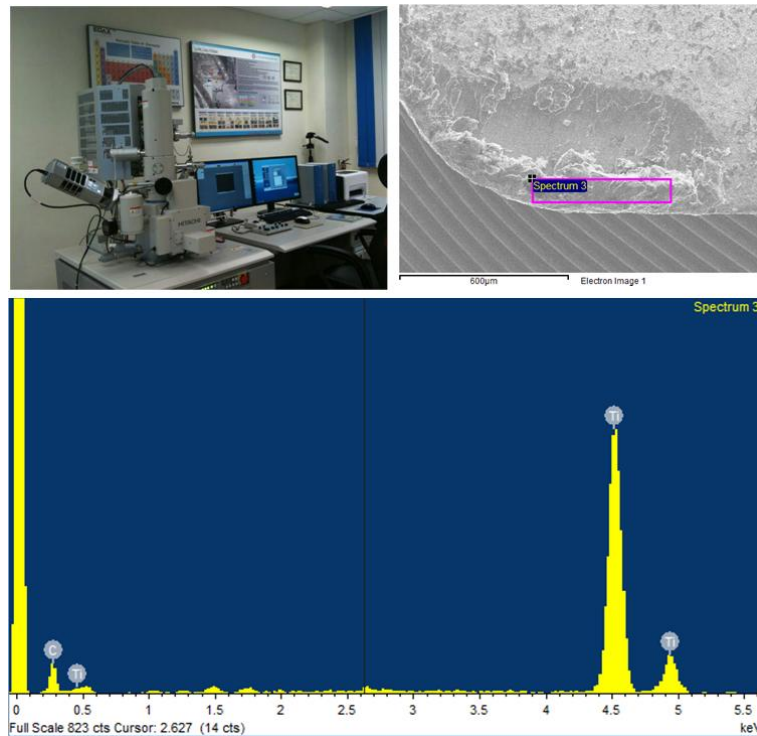
Fig. 7-21 : SEM + EDX machine and the results of an internally cooled carbide tool

The cutting inserts used in the experiment have been inspected under TESA vision system, and the rake face images of the inserts were consolidated in Fig. 7-22. Adhesion wear can be seen on all the cutting inserts. Oxidation wear which to some extent is useful for machining can be observed in Fig. 7-22(a) and Fig. 7-22(b). However, due to absence of cooling mechanism in Fig. 7-22(b) the temperature rise caused the rapid tool failure due to intensifying of oxidation wear and this can be observed from the notch generation and chipping along the edge of the cutting insert. Delamination of the diamond coating can also be detected on this tool as such in Fig. 7-23. The generation of notch, chipping and delamination of diamond coating resulted in a very unfavourable cutting edge and a degradation of the machine surface as detected in Fig. 7-23. Both cases of uncoated tools showed almost the same rake faces condition. From these observations it is understandable that machinining hard-to-cut materials such

as titanium causes the cutting tool to experience the combination effect of intense stresses and temperatures especially at the contact region. A self lubrication property of diamond is handy to aid the machining of these materials.
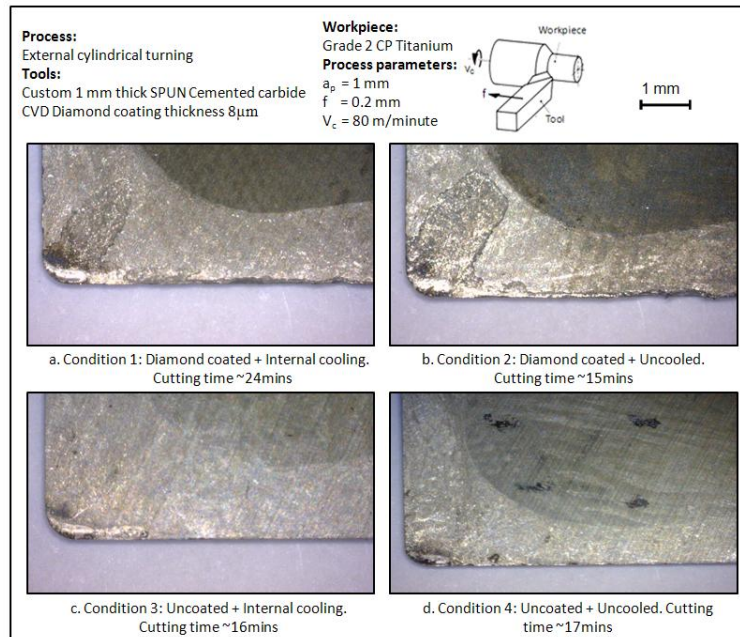
Fig. 7-22 : Cutting edges of used carbide inserts after dry machining grade 2 CP titanium
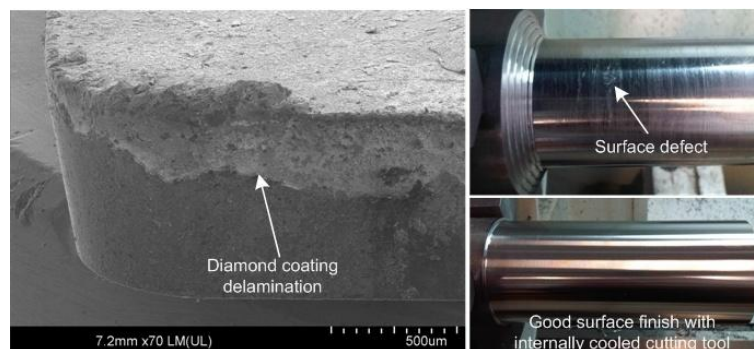
Fig. 7-23 : SEM image of diamond coating delamination and the surface finish of internally cooled and uncooled cutting tools

7.4.   Inlet-outlet temperature difference

The temperature difference between the inlet and outlet represents the amount of heat removed from the cutting insert by the cooling fluid. Based on the energy equation

$$E = \dot{m}_c \cdot c_p \cdot \Delta\theta \qquad\qquad (7.1)$$

Denoting E is the energy absorbed by the water, $\dot{m}_c$ is the mass flow of the water, c_p is specific heat capacity and $\Delta\theta$ is the difference in temperatures at the inlet and outlet. With the constant mass flow supplied the amount of energy absorbed is linearly proportional with the temperature difference. The higher heat created at the heat sources as in the case of worn tool, BUEs occurrence or abrupt tool failure will be reflected with the increase in temperature difference between the inlet and outlet.

Fig. 7-24 depicts the acquired cutting force and temperature difference of the inlet and outlet when three common phenomena in machining occur (smooth cut, BUE and tool wear). It can be seen that the temperature difference at the inlet and outlet imitates the cutting force with some delay. Cutting force monitoring is a common process variable that is used in process condition monitoring system. The nominal cutting force of about 50 N in smooth cut has doubled with the presence of BUE or when the wear took place, and the same order can be observed with the temperature difference when the temperature increases from 1°C in good condition to over 2°C when the onset of tool failure. The ability of the difference of the inlet and outlet temperatures to detect the abnormality in machining offers great potential for further development of a smart and cost effective tool condition monitoring technique.
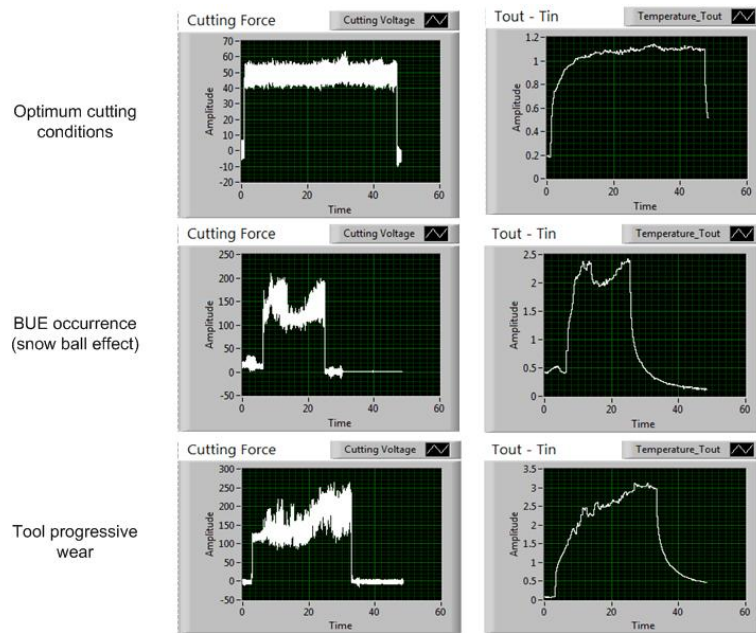
Fig. 7-24 : The readings of the cutting force and the temperature difference at
the inlet and outlet in different machining phenomena

7.5.   **Conclusion**

Machining AA6082

Challenges in machining AA6082

 (1) Material tends to form welded junction at the contact interface.

 (2) BUEs occur at elevated temperature shorten tool life, damage work
      surface and/ or increase machine down time

 (3) Small range of optimum cutting condition

Advantages of internally cooled cutting tools:

 (1) Hardly any BUE found in machining with internally cooled cutting tools.

 (2) Better quality and more predictable surface finish for extended tool life.

 (3) Enable machining at a wider range of cutting speeds.

Proposal for improvement:

(1) Longer cutting time to investigate the performance of internally cooled cutting tool in terms of tool lifespan, wear mechanisms and machined surface quality.

(2) Introduction of chip breaker on the tool as long swarf that gathers around the tool affects measurement accuracy.

(3) Perform cutting trials on other machine tool with higher spindle speed capabilities to observe the performance of the internally cooled cutting speed in high speed machining.

Machining EN32B

(1) Cutting temperature and surface roughness in machining EN32B are directly influenced by feedrate. The feedrate linearly controls the rise in cutting temperature and the generated surface roughness.

(2) Cutting temperatures and surface finish qualities showed significant improvement when applying internally cooled cutting tool.

(3) Thermo-chemical-mechanical interactions during dry machining of EN32B should be further analysed in order to understand the effects of internal cooling. The prepared framework of this research could not explain scientifically the non-linear relationship between the cutting temperature and surface roughness.

(4) Based on the positive outcomes of machining titanium, a cutting trial with the application of diamond coated internally cooled cutting tool in cutting EN32B could provide useful information to improve EN32B machining performance.

Machining grade 2 CP titanium

(1) Machining of difficult-to-cut materials such as titanium in a contamination free environment has been always a challenge for manufacturing practitioner due to the combination effect of intense mechanical stresses and temperature at the cutting tip causes unpredictable surface finish defect and abrupt tool failure.

(2) CVD coating diamond on the insert and application of internal cooling have been proven as a good pragmatic solution to overcome these issues. Less adhesion and thermally induced wear has been observed in turning of grade 2 CP titanium with the diamond coated internally cooled tool at recommended cutting parameters (machinability).

(3) Conventional DM with CVD diamond coated insert produced short tool life and bad surface finish due to diamond coating delamination. The defect is because of the limitation of the CVD diamond coating to withstand the combination of high pressure and high temperature in the absence of cooling fluid.

(4) Machining with CVD diamond coated internally cooled tool has produced significant improvement in surface roughness and could extend the tool life up to 30% higher than conventional machining.

(5) The improvements paved a potential advantage for higher productivity and improved surface finish quality in turning of high strength materials using internally cooled cutting tools.

The temperature difference between the inlet and outlet show agreement with the cutting force obtained. The changes in cutting force due to BUE and tool wear can also be detected with the change in temperature difference. This is beneficial in the development of smart and cost effective on-line monitoring system for adaptive machining.

Chapter 8:   Conclusions and Recommendation for Future Work

8.1.   Conclusions

The works throughout this research have demonstrated the ability of the research approach to answer the ten questions that have been formulated at the beginning of this thesis.

(1) Accurate cutting temperature

Cutting temperature is dependent on temporal and spatial uncertainties, which makes the measuring of it precisely, accurately and consistently is difficult. Throughout this research three measurement equipment have been tested, viz. thermocouple, IR video camera and pyrometer. Embedded thermocouple is found to offer the most economical and viable solution for acquiring the tool temperature in the high dynamic and hostile environment of machining. Labourious work particularly in determining the emissivities of different metal surfaces in machining operation makes the utilisation of IR camera the least feasible technique to provide feedback sensor to the plug-and-produce smart cutting tool. On the other hand, the measurement recorded by the thermocouple by means of heat conducted to the tool is more accurate and reproducible.

(2) Efficient cooling techniques

Modeling and simulation of the combined heat transfer and fluid flow of internally cooled cutting tool have provided thermo-mechanical fundamental understanding of the behaviour of the internal cooling technique. The internal

cooling that have been modelled are manifold micro-channel, jet cooling and open plan cooling designs. The boundary conditions obtained experimentally have been used to assess the effectiveness of the cooling techniques applied. The heat transfer coefficient, friction coefficient and pressure drop are analysed to determine the most optimum cooling technique. Jet cooling micro-channel is found to have the most optimum cooling capability to be applied in the specified machining procedures.

(3) Structural strength with the inclusion of micro-channel

The structural modeling of the cutting tool design allows the optimisation of the design parameters of the internally cooled cutting tools with particular consideration of mechanical strength. Experimental study has been carried out by machining grade 2 CP titanium to determine the tool-chip contact area and the cutting forces exerted. An important finding of the study indicates that an inclusion of a micro-channel of $0.8\mu m$ diameter with 1mm distance to the cutting edge for an insert made of WC exhibits structural strength with a safety factor of higher than 1.5 in the nominal operating condition.

(4) Effectiveness of internal cooling in reducing cutting temperature

Cutting tool and workpiece are subjected to the combination of high thermal stresses and mechanical pressure in machining with the absence of cooling fluid. In moderate cut such as in machining aluminium alloy AA6082 and finishing operation of mild steel EN32B, internal cooling could efficiently remove the heat generated by the process of chip formation but no evidence of machining performance improvement observed in machining hard and difficult materials. An implication of this is the possibility that the inefficiency of the cooling mechanism is due to the increase in friction coefficient between the

sliding chip and the rake face of the tool at elevated temperature due to no application of lubrication.

(5) Optimum cooling conditions

One of the more significant findings emerged from this research is that the success of the application of smart cutting tool in the ECMP requires more than just eliminating flood coolant and removal of maximum generated heat; it requires a methodological approach in controlling of optimum heat/ cutting condition in the overall process. The experimental cutting trials have found that generally as the cutting speed increases the surface roughness reduces. Growth of welded metals were observed at certain transition range of cutting speed for all materials; AA6082, EN32B and CP titanium. The results of machining mild steel EN32B indicate that with the aim of maximising MRR at the maximum cutting speed of 200m/min, the surface finish quality can be improved by 7% when the internal coolant with flow rate of 2.0l/min is applied.

(6) Cutting temperature correlation with the tool wear

The development of tool wear limits the tool life. Inarguably cutting temperature determines the wear mechanisms; i.e. abrasion, adhesion, diffusion, oxidation or abrupt tool failure, but surprisingly the development of total wear is not in trend with the cutting temperature for all cases. It is difficult to explain this result and interpret the correlation between the tool wear and the cutting temperature without a dedicated study on the effect of chemical reaction at the tribological contact surfaces between the chip and the tool and between the finished work surface and the flank face. The present results are, however, significant in at least two respects; (1) the cutting temperature influences the activation of adhesion, oxidation and diffusion wear and (2)

optimum cutting temperature can minimise the development of tool wear mechanisms.

(7) Machining of different materials

Machining trials have been performed on three different materials, viz. aluminium alloy AA6082, mild steel EN32B and grade-2 CP titanium. Selected materials were chosen because their machinabilities represent three important groups of materials in industry, i.e. soft-ductile material, hard brittle-material and difficult-to-cut material. The applications of internally cooled cutting tool in ECMP of aluminium alloy AA6082 were the most successful as it could solve the common BUE problems in machining adhesive-prone ductile aluminium alloy. On the other hand, the most interesting finding was obtained in machining mild steel EN32B. Generally in machining EN32B, acceptable surface finish was obtained at low cutting speed where the cutting temperature is low. However, at middle cutting speed of 150 m/min, a surprise phenomenon where the supply of internal cooling fluid of 1 l/min resulted the worst surface finish quality. This finding has important implications for determining the optimum cutting conditions in machining this type of material. The application of internally cooled cutting tool in ECMP of difficult-to-cut material grade 2 CP titanium shows that improvement can be obtained if the insert is applied with self-lubricating CVD diamond coating. Without internal cooling the ECMP with CVD diamond coated insert produced short tool life due to the delamination of diamond coating.

(8) Adaptive machining in controlling tool wear

Adaptive machining by controlling the optimum cutting temperature offers potential solution for controlling the activation of tool wear mechanisms in

ECMP. Machining trials of mild steel EN32B with internally cooled cutting tools (flow rate 0.1 l/min) indicate that higher degree of progressive wears was observed in non-adapted cutting speed machining. By adapting the cutting speed in controlling the cutting temperature, critical temperature at where the thermal induced wear is activated could be avoided.

(9) Adaptive control technique to apply internally cooled cutting tool

Returning to the adaptive control techniques formulated at the beginning of this thesis, it is now possible to state that the utilisation of real time and on-line adaptive control algorithm is not trivial to be realised. A holistic fundamental study of the thermal-chemical and physical interactions in the complex machining process is required.

Technological aspects of machine tool CNC control, reliable sensor fusion, real-time capability of data acquisition system and self-learning ability of the data processing units are also demanded in dealing with the challenge in interpreting the ever-lagged measured temperature in real time control. The approach of implementing on-line adaptive control constraint (ACC) has numbers of attractive aims in this research: (1) to observe the machining performance of internally cooled smart cutting tools in adaptive machining, (2) to evaluate the performance of the thermal sensors in on-line communication, and (3) to assess the effect of critical temperature in activating wear mechanisms. The experimental trials indicate that by applying ACC in controlling the adaptive machining with internally cooled smart cutting tools, the tool life can be extended and higher degree of surface roughness accuracy can be obtained.

(10) Inlet-outlet temperature difference

The temperature difference between the inlet and outlet fluid is associated with the amount of heat removed from the cutting tool. The readings of the temperature difference between the inlet and outlet show agreement with the cutting force obtained. The agreement between the temperature and force signal in detecting the abnormalities in machining indicates that the difference in the inlet and outlet temperatures can be utilised for condition monitoring signal. Major abnormality of machining conditions such as BUE and tool wear that are normally detected by the cutting force can also be indirectly detected by observing the inlet-outlet temperature difference. This is beneficial in the development of smart and cost effective on-line monitoring system for adaptive machining.

8.2.   **Contributions to knowledge**

Major contributions to the knowledge can be summarised as follows:

(1) An optimal design of the internally cooled cutting tool supported by the CFD analysis. The cutting tool has successfully been tested in adaptive machining of materials, including adhesive-prone aluminium alloy AA6082, mild steel EN32B and grade 2 CP titanium.

(2) Development of the hybrid models that can be used to predict the internally cooled cutting tool performance.

(3) Investigation on the critical temperature through which the rapid failure of the tool has been determined and the optimum region for the minimum occurrence of tool wear has been identified.

(4) The development of adaptive machining framework for application of internally cooled cutting tool. The framework has been tested with two strategies:

- using optimum force constraint to adapt the machining feedrate, and
- using optimum temperature region to cognitively adapt coolant flow rate and cutting speed.

8.3.   **Recommendations for future work**

(1) Improve the design of the internally cooled tool with the chip breaker. Chip management is critical in ECMP as the friction between the tool and the chip influence the heat generation at the secondary zone.

(2) The cooling efficiency of the micro channel should be explored when embedding the cutting tool with multiple channels. The increase in contact area can improve the heat removal rate.

(3) The tool life/ wear rate model for internally cooled cutting tool needs to be developed. The previous work on tool life/ wear rate model on conventional cutting tool is a good reference to follow. Hybrid tool life model with CFD and heat transfer model will be novel and beneficial to the manufacturing community.

(4) Machining should be performed with wider range of material such as explosive-prone magnesium, hard-to-cut Inconel and composite materials such as MMC.

References

Abdel-Aal, H.A., Nouari, M. and Mansori, M.E. (2009) "Tribo-energetic correlation of tool thermal properties to wear of WC-Co inserts in high speed dry machining of aeronautical grade titanium alloys", *Wear,* vol. 266, no. 3–4, pp. 432-443.

Abukhshim, N.A., Mativenga, P.T. and Sheikh, M.A. (2006) "Heat generation and temperature prediction in metal cutting: A review and implications for high speed machining", *International Journal of Machine Tools and Manufacture,* vol. 46, no. 7–8, pp. 782-800.

Abukhshim, N.A., Mativenga, P.T. and Sheikh, M.A. (2005) "Investigation of heat partition in high speed turning of high strength alloy steel", *International Journal of Machine Tools and Manufacture,* vol. 45, no. 15, pp. 1687-1695.

Adams, T.M., Abdel-Khalik, S.I., Jeter, S.M., Qureshi, Z.H. (1998), "An experimental investigation of single-phase forced convection in microchannels", *International Journal of Heat and Mass Transfer*, vol. 41, no. 6–7, pp. 851-857

Arrazola, P.-., Garay, A., Iriarte, L.-., Armendia, M., Marya, S. and Le Maître, F. (2009) "Machinability of titanium alloys (Ti6Al4V and Ti555.3)", *Journal of Materials Processing Technology,* vol. 209, no. 5, pp. 2223-2230.

Arsecularatne, J. A., Zhang, L. C., & Montross, C. 2006. "Wear and tool life of tungsten carbide, PCBN and PCD cutting tools. " *International Journal of Machine Tools and Manufacture*, *46*(5), 482-491.

Astakhov, V.P. (2006) *Tribology of Metal Cutting*, Elsevier, Amsterdam.

Astakhov, V.P. (2004) "The assessment of cutting tool wear", *International Journal of Machine Tools and Manufacture*, vol. 44, no. 6, pp. 637-647.

Attanasio, A., Ceretti, E., Fiorentino, A., Cappellini, C. and Giardini, C. (2010) "Investigation and FEM-based simulation of tool wear in turning operations with uncoated carbide tools", *Wear*, vol. 269, no. 5–6, pp. 344-350.

Axinte, D.A., Belluco, W. and De Chiffre, L. (2001) "Reliable tool life measurements in turning — an application to cutting fluid efficiency evaluation", *International Journal of Machine Tools and Manufacture*, vol. 41, no. 7, pp. 1003-1014.

Ay, H. and Yang, W. (1998) "Heat transfer and life of metal cutting tools in turning", *International Journal of Heat and Mass Transfer*, vol. 41, no. 3, pp. 613-623.

Bacci da Silva, M. and Wallbank, J. (1999) "Cutting temperature: prediction and measurement methods—a review", *Journal of Materials Processing Technology*, vol. 88, no. 1–3, pp. 195-202.

Bahi, S., Nouari, M., Moufki, A., Mansori, M.E. and Molinari, A. (2012) "Hybrid modeling of sliding–sticking zones at the tool–chip interface under dry machining and tool wear analysis", *Wear*, vol. 286–287, pp. 45-54.

Barry, J. and Byrne, G. (2002) "Chip Formation, Acoustic Emission and Surface White Layers in Hard Machining", *CIRP Annals - Manufacturing Technology,* vol. 51, no. 1, pp. 65-70.

Basti, A., Obikawa, T. and Shinozuka, J. (2007) "Tools with built-in thin film thermocouple sensors for monitoring cutting temperature", *International Journal of Machine Tools and Manufacture,* vol. 47, no. 5, pp. 793-798.

Beckhoff Automation LLC (2001) *Beckhoff Automation LLC, (Nov2001) "Using National Instruments LabView with TwinCAT I/O", APP-NOTE 500031 Beckhoff Application Note.,* APP-NOTE 500031 Beckhoff Application Note, Minneapolis.

Bermingham, M.J., Kirsch, J., Sun, S., Palanisamy, S. and Dargusch, M.S. (2011) "New observations on tool life, cutting forces and chip morphology in cryogenic machining Ti-6Al-4V", *International Journal of Machine Tools and Manufacture,* vol. 51, no. 6, pp. 500-511.

Bermingham, M.J., Palanisamy, S., Kent, D. and Dargusch, M.S. (2012) "A comparison of cryogenic and high pressure emulsion cooling technologies on tool life and chip morphology in Ti–6Al–4V cutting", *Journal of Materials Processing Technology,* vol. 212, no. 4, pp. 752-765.

Bin, Z., Chuanzhen, H., Ming, C., Meilin, G. and Hanlian, L. (2007) "High-temperature oxidation behavior and mechanism of Si3N4/Si3N4w/TiN nanocomposites ceramic cutting tool materials", *Materials Science and Engineering: A,* vol. 459, no. 1–2, pp. 86-93.

[Online] Bititci, U., Maguire, C., and Gregory, I. (2011) *Adaptive Capability- A must for Manufacturing SMEs of the Future*. Available at: http://www.futuresme.eu/docs/research-reports/2011/01/26/adaptive-capability---a-must-for-smes.pdf (Accessed: October 2012).

[Online] BMandF *Beverage Machine and Fabricators, Inc.* Available at: www.bevmachine.com (Accessed: December 2012).

Brinksmeier, E., Aurich, J.C., Govekar, E., Heinzel, C., Hoffmeister, H.-., Klocke, F., Peters, J., Rentsch, R., Stephenson, D.J., Uhlmann, E., Weinert, K. and Wittmann, M. (2006) "Advances in Modeling and Simulation of Grinding Processes", *CIRP Annals - Manufacturing Technology*, vol. 55, no. 2, pp. 667-696.

Brockhoff, T. and Walter, A. (1998) "Fluid Minimization in Cutting and Grinding, Abrasives", *Journal for Abrasive Engineering Society*, pp. 38-42.

Byers, J.P. (2006) *Metalworking fluids*, 2nd edn, Taylor and Francis, London.

Byrne, G., Dornfeld, D. and Denkena, B. (2003) "Advancing Cutting Technology", *CIRP Annals - Manufacturing Technology*, vol. 52, no. 2, pp. 483-507.

Byrne, G. and Scholta, E. (1993) "Environmentally Clean Machining Processes — A Strategic Approach", *CIRP Annals - Manufacturing Technology*, vol. 42, no. 1, pp. 471-474.

Carslaw, H.S. (1959) *Conduction of heat in solids*, 2nd edn, Clarendon, Oxford.

Carvalho, S.R., Lima e Silva, S.M.M., Machado, A.R. and Guimarães, G. (2006) "Temperature determination at the chip–tool interface using an inverse thermal model considering the tool and tool holder", *Journal of Materials Processing Technology,* vol. 179, no. 1–3, pp. 97-104.

Ceretti, E., Filice, L., Umbrello, D. and Micari, F. (2007) "ALE Simulation of Orthogonal Cutting: a New Approach to Model Heat Transfer Phenomena at the Tool-Chip Interface", *CIRP Annals - Manufacturing Technology,* vol. 56, no. 1, pp. 69-72.

Chao, B.T. and Trigger, K.J. (1958) "Temperature distribution at tool-chip and tool-work interface in metal cutting", *Wear,* vol. 80, no. 2, pp. 311-320.

Che Ghani, S., Cheng, K., Sun, X., Bateman, R. (2011a) "Modeling and analysis of the temperature distribution of a micro-channel internally cooled smart cutting tool in machining AlSi7", 4M Conference, Stuttgart, Germany.

Che Ghani, S., Cheng, K., Sun, X., Bateman, R., (2011b) "Optimizing heat transfer rate in an internally cooled cutting tool: FE- based design analysis and experimental study", *Key Engineering Materials,* vol. 496, pp. 188-193.

Childs, T.H.C. (2000) *Metal machining : theory and applications,* Arnold, London.

Choudhury, S.K., Kumar, E. and Ghosh, A. (1999) "A scheme of adaptive turning operations", *Journal of Materials Processing Technology,* vol. 87, no. 1–3, pp. 119-127.

Chungchoo, C. and Saini, D. (2002) "A computer algorithm for flank and crater wear estimation in CNC turning operations", *International Journal of Machine Tools and Manufacture,* vol. 42, no. 13, pp. 1465-1477.

Connolly, R. and Rubenstein, C. (1968) "The mechanics of continuous chip formation in orthogonal cutting", *International Journal of Machine Tool Design and Research,* vol. 8, no. 3, pp. 159-187.

Cotterell, M. and Byrne, G. (2008) "Dynamics of chip formation during orthogonal cutting of titanium alloy Ti–6Al–4V", *CIRP Annals - Manufacturing Technology,* vol. 57, no. 1, pp. 93-96.

Cus, F., Zuperl, U., Kiker, E. and Milfelner, M. (2008) "Adaptive self-learning controller design for feedrate maximisation of machining process", *Journal of Achievements in Materials and Manufacturing Engineering,* vol. 31, no. 2, pp. 469-476.

Dasch, J.M., Ang, C.C., Wong, C.A., Waldo, R.A., Chester, D., Cheng, Y.T., Powell, B.R., Weiner, A.M. and Konca, E. (2009) "The effect of free-machining elements on dry machining of B319 aluminum alloy", *Journal of Materials Processing Technology,* vol. 209, no. 10, pp. 4638-4644.

Davies, M.A., Chou, Y. and Evans, C.J. (1996) "On Chip Morphology, Tool Wear and Cutting Mechanics in Finish Hard Turning", *CIRP Annals - Manufacturing Technology,* vol. 45, no. 1, pp. 77-82.

Davies, M.A., Ueda, T., M'Saoubi, R., Mullany, B. and Cooke, A.L. (2007) "On The Measurement of Temperature in Material Removal Processes", *CIRP Annals - Manufacturing Technology,* vol. 56, no. 2, pp. 581-604.

Davis, J., Edgar, T., Porter, J., Bernaden, J. and Sarli, M. (2012) "Smart manufacturing, manufacturing intelligence and demand-dynamic performance", *Computers and Chemical Engineering,* vol. 47, pp. 145-156.

De Chiffre, L. and Belluco, W. (2000) "Comparison of Methods for Cutting Fluid Performance Testing", *CIRP Annals - Manufacturing Technology,* vol. 49, no. 1, pp. 57-60.

[Online] Department of Trade and Industry (2000) *A guide to biological treatment for metalworking fluid disposal* . Available at: biowise.org.uk/core_files/MWFs.pdf (Accessed: September 2011).

D'Errico, G.E. (1998) "An adaptive system for turning process control based on tool temperature feedback", *Journal of Materials Processing Technology,* vol. 78, no. 1–3, pp. 43-47.

Deshayes, L., Welsch, L., Donmez, A., Ivester, R., Gilsinn, D., Rhorer, R., Whitenton, E. and Potra, F. (2006) "Smart machining systems: issues and research trends", *Innovation in Life Cycle Engineering and Sustainable Development*, Springer Netherlands, , pp. 363-380.

Devillez, A., Schneider, F., Dominiak, S., Dudzinski, D. and Larrouquere, D. (2007) "Cutting forces and wear in dry machining of Inconel 718 with coated carbide tools", *Wear,* vol. 262, no. 7–8, pp. 931-942.

Dimla Snr., D.E. (2000) "Sensor signals for tool-wear monitoring in metal cutting operations—a review of methods", *International Journal of Machine Tools and Manufacture,* vol. 40, no. 8, pp. 1073-1098.

Dogu, Y., Aslan, E. and Camuscu, N. (2006) "A numerical model to determine temperature distribution in orthogonal metal cutting", *Journal of Materials Processing Technology,* vol. 171, no. 1, pp. 1-9.

Dutt, R.P. and Brewer, R.C. (1965) "On the theoretical determination of the temperature field in orthogonal machining'', *International Journal of Production Research,* vol. 4, no. 2, pp. 91-114.

El Hakim, M.A., Abad, M.D., Abdelhameed, M.M., Shalaby, M.A. and Veldhuis, S.C. (2011) "Wear behavior of some cutting tool materials in hard turning of HSS", *Tribology International,* vol. 44, no. 10, pp. 1174-1181.

Ezugwu, E.O. and Wang, Z.M. (1997) "Titanium alloys and their machinability—a review", *Journal of Materials Processing Technology,* vol. 68, no. 3, pp. 262-274.

Ezugwu, E.O., Bonney, J., Da Silva, R.B. and Çakir, O. (2007) "Surface integrity of finished turned Ti–6Al–4V alloy with PCD tools using conventional and high pressure coolant supplies", *International Journal of Machine Tools and Manufacture,* vol. 47, no. 6, pp. 884-891.

Falkinham III, J.O. (2002) "Nontuberculous mycobacteria in the environment", *Clinics in Chest Medicine,* vol. 23, no. 3, pp. 529-551.

Fang, N. and Wu, Q. (2009) "A comparative study of the cutting forces in high speed machining of Ti–6Al–4V and Inconel 718 with a round cutting edge tool", *Journal of Materials Processing Technology,* vol. 209, no. 9, pp. 4385-4389.

Frankel, P.G., Withers, P.J., Preuss, M., Wang, H.-., Tong, J. and Rugg, D. (2012) "Residual stress fields after FOD impact on flat and aerofoil-shaped leading edges", *Mechanics of Materials,* vol. 55, pp. 130-145.

Fratila, D. (2010) "Macro-level environmental comparison of near-dry machining and flood machining", *Journal of Cleaner Production,* vol. 18, no. 10–11, pp. 1031-1039.

Frost, T. (2008) *Drehen mit geschlossenem Innenkuehlsystem*, Technische Universitaet Berlin.

Fu, P., Li, W. and Guo, L. (2011) "Fuzzy Clustering and Visualization Analysis of Tool Wear Status Recognition", *Procedia Engineering,* vol. 23, pp. 479-486.

Gekonde, H.O. and Subramanian, S.V. (2002) "Tribology of tool–chip interface and tool wear mechanisms", *Surface and Coatings Technology,* vol. 149, no. 2–3, pp. 151-160.

Gente, A., Hoffmeister, H.-. and Evans, C.J. (2001) "Chip Formation in Machining Ti6Al4V at Extremely High Cutting Speeds", *CIRP Annals - Manufacturing Technology,* vol. 50, no. 1, pp. 49-52.

Ghosh, R., Zurecki, Z. and Grimm, L.M. (2005) Method for cutting workpieces with the provision of cooling of the cutting tool, EP1637257 A1, European Patent.

Grzesik, W. (2008) *Advanced machining processes of metallic materials : theory, modeling and applications,* Elsevier, Oxford.

Hahn, R.S. (1951) "On the Temperature Developed at the Shear Plane in the Metal Cutting Process", *Proc. of First U.S. National Congress of Applied Mechanics,* pp. 661-666.

Hastings, W.F., and Oxley, P.L.B., (1976) "Predicting tool life from fundamental work material properties and cutting conditions", *CIRP Annals,* pp. 105-109.

Heisel, C., Silva, M., and Schmalzried, T.P. (2004) "Bearing surface options for total hip replacement in young patients", *The Journal of Bone and Joint Surgery,* vol. 85-A, no. 7, pp. 1365-1379.

Helu, M., Behmann, B., Meier, H., Dornfeld, D., Lanza, G. and Schulze, V. (2012) "Impact of green machining strategies on achieved surface quality", *CIRP Annals - Manufacturing Technology,* vol. 61, no. 1, pp. 55-58.

Hibbeler R. C. (2008) *Mechanics of Materials- seventh SI edition ,* 7th edn, Pearson Ed Asia.

Hosokawa, A., Ueda, T., Onishi, R., Tanaka, R. and Furumoto, T. (2010) "Turning of difficult-to-machine materials with actively driven rotary tool", *CIRP Annals - Manufacturing Technology,* vol. 59, no. 1, pp. 89-92.

[Online] HSE *Health and Safety Executive*. Available at: http://www.hse.gov.uk/metalworking/index.htm (Accessed: December 2012).

Incropera, F. P., Dewitt, D. P. (2007) *Fundamentals of heat and mass transfer*, 6th edn, Wiley; John Wiley, Hoboken, N.J.; Chichester.

[Online] International Aerospace Quality Group (2007) *Foreign Object Debris/Foreign Object Damage (FOD) Prevention Training Program* . Available at: http://www.sae.org/iaqg/. (Accessed: September 2011).

ISO3685:1993, International Organization for Standardization.(1993)*Tool-life testing with single-point turning tools = : Essais de durée de vie des outils de tournage à partie active unique.*2nd edn , International Organization for Standardization , Genève, Switzerland.

Ippolito, R., Tornincasa, S. and Levi, R. (1988) "High Speed Machining: Tool Performance and Surface Finish in Steel Turning", *CIRP Annals - Manufacturing Technology*, vol. 37, no. 1, pp. 105-108.

Iqbal, S.A., Mativenga, P.T. and Sheikh, M.A. (2009) "A comparative study of the tool–chip contact length in turning of two engineering alloys for a wide range of cutting speeds", *The International Journal of Advanced Manufacturing Technology*, vol. 42, no. 1-2, pp. 30-40.

Jacobson, N.S., Opila, E.J. and Lee, K.N. (2001) "Oxidation and corrosion of ceramics and ceramic matrix composites", *Current Opinion in Solid State and Materials Science*, vol. 5, no. 4, pp. 301-309.

[Online] Jerard, R. B., Fussel, B. K., Xu, M. and Schuyler, C. (2009) *A Testbed for Research on Smart Machine Tools*. Available at: http://smartmachiningsystems.com/posters/PT4_sms.1.revised.final.pdf (Accessed: June 2010).

Jawahir, I. S., Li, P. X., Gosh, R., & Exner, E. L. 1995. "A new parametric approach for the assessment of comprehensive tool wear in coated grooved tools. " *CIRP Annals-Manufacturing Technology*, *44*(1), 49-54.

Joseph, D. D., Yang, B. H. (2010). "Friction factor correlations for laminar, transition and turbulent flow in smooth pipes", *Physica D: Nonlinear Phenomena*, *239*(14), pp. 1318-1328.

Kamata, Y. and Obikawa, T. (2007) "High speed MQL finish-turning of Inconel 718 with different coated tools", *Journal of Materials Processing Technology*, vol. 192–193, pp. 281-286.

Kandlikar, S.G. and Grande, W.J. (2003) "Evolution of Microchannel Flow Passages--Thermohydraulic Performance and Fabrication Technology", *Heat Transfer Engineering*, vol. 24, no. 1, pp. 3-17.

Khan, A.A. and Ahmed, M.I. (2008) "Improving tool life using cryogenic cooling", *Journal of Materials Processing Technology*, vol. 196, no. 1–3, pp. 149-154.

Kilic, D.S. and Raman, S. (2007) "Observations of the tool–chip boundary conditions in turning of aluminum alloys", *Wear*, vol. 262, no. 7–8, pp. 889-904.

Kitagawa, T., Kubo, A. and Maekawa, K. (1997) "Temperature and wear of cutting tools in high-speed machining of Inconel 718 and Ti6Al6V2Sn", *Wear,* vol. 202, no. 2, pp. 142-148.

Klocke, F. and Eisenblätter, G. (1997) "Dry Cutting", *CIRP Annals - Manufacturing Technology,* vol. 46, no. 2, pp. 519-526.

Komanduri, R. (1982) "Some clarifications on the mechanics of chip formation when machining titanium alloys", *Wear,* vol. 76, no. 1, pp. 15-34.

Komanduri, R. and Von Turkovich, B.F. (1981) "New observations on the mechanism of chip formation when machining titanium alloys", *Wear,* vol. 69, no. 2, pp. 179-188.

Kone, F., Czarnota, C., Haddag, B. and Nouari, M. (2011) "Finite element modeling of the thermo-mechanical behavior of coatings under extreme contact loading in dry machining", *Surface and Coatings Technology,* vol. 205, no. 12, pp. 3559-3566.

Koren, Y. 1977. *Flank wear model of cutting tools using control theory*. Department of Mechanical Engineering, Technion, Israel Inst. of Techn.

Koren, Y. (June 1988) "Adaptive Control Systems for Machining", *American Control Conference,* Atlanta, pp. 1161-1167.

Korkut, I., Boy, M., Karacan, I. and Seker, U. (2007) "Investigation of chip-back temperature during machining depending on cutting parameters", *Materials and Design,* vol. 28, no. 8, pp. 2329-2335.

Kouadri, S., Necib, K., Atlati, S., Haddag, B. and Nouari, M. (2013) "Quantification of the chip segmentation in metal machining: Application to machining the aeronautical aluminium alloy AA2024-T351 with cemented carbide tools WC-Co", *International Journal of Machine Tools and Manufacture,* vol. 64, pp. 102-113.

Kountanya, R. (2008) "Cutting tool temperatures in interrupted cutting—The effect of feed-direction modulation", *Journal of Manufacturing Processes,* vol. 10, no. 2, pp. 47-55.

Kremer, A. and El Mansori, M. (2011) "Tool wear as-modified by particle generation in dry machining", *Wear,* vol. 271, no. 9–10, pp. 2448-2453.

Kustas, F.M., Fehrehnbacher, L.L. and Komanduri, R. (1997) "Nanocoatings on Cutting Tools For Dry Machining", *CIRP Annals - Manufacturing Technology,* vol. 46, no. 1, pp. 39-42.

Kwon, Y. and Fischer, G.W. (2003) "A novel approach to quantifying tool wear and tool life measurements for optimal tool management", *International Journal of Machine Tools and Manufacture,* vol. 43, no. 4, pp. 359-368.

Lahres, M. and Jörgensen, G. (1997) "Properties and dry cutting performance of diamond-coated tools", *Surface and Coatings Technology,* vol. 96, no. 2–3, pp. 198-204.

Lalwani, D.I., Mehta, N.K. and Jain, P.K. (2008) "Experimental investigations of cutting parameters influence on cutting forces and surface roughness in finish

hard turning of MDN250 steel", *Journal of Materials Processing Technology,* vol. 206, no. 1–3, pp. 167-179.

Launder, B.E. and Sharma, B.I. (1974) "Application of the energy-dissipation model of turbulence to the calculation of flow near a spinning disc", *Letters in Heat and Mass Transfer*, vol. 1, no. 2, pp. 131-137.

Lau, W. S., Venuvinod, P. K. and Rubenstein, C. 1980. "The relation between tool geometry and the Taylor tool life constant." *International Journal of Machine Tool Design and Research* 20.1: 29-44.

Lee, L.C., Liu, X.D. and Lam, K.Y. (1995) "Determination of stress distribution on the tool rake face using a composite tool", *International Journal of Machine Tools and Manufacture,* vol. 35, no. 3, pp. 373-382.

Li, K. and Liang, S.Y. (2007) "Modeling of cutting forces in near dry machining under tool wear effect", *International Journal of Machine Tools and Manufacture,* vol. 47, no. 7–8, pp. 1292-1301.

Liang, L., Xu, H. and Ke, Z. (2013) "An improved three-dimensional inverse heat conduction procedure to determine the tool-chip interface temperature in dry turning", *International Journal of Thermal Sciences,* vol. 64, pp. 152-161.

Lim, R.J., Benjamin Yen and Wei Zhang (2000) "Just-in-time scheduling with machining economics for single-machine turning process", *Journal of Manufacturing Systems,* vol. 19, no. 4, pp. 219-228.

List, G., Nouari, M., Géhin, D., Gomez, S., Manaud, J.P., Le Petitcorps, Y. and Girot, F. (2005) "Wear behaviour of cemented carbide tools in dry machining of aluminium alloy", *Wear,* vol. 259, no. 7–12, pp. 1177-1189.

List, G., Sutter, G. and Bouthiche, A. (2012) "Cutting temperature prediction in high speed machining by numerical modeling of chip formation and its dependence with crater wear", *International Journal of Machine Tools and Manufacture,* vol. 54–55, pp. 1-9.

Lo Casto, S., Lo Valvo, E., Piacentini, M., Ruisi, V.F., Lucchini, E., Maschio, S. and Lonardo, P. (1994) "Cutting Temperatures Evaluation in Ceramic Tools: Experimental Tests, Numerical Analysis and SEM Observations", *CIRP Annals - Manufacturing Technology,* vol. 43, no. 1, pp. 73-76.

Loewen, E.G. and Shaw, M.C. (1954) "On the Analysis of Cutting Tool Temperatures", *Transactions of the ASME: Joiurnal of Engineering for Industry,* vol. 76, pp. 217-231.

Mackerle, J. (2003) "Finite element analysis and simulation of machining: an addendum: A bibliography (1996–2002)", *International Journal of Machine Tools and Manufacture,* vol. 43, no. 1, pp. 103-114.

Malekian, M., Park, S.S. and Jun, M.B.G. (2009) "Tool wear monitoring of micro-milling operations", *Journal of Materials Processing Technology,* vol. 209, no. 10, pp. 4903-4914.

Marksberry, P.W. and Jawahir, I.S. (2008) "A comprehensive tool-wear/tool-life performance model in the evaluation of NDM (near dry machining) for sustainable manufacturing", *International Journal of Machine Tools and Manufacture,* vol. 48, no. 7–8, pp. 878-886.

Maropoulos, P.G. and Alamin, B. (1996) "Integrated tool life prediction and management for an intelligent tool selection system", *Journal of Materials Processing Technology,* vol. 61, no. 1–2, pp. 225-230.

Masory, O., Koren, Y. and Weill, R. (1980) "Adaptive Control System for Turning", *CIRP Annals - Manufacturing Technology,* vol. 29, no. 1, pp. 281-284.
Mathew, P. (1989) "Use of predicted cutting temperatures in determining tool performance", *International Journal of Machine Tools and Manufacture,* vol. 29, no. 4, pp. 481-497.

McPhail, S. J. (2009) "Single-phase fluid flow and heat transfer in microtubes".

Meng, Q., Arsecularatne, J.A. and Mathew, P. (2000) "Calculation of optimum cutting conditions for turning operations using a machining theory", *International Journal of Machine Tools and Manufacture,* vol. 40, no. 12, pp. 1709-1733.

Mills, B. (1996) "Recent developments in cutting tool materials", *Journal of Materials Processing Technology,* vol. 56, no. 1–4, pp. 16-23.

Molinari, A. and Moufki, A. (2005) "A new thermomechanical model of cutting applied to turning operations. Part I. Theory", *International Journal of Machine Tools and Manufacture,* vol. 45, no. 2, pp. 166-180.

Molinari, A. and Nouari, M. (2002) "Modeling of tool wear by diffusion in metal cutting", *Wear,* vol. 252, no. 1–2, pp. 135-149.

Movahhedy, M., Gadala, M.S. and Altintas, Y. (2000) "Simulation of the orthogonal metal cutting process using an arbitrary Lagrangian–Eulerian finite-element method", *Journal of Materials Processing Technology,* vol. 103, no. 2, pp. 267-275.

N Gane and, J.M.C. (1970) "The deformation behaviour of crossed diamond wedges in the scanning electron microscope", *Journal of Physics D: Applied Physics,* vol. 3, no. 2, pp. 121.

[Online] National Institute for Occupational Safety and Health. (1998) *What you need to know about occupational exposure to metalworking fluids*. Available at: http://www.cdc.gov/niosh/docs/98-116/ (Accessed: July 2010).

[Online] National Institute of Standards and Technology. (2002) *The Smart Machine Tools Technology Workshop*. Dec. 9-11, Gaithersburg, MD. Available at: http://www.mel.nist.gov/proj/sms.htm (Accessed: July 2010).

Niebel, B. W., Draper, A. B., & Wysk, R. A. 1989. *Modern manufacturing process engineering*. New York: McGraw-Hill

Nouari, M., List, G., Girot, F. and Coupard, D. (2003) "Experimental analysis and optimisation of tool wear in dry machining of aluminium alloys", *Wear,* vol. 255, no. 7–12, pp. 1359-1368.

O'Sullivan, D. and Cotterell, M. (2001) "Temperature measurement in single point turning", *Journal of Materials Processing Technology*, vol. 118, no. 1–3, pp. 301-308.

Obikawa, T. and Shinozuka, J. (2004) "Monitoring of flank wear of coated tools in high speed machining with a neural network ART2", *International Journal of Machine Tools and Manufacture*, vol. 44, no. 12–13, pp. 1311-1318.

Olovsson, L., Nilsson, L. and Simonsson, K. (1999) "An ALE formulation for the solution of two-dimensional metal cutting problems", *Computers and Structures*, vol. 72, no. 4–5, pp. 497-507.

Oxley, P. L. B. 1989. *The mechanics of machining: an analytical approach to assessing machinability*. New York: E. Horwood.

Pan Fu, Hope, A.D. and King, G.A. (1998) "A neurofuzzy classification network and its application", *1998 IEEE International Conference on Systems, Man, and Cybernetics*, San Diego, pp. 4234.

Pandey, G., Deffor, H., Thostenson, E.T. and Heider, D. (2013) "Smart tooling with integrated time domain reflectometry sensing line for non-invasive flow and cure monitoring during composites manufacturing", *Composites Part A: Applied Science and Manufacturing*, vol. 47, pp. 102-108.

Papautsky, I., Ameel, T., and Frazier, A. B., (2001), "A review of laminar single-phase flow in microchannels." *ASME, Proceedings of Int. Mech. Eng Congress Expos Proc (IMECE)*. vol. 2.

Patankar, S.V., (1980) *Numerical Heat Transfer and Fluid Flow,* Taylor and Francis, London.

Petukhov, B.S. "Heat Transfer and Friction in Turbulent Pipe Flow with Variable Physical Properties", *Advances in Heat Transfer*, Elsevier, pp. 503-564.

Pintaude, G., Bernardes, F.G., Santos, M.M., Sinatora, A. and Albertin, E. (2009) "Mild and severe wear of steels and cast irons in sliding abrasion", *Wear,* vol. 267, no. 1–4, pp. 19-25.

Popke, H., Emmer, T. and Steffenhagen, J. (1999) "Environmentally clean metal cutting processes—machining on the way to dry cutting", *Proceedings of the Institution of Mechanical Engineers, Part B: Journal of Engineering Manufacture,* vol. 213, no. 3, pp. 329-332.

Prasad, B. (1996) *Concurrent Engineering Fundamentals Integrated Product and Process Organisation,* IPTR Prentice-Hall, Upper Saddle River, New Jersey.

Pugh, S. and Clausing, D. (1996) *Creating Innovative Products Using Total Design: The Living Legacy of Stuart Pugh* Addison-Wesley Longman Publishing Co., Inc., Boston, MA.

Quazi, H.A., Khoo, Y., Tan, C. and Wong, P. (2001) "Motivation for ISO 14000 certification: development of a predictive model", *Omega,* vol. 29, no. 6, pp. 525-542.

Rech, J. (2006) "Influence of cutting tool coatings on the tribological phenomena at the tool–chip interface in orthogonal dry turning", *Surface and Coatings Technology*, vol. 200, no. 16–17, pp. 5132-5139.

Risbood, K.A., Dixit, U.S. and Sahasrabudhe, A.D. (2003) "Prediction of surface roughness and dimensional deviation by measuring cutting forces and vibrations in turning process", *Journal of Materials Processing Technology*, vol. 132, no. 1–3, pp. 203-214.

[Online] Rockwell Automation . (1998) *What is smart manufacturing?*. Available at: https://smart-process-manufacturing.ucla.edu/about/news/time-magazine-what-is-smart-manufactuing.pdf (Accessed: July 2010).

Rosenman, K.D., Reilly, M.J. and Kalinowski, D. (1997) "Work-related asthma and respiratory symptoms among workers exposed to metal-working fluids", *American Journal of Industrial Medicine*, vol. 32, no. 4, pp. 325-331.

[Online] RPM *Reed Prototype and Machining*. Available at: http://www.magnesiummachining.com (Accessed: September 2012).

Salahshoor, M. and Guo, Y.B. (2011) "Cutting mechanics in high speed dry machining of biomedical magnesium–calcium alloy using internal state variable plasticity model", *International Journal of Machine Tools and Manufacture*, vol. 51, no. 7–8, pp. 579-590.

[Online] Sandvik (2012) *Wear on cutting edges*. Available at: http://www.sandvik.coromant.com/enb/knowledge/materials/cutting_tool_materials/wear_on_cutting_edges/Pages/default.aspx (Accessed: October 2012).

Schulz, H. and Moriwaki, T. (1992) "High-speed Machining", *CIRP Annals - Manufacturing Technology,* vol. 41, no. 2, pp. 637-643.

Sharma, V.S., Dogra, M. and Suri, N.M. (2009) "Cooling techniques for improved productivity in turning", *International Journal of Machine Tools and Manufacture,* vol. 49, no. 6, pp. 435-453.

Sharp, K.V. and Adrian, R.J. (2004) "Transition from laminar to turbulent flow in liquid filled microtubes", *Experiments in Fluids,* vol. 36, no. 5, pp. 741-747.

Shaw, M.C. (1984) *Metal cutting principles,* Clarendon.

Shen, C.H. (1996) "The importance of diamond coated tools for agile manufacturing and dry machining", *Surface and Coatings Technology,* vol. 86–87, Part 2, pp. 672-677.

Shimada, S., Tanaka, H., Higuchi, M., Yamaguchi, T., Honda, S. and Obata, K. (2004) "Thermo-Chemical Wear Mechanism of Diamond Tool in Machining of Ferrous Metals", *CIRP Annals - Manufacturing Technology,*vol. 53, no. 1, pp. 57-60.

Shokrani, A., Dhokia, V. and Newman, S.T. (2012) "Environmentally conscious machining of difficult-to-machine materials with regard to cutting fluids", *International Journal of Machine Tools and Manufacture,* vol. 57, pp. 83-101.

Soares, C. (1999) *Environmental Technology and Economics : Sustainable Development in Industry,* Butterworth-Heinemann, Boston ; Oxford.

Sreejith, P.S. and Ngoi, B.K.A. (2000) "Dry machining: Machining of the future", *Journal of Materials Processing Technology,* vol. 101, no. 1–3, pp. 287-291.

Stephenson, D.A. (2006) *Metal Cutting Theory and Practice,* 2nd edn, CRC; Taylor and Francis distributor, New York; London.

Strenkowski, J.S., Hsieh, C.C. and Shih, A.J. (2004) "An analytical finite element technique for predicting thrust force and torque in drilling", *International Journal of Machine Tools and Manufacture,* vol. 44, no. 12–13, pp. 1413-1421.

Sun, X., Bateman, R., Cheng, K., and Che Ghani, S. (2011) "Design and analysis of an internally cooled smart cutting tool for dry cutting", *Part B Journal Engineering Manufacture, Proc. IMechE,* vol. 225, pp. 1-7.

Sutter, G. and Ranc, N. (2007) "Temperature fields in a chip during high-speed orthogonal cutting—An experimental investigation", *International Journal of Machine Tools and Manufacture,* vol. 47, no. 10, pp. 1507-1517.

Tabor, D. (1970) "The hardness of solids", *Review of Physics in Technology*, vol. 1, no. 3, pp. 145.

Tabor, D. (1956) "The physical meaning of indentation and scratch hardness", *British Journal of Applied Physics,* vol. 7, no. 5, pp. 159.

Tabor, D. (1954) "Mohs's Hardness Scale - A Physical Interpretation", *Proceedings of the Physical Society.Section B,* vol. 67, no. 3, pp. 249.

Takeyama, H. and Murata, R. (1963) "Basic Investigation of Tool Wear", *J. Eng. for Industry,* vol. 85, no. 1, pp. 33-37.

Tasdelen, B., Thordenberg, H. and Olofsson, D. (2008) "An experimental investigation on contact length during minimum quantity lubrication (MQL) machining", *Journal of Materials Processing Technology,* vol. 203, no. 1–3, pp. 221-231.

Tay, A.A.O. (1993) "A review of methods of calculating machining temperature", *Journal of Materials Processing Technology,* vol. 36, no. 3, pp. 225-257.

Tay, A.O., Stevenson, M.G. and De Vahl Davis, G. (1974) "Using the Finite Element Method to Determine Temperature Distributions in Orthogonal Machining", *Proceedings of the Institution of Mechanical Engineers,*vol. 188, no. 1, pp. 627-638.

Trent, E.M. and Paul K Wright (2000) *Metal cutting,* 4th edn, Butterworth-Heinemann, Woburn Massachusetts.

Trigger, K.J. and Chao, B.T. (1951) "An Analytical Evaluation of Metal Cutting Temperatures ", *Transactions of the ASME: Journal of Engineering for Industry,* vol. 73, pp. 57-68.

Ueda, K. and Manabe, K. (1993) "Rigid-Plastic FEM Analysis of Three-Dimensional Deformation Field in Chip Formation Process", *CIRP Annals - Manufacturing Technology,* vol. 42, no. 1, pp. 35-38.

Ueda, T., Hosokawa, A., Oda, K. and Yamada, K. (2001) "Temperature on Flank Face of Cutting Tool in High Speed Milling", *CIRP Annals - Manufacturing Technology,* vol. 50, no. 1, pp. 37-40.

Ueda, T., Sato, M. and Nakayama, K. (1998) "The Temperature of a Single Crystal Diamond Tool in Turning", *CIRP Annals - Manufacturing Technology,* vol. 47, no. 1, pp. 41-44.

Usui, E., Shirakashi, T. and Kitagawa, T. (1984) "Analytical prediction of cutting tool wear", *Wear,* vol. 100, no. 1–3, pp. 129-151.

van Luttervelt, C.A., Childs, T.H.C., Jawahir, I.S., Klocke, F., Venuvinod, P.K., Altintas, Y., Armarego, E., Dornfeld, D., Grabec, I., Leopold, J., Lindstrom, B., Lucca, D., Obikawa, T., Shirakashi and Sato, H. (1998) "Present Situation and Future Trends in Modeling of Machining Operations Progress Report of the CIRP Working Group 'Modeling of Machining Operations'", *CIRP Annals - Manufacturing Technology,* vol. 47, no. 2, pp. 587-626.

Venkatesh, V.C., Ye, C.T., Quinto, D.T. and Hoy, D.E.P. (1991) "Performance Studies of Uncoated, CVD-Coated and PVD-Coated Carbides in Turning and Milling", *CIRP Annals - Manufacturing Technology,* vol. 40, no. 1, pp. 545-550.

Wang, C., Bin Che Ghani, , S., Cheng, K., and Rakowski, R., (2012) "Adaptive smart machining based on using constant cutting force and a smart cutting tool ", *Part B Journal Engineering Manufacture, Proc. IMechE,*vol. 226, pp. 1-5.

Wang, H. P. B., & Wysk, R. A. (1986). "An expert system for machining data section." *Computers & Industrial Engineering*, *10*(2), 99-107

Wang, Z.Y., Rajurkar, K.P., Fan, J., Lei, S., Shin, Y.C. and Petrescu, G. (2003) "Hybrid machining of Inconel 718", *International Journal of Machine Tools and Manufacture,* vol. 43, no. 13, pp. 1391-1396.

Weinert, K., Inasaki, I., Sutherland, J.W. and Wakabayashi, T. (2004) "Dry Machining and Minimum Quantity Lubrication", *CIRP Annals - Manufacturing Technology,* vol. 53, no. 2, pp. 511-537.

Weinert, K. and König, W. (1993) "A Consideration of Tool Wear Mechanism when Machining Metal Matrix Composites (MMC)", *CIRP Annals - Manufacturing Technology,* vol. 42, no. 1, pp. 95-98.

Welty, J.R. (2008) *Fundamentals of Momentum, Heat, and Mass Transfer,* 5th edn, Wiley, Hoboken, NJ.

Whitelaw, K. (1997) *ISO 14001 Environmental Systems Handbook,* Butterworth Heinemann, Oxford.

Wright, P.K., Horne, J.G. and Tabor, D. (1979) "Boundary conditions at the chip-tool interface in machining: Comparisons between seizure and sliding friction", *Wear,* vol. 54, no. 2, pp. 371-390.

Xie, L.-., Schmidt, J., Schmidt, C. and Biesinger, F. (2005) "2D FEM estimate of tool wear in turning operation", *Wear,* vol. 258, no. 10, pp. 1479-1490.

Yang, L.J. (2001) "Determination of the wear coefficient of tungsten carbide by a turning operation", *Wear,* vol. 250, no. 1–12, pp. 366-375.

Yildiz, Y. and Nalbant, M. (2008) "A review of cryogenic cooling in machining processes", *International Journal of Machine Tools and Manufacture,* vol. 48, no. 9, pp. 947-964.

Young, H. (1996) "Cutting temperature responses to flank wear", *Wear,* vol. 201, no. 1–2, pp. 117-120.

Yousefi, R. and Ichida, Y. (2000) "A study on ultra–high-speed cutting of aluminium alloy: Formation of welded metal on the secondary cutting edge of the tool and its effects on the quality of finished surface", *Precision Engineering,* vol. 24, no. 4, pp. 371-376.

Yu, D., Warrington, R., Barron, R., and Ameel, T. (1995) "An experimental and theoretical investigation of fluid flow and heat transfer in microtubes", In *ASME/JSME Thermal Engineering Conference,* vol. 1, no. 52, pp. 523-530, Pergamon.

Zacharisen, M.C. and Fink, J.N. (2011) "Hypersensitivity Pneumonitis and Related Conditions in the Work Environment", *Immunology and Allergy Clinics of North America,* vol. 31, no. 4, pp. 769-786.

Zaghbani, I. and Songmene, V. (2009) "Estimation of machine-tool dynamic parameters during machining operation through operational modal analysis", *International Journal of Machine Tools and Manufacture,* vol. 49, no. 12–13, pp. 947-957.

Zdeblick, W. J., De Vor, R. E., & Kahles, J. F. 1981. "A comprehensive machining cost model and optimization technique. " *CIRP Annals-Manufacturing Technology*, *30*(1), 405-408

Zhou, Q., Hong, G.S. and Rahman, M. (1995) "A new tool life criterion for tool condition monitoring using a neural network", *Engineering Applications of Artificial Intelligence,* vol. 8, no. 5, pp. 579-588.

Appendix A: List of Publications Arising from This Research

(1) Sun, X., Bateman, R., Cheng, K., Che Ghani, S. (2011), "Design and analysis of an internally cooled smart cutting tool for dry cutting", *Part B Journal Engineering Manufacture*, Proc. IMechE Vol. 225, pp. 1-7.

(2) Wang, C., Bin Che Ghani, S., Cheng, K., Rakowski, R., (2012), "Adaptive smart machining based on using constant cutting force and a smart cutting tool", Part B Journal Engineering Manufacture, Proc. IMechE Vol. 226, pp. 1-5.

(3) Che Ghani, S., Cheng K., Sun X., Bateman, R. (September 2011) "Optimizing heat transfer rate in an internally cooled cutting tool: FE- based design analysis and experimental study", ICPM 2011, Liverpool, UK.

(4) Che Ghani, S., Cheng, K., Sun, X., Bateman, R. (November 2011) "Modeling and analysis of the temperature distribution of a micro-channel internally cooled smart cutting tool in machining AlSi7", 4M Conference, Stuttgart, Germany.

(5) Che Ghani, S., Cheng, K., Sun, X., Bateman, R., (2011) "Optimizing heat transfer rate in an internally cooled cutting tool: FE- based design analysis and experimental study", *Key Engineering Materials*, vol. 496, pp. 188-193.

(6) Che Ghani, S., Cheng, K., Minton, T., Bateman, R. (June 2013) "Adaptive machining of titanium, steel and aluminium with internally cooled smart cutting", FAIM2013, Porto, Portugal.

Appendix B: Equipment and Machine Tool Used in the Research

Metrology methods

The performance of the smart tool in ECMP is assessed by proper equipment. Process variables including cutting forces, cutting temperatures, surface roughness and wear faces describes the useful of a cutting tool.

Dynamometer

Dynamometer is the most common and effective tool to measure cutting force. The forces generated in machining operations, reflecting interaction between cutting tools and work materials, have a direct impact on cutting performance such as tool wear or failure, quality of machined surface and accuracy of components. Therefore, it is necessary to characterize these forces quantitatively and precisely so as to examine, evaluate and optimize cutting processes. A force dynamometer is capable of performing the function accurately both in magnitude and direction by creating electrical signals proportional to the forces in three orthogonal directions. Ideally, a dynamometer should be developed and configured with high sensitivity, high rigidity, high natural frequency response, high linearity, low drift and low measuring threshold in order to achieve better static and dynamic characteristics.

Kistler three-component piezoelectric dynamometer Model 9257B is among the most widely used for force measurement in literature (Bahi et al., 2012). The dynamometer uses four three-component force transducers fitted under high preload between a base plate and a top plate. The transducers consists of three

pairs of quartz plates; i.e. one sensitive to pressure in the z direction and the other two responding to shear in the x and y directions respectively. Quartz is a piezoelectric material that produces electrical charge under the mechanical load. The signals obtained from the sensors are processed in a way to measure multi-components of forces and moments. The eight output signals are available at the 9-conductor flange socket. The dynamometer is heavy-duty equipment as the chassis of it is dustproof and waterproof. This makes the equipment suitable to be used in hostile machining environment.

Fig. B.1: Dynamometer Kistler 9257B

Thermocouples

The working principles of thermocouple (TC) are based on the correlation between the temperature and voltage generated from joints of two dissimilar materials. The correlation of thermal induced current and voltage drop is explained in Seebeck effect (Davies, et al., 2007). TC is a popular device used in measuring cutting temperature owe to their advantages, such as (1) cost effective, (2) rugged, (3) versatile and available for many temperature ranges, (4) reasonably stable and reproducible, (5) easy to calibrate and (6) relatively

quick response. The biggest challenge in applying TC in machining is related to the positioning of TC. Besides the risk of damaging the TC if it is to be put too near to the cutting edge, the TC is also subjected to large uncertainty due to large temperature gradient and rapid change in temperature. To overcome this issue Basti et al. (2007) has introduced thermo-film thermocouple (TFT) and the concept of this TC is shown in Fig. B. 2. TFT thermocouple consists of two dissimilar materials (Ni and Ni-Cr) and are joined together to make up hot and cold junction. The hot junction is fabricated at the cutting edge and the cold junction is placed on the rake face but quite remote from the cutting region.
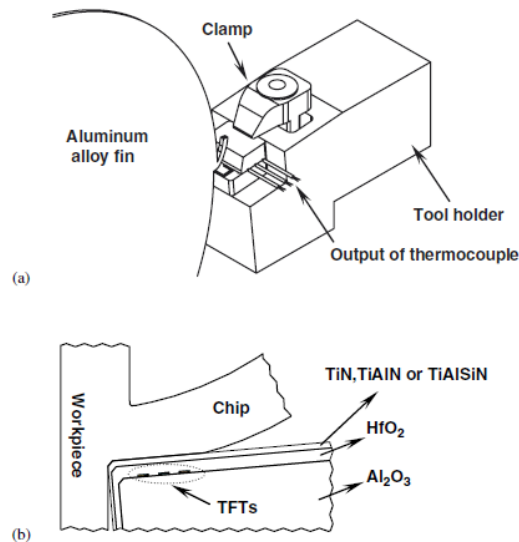
Fig. B. 2: A concept of thin-film thermocouple integrated to a cutting tool by Basti et. al. (2007)

Thermocouple gets easily broken in machining. Korkut et. al. (2007) in their report has used mineral isolated K-type thermocouple attached to an insert to measure the cutting temperature. Then, Inconel 600 was used a protective cover of the thermocouple against mechanical impact and chemical and physical wear during machining.

Infrared camera (IR camera) and Pyrometer

Application of IR camera and pyrometer in measuring cutting temperature has been increasingly popular in recent years. The major advantage of IR camera and pyrometer against thermocouple is that it is non-intrusive so it will not alter the temperature field (O' Sullivan, et al., 2001). The capability to capture live temperature field by IR camera and temperature spot by pyrometer is also useful in highly dynamic machining process. IR camera and pyrometer requires the emissivity determination. Emissivity is material specific describes the quantification of the efficiency of a surface condition for radiation of energy in a defined waveband and at a given temperature. The procedure to calibrate the IR camera accurately is documented nicely by Liang et. al. (2013). They have calibrated the IR camera model Thermo-Vision A200 against the black body by heating the insert in the range 30°C to 900°C.

3D surface profiler

A 3D surface profiler is an instrument for quantifying and characterising a surface texture. The characterisation of a surface typically includes surface roughness and surface shape measurements. In most cases, surface profilers are used for 3D surface roughness measurement and analysis. Surface roughness reflects characteristic marks left by the machining process, which is a direct indicator for the quality of a machined surface, and it can affect the functionality of a machined component. Therefore, ability to measure surface topography and texture accurately in 3D is a crucial concern for industrial applications especially in crucial industries in ECMP such as biomedical and aerospace. Fig. 2.22 shows some typical non-contact and contact 3D surface metrology instruments.
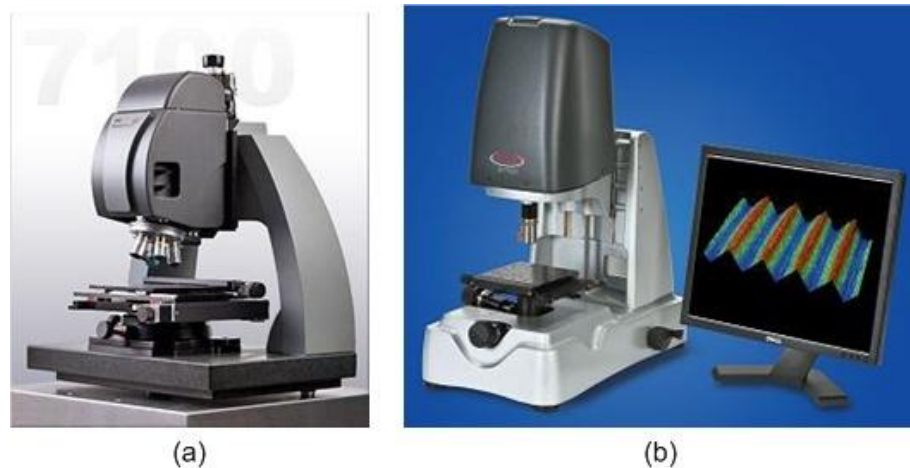
Fig. B.3: Commercial surface profiler in the market; (a) Zygo New View™ 7100 (Zygo, 2010) and (b) Wyko NT9080 (Veeco, 2010)

Microscopes

Application of microscopes in the research area of machining is mainly for examination of surface condition (Lo Casto, et al.,1994; El Hakim, et al., 2011). The surface conditions studies include the observation about the wear mechanism, measurement of micro features geometry, inspection about coatings integrity and investigation about the thermo-chemical tool-work interactions. The function of conventional optical microscopes that is used to magnify an object at the expense of loss of field depth has been improved with the digital microscopes which are not only capable of capturing micro-scale image with the magnification up to 5000× (Keyence Digital Microscope VHX-2000), but it can also stitch the captured images thus a wider scope can be inspected.

Another type of microscope is scanning electron microscope (SEM) combined with energy disperse X-ray (EDX). SEM can be utilised in high resolution inspection of all materials. SEM in combination with EDX is also possible to determine the element contained in a material. This function can be used in machining to investigate the surface tribology of a cutting tip after machining.

Chemical reaction due to thermal induced wear mechanism such as diffusion and oxidation has been investigated before by El Hakim et. al. (2011) using this equipment.

The list of machine tools and equipment used throughout this research can be found in Table B-1.

Table B-1: List of machine tools, equipment and tools used in the research

CNC machine tool	1. KERN 5-Axis CNC Micro-Machining Centre 2. Colchester Harrison 600 Group Alpha 1350XS CNC lathe
Cutting insert	1. SNUN120408 uncoated WC 2. SNUN120408 Ti-N coated WC 3. SNUN120408 HSS 4. SPUN12xx08 uncoated WC 5. SPUN12xx08 CVD diamond coated WC
Tool holder	CSBNR 2525M12-4
Work materials	1. Aluminium alloy AA6082-T6 2. AISI7 3. Mild Steel EN32B 4. CP Grade2 Titanium
On-line measuring equipment	1. Micro-Epsilon pyrometer CTLM3-H1-CF2 2. Optris PI IR camera PI160 3. Thermocouple K type (Chromel- Alumel) 4. Kistler 3-Axis force dynamometer 9257B with double charge amplifiers 5070A

	5. Digital microscope Dino-Lite AD413TL
Real-time electronic data acquisition system	1. 16 Channel Thermocouple module NI9213 2. Voltage AO module NI9264 3. 8 slots DAQ chassis NIcDAQ 9172 4. Electronics module for micro-epsilon CTLM pyrometer
Metrology	1. White light interferometer Zygo NewView 5000 2. Field emission scanning electron microscope Zeiss Supra 35VP 3. Optical microscope TESA VISIO-200 4. FESEM Hitachi S3000 with EDX

Appendix C: Technical Drawing of Cooling Adapter

These are the drawings of cooling adapters. The first drawing is the adapter for bottle cap shaped insert and the second one is for the 1mm thickness insert plate.

The angle between axis a and surface X is 22.82 degree
The angle between axis a and surface Y is 34.69 degree
The angle between axis b and surface X is 43.71 degree
The angle between axis b and surface Y is 41.06 degree
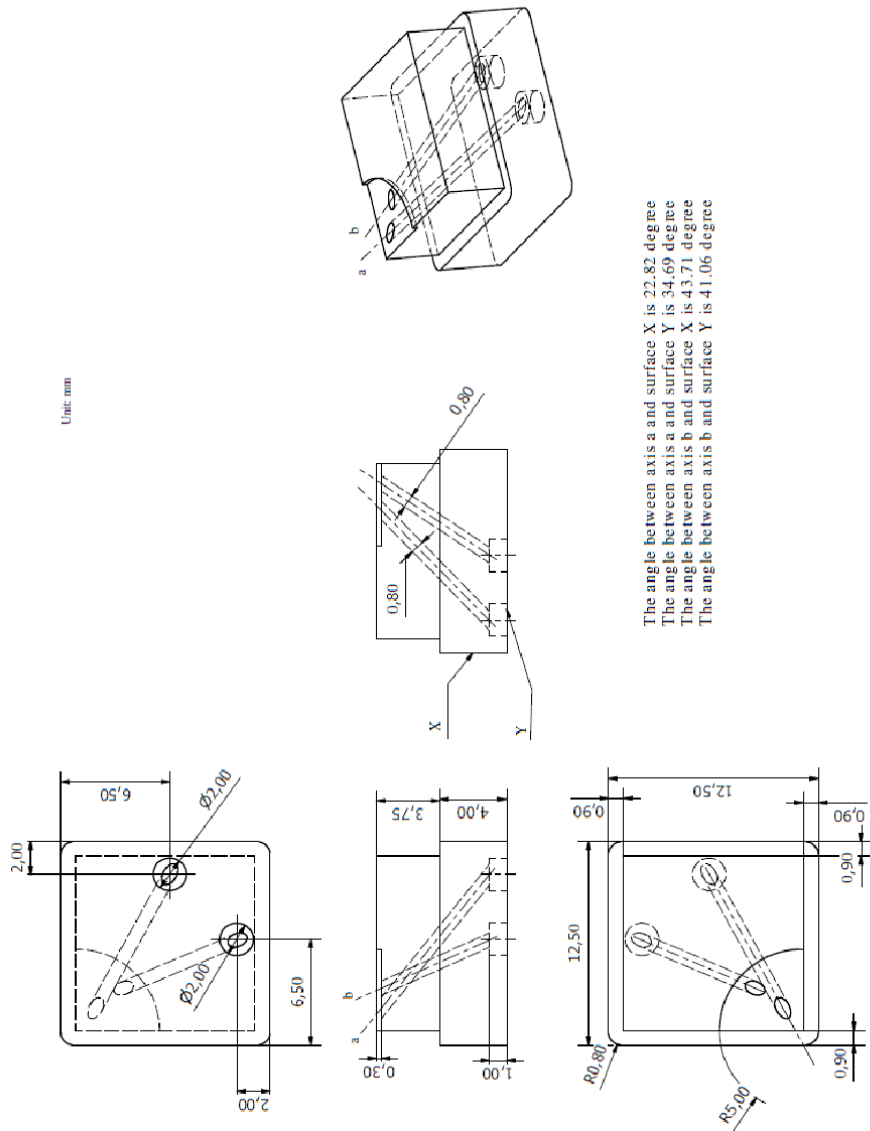
Cooling adapter for bottle cap shape insert
Designer: Sarah Sun
Date: 04/11/2010
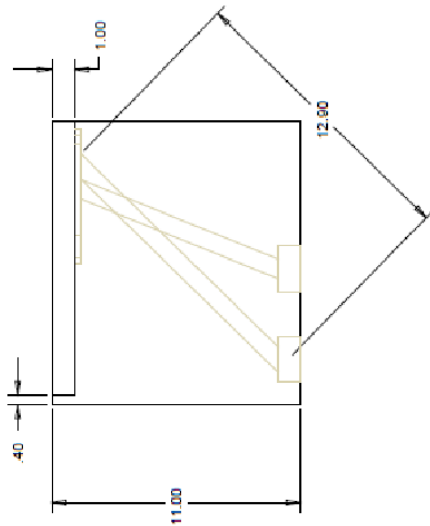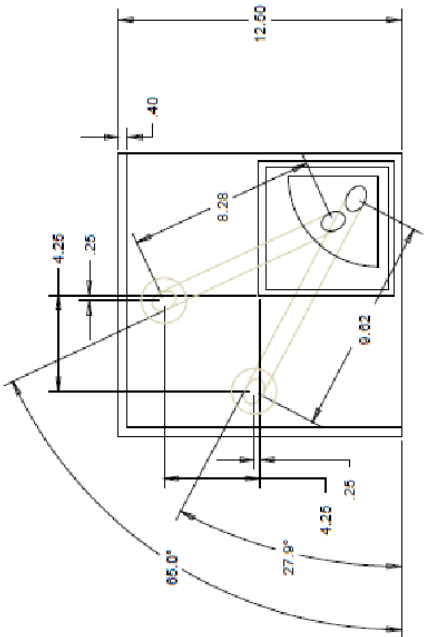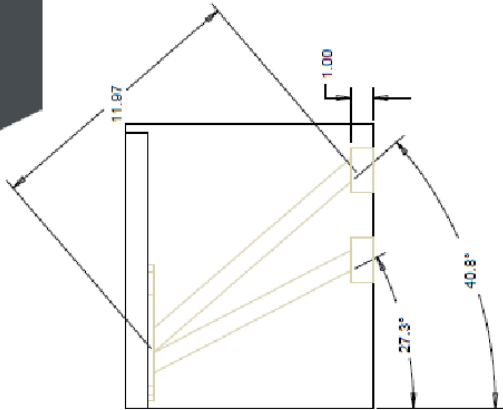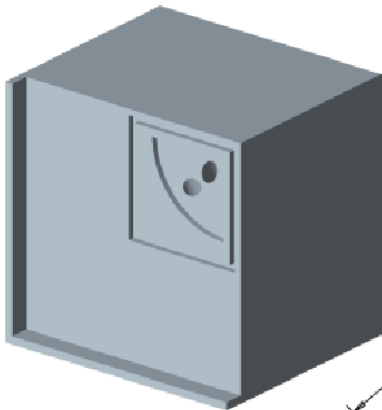
Cooling Adapter: Optimised design
Designer: Saiful Che Ghani
Date: 04/07/2012

Appendix D: 5-Axis CNC Programme

The cooling adapter has been fabricated in house on the 5-Axis Kern CNC centre. The coding for precision machining of micro channels (see Appendix C) is displayed in this appendix.

<u>Hole a</u>

```
0  BEGIN PGM PYMAKEHOLE2 MM
1  TOOL CALL 2 Z S20000
2  L M3
3  L M140 MB MAX
4  CALL LBL 99
5  CYCL DEF 7.0 DATUM SHIFT
6  CYCL DEF 7.1 X-2,85
7  CYCL DEF 7.2 Y-2,85
8  CYCL DEF 19.0 WORKING PLANE
9  CYCL DEF 19.1 B-38 C+66,41
10  L B+Q121 C+Q122 R0 F MAX
11  CYCL DEF 200 DRILLING ~
    Q200=2   ;SET-UP CLEARANCE ~
    Q201=-0,5 ;DEPTH ~
    Q206=8   ;FEED RATE FOR PLNGNG ~
    Q202=0,05 ;PLUNGING DEPTH ~
    Q210=0   ;DWELL TIME AT TOP ~
    Q203=+0  ;SURFACE COORDINATE ~
    Q204=50  ;2ND SET-UP CLEARANCE ~
    Q211=3   ;DWELL TIME AT DEPTH
12  L X+0 Y+0 R0 F MAX
13  L Z+5 R0 F MAX
14  L M99
15  L M140 MB MAX
16  TOOL CALL 2 Z S15000
17  L M15
18  L X+0 Y+0 R0 F MAX
```

```
19  CYCL DEF 200 DRILLING ~
    Q200=2   ;SET-UP CLEARANCE ~
    Q201=-1  ;DEPTH ~
    Q206=8   ;FEED RATE FOR PLNGNG ~
    Q202=0,1 ;PLUNGING DEPTH ~
    Q210=0   ;DWELL TIME AT TOP ~
    Q203=+0  ;SURFACE COORDINATE ~
    Q204=50  ;2ND SET-UP CLEARANCE ~
    Q211=0   ;DWELL TIME AT DEPTH
20  CYCL CALL
21  L M140 MB MAX
22  TOOL CALL 7 Z S8000
23  L M15
24  L X+0 Y+0 R0 F MAX
25  CYCL DEF 200 DRILLING ~
    Q200=2   ;SET-UP CLEARANCE ~
    Q201=-12 ;DEPTH ~
    Q206=20  ;FEED RATE FOR PLNGNG ~
    Q202=0,2 ;PLUNGING DEPTH ~
    Q210=0   ;DWELL TIME AT TOP ~
    Q203=+0  ;SURFACE COORDINATE ~
    Q204=50  ;2ND SET-UP CLEARANCE ~
    Q211=0   ;DWELL TIME AT DEPTH
26  CYCL CALL
27  L M140 MB MAX
28  CALL LBL 99
29  L B+Q121 C+Q122 R0 F MAX
30  L M30
31  LBL 99
32  CYCL DEF 7.0 DATUM SHIFT
33  CYCL DEF 7.1 X+0
34  CYCL DEF 7.2 Y+0
35  CYCL DEF 7.3 Z+0
36  CYCL DEF 19.0 WORKING PLANE
37  CYCL DEF 19.1 B+0 C+0
38  CYCL DEF 19.0 WORKING PLANE
```

39 CYCL DEF 19.1

40 LBL 0

41 END PGM PYMAKEHOLE2 MM

Hole b

0 BEGIN PGM PYMAKEHOLE3 MM

1 TOOL CALL 2 Z S20000

2 L M3

3 L M140 MB MAX

4 CALL LBL 99

5 CYCL DEF 7.0 DATUM SHIFT

6 CYCL DEF 7.1 X-4,35

7 CYCL DEF 7.2 Y-4,35

8 L X+0 Y+0 Z+20 F MAX

9 CYCL DEF 19.0 WORKING PLANE

10 CYCL DEF 19.1 B-46,63 C+28,14

11 L B+Q121 C+Q122 R0 F MAX

12 CYCL DEF 200 DRILLING ~

   Q200=2   ;SET-UP CLEARANCE ~

   Q201=-0,4 ;DEPTH ~

   Q206=12   ;FEED RATE FOR PLNGNG ~

   Q202=0,1 ;PLUNGING DEPTH ~

   Q210=0   ;DWELL TIME AT TOP ~

   Q203=+0   ;SURFACE COORDINATE ~

   Q204=50   ;2ND SET-UP CLEARANCE ~

   Q211=2   ;DWELL TIME AT DEPTH

13 L X+0 Y+0 R0 F MAX

14 L Z+5 R0 F MAX

15 L M99

16 L M140 MB MAX

17 TOOL CALL 2 Z S15000

18 L M15

19 L X+0 Y+0 R0 F MAX

20 CYCL DEF 200 DRILLING ~

   Q200=2   ;SET-UP CLEARANCE ~

   Q201=-1,2 ;DEPTH ~

```
    Q206=12  ;FEED RATE FOR PLNGNG ~
    Q202=0,2 ;PLUNGING DEPTH ~
    Q210=3   ;DWELL TIME AT TOP ~
    Q203=+0  ;SURFACE COORDINATE ~
    Q204=50  ;2ND SET-UP CLEARANCE ~
    Q211=0   ;DWELL TIME AT DEPTH
21  CYCL CALL
22  L M140 MB MAX
23  TOOL CALL 7 Z S8000
24  L M15
25  L X+0 Y+0 R0 F MAX
26  CYCL DEF 200 DRILLING ~
    Q200=2   ;SET-UP CLEARANCE ~
    Q201=-13,3 ;DEPTH ~
    Q206=12  ;FEED RATE FOR PLNGNG ~
    Q202=0,2 ;PLUNGING DEPTH ~
    Q210=0   ;DWELL TIME AT TOP ~
    Q203=+0  ;SURFACE COORDINATE ~
    Q204=50  ;2ND SET-UP CLEARANCE ~
    Q211=0   ;DWELL TIME AT DEPTH
27  CYCL CALL
28  L M140 MB MAX
29  CALL LBL 99
30  L B+Q121 C+Q122 R0 F MAX
31  L M30
32  LBL 99
33  CYCL DEF 7.0 DATUM SHIFT
34  CYCL DEF 7.1 X+0
35  CYCL DEF 7.2 Y+0
36  CYCL DEF 7.3 Z+0
37  CYCL DEF 19.0 WORKING PLANE
38  CYCL DEF 19.1 B+0 C+0
39  CYCL DEF 19.0 WORKING PLANE
40  CYCL DEF 19.1
41  LBL 0
42  END PGM PYMAKEHOLE3 MM
```

Appendix E: Geometry for Indexable Inserts

The identification of single point turning tool as described by Mitsu according to the ISO standards for indexable inserts geometry is shown in this appendix.

Triangular insert with a facet (Secondary Cutting Edge)

① Symbol for Insert Shape
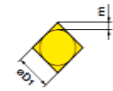
Symbol	Insert Shape	
H	Hexagonal	
O	Octagonal	
P	Pentagonal	
S	Square	
T	Triangular	
C	Rhombic80°	
D	Rhombic55°	
E	Rhombic75°	
F	Rhombic50°	
M	Rhombic86°	
V	Rhombic35°	
W	Trigon	
L	Rectangular	
A	Parallelogram85°	
B	Parallelogram82°	
K	Parallelogram55°	
R	Round	

③ Symbol for Tolerance Class

Symbol	Tolerance of Nose Height m (mm)	Tolerance of Inscribed Circle øD₁ (mm)	Tolerance of Thickness S₁ (mm)
A	±0.005	±0.025	±0.025
F	±0.005	±0.013	±0.025
C	±0.013	±0.025	±0.025
H	±0.013	±0.013	±0.025
E	±0.025	±0.025	±0.025
G	±0.025	±0.025	±0.13
J	±0.005	±0.05−±0.15	±0.025
K*	±0.013	±0.05−±0.15	±0.025
L*	±0.025	±0.05−±0.15	±0.025
M*	±0.08−±0.18	±0.05−±0.15	±0.13
N*	±0.08−±0.18	±0.05−±0.15	±0.025
U*	±0.13−±0.38	±0.08−±0.25	±0.13

The surface of insert with ★ mark is sintered.

Detail of M Class Insert Tolerance

● Tolerance of Nose Height (mm)

D.I.C.	Triangular	Square	Rhombic 80°	Rhombic 55°	Rhombic 35°	Round
6.35	±0.08	±0.08	±0.08	±0.11	±0.16	−
9.525	±0.08	±0.08	±0.08	±0.11	±0.16	−
12.70	±0.13	±0.13	±0.13	±0.15	−	−
15.875	±0.15	±0.15	±0.15	±0.18	−	−
19.05	±0.15	±0.15	±0.15	±0.18	−	−
25.40	−	±0.18	−	−	−	−
31.75	−	±0.20	−	−	−	−

● Tolerance of Inscribed Circle (mm)

D.I.C.	Triangular	Square	Rhombic 80°	Rhombic 55°	Rhombic 35°	Round
6.35	±0.05	±0.05	±0.05	±0.05	±0.05	−
9.525	±0.05	±0.05	±0.05	±0.05	±0.05	±0.05
12.70	±0.08	±0.08	±0.08	±0.08	−	±0.08
15.875	±0.10	±0.10	±0.10	±0.10	−	±0.10
19.05	±0.10	±0.10	±0.10	±0.10	−	±0.10
25.40	−	±0.13	−	−	−	±0.13
31.75	−	±0.15	−	−	−	±0.15

③ Symbol for Tolerance Class

C N M G

① ③ ② ④

② Symbol for Normal Clearance

Symbol	Normal Clearance	
A	3°	
B	5°	
C	7°	
D	15°	
E	20°	
F	25°	
G	30°	
N	0°	
P	11°	
O	Other Normal Clearance	
	Major Normal Clearance	

④ Symbol for Fixing and/or for Chip Breaker

Metric

Symbol	Hole	Hole Configuration	Chip Breaker	Figure	Symbol	Hole	Hole Configuration	Chip Breaker	Figure
W	With Hole	Cylindrical Hole + One Countersink (40−60°)	No		A	With Hole	Cylindrical Hole	No	
T	With Hole	One Countersink (40−60°)	One Sided		M	With Hole	Cylindrical Hole	One Sided	
Q	With Hole	Cylindrical Hole +	No		G	With Hole	Cylindrical Hole	Double Sided	
U	With Hole	Double Countersink (40−60°)	Double Sided		N	Without Hole	−	No	
B	With Hole	Cylindrical Hole + One Countersink (70−90°)	No		R	Without Hole	−	One Sided	
H	With Hole	One Countersink (70−90°)	One Sided		F	Without Hole	−	Double Sided	
C	With Hole	Cylindrical Hole +	No		X	−	−	−	Special Design
J	With Hole	Double Countersink (70−90°)	Double Sided						

Appendix F: Calibration Certificate of Kistler Dynamometer

The calibration certificate of dynamomter model 9257B is required for the setting of charge amplifier.

KISTLER
measure. analyze. innovate.

Kalibrierschein KRAFT
Calibration Certificate FORCE

Type **9257B**   Serial No. **554468**

Kalibriert durch Calibrated by	Datum Date
S. Mogavero	15.01.2009

Referenzgeräte Reference Equipment	Typ Type	Serien-Nr. Serial No.
Gebrauchsnormal Working Standard	Kistler 9251A	1748038
Ladungskalibrator Charge Calibrator	Kistler 5395A	530634

Umgebungstemperatur Ambient Temperature °C	Relative Feuchte Relative Humidity %
22	38

Messergebnisse Results of Measurement

Kalibrierter Bereich Calibrated Range kN	Empfindlichkeit Sensitivity pC / N	Linearität Linearity ≤ ± %FSO	Übersprechen Cross talk %	 %
Fx 0 … 5	-7,937	0,05	$Fx \rightarrow Fy$ 1,0	$Fx \rightarrow Fz$ 0,2
Fx 0 … 0,5	-7,947	0,03	$Fx \rightarrow Fy$ 0,9	$Fx \rightarrow Fz$ 0,3
Fx 0 … 0,05	-7,969	0,15		
Fy 0 … 5	-7,929	0,03	$Fy \rightarrow Fx$ 0,7	$Fy \rightarrow Fz$ 0,1
Fy 0 … 0,5	-7,935	0,03	$Fy \rightarrow Fx$ 0,6	$Fy \rightarrow Fz$ 0,2
Fy 0 … 0,05	-7,932	0,15		
Fz 0 … 10	-3,721	0,06	$Fz \rightarrow Fx$ 0,5	$Fz \rightarrow Fy$ 0,0
Fz 0 … 1	-3,724	0,08	$Fz \rightarrow Fx$ 0,5	$Fz \rightarrow Fy$ 0,0
Fz 0 … 0,1	-3,720	0,07		

Messverfahren Measurement Procedure	Kontinuierliche Kalibrierung, Vergleichsverfahren Continuous Calibration, Comparison Method

Kistler betreibt die SCS Kalibrierstelle Nr. 049, akkreditiert nach ISO 17025. SCS Kalibrierzertifikate sind auf Bestellung erhältlich.
Kistler operates the SCS Calibration Laboratory No. 049, which is accredited per ISO 17025. SCS Calibration Certificates are available on request.

Bestätigung Confirmation

Das oben durch die Serienummer identifizierte Gerät entspricht der Vereinbarung der Bestellung und hält die Herstelltoleranzen gemäss den Spezifikationen der Datenblätter ein. Dieses Dokument erfüllt die Anforderungen von EN 10204 Abnahmeprüfzeugnis "3.1". Alle Messmittel sind auf nationale Normale rückverfolgbar. Das Kistler Qualitätsmanagement System ist nach ISO 9001 zertifiziert. Dieses Dokument ist ohne Unterschrift gültig.
The equipment mentioned above and identified by Serial Number complies with the agreement of the order and meets the manufacturing tolerances specified in the data sheets. This document fulfils the requirements of EN 10204 Inspection Certificate "3.1". All measuring devices are traceable to national standards. The Kistler Quality Management System is certified per ISO 9001. This document is valid without a signature.

Kistler Instrumente AG
Eulachstrasse 22	Tel. +41 52 224 11 11	ZKB Winterthur BC 732	IBAN: CH67 0070 0113 2003 7462 8
PO Box	Fax +41 52 224 14 14	Swift: ZKBKCHZZ80A	VAT: 229 713
CH-8408 Winterthur	info@kistler.com	Account: 1132-0374.628	ISO 9001 certified

www.kistler.com

Seite page 1 / 1

Appendix G: Technical specifications for thermal grease/ sealant

HYLOMAR UNIVERSAL BLUE

Non-setting gasket compound

Description

Hylomar Universal Blue is a polyester urethane based sealant that is non-setting and non-hardening even at high temperatures. The compound is resistant to a wide range of fluids including all industrial fuels, oils, water and brine, air, turbine and piston engine combustion products, water, water/glycol and methanol mixtures, petroleum and synthetic diester lubricating oils, gasoline and kerosene fluids (Avtur & Avcat) and fluorocarbon refrigerants. Hylomar Universal Blue can be used to seal joint faces or threaded parts.

Physical Properties

Chemical Basis	Polyester Urethane
Temperature range	-50°C to 250°C
LIGHT GRADE	
Film Thickness	0.015 mm
Surface Finish Max	2.0 µm
Area covered by 100g	1.875m²
Product coverage after drying	2mg/cm²
MEDIUM GRADE	
Film Thickness	0.03 mm
Surface Finish Max	3.0 µm
Area covered by 100g	1.275m²
Product coverage after drying	4mg/cm²
HEAVY GRADE	
Film Thickness	0.09 mm
Surface Finish Max	3.5 µm
Area covered by 100g	0.56m²
Product coverage after drying	12mg/cm²

Instructions for use

Hylomar Universal Blue should be applied to clean dry surfaces. Apply a thin film or bead to one or both surfaces. Once applied, sufficient time should be allowed for the solvent to evaporate. Unlimited assembly time allows precise alignment of joints to be made. Due to the nature of the compound, fasteners may be required to be re-tightened to the correct torque.

Hylomar Universal Blue can be removed from dismantling components by rubbing with a cloth soaked with Acetone. No scraping is necessary.

Appendix H: CFD Simulation Results

Design	Picture	Description	Geometry/dimensions	Fluid Input variables	Other features	Mechanical stress input	Minimum principle stress on cutting tip Gpa	Maximum fluid speed m/s	Maximum Fluid temperature K (°C)	Maximum cutting temperature K (°C)
Monolithic insert		Monolithic insert for heat flux simulation and heat distribution throughout the insert	12.7 x 12.7 x 5mm. No cooling geometry		No			N/A	N/A	627K (353.9°C)
Mark I		Single cooling channel as chamfered edge. Vertical inlet/outlets	12.7 x 12.7 x 5mm. cooling geometry. 1mm chamfer	Heat flux: 5 W/mm² Fluid speed: 0.02 m/s	No	Fc = 200N Ff = 50N Fp = 100N	1.24 GPa	N/A	N/A	549.1K (275.95°C)
				Fluid speed 0, ConTemp turned off				N/A	N/A	801K (527.85°C)
Ebert I		Open plan geometry, slotted inlet/outlet, insert supported by pegs	12.7 x 12.7 x 5mm. Pegs	Heat flux 60 W/mm2 Fluid speed: 0.2 m/s	Tappered inlet/outlet	Fc = 200N Ff = 50N Fp = 100N	1.96 Gpa	13.8m/s	1500K	3580K
				Fluid speed: 2 m/s				22.9m/s	1080K	3370K
			12.7 x 12.7 x 5mm	Heat flux 60 W/mm2 Fluid speed: 0.2 m/s	Tappered inlet/outlet	Fc = 200N Ff = 50N Fp = 100N	1.96 Gpa	14.11m/s	1800K	3580K
				Fluid speed: 2 m/s				14.11m/s	1010K	3250K
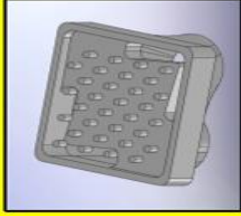
Design	Picture	Description	Geometry dimensions	Fluid input variables	Other features	Mechanical stress input	Minimum principle stress on cutting tip Gpa	Maximum fluid speed m/s	Maximum Fluid temperature K (°C)	Maximum cutting temperature K (°C)
Manifold 1 channel		Single channel manifold designs, slanted inlet/outlet	12.7 x 12.7 x 5mm, 0.8mm inlet/outlet, Xmm manifold channel	Heat flux: 5 W/mm² Fluid speed: 0.2 m/s. Fluid speed: 2 m/s	No	Fc = 200N Ff = 50N Fp = 100N				
Manifold 2 channel		2 channel manifold designs, slanted inlet/outlet	12.7 x 12.7 x 5mm, 0.8mm inlet/outlet, Xmm for each manifold channel	Heat flux: 5 W/mm² Fluid speed: 0.2 m/s Fc = 200N Ff = 50N Fp = 100N. Fluid speed: 2 m/s	No	Fc = 200N Ff = 50N Fp = 100N				
Manifold 3 channel		3 channel manifold designs, slanted inlet/outlet	12.7 x 12.7 x 5mm, 0.8mm inlet/outlet, Xmm for each manifold channel	Heat flux: 5 W/mm² Fluid speed: 0.2 m/s. Fluid speed: 2 m/s	No	Fc = 200N Ff = 50N Fp = 100N				
Manifold 4 channel		4 channel manifold designs, slanted inlet/outlet	12.7 x 12.7 x 5mm, 0.8mm inlet/outlet, Xmm for each manifold channel	Heat flux: 5 W/mm² Fluid speed: 0.2 m/s. Fluid speed: 2 m/s	No	Fc = 200N Ff = 50N Fp = 100N				
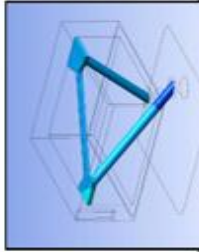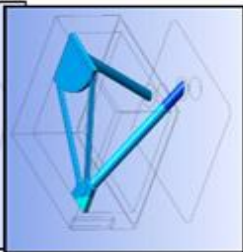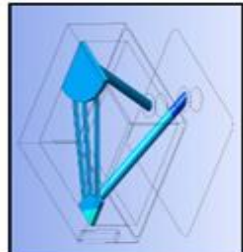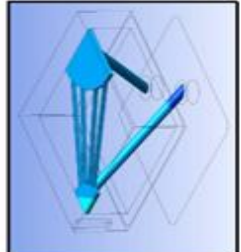
Design	Picture	Description	Geometry dimensions	Fluid Input variables	Other features	Mechanical stress input	Minimum principle stress on cutting tip Gpa	Maximum fluid speed m/s	Maximum Fluid temperature K (°C)	Maximum cutting temperature K (°C)
Manifold 0 channel		0 channel direct flow design, slanted inlet/outlet	12.7 x 12.7 x 5mm. 0.8mm inlet/outlet.	Heat flux: 5 W/mm² Fluid speed: 0.2 m/s F_c =100N Fluid speed: 2 m/s	No	F_c = 200N Ff = 50N Fp = 100N				
Diamond coated 0 channel design		0 channel direct flow design, slanted inlet/outlet, 5µm Diamond coating layer	12.7 x 12.7 x 5mm. 0.8mm inlet/outlet. 5µm diamond layer	Heat flux: 5 W/mm² Fluid speed: 0.2 m/s Fluid speed: 2 m/s	Diamond coated insert (External surface only)	F_c = 200N Ff = 50N Fp = 100N				
Diamond coated 0 channel design		0 channel direct flow design, slanted inlet/outlet, 5µm Diamond coating layer	12.7 x 12.7 x 5mm. 0.8mm inlet/outlet. 5µm diamond layer	Heat flux: 5 W/mm² Fluid speed: 0.2 m/s F_c =100N Fluid speed: 2 m/s	Diamond coated insert (All insert surfaces)	F_c = 200N Ff = 50N Fp = 100N				
0 channel manifold design		0 channel direct flow design, slanted inlet/outlet, Ethylene glycol 25%	12.7 x 12.7 x 5mm. 0.8mm inlet/outlet.	Heat flux: 5 W/mm² Fluid speed: 0.2 m/s F_c =100N Fluid speed: 2 m/s	Alternative coolant: Ethylene glycol 25%	F_c = 200N Ff = 50N Fp = 100N		0.622m/s		422 (148.85°C)
0 channel manifold design		0 channel direct flow design, slanted inlet/outlet, Propylene glycol 25%	12.7 x 12.7 x 5mm. 0.8mm inlet/outlet.	Heat flux: 5 W/mm² Fluid speed: 0.2 m/s F_c =100N Fluid speed: 2 m/s	Alternative coolant: Propylene glycol 25%	F_c = 200N Ff = 50N Fp = 100N		191m/s ? 0.618m/s		414K (140°C) 428K (154.85°C)
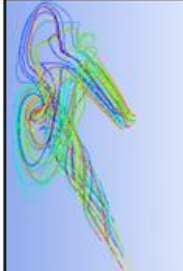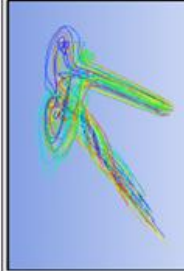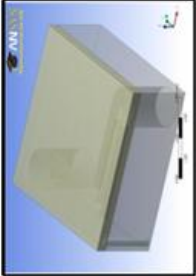
Design	Picture	Description	Geometry dimensions	Fluid Input variables	Other features	Mechanical stress input	Minimum principle stress on cutting tip Gpa	Maximum fluid speed m/s	Maximum Fluid temperature K (°C)	Maximum cutting temperature K (°C)
Malpensa I		2 channel design, vertical inlet/outlet, 0.8mm cooling channels. 0.6mm thermocouple	12.7 x 12.7 x 5mm. 3mm inlet/outlet. 0.8mm x 1mm cooling channels	Heat flux: 5 W/mm² Fluid speed: 0.2 m/s Fc = 200N Fr= 50N Fp = 100N / Fluid speed: 2 m/s	Thermocouple placed between cooling channels	Fc = 200N Ff = 50N Fp = 100N		13.8m/s	310K (37°C) [296K (22.9°C) Thermocouple temperature]	392.7K (119.6°C)
Malpensa II		2 channel design, vertical inlet/outlet, 0.8mm cooling channels. 0.6mm thermocouple	12.7 x 12.7 x 5mm. 3mm inlet/outlet. 0.8mm x 1mm cooling channels	Heat flux: 5 W/mm² Fluid speed: 0.2 m/s Fc = 200N Fr= 50N Fp = 100N / Fluid speed: 2 m/s	Thermocouple placed infront of cooling channels, as close to the tip as possible	Fc = 200N Ff = 50N Fp = 100N		13.4m/s	298.5K (25.4°C) [307K (33.9°C) Thermocouple temperature]	388.6K (115.5°C)
Malpensa III		3 channel design, vertical inlet/outlet, 0.8mm cooling channels. 0.6mm thermocouple	12.7 x 12.7 x 5mm. 3mm inlet/outlet. cooling channels I 0.8 x 1mm, II 0.8 x 0.55mm, III 0.8 x 0.45mm	Heat flux: 5 W/mm² Fluid speed: 0.2 m/s Fc = 200N Fr= 50N Fp = 100N / Fluid speed: 2 m/s	Thermocouple placed infront of cooling channels, as close to the tip as possible, cross section of channels adjusted to equalise pressure drop	Fc = 200N Ff = 50N Fp = 100N	0.742359GPa	11.9 m/s max 3 m/s ave		
Malpensa III		3 channel design, vertical inlet/outlet, 0.8mm cooling channels. 0.6mm thermocouple, with an increased inlet velocity	12.7 x 12.7 x 5mm. 3mm inlet/outlet. cooling channels I 0.8 x 1mm, II 0.8 x 0.55mm, III 0.8 x 0.45mm	Heat flux: 5 W/mm² Fluid speed: 3m/s / Fluid speed: 5 m/s	Thermocouple placed infront of cooling channels, as close to the tip as possible, cross section of channels adjusted to equalise pressure drop	Fc = 200N Ff = 50N Fp = 100N		30.15 m/s max 7 m/s		
First prototype open plan design				Fluid speed: 0.2 m/s / Fluid speed: 10 m/s			0.74GPa	1236 m/s max 70 m/s ave		